



United States
Department of
Agriculture

Agricultural
Research
Service

ARS-76

October 1989

ENGINEERING DIV.
LIBRARY

Scour at Cantilevered Pipe Outlets

Plunge Pool Energy Dissipator Design Criteria

Property of
Flood Control District of MC Library
Please Return to
2801 W. Durango
Phoenix, AZ 85009

2890-1 33943

ABSTRACT

Blaisdell, Fred W., and Clayton L. Anderson. 1989. Scour at Cantilevered Outlets: Plunge Pool Energy Dissipator Design Criteria. U.S. Department of Agriculture, Agricultural Research Service, ARS-76, 171 pp.

Cantilevered pipe spillway outlets are used at most farm-pond and many upstream flood-control principal spillways. Allowing pipe spillways to scour their own energy dissipation pools may be acceptable for small farm ponds. However, preexcavated and riprap-lined plunge pools or more elaborate stilling basins may be required for larger, upstream flood-control reservoirs that flow at full capacity for prolonged periods.

An extensive literature review on the general principles of local scour at pipe outlets revealed little practical information on scour and prevention of scour at culvert outlets: There was no specific information on the design of plunge pool energy dissipators for pipe spillways.

Presented herein are a research plan to provide the needed information, a description of the special experimental apparatus and instrumentation constructed for this study, and an explanation of the experimental methods used. Background information is: a description of the scour process, a method of computing the ultimate scour hole dimensions from short-time tests of the scour progress, and the geometry of the jet after emerging from the pipe. The test program completed and a summary of the test data define the scope of the tests.

Equations and procedures for the design of cantilevered pipe spillway plunge pool energy dissipators resulted from a detailed analysis of the experimental data. The design procedure and equations are summarized in chapter XII, and examples are given.

KEYWORDS: beaching, cantilevered pipe outlet, cantilevered pipe spillway, energy dissipator, energy-dissipation pool, erosion, flood control, jet trajectory, nonerodible layer, pipe spillway, plunge pool, riprap, scour, scour hole, spillway, stilling basin, tailwater, time progression of scour

Trade names are used in this publication solely to provide specific information. Mention of a trade name does not constitute a guarantee or warranty of the product by the U.S. Department of Agriculture or an endorsement by the Department over other products not mentioned.

Copies of this publication may be purchased from the National Technical Information Service, 5285 Port Royal Road, Springfield, VA 22161.

ARS has no additional copies for free distribution.

ENGINEERING DIVISION

United States
Department of
Agriculture

**Agricultural
Research
Service**

ARS-76

Scour at Cantilevered Pipe Outlets

Plunge Pool Energy Dissipator Design Criteria

In Cooperation With the
Minnesota Agricultural Experiment Station

and

St. Anthony Falls Hydraulic Laboratory,
University of Minnesota

ENGINEERING DIVISION

SUMMARY

In chapter I the use of cantilevered outlets is explained, and scour holes that develop at cantilevered pipe outlets are pictured. Attempts to use riprap to prevent scour or to line plunge-pool energy dissipators are shown sometimes to be unsuccessful. The product of the research reported here is an explanation of and procedures for solving the problem of how to size riprap and shape a plunge-pool energy dissipator.

Previous work pertinent to our study is discussed in chapter II. Few studies involved three-phase flow such as is experienced at cantilevered pipe outlets. The value of the literature review is in evaluating general principles of local scour by jets, relevant sediment characteristics, scour pattern similarity, rate and maximum depth of scour, and pertinent parameters and relationships. The extensive tests at Colorado State University published from 1949 to 1983 proved to be of little practical value because the short scour periods and the methods of experimentation did not produce stable scour holes. The University of Alberta studies published between 1977 and 1983 were of limited practical use because they showed inconsistencies, were not correlated, and parameters necessary for their practical application were not determined. Limited studies at the University of Cincinnati were used by the Soil Conservation Service to develop their Design Note No. 6 giving criteria for the design of armored scour holes. These armored scour holes were later found to scour at the downstream end. Studies at the Waterways Experiment Station and at other locations involved culvert scour only. Quotations from three recent publications on scour by two-dimensional jets are given because they summarize information on scour formulas developed from both model and prototype measurements. Despite the large amount of work cited and not cited, the available published material on scour by jets proved to be mostly of only general, not specific or practical, value to us.

The research plan and its history are given in chapter III. Variables included six dimensionless discharges $Q/\sqrt{gD^5}$ ranging from 0.5 to 5.0, five uniform bed materials ranging from 0.5 mm to 8 mm, seven pipe invert heights ranging from 2 pipe diameters below to 8 pipe diameters above the tailwater surface, three geometric standard deviations of bed material size ranging from 1.22 to 1.76, several pipe slopes with most having the pipe horizontal, and a single 1-inch-diameter pipe. Some features of the original test plan were eliminated because they were found to be unnecessary for achieving the desired objective. Added was an impermeable layer in the bed to evaluate the effect of a rock ledge or soil layer resistant to scour.

The experimental apparatus is described in chapter IV. The tests were conducted in duplicate channels so that two tests

could be run simultaneously and thereby increase the efficiency of personnel utilization. All construction materials were corrosion resistant. The water was recirculated, filtered, and temperature controlled. Data on the bed scour were obtained semiautomatically using a bed level probe. Cross and longitudinal sections were recorded numerically on punched paper tape and graphically by a X-Y recorder. Uniform size bed material was used to evaluate the scour produced by flow from the cantilevered pipe.

The experimental methods are described in chapter V. Before each test the bed was screeded level a half pipe diameter above the tailwater level and a pilot channel was screeded in the level bed. The flow was stopped periodically during the scour progress, the scour hole was measured, and pertinent data were recorded both manually and on punched paper tape. The punched paper tapes were processed by computer to provide a hard copy of the recorded data, a contour map of the scour hole, and selected scour hole profiles.

The scouring process is described in chapter VI under subheadings describing how the scour hole shape is affected by the discharge, beaching, removal of suspended material, progression with time, and repeatability of the tests. Also described are qualitative comparisons of the similarity of field scour holes to those observed during the small scale laboratory tests.

Equations describing the increase of the dimensions of the scour hole with time are discussed in chapter VII. Described is the use of the hyperbolic, logarithmic velocity-of-scour method to compute the asymptotic or ultimate maximum scour depth from measurements made after shorter time periods.

It is the path and size of the jet from the cantilevered pipe that determine the location of the scour. Equations defining the jet properties are derived in chapter VIII.

The test numbers and the test variables actually used are summarized in chapter IX. The test conditions and the resulting observations are also summarized.

The test data are analyzed and the results of the tests are discussed and presented in chapter X. This is a long chapter, but the preceding sentence summarizes its contents adequately.

The plunge pool must be designed for a range of flows, so the designed pool shape must be a composite of the pool shapes for the anticipated range of flows. This procedure is given in chapter XI.

ENGINEERING DIVISION

The procedure for the design of plunge pool energy dissipators is given in chapter XII. All of the required equations are assembled in chapter XII for convenience of use. The degree of conservatism of the equations compared to the experimental holes is also given.

In chapter XIII there are examples of the application of the recommended design procedure to typical field conditions that have been experienced by the Soil Conservation Service.

Our conclusions regarding this study are given in chapter XIV.

The references cited in this report follow chapter XIV.

ACKNOWLEDGMENTS

All Agricultural Research Service professionals at the St. Anthony Falls Hydraulic Laboratory participated to some degree in this research. Each contributed ideas, comments, and constructive criticisms to those actually performing the work. The major contributions of each are acknowledged:

Fred W. Blaisdell conceived and supervised the study, wrote the research plan, designed the experimental apparatus, conceived the hyperbolic velocity-of-scour procedure, performed many of the analyses, developed the contour envelope curves and their equations, and wrote most of the report.

Clayton L. Anderson supervised sieving the bed material, designed the sand mixtures to ensure a well-graded size distribution within the size range of the uniform-sized and graded bed materials, built the first experimental apparatus, supervised or conducted the experiments, supervised and/or planned or modified the computer programs, analyzed the computer-generated contour plots to develop the normalized contour coordinates, did the hyperbolic velocity-of-scour analysis and the densimetric Froude number analysis, and wrote the initial draft of parts of the test results chapter.

Kesavarao Yalamanchili analyzed the contour maps and selected the normalizing parameters, thus making possible the reduction of the scour hole contour maps to a common base. He also made a few tests.

Elton A. Hallauer of the North Central Soil Conservation Research Center at Morris, MN, wrote the original computer and plotting programs.

George G. Hebaus was consulted frequently throughout the study. He made major contributions to the hyperbolic velocity-of-scour procedure and to computer programming, and participated in all staff conferences in which the adequacy of the information and the conclusions and recommendations were evaluated.

Karl F. Wikstrom, principal engineering assistant on the St. Anthony Falls Hydraulic Laboratory staff, performed a majority of the experiments and prepared the photographic record of the tests. His meticulous attention to detail contributed greatly to the quality of the research.

The professional staff of the St. Anthony Falls Hydraulic Laboratory were consulted frequently throughout the study. Their input contributed to the research in numerous ways. The experimental apparatus was largely constructed by the laboratory's shop personnel.

CONTENTS

Chapter

- I. Introduction, 1
- II. Previous work (with comments), 4
 - General principles, 4
 - Scour at culvert outlets, 10
 - Scour by two-dimensional jets, 30
- III. Research plan, 36
 - Research outline of 1950, 37
 - Experimental outlines of 1954 to 1968, 42
 - Research outline of 1968, 42
 - Work unit/work project numbers 3504-15070-001 and 3504-20810-001, 43
 - Impermeable layer, 43
- IV. Experimental apparatus, 44
 - Turbine room channel, 44
 - Main floor channels, 48
 - Data acquisition apparatus, 52
 - Bed material, 55
- V. Experimental methods, 58
 - Bed preparation, 58
 - Starting a test, 58
 - Test data, 60
 - Data processing, 61
- VI. Scouring process, 62
 - Scour hole shape, 62
 - Prototype similarity, 69
- VII. Time development of scour, 72
- VIII. Jet properties, 76
 - Jet trajectory, 76
 - Plunge velocity and diameter, 78
- IX. Data summary, 79

X.	Analyses of test results, 102
	Beaching limit, 102
	Dimensionless contour analysis, 105
	Parameter evaluation, 110
	Comparison of computed and experimental scour holes, 137
	Effect of nonerrodible layer, 140
XI.	Composite scour hole (and plunge pool), 145
	Description of test, 145
	Test results, 145
	Comparison with computed contours, 146
	Suggested design procedure, 150
XII.	Plunge pool energy dissipator design procedure, 151
	Limiting discharge, 151
	Jet computations, 151
	Densimetric Froude number, 152
	Ultimate maximum scour hole or plunge pool depth, 153
	Scour hole location, 153
	Scour hole shape, 154
	Time progression of scour, 154
	Agreement of equations with experimental holes, 155
	Composite plunge pool energy dissipator, 155
	Effect of nonerrodible layer, 156
XIII.	Examples of application of results, 157
	Example values, 157
	Beaching limit, 158
	Jet computations, 158
	Plunge pool (or scour hole) dimensions, 158
XIV.	Conclusions, 164
	References, 165

SYMBOLS

a	x-axis coefficient for the contour ellipse
A	semitransverse axis of the rectangular hyperbola
b	y-axis coefficient for the contour ellipse
B	semiconjugate axis of the hyperbola
d	bed material diameter
d_{15}	bed material diameter 15% of which by weight is finer
d_{50}	bed material diameter 50% of which by weight is finer
d_{84}	bed material diameter 84% of which by weight is finer
D	pipe diameter
D_p	plunge diameter of jet; diameter of the jet at the tailwater surface
e	Naperian or natural logarithmic base
F_d	densimetric Froude number = $\frac{V_p}{\sqrt{gd_{50}(\rho_s - \rho)/\rho}}$
g	acceleration due to gravity
L	length of scour hole
n	an integer
Q	discharge
s	Beltaos distance between the jet center line and the stagnation point
S	sine of the angle of the pipe with the horizontal
t	time; seconds in the hyperbolic equation; minutes for test data
V_o	velocity of jet emerging from the pipe
V_p	jet plunge velocity; velocity at which the jet enters the tailwater surface
$V_{p,h}$	horizontal component of the jet plunge velocity
$V_{p,v}$	vertical component of the jet plunge velocity

V_{Z_m}	average velocity by which the scour depth increases = Z_m/t
V	volume of scour
W	width of the scour hole
W_m	maximum width of the scour hole
$W_{m,tw}$	maximum scour hole width at the tailwater surface
x	abscissa in the equation for the hyperbola
x	abscissa for the jet coordinates
x	longitudinal axis for the contour ellipse
x_{ds}	longitudinal axis for the downstream half of the contour ellipse
x_{us}	longitudinal axis for the upstream half of the contour ellipse
X	distance from the pipe exit
X_b	distance from the pipe exit to the beginning of the scour hole
$X_{b,tw}$	distance from the pipe exit to the upstream end of the scour hole at the tailwater surface
X_e	distance from the pipe exit to the downstream end of the scour hole
$X_{e,tw}$	distance from the pipe exit to the downstream end of the scour hole at the tailwater surface
X_j	computed distance from the pipe exit to the point where the jet reaches the elevation of the maximum depth of scour
X_m	distance from the pipe exit to the maximum depth of scour
$X_{m,a}$	average distance from the pipe exit to the center of the scour hole or plunge pool
$X_{m,b}$	distance from the pipe exit to the center of the upstream semiellipse

$X_{m,c}$	length of the parallel-sided center section between the upstream and downstream semiellipses
$X_{m,e}$	distance from the pipe exit to the center of the downstream semiellipse
X_p	computed distance from the pipe exit to the point at which the jet enters the tailwater surface; distance to the jet plunge point
y	ordinate in the equation for the hyperbola
y	transverse axis for the contour ellipse
y_o	offset of the origin of the hyperbola on the y-axis
Y	transverse distance from the center line
z	ordinate for the jet coordinates
Z	distance from the tailwater surface
Z_m	maximum depth of scour below the tailwater surface; Z_m is negative
$Z_{m,t}$	time-dependent depth of scour below the tailwater surface
$Z_{m,u}$	ultimate maximum depth of scour below the tailwater surface; depth of scour at infinite time; asymptote of the hyperbola; $Z_{m,u}$ is negative
Z_p	height of the pipe invert above (+) or below (-) the tailwater surface
Z_{tw}	tailwater depth above the original bed
0_{corr}	correction to the value of X_m to locate the center of each elliptical contour
α	angle with the horizontal at which the jet enters the tailwater surface; angle of inclination of the submerged jet
γ	specific weight of water
γ_s	particle specific weight
Δ	difference

$\Delta\gamma$	$\gamma_s - \gamma$
$\Delta\rho$	$\rho_s - \rho$
σ	geometric standard deviation of particle sizes
τ	shear stress
τ_c	critical shear stress
ϕ	function
ρ	fluid density
ρ_s	bed material (sediment) density
ω	fall velocity of bed material
ω_m	mean fall velocity of bed material

SCOUR AT CANTILEVERED PIPE OUTLETS:
PLUNGE POOL ENERGY DISSIPATOR DESIGN CRITERIA

Fred W. Blaisdell and Clayton L. Anderson

I. INTRODUCTION

Pipe spillways with cantilevered outlets have been used by the Soil Conservation Service (SCS) of the U.S. Department of Agriculture at many of the principal spillways for relatively small farm ponds and relatively large upstream floodwater protection and water conservation structures since the creation of SCS in the 1930's. Particularly for farm ponds, these outlets have been allowed to erode their own scour holes to form energy dissipation pools at the pipe exits. The purpose of the cantilevered pipe is to ensure that the scour occurs far enough downstream to forestall damage to the dam. The bent supporting the cantilevered pipe must, of course, extend below the anticipated depth of scour.

A large majority of these cantilevered pipe outlets with self-formed scour holes have performed satisfactorily, particularly where the soil is cohesive. Figure I-1 shows a small (4-ft-deep by 10-ft-wide by 18-ft-long) scour hole; and figure I-2, moderate scour at a large cantilevered pipe exit. In the latter figure, note the small depth of scour at the supporting bent. Although the design of cantilevered pipe outlets anticipates some scour at the bent, in many cases there is no scour there. In rocky soil, natural armoring helps limit the scour hole size, as shown, for example, in figure I-3. The material eroded from the scour hole has deposited in the entrance to the downstream channel because it is too heavy to be transported further. Low flows now pass around the edges of the deposit. Figure VI-6 shows another example of a typical satisfactory scour hole. At some pipe outlets, on the other hand, the size of the scour hole has been excessive, so the hole periphery has had to be riprapped to prevent further enlargement. Figure I-4 shows such a scour hole. See figure VI-7 for another view of this outlet and figure VI-10 for a similar scour hole in Louisiana. At other pipe outlets the scour has extended upstream far enough and deep enough to undermine the bent and cause the outlet to fail. We have observed this problem only in sandy, noncohesive soils.

Blaisdell is a research hydraulic engineer, formerly at the St. Anthony Falls Hydraulic Laboratory, USDA-ARS, Third Avenue SE at Mississippi River, Minneapolis, MN 55414, and presently a collaborator associated with the Water Conservation Structures Laboratory, USDA-ARS, 1301 North Western Street, Stillwater, OK 74075; Anderson was an ARS research hydraulic engineer, formerly at the St. Anthony Falls Hydraulic Laboratory.



Figure I-1
Scour hole in good sod. Goodhue
County, MN.



Figure I-2
Scour hole at exit of a 4-foot cantilevered
pipe outlet. Goodhue County, MN.



Figure I-3
Self-formed scour hole in rocky soil.
Structure No. 5, South Branch,
Potomac River, WV.



Figure I-4
An excessively wide scour hole. Structure No. 44,
Middle Broad River, GA.

Riprap- or rock-lined stilling basins have been used at some pipe outlets to forestall the damage mentioned in the preceding paragraph. Not all these attempts have been successful. Figure I-5 shows an example. Although there is no scour near the pipe exit and the outlet is in no danger of being undermined, riprap along the sides at the midlength of the downstream protection has been scoured and deposited on the bed further downstream.

Based on a few tests at the University of Cincinnati (Seaburn and Laushey 1967, and Laushey et al. 1967) and other information, Culp (1968) prepared SCS Design Note No. 6, "Armored Scour Hole for Cantilever Outlet." The limited data used to develop this design note proved to be adequate, with the exception that many States have reported erosion of the riprap at the downstream end of the hole and deposition of this riprap in the entrance of the downstream channel. Design Note No. 6 requires the construction of an energy dissipation pool whose depth depends on the discharge and riprap size. If the flow from the pipe discharges onto a rock ledge, obtaining the required depth may require blasting a hole in the ledge, as has been done at the outlet shown in figure I-6. The soil above the ledge has been riprapped. Note that some rock has eroded and deposited in the entrance of the downstream channel.

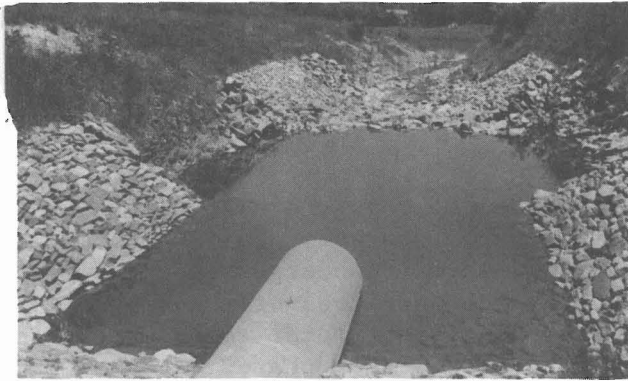


Figure I-5
Flow has damaged this riprapped outlet.
Site No. 14, New Creek, Potomac River, WV.



Figure I-6
Plunge pool blasted in rock ledge and riprapped
above ledge. Rock deposit in entrance to
downstream channel. Structure No. 4, West Point
Remove Watershed, Conway, Pope, and Van Buren
Counties, AR.

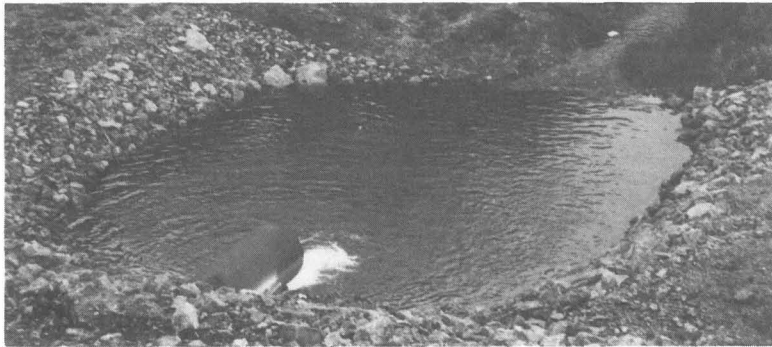


Figure I-7
Preshaped and riprapped plunge pool
energy dissipator. Structure No. 1,
West Fork, Kickapoo River, WI.

That information was needed on the anticipated scour hole size is obvious from the preceding statements. The needed information is provided by the research reported here. Products of the research are: Criteria for the design of cantilevered-outlet plunge-pool energy dissipators; determination of the reason for and means of preventing extreme widening like that shown in figure I-4; determination of the correct size and placement of riprap to prevent damage like that shown in figure I-5; explanation of how to estimate the progression of scour with time; computation of the ultimate size of the scour hole in various-size noncohesive bed materials typically shown in figure I-3; explanation of the effect of a rock ledge like that shown in figure I-6; and suggestions for the design of plunge pools that have a rock ledge for a bottom.

A riprapped, preformed plunge-pool energy dissipator such as might result from application of the information in this publication is shown in figure I-7.

II. PREVIOUS WORK (WITH COMMENTS)

The majority of past studies of local scour have involved only two-phase flow: water and sediment. However, the flow from cantilevered pipe outlets and culverts discharges into air or close to the air-water surface and thus involves three phases: air, water, and sediment. Few studies of local scour have been performed with the involvement of the three phases, such as is experienced at most cantilevered pipe spillway outlets.

Furthermore, in most past studies the sediment and scour have been totally submerged, even if the scouring jet discharges into air before entering the water. In practice, the sediment is exposed to the atmosphere at the periphery of the scour hole. Studies involving this latter--and practical--condition are extremely limited.

Many of the earlier studies were to investigate the nature of scour and were two-dimensional. Although many studies have involved three dimensions, most have involved only two-phase flow and thus are of extremely limited usefulness when applied to the three-dimensional practical case of scour at cantilevered pipe spillway and culvert outlets.

A literature survey was initiated in 1948 when this study was conceived. The annotated card file listing authors and coauthors of each title now (1988) contains some 1,220 cards. Selected titles especially pertinent to the current study are listed in the bibliography. Some of these bibliographic listings are referred to throughout this report.

A survey of the bibliographic cards revealed the two earliest publications to be by Rouse in 1940 and Laursen in 1952. The number of publications indicates that interest in local scour increased in the 1950's and was high in the 1960's.

Previous work which helped establish the principles and procedures involved in studies of local scour will be discussed first. Published results of studies of scour at culvert outlets and scour by two-dimensional jets will follow.

General Principles

Rouse (1940) used a two-dimensional submerged jet directed vertically downward along a vertical wall onto a sand bed to develop his "Criteria for Similarity in the Transportation of Sediment" while at the Soil Conservation Service-California Institute of Technology Cooperative Laboratory. A number of his statements remain pertinent even today, and they will be noted under applicable subject headings.

Laursen (1952) used a two-dimensional horizontal submerged jet located at the original bed level to acquire experimental data. In his study, as in Rouse's and ours, the sediment was lifted from the scour hole by suspension. Laursen, also like Rouse and us, developed parameters enabling the collapse of data for the relationship between scour and time into a single curve.

Laursen's (1952, pp. 180-181; also Vanoni 1975, p. 48) major contribution is his list of four general characteristics of local scour:

1. The rate of scour will equal the difference between the capacity for transport out of the scoured area and the rate of supply of material to that area.
2. The rate of scour will decrease as the flow section is enlarged.
3. There will be a limiting extent of scour.
4. This limit will be approached asymptotically.

These characteristics have received general acceptance and are pertinent to the present study.

Detailed comments on previous work could be included here but are not. Instead, the reader is referred to the comprehensive and authoritative information given in Vanoni (1975), particularly chapter II, section C, subsections 19, pp. 47-49 ("Local Scour") and 20, pp. 49-58 ("Scour by Jets").

Sediment Characteristics

The properties of sediment are described in considerable detail in Vanoni (1975, pp. 19-38). The properties discussed--all highly important in sediment transport and local scour--are particle size, shape, specific weight, fall velocity (in detail), and size-frequency distribution.

Rouse (1940) devotes several pages to the sediment characteristics and points out the importance of the mean size d_{50} and geometric standard deviation σ on sediment transport. But in the section "Similarity in Scour Phenomena," Rouse states that "sedimentation transportation is a combination of two distinct types of motion--that of a fluid relative to geometrical boundaries, and that of granular solids relative to the moving fluid, the latter motion producing in addition a gradual change in the geometrical boundary." Assuming that "the relative motion between sediment and fluid is proportional to the normal settling velocity", Rouse used the sediment fall velocity and its geometric standard deviation to characterize his sediment

properties. Certainly this is a legitimate substitution for the mean size and its geometric standard deviation. However, because sieve sizes are more readily obtainable, we characterized our sediment with d_{50} and σ .

Anderson et al. (1970) show by the straight line in their figure 8 that similarity of critical shear stress can be achieved with sediment particles as small as 0.2 mm. In our studies the minimum size was 0.5 mm.

Rouse's bed materials were all of uniform size, as were most of ours. Little and Mayer (1976) have shown that the bed will not armor if the geometric standard deviation is less than 1.3. We have assumed this to be the upper limit for uniform sized bed material. Our uniform sized bed materials had standard deviations ranging from 1.22 to 1.26. But even those few experiments of ours with graded bed material had so few large particles that they did not adequately armor the bed. As a result, the effect of the geometric standard deviation was not found.

Scour Pattern Similarity

Through the use of suitable parameters, Rouse and Laursen were able to collapse their scour data into a single curve. Rouse used the jet thickness to normalize his scour depth. Laursen (1952, fig. 3; also Vanoni 1975, fig. 2.16) used the distance to the crest of the dune (the deposit of bed material from the scour hole) to collapse the scour patterns at successive times into a single curve. This use of suitable parameters to collapse scour dimensions is typical of what others, including ourselves, have subsequently found. However, Laursen's normalizing parameter is a function of the developing scour hole geometry, and the geometry cannot be reproduced by others until the normalizing parameter is defined in terms that are independently definable. Rajaratnam and colleagues (Rajaratnam and Berry 1977; Rajaratnam and Beltaos 1977; Rajaratnam 1981a-d, 1982; Rajaratnam et al. 1981; Rajaratnam and Macdougall 1983) have used what he calls an approximate asymptotic state dimension as a normalizing parameter, which he defines using a function containing the densimetric Froude number.

To determine a scour depth parameter, Rouse extended the slope of the dune back to his vertical wall. For our experiments Yalamanchili, a former associate of the authors, similarly found that the best definition of the length and width of the scour hole was obtained by extending the slope of the eroded hole to the water surface. Therefore, to normalize our scour hole contour coordinates, our normalizing distances are the distances from the center of the scour hole to the points where the projections of the scour-hole end- and side-slopes intersect the water surface. These normalizing distances were in turn normal-

ized by the maximum depth of the scour hole, and the maximum depth of the scour hole was defined in terms of the densimetric Froude number. Thus, the scour hole dimensions can be computed by working backwards after computing the densimetric Froude number from the pipe velocity, the sediment size and its relative density, and the acceleration of gravity.

Rate of Scour

Rouse's experiments show the progression of scour with time to be a linear relationship between the dimensionless scour depth and the logarithm of dimensionless time. As Rouse notes, this relationship indicates "no equilibrium of scour . . . , the removal of material continuing as an exponential function of time"

Anderson (Vanoni 1975, pp. 50-52) discusses in some detail the relationships that define the progression of scour with time and the implications of the various functions. He ends with the statement: "In the absence of an analytical solution that describes the entire range, recourse must be had to empirical descriptions of the various significant parts of the entire curve." These parts are the exponential function for small values of time, the logarithmic function for larger values of time, either function for intermediate times, and possibly some other function for times approaching the equilibrium scour time. Although the data cited by Anderson do not show it, Rajaratnam's data (Rajaratnam and Berry 1977; Rajaratnam 1981a, b, c) do show a deviation from the logarithmic function as the scour approaches its asymptotic limit. Sarma and Sivasankar (1967) conclude, "(a) progress of scour is not strictly logarithmic but is only approximate to it over certain ranges of scour depths [sic] and time, and (b) the scour-time relationship is a \tan^{-1} -function."

Anderson (Vanoni 1975, pp. 54-57) shows how the individual scour dimensions vs. logarithm of scour time curves can be collapsed to a single curve. Robinson (1971) also used this method when analyzing the data he obtained on scour at cantilevered pipe outlets in our earlier tests.

Nik Hassan and Narayanan (1985) conducted experiments on scour rates in uniform 0.5-mm-, 0.8-mm- and 1.65-mm-size sands downstream of a horizontal apron by a deeply submerged two-dimensional jet, and measured the velocity profiles in stabilized scour holes. Based on their experiments, they present and evaluate a "semi-empirical theory" defining the rate of scour. Their dimensionless equation is

$$\frac{dh}{dt} = \beta_1 \left[\frac{U_m^2}{g(s-1)h} \right]^n U_m \left[\frac{U_m^2}{g(s-1)D} \right]$$

where h is the maximum scour depth below the apron, t is the time, U_m is the maximum mean velocity at the vertical section passing through the position of the maximum scour depth, g is the acceleration due to gravity, s is the relative density of the sediment, and D is the sediment size. The quantities in brackets are squares of the Froude number, the first being a flow Froude number modified by the sediment density and the second being a densimetric Froude number. Our analyses used similar dimensionless numbers.

Nik Hassan and Narayanan found that the best shape of the curve of h versus t for all experimental results was obtained for $n = 2$. The coefficient of proportionality β_1 was found to be a function of D/δ_{1A} as shown in their figure 11, where δ_{1A} is the length scale for the outer layer at the end of the apron--the distance on the vertical velocity profile between U_{mA} and $U_{mA}/2$.

Thomas (1971, 1972) has developed a theoretical equation for the time development of scour. His equation computes the rate of increase or velocity of scour depth--a quantity apparently unused by others. Two of Thomas' conclusions read:

3. Both theory and experiments show that there is a certain time t_k , which we call "critical", in which the characteristics of the time course of the scour depth and the velocity of the creation of the scour depth change.
4. Experiments have proved the quantitative agreement between the theoretically determined time pattern of the local scour depths and the velocity of its formation and that for time $t \gg 0$.

Additional information and comment of Thomas' work can be found in Blaisdell et al. (1981) and in chapter VII of this publication, where the velocity-of-scour approach was used to determine the ultimate scour dimensions.

Maximum Depth of Scour

Because the logarithmic relationship indicates that the scour has no limit, Anderson (Vanoni 1975, p. 52) describes a "practical equilibrium" after which the time-development of scour becomes "virtually imperceptible." Nevertheless, we found scour continuing logarithmically even after 14 months, although the movement of individual grains of bed material was infrequent. It is obvious that the practical limit is an uncertain value that may be evaluated differently by each individual. Although Anderson (Vanoni 1975, pp. 57-58) presents a method to evaluate the practical limit, the personal factor remains. Therefore, Blaisdell et al. (1981) developed a hyperbolic logarithmic velocity-of-scour procedure that can be used to determine the asymptotic or ultimate scour depth from

measurements made as the scour progresses, thus eliminating the variable practical limits of scour used by many analysts. The application of this method to our data is described in chapter VI.

The Nik Hassan and Narayanan (1985) equation for the rate of scour presented previously can be written as

$$\frac{1}{3} \frac{dh^3}{dt} = \beta_1 \left[\frac{U_m^2}{g(s-1)} \right]^2 U_m \left[\frac{U_m^2}{g(s-1)D} \right]$$

to show that there is no limit to the maximum depth of scour. We also found this to be the case.

Sarma (1967) also recognized the limitation of the logarithmic relationship. After listing several functions that would pass through zero scour at zero time and asymptotically approach a limit at infinite time to define a maximum scour depth, he selected a function which related the maximum scour depth to the inverse tangent of the time.

Rajaratnam and Berry (1977, p. 283) discuss an "approximate asymptotic state" of scour, so called because "even after a very long time . . . there were occasional turbulent bursts, randomly distributed (near the bed) which caused local (or spot) erosion and the eroded material was transported (rather at a very low rate) out of the hole . . . even after the other scour characteristics became (almost) time-invariant." Blinco and Simons (1973) give references to and have themselves studied the bursting phenomenon. We also observed these occasional turbulent bursts which disturbed the bed locally and allowed the flow to transport the temporarily suspended sediment for short distances.

Disturbed Scour Depth

Rajaratnam (1981a, 1982) shows that the maximum depth of scour with the jet on--the dynamic scour depth--is as much as 1.4 times the depth of scour with the jet off--the static depth of scour. The lesser depth with the jet off is due to the volume of suspended sediment that deposits in the scour hole when the flow stops. The suspended sediment is vividly shown in figure 12 of Rajaratnam et al. (1981, p. 27). Earlier, Rajaratnam cited a value of 3 times the static depth for circular jets (1981c) and 1.25 times the static depth for plane jets impinging obliquely (Rajaratnam et al. 1981). We also observed a difference caused by turbulence--suspended bed material being deposited in the scour hole when the jet was diverted for

measurement of the scoured bed. This is the reason for our suspended-material-removed tests, described later, which produced the dynamic or maximum clear-water scour depth.

Densimetric Froude Number

Rajaratnam and colleagues (Rajaratnam and Berry 1977; Rajaratnam 1981a-d, 1982; Rajaratnam et al. 1981; Rajaratnam and Macdougall 1983) include the densimetric Froude number in their relationships defining the asymptotic scour depth. We also expressed our ultimate scour depth in terms of the densimetric Froude number.

Some of Rajaratnam's relationships are well defined, and some are not. Some of his relationships are linear, while for others the rate of increase in maximum scour depth decreases as the densimetric Froude number increases. For our experiments, the data scatter and envelope curves are used to define the relationship between the maximum scour depth and the densimetric Froude number. This relationship is exponential, and approaches a limiting maximum depth of scour as the densimetric Froude number increases.

Scour at Culvert Outlets

Scour at culvert outlets has been studied at the Colorado State University, University of Cincinnati, and U.S. Army Engineer Waterways Experiment Station. The University of Cincinnati studies were used by Culp (1968) to develop Soil Conservation Service Design Note No. 6. These studies will be discussed under their respective subheadings, with the symbols changed to conform to our usage.

Colorado State University

Scour by two- and three-dimensional jets has been studied at Colorado State University for many years. The earliest thesis we have is by Doddiah (1949), and the most recent paper is by Abt et al. (1985). For all of the earlier tests the jets plunged into a deep tailwater pool, and the erosion and deposition of eroded material took place below the water surface: There were no exposed boundaries of the scour hole and the scoured material was deposited at the periphery of the scour hole. For their tests with shallow tailwater, the scoured material was first deposited at the edge of the scour hole and then washed downstream. In these respects, many of the Colorado tests did not represent practical conditions. They do, however, help to understand the scouring process. The studies will be presented in chronological order.

Doddiah's (1949) experiments compared the scour caused by hollow and solid jets directed vertically downward at the uniformly

sized bed from above the tailwater. For a given jet area, the resulting scour indicates a single trend. The scour depth in relatively uniform bed material was found to depend on the jet area and velocity, the fall velocity of the bed material, the depth of the tailwater, and the duration of the scour. No equilibrium was achieved. As would be expected, the scour depth approached zero as the ratio of the jet velocity to the scour velocity approached unity. Interestingly, scour increased with an increase in tailwater depth until the tailwater depth reached a critical value. This critical depth was also found by other Colorado investigators. Further increase in the tailwater diminished the scour depth.

Thomas' (1953) experiments used a variable height free overfall and a 1 to 4 range of unit discharges. The nappe impinged on a tailwater of variable depth. The scour took place in two 6-mm-mean-sized gravels having geometric standard deviations based on the fall velocity of 1.17 for the uniform material and 1.33 for the graded material. Thomas' findings agreed with those of Doddiah with respect to critical tailwater depth, no equilibrium scour depth, and erosion of the downstream deposit at low tailwater depths. Equations for the scour depth below the original bed ($Z_m - Z_{tw}$) relative to the tailwater depth Z_{tw} are in terms of the height of fall from the crest to the original bed H , the discharge per unit crest length q , the time t , and the geometric mean fall velocity of the bed material ω_m . For the uniform bed material,

$$\frac{Z_m - Z_{tw}}{Z_{tw}} = (0.29 + 0.070 \log \frac{qt}{H^2}) \left(\frac{q}{H\omega_m}\right)^{1/2} \left(\frac{H}{Z_{tw}}\right)^3 (q/H\omega_m)^{1/3} \quad (\text{II-1})$$

and for the graded bed material,

$$\frac{Z_m - Z_{tw}}{Z_{tw}} = (0.45 + 0.040 \log \frac{qt}{H^2}) \left(\frac{q}{H\omega_m}\right)^{2/3} \left(\frac{H}{Z_{tw}}\right)^2 (q/H\omega_m)^{1/6} \quad (\text{II-2})$$

Hallmark (1955) also studied scour at the base of a free overfall with emphasis on armorplating. As would be expected, armorplating decreased the rate of scour, a relatively small amount of armorplating causing a relatively large decrease in the scour rate. The armorplate should be graded rather than uniform with its minimum size about the same as the maximum size of the bed material.

Smith (1957a,b) conducted 12 series of tests totaling 66 experiments for the Agricultural Research Service using an

8-inch-diameter horizontal pipe cantilevered 4 ft above a submerged bed composed of graded material of 2.32 mm mean size ($0.0114D$, where D is the pipe diameter) having a geometric standard deviation of 1.71. The mean measured fall velocity of the bed material ω_m was 0.700 ft/s. The series included four discharges Q (0.5, 1.0, 1.5 and 2.0 ft³/s or 0.24, 0.49, 0.73 and $0.97 Q/\sqrt{gD^5}$), three tailwater depths Z_{tw} (0.5, 1.0 and 1.5 ft or 0.75, 1.5 and $2.25D$), and one height of fall H (4 ft or $6D$). Based on his experiments, Smith (1957b) proposes a "standard preshaped scour hole." The center of the hole is located at

$$X_m = X_p + Z_{tw} \cos \alpha + 0.6 V^{1/3} \quad (\text{II-3})$$

where

X_m is the horizontal distance from the end of the pipe to the center of the scour hole,

$X_p + Z_{tw} \cos \alpha$ is the horizontal distance from the end of the pipe to the point of impingement of the jet on the bed $= V_o \cos(\sin^{-1} S) [2(Z_p + Z_{tw})/g]^{1/2}$ (an equation that is not strictly correct, because (1) it represents a free-falling jet, whereas the jet is not free falling after it enters the tailwater, and (2) the jet continues on the slope at which it enters the tailwater until it impinges on the bottom of the scour hole),

$Z_p + Z_{tw}$ is the height of the fall from the pipe center line to the original bed,

$V_o \cos(\sin^{-1} S)$ is the horizontal velocity of the jet at the pipe exit,

g is the acceleration due to gravity, and

V is the volume of scour.

Smith's (1957a,b) standard preshaped scour hole is a truncated inverted cone. From the experimental data, Smith proposes that the preshaped hole have

$$\text{a top diameter of } 2.5 V_t^{1/3} \quad (\text{II-4})$$

$$\text{a bottom diameter of } 0.4 V_t^{1/3} \quad (\text{II-5})$$

$$\text{a depth of } 0.5 V_t^{1/3} \quad (\text{II-6})$$

where V_t is the volume of scour at time t . However, the equation for the volume of a cone is incorrect, so these values are questionable. In addition, they are based on a limited volume of data and on test times limited by the narrow test channel to less than one hour for some tests because the wall distorted the scour hole shape as the hole size increased.

Smith (1961) later used a correct equation for the volume of a cone and revised the preshaped scour hole equations to

$$\text{top diameter} = 2.38 V_t^{1/3} \quad (\text{II-7})$$

$$\text{bottom diameter} = 0.65 V_t^{1/3} \quad (\text{II-8})$$

$$\text{maximum depth} = 0.50 V_t^{1/3} \quad (\text{II-9})$$

where the maximum depth is now the depth at the apex of a cone obtained by projecting the side slopes of the scour hole to their point of intersection. The maximum depth is greater than the depth measured to the bottom of the observed hole. These equations are also given in Smith and Hallmark (1961). Smith's (1957b) equation for the location of the scour hole was not corrected in Smith (1961).

Smith (1957a,b) presents equations for $V^{1/3}$ after 100 hours of scour in terms of the height of fall, the energy of the jet at the tailwater surface, the mean fall velocity of the bed material, and the density of water. These equations are for three tailwater depths less than the critical depth and for tailwater depths greater than the critical depth. The critical depth is also defined in terms of the same parameters.

Iwagaki et al. (1958) present a theoretical study of the mechanics of scour by a three-dimensional jet. For our study, the value of the theoretical analysis lies in the selection of the pertinent parameters and methods of analysis. Quoting from pages 54 and 55,

This theoretical investigation with the experimental verifications for the two cases of vertical and inclined jets from non-submerged outlets indicates the following:

1. The rate of scour by a jet issuing in or into still water from a submerged or non-submerged outlet is governed by the characteristics of jet diffusion. In the case of a submerged outlet the depth of scour varies with the power law with respect to time, and in the case of a non-submerged outlet, the variation of the scour depth follows the logarithmic law with respect to time.

2. The dimensionless parameters defining the depth of scour with respect to time, are $(Z_m - Z_{tw})/D_p \sin \alpha$ and $(d_{50}/D_p \sin \alpha)(V_{p,v}t/Z_{tw})$.
3. The effect of sediment characteristics can be expressed by the parameter $V_{p,v}^2/[(\rho_s/\rho) - 1]gd_{50} [= F_d^2]$; however, its validity has not been established by experimental data because of the narrow range of sediment sizes used in the experiments.
4. The tail water depth is introduced by the dimensionless parameter $Z_{tw}/D_p \sin \alpha$.
5. The angle of impingement of the jet α indicates a significant influence on the depth of scour in the case of the non-submerged outlet.
6. The dimensionless form for the final depth of scour should be of the form $Z_{m,u}/D_p \sin \alpha$ which is expressed by power and logarithmic equations with other parameters for the cases of submerged and non-submerged outlets respectively.

The symbols used in the quotation are defined as follows:

- d_{50} is the median diameter of the sediment particles,
- D_p is the jet diameter at the water surface,
- F_d is what we call the densimetric Froude number, although it is not so called by the authors,
- t is the time,
- $V_{p,v}$ is the vertical velocity of the jet at the water surface,
- Z_{tw} is the tailwater depth,
- α is the angle of the jet at the water surface,
- ρ is the density of water, and
- ρ_s is the density of the sediment.

Smith (1961, p. 7) quotes Iwagaki's equation for the depth of scour for an inclined jet as

$$\frac{Z_m - Z_{tw}}{\sqrt{A_p} \sin \alpha} = Y \left[\log \left(\frac{d_{50}}{\sqrt{A_p} \sin \alpha} \frac{V_{p,v}t}{Z_{tw}} \right) + \log Z \right]$$

where A_p is the plunge area of the jet, and Y and Z are empirical functions of $\sin \alpha$.

Smith (1961) continued his studies, begun under Agricultural Research Service sponsorship, under the sponsorship of the Bureau of Public Roads. Equations II-7, II-8 and II-9 and a time of 100 hours to represent a nearly asymptotic scour hole size were used to compute a design size of scour hole in gravel. Then, riprap-protected holes having volumes $1/8$, $1/4$ and $1/2$ the design volume were tested. The $1/8$ -volume hole was so small that the jet was deflected instead of having its energy dissipated in the basin. The $1/2$ -volume hole was larger than necessary. The $1/4$ -volume armored hole exhibited the best performance. Dumping the riprap in a pile in the basin was more effective than placing the riprap uniformly over the basin surface. The most effective point of placement of the dumped riprap in the hole was slightly downstream of the junction of the impinging jet with the original bed level. Of course, the jet impinges on the hole surface downstream of the point of impingement with the original bed level, so this is the logical point for dumping the riprap.

For the limited conditions tested, Smith gives the amount of riprap needed as 10% of the volume of the preshaped basin. The minimum riprap size should be the maximum size of the bed material. The maximum size should resist erosion at the peak flow. Smith states: "No quantitative studies have been made on determining criteria for the maximum diameter." Smith used channels with vertical side walls having widths of 7.5, 15 and 30 pipe diameters and found that the rate and volume of scour increased with the test channel width. Smith explains that side eddies increase in magnitude and stability as the channel becomes wider, and that these eddies transport material upstream. He also notes that rigid boundaries are seldom encountered at culverts. One trapezoidal channel with a 7.5-pipe-diameter bottom width was tested. Armoring of the banks was found to be necessary to prevent erosion by waves generated by the flow in the basin.

The value of Smith's study for the Bureau of Public Roads is in indicating trends. The study is so limited that its practical usefulness is minimal.

Shen et al. (1966) conducted an analytical and experimental study of the basic mechanism of local scour at bridge piers. As part of that study, Karaki and Haynie (1963) prepared a bibliography with brief abstracts of 307 papers. Many of the citations apply also to local scour, and they are included in the more extended card file prepared as part of the present study.

Opie (1967) reports tests conducted for the Wyoming State Highway Department on scour in riprap placed level with the pipe

invert. Pipe sizes were 1.015, 1.45 and 3.00 ft. Discharges ranged from $Q/\sqrt{gD^5} = 0.34$ to 1.58. Seven rounded and angular bed materials having sizes ranging from $d_{50} = 25$ mm to 204 mm and having geometric standard deviations σ ranging from 1.24 to 2.97 were used.

Opie makes several observations:

1. From a practical standpoint, the amount of scour in the material sizes tested was not dependent upon time erosion was rapid and the final "stable" scour hole for that flow formed in minutes rather than hours.
2. The depth of scour was reduced greatly by increasing the tailwater to approximately the level of the top of the pipe. Also, the position of maximum scour was moved downstream.
3. For depths of tailwater below the centerline of the pipe, the effect of tailwater depth on depth of scour was small.
4. Where there was a wide gradation of angular material, "armoring" took place on the downstream face of the scour hole
6. Once the scour hole formed and the dune was established, a significant quantity of water was deflected laterally and escaped down the extreme sides of the bed, at velocity liable to cause scour in unprotected fill. [This is typical of deposition of material scoured at pipe outlets, and is a reason for insuring that such scour will not occur.]

In his analysis, Opie found "that there is a direct correlation, within the accuracy of the experiments, between: the length of scour, the depth of scour, the width of scour, and, as a result, the cube root of the volume of scour." Having established these correlations, the only parameter required to design a stilling basin is the maximum depth of scour Z_m . Opie used the relationship $Z_m - Z_{TW} = \phi(\rho QV_O/B)(d_{84}^2/\Delta\gamma d_{84}^3)$. The term $(\rho QV_O/B)$ represents the potential force of the jet per unit width B . Here ρ is the density of water, Q is the discharge, and V_O is the velocity in the pipe. In the second parentheses, d_{84}^2 represents the area a particle presents to the flow, and $\Delta\gamma d_{84}^3$ is the submerged weight of the particle. The selection of d_{84} as the particle diameter was arbitrary, and $\Delta\gamma$ is the submerged specific weight of the particle.

Opie plotted the terms in this equation to define ϕ . In foot-pound-second units, we find that $Z_m - Z_{tw} = 0.5 + 0.125 \rho Q V_o / B \Delta \gamma d_{84}$ for values of $(\rho Q V_o / B \Delta \gamma d_{84})$ between 2 and 10. For rounded bed materials, ϕ is well defined, whereas for angular bed materials the definition is poor.

Opie points out: "The curves were developed from a limited number of experiments on uniformly graded materials whose size varied over a relatively narrow range in each experiment." With regard to uniformity of the bed material, our analysis indicates that five of the seven bed materials had standard geometric deviations of less than 1.3 (Little and Mayer's (1976) definition of the upper limit of uniformly graded material.), and two bed materials had deviations exceeding this value. Opie emphasizes that the number of experiments is limited and that the results should not be extrapolated beyond the limits of his experiments.

Stevens (1969) reports 259 tests funded by the Colorado State University and the Wyoming Highway Department. Variables include pipes 6, 12, 18 and 36 inches in diameter; 10 sizes of angular and rounded rock with d_{50} from 0.54 to 7.00 inches having geometric standard deviations ranging from 1.05 to 4.29; pipe slopes of 0 and 3.75%; relative discharges $Q/\sqrt{gD^5}$ from 0.1 to 1.59; and plain or flared end sections. The tailwater was varied from $0D$ to about $1D$.

Froude law scaling was shown to be valid by comparing scour hole dimensions at $Q/\sqrt{gD^5} = 1.0, 1.3$ and 1.4 for 6-inch and 18-inch pipes and angular stone of $d_{50}/D = 0.20$ and $\sigma = 1.3$. Scour hole depths, widths and lengths for comparative tests were well within the limits of precision of scour tests. Referring to a Ph.D. dissertation (Abt 1980) and unpublished data (M.J. McGowan 1980, unpublished research data for the Department of Transportation on scour at culvert outlets; Colorado State University, Ft. Collins), Mendoza-Cabrales (1980, p. 23 and fig. 3) also presents data showing Froude law similarity of scour depths, lengths and volumes for a range of dimensionless discharges from about 0.44 to 2.5. The scale ratio was 1:5. Even though the same (unscaled) bed material was used at both model sizes, similarity of the scour dimensions was within the limits of experimental precision.

Like other Colorado State University researchers, Stevens presents curves (1969, fig. 21) showing, for a constant discharge, the existence of a critical tailwater depth at which the scour hole depth is a maximum. However, Stevens presents other curves (1969, figs. 21a, 22, 23) where the scour hole depth decreases (to zero for some conditions) as the tailwater depth increases. Stevens' explanation for the decrease in scour depth

for low tailwater levels is the mound deposited downstream of the scour hole over which the flow cannot discharge material even though rock is in motion in the scour hole. Obviously, the ultimate scour depth had not been reached. Scour resumed when, for special tests, Stevens removed the mound and resumed the flow. A projection of the curve of mound height vs. scour depth to a zero mound height--the condition for a stable hole--produced a threefold increase in the scour depth.

Stevens states that incipient motion depends on discharge and tailwater depth and that "the dependence is even greater than has been reported by Seaburn and Laushey."

A test with a hydrograph of discharges showed that the scour produced by the maximum discharge was increased by a lesser discharge. The lesser discharge scour was deposited in the scour hole and was swept out by a subsequent maximum discharge. We also observed this sequence of events, which indicates that the plunge pool should be designed for a range of discharges instead of the maximum discharge alone.

Stevens presents examples of the design of riprapped basins.

Simons et al. (1970, chapter IV, "Rock Riprapped Basins") show how to design standard riprapped nonscouring, hybrid, and scoured basins. As noted by Stevens (1969, chapter V, "Summary," item 4), and stated by Simons et al. (1970, p. 45) for the scoured basin: "The mound is an integral part of the structure and if it is somehow removed the scour hole would deepen and penetrate the apron resulting in partial failure or failure of the basin."

In Simons et al. (1970) design examples for rock riprapped basins are presented in appendix A, section D, pp. 86-129. Field checks of the design procedure are in section F, pp. 133-139. For the example presented, the agreement of the design procedure with the observed dimensions was excellent for the scour depth, very good for the width of the hole (57 ft computed, 60 ft observed), good for the length of basin to length of scour hole ratio (1.9 computed, 1.6 observed), and fair for the scour hole length (158 ft computed, 105 ft observed).

The design information presented by Simons et al. (1970) is available in abridged form in Stevens et al. (1971).

Ruff and Abt (1980) and Abt (1980) made 12 scour experiments for the Federal Highway Administration in 0.15-mm-mean-size SC cohesive soil composed of 58% sand and 28% clay compacted to $90 \pm 12\%$ of optimum density. Three smooth circular pipes with inside diameters of 10-1/4, 13-1/2 and 17-1/2 inches were used. Each pipe was tested using $Q/\sqrt{gD^5} = 0.5, 1.0, 1.5$ and 2.0. The

tailwater was $0.45D \pm 0.05D$ because the scour depth is greatest at this or lesser depths. Data were collected at scour times of 31.6, 100, 316 and 1000 min.

The scour depth $Z_m - Z_{tw}$, length L , width W and volume V in terms of the pipe diameter D were related to the discharge intensity $Q/\sqrt{gD^5}$ and modified shear number $\tau_c/\rho V_o^2$ using logarithmic relationships. Here τ_c is the critical shear stress, ρ is the fluid density, and V_o is the velocity at the culvert outlet. Equations express each of these relationships, and, despite the limited number of experiments, design procedures are proposed.

The information reported by Ruff and Abt (1980) has also been published by Abt and Ruff (1981 and 1982).

Mendoza-Cabrales (1980) made tests in a 4-ft-wide channel with and without a headwall at the exit of a 4-inch-diameter culvert. Cross sections and comments make it obvious that the scour patterns at the channel edges were affected by the channel sidewalls. The bed material properties were: Mean diameter $d_{50} = 1.84$ mm [$d_{50}/D = 0.0181$], geometric standard deviation $\sigma = 1.33$, settling velocity $\omega = 0.89$ ft/s, and critical velocity $V_c = 0.214$ ft/s. The bed surface was at the pipe invert elevation. The tailwater was $0.4D$ above the pipe invert. Seven dimensionless discharges $Q/\sqrt{gD^5}$ ranging from 0.44 to 2.50 were used. Point depths throughout the scour hole for both the headwall and no headwall conditions are listed in their appendix II for eight durations of scour ranging from 14 to 1000 min.

In contrast to other Colorado studies, Mendoza-Cabrales uses an exponential equation to relate the depth $d = (Z_m - Z_{tw})$, length L , and volume V of scour measured at the original bed level at each time t to the scour values at the maximum time of 1000 min designated by the subscript m . Letting S be the dimensionless variable, values of a and b in the equation

$$S = 1 - e^{-(at + b)} \quad (\text{II-10})$$

were determined. They are:

<u>Variable</u>	<u>No headwall</u>		<u>Headwall</u>	
	<i>a</i>	<i>b</i>	<i>a</i>	<i>b</i>
d/d_m	0.14	+0.90	0.14	+0.74
L/L_m	0.14	+0.47	0.14	+0.41
V/V_m	0.18	-0.31	0.18	-0.25

The logic for using exponential curves is fine, but the poor fit to the data indicates that other factors may influence the scour progress. The logic is good because exponential equations give values of the scour at any time that become asymptotic to the maximum scour at the maximum time tested. Thus, the exponential equation produces limiting scour dimensions. In contrast, the power equation used by other Colorado investigators to express the variation of scour dimensions with time produces no limit to the maximum scour dimensions. We used a different method to express the progression of scour with time (see chapter VII) but did use exponential equations to relate the relative ultimate (asymptotic) depth of scour and the densimetric Froude number.

Mendoza-Cabrales (1980) also presents curves of the maximum scour dimensions relative to the pipe diameter D as a function of the dimensionless discharge. The power equation

$$\frac{S_m}{D} = a \left(\frac{Q}{\sqrt{gD^5}} \right)^b \quad (\text{II-11})$$

was used, where a and b are:

<u>Variable</u>	<u>No headwall</u>		<u>Headwall</u>	
	a	b	a	b
d_m/D	2.14	0.35	2.09	0.35
L_m/D	19.63	0.42	19.26	0.40
V_m/D^3	182.55	1.53	156.28	1.32

The fit of the data to the curves defined by these values of a and b is good. However, plots show that the differences between the headwall and no headwall data are so small that single values of a and b would represent the data well within the limits of precision of the measurements. In any case, we maintain that scour continues indefinitely. As a result, the maximum scour dimensions defined by equation II-11 and the accompanying tabulation, which are based on tests run for a maximum of 1000 min, must be much less than the ultimate maximum values.

Mendoza-Cabrales comments that for the no headwall condition the scour directly under the culvert outlet is about 0.4 as deep as the maximum scour depth. However, for the headwall condition, the scour at the headwall extends to the maximum depth observed in the scour hole. This maximum scour depth is located between 0.30 and 0.40 of the maximum scour length for either headwall condition.

Mendoza-Cabrales' (1980) results were published by Mendoza et al. (1983).

Shaikh (1980) made two series of four tests each. The difference between series was the geometric standard deviation of the bed material σ : for the uniform material $\sigma = 1.32$ and for the graded material $\sigma = 4.87$. The uniform material size was $d_{50} = 7.62$ mm and the graded bed material size was 7.34 mm--close to the same. The culvert diameter was 10-1/4 inches and the test channel was 20 ft wide, a width of $23D$. The horizontal bed surface was at the pipe invert elevation. Tailwater depth was $0.45D \pm 0.05D$. Dimensionless discharges used were $Q/\sqrt{gD^5} = 0.5, 1.0, 1.5$ and 2.0 . Scour holes were measured after 31.6, 100 and 316 min. The scour measurement data are listed in an appendix.

Shaikh comments: "with graded gravel . . . the fine and coarse particles were segregated. A portion of the coarse particles settled at the bottom of the scour hole while the fine particles were deposited at the sides of the scour hole and around the edge of the mound."

Power equations were used to fit curves to the data. The relation between the ratio of the maximum scour after 316 min $d_{m,316} = (Z_{m,316} - Z_{tw})$ to the pipe diameter D and the dimensionless discharge is

$$\frac{d_{m,316}}{D} = \frac{Z_{m,316} - Z_{tw}}{D} = a \left(\frac{Q}{\sqrt{gD^5}} \right)^b \quad (\text{II-12})$$

where for uniform bed material $a = 1.81$ and $b = 0.45$, and for graded bed material $a = 1.49$ and $b = 0.51$.

The progression of scour with time t in minutes for both uniform and graded bed material is

$$\frac{d_m}{d_{m,316}} = \frac{Z_m - Z_{tw}}{Z_{m,316} - Z_{tw}} = 1.0 \left(\frac{t}{316} \right)^{0.03} \quad (\text{II-13})$$

Equations II-12 and II-13 can be combined to give

$$\frac{d_m}{D} = \frac{Z - Z_{tw}}{D} = a \left(\frac{Q}{\sqrt{gD^5}} \right)^b \left(\frac{t}{316} \right)^{0.03} \quad (\text{II-14})$$

The length L , width W and volume V of the scour hole in terms of the pipe diameter D are related to the relative maximum scour depth d/D . In the equation

$$\text{variable} = a \left(\frac{Z - Z_{tw}}{D} \right)^b \quad (\text{II-15})$$

the variables and their corresponding a and b values are:

Variable	Uniform		Graded	
	a	b	a	b
L/D	4.78	1.85	7.95	1.16
W/D	4.48	1.25	4.46	1.66
V/D	12.55	2.96	9.19	3.97

Kloberdanz (1982) made six tests of the scour produced by a 4-inch-diameter culvert after 14, 44, 141, 268 and 316 min in a bed of 2.00-mm median diameter [$d_{50}/D = 0.0197$] and 4.38-geometric-standard-deviation sand having a fall velocity of 27.3 cm/s (0.90 ft/s). Discharges ranged from 0.11 to 0.73 ft³/s [$Q/\sqrt{gD^5} = 0.3$ to 2.0]. The tailwater depth was 0.45D above the pipe invert, and the bed was level with the pipe invert. In his appendix B are tabulated the scour-hole cross-section elevations at several distances downstream from the pipe exit for each time of scour and for $Q/\sqrt{gD^5} = 0.3, 0.4, 0.5, 1.0, 1.5$ and 2.0. For relative discharges of 1.5 and 2.0, the bed scoured to the boundary of the 4-ft-wide test channel in less than the 14-min minimum scour time. Boundary interference must have affected these results.

Kloberdanz observes: "Segregation of particles in the scour hole was observed at the conclusion of each test. Armoring of the scour holes consistently occurred for each test." This is expected because of the large geometric standard deviation of the bed material. To avoid segregation and armoring, we used uniform size bed materials for our research.

Like Mendoza-Cabrales (1980), Kloberdanz uses an exponential equation to relate the depth $d = (Z - Z_{tw})$, width W , length L and volume V of scour measured at the original bed level at each time t to the scour values at the maximum time of 316 min,

designated by the subscript m . Values of a and b for the variable S in equation II-10 are:

<u>Variable</u>	<u>a</u>	<u>b</u>
d/d_m	0.015	0.96
W/W_m	0.015	0.52
L/L_m	0.016	1.88
V/V_m	0.015	0.47

Kloberdanz also presents curves of the maximum scour dimensions after 316 min relative to the pipe diameter D as a function of the dimensionless discharge. The power equation II-11 was used, where a and b are:

<u>Variable</u>	<u>a</u>	<u>b</u>
d_m/D	1.25	0.87
W_m/D	9.75	0.87
L_m/D	13.49	0.37
V_m/D	36.16	2.08

The fit of the data to the curves defined by these values of a and b is good.

Our experience is that scour continues indefinitely and that much scour can occur after the 316-min limit used by Kloberdanz; thus, the maximum values given by equation II-11 and the accompanying tabulation may be much less than the ultimate maximum values.

Kloberdanz also combined his data with the data obtained by others. These results were published by Abt et al. (1984). They are presented below.

Ruff et al. (1982), in a report prepared for the Federal Highway Administration, present detailed data and analyses of the Colorado experiments.

Abt et al. (1984) have correlated the studies by Ruff et al. (1982), Mendoza-Cabrales (1980), Mendoza et al. (1983), Kloberdanz (1982) and Shaikh (1980). For these tests, pipes 4

and 10 inches in diameter extended about $7D$ through headwalls into 4- and 20-ft-wide flumes. Noncohesive material of $d_{50} = 0.22, 1.86, 2.00, 7.62$ and 7.34 mm and $\sigma = 1.26, 1.33, 4.38, 1.32$ and 4.78 , respectively, was leveled to the pipe invert elevation. The tailwater depth was $0.45D$. The dimensionless discharge $Q/\sqrt{gD^5}$ ranged from 0.3 to 3.1--a wider range than for most of the Colorado experiments. Data collection was at 31, 100 and 316 min or more from the beginning of each test, but the correlation is for a scour time of 316 min. The power equation

$$S = a\left(\frac{Q}{\sqrt{gD^5}}\right)^b \quad (\text{II-16})$$

was used to represent the data. Initially $S = (Z_m - Z_{tw})/D$ or $d_m/D, W_m/D, L_m/D$, and V_m/D^3 , where the subscripts indicate maximum scour values after 316 min, and $d = (Z - Z_{tw})$ is the depth, W is the width, L is the length, and V is the volume of the scour hole. These values were measured with respect to the original bed level. After a sensitivity analysis, an attempt was made to improve the coefficient of determination r^2 by including the bed material properties. The equation then became

$$S_\sigma^{0.4} = a\left[\frac{Q}{\sqrt{gD^5}} \left(\frac{d_{50}}{D}\right)^{0.2}\right]^b \quad (\text{II-17})$$

The values of a, b and r^2 in equations II-16 and II-17 are:

Variable	Equation II-16			Equation II-17		
	a	b	r^2	a	b	r^2
d_m/D	1.77	0.63	0.72	3.65	0.57	0.83
W_m/D	8.73	0.66	0.79	19.25	0.64	0.81
L_m/D	17.98	0.58	0.70	35.22	0.51	0.70
V_m/D^3	97.04	1.92	0.76	550	1.71	0.76

Although the sensitivity analysis resulted in a considerable improvement of the coefficient of determination for $d_m/D = (Z_m - Z_{tw})/D$ and a slight improvement for W_m/D , there was no improvement for L_m/D and V_m/D^3 .

Comments: All of the Colorado studies have a deposit of eroded material downstream of the scour hole, and this deposit is required if the equations for the scour hole are to be valid. Simons et al. (1970, p. 45) specifically mention this requirement. This deposit could be obtained by placing riprap level with the pipe invert to a depth exceeding the depth of

scour. Subsequent scour would produce the mound. However, if the scour hole is preformed and is stable, there will be no mound and the Colorado analyses will not be valid. An object of our study was to determine the ultimate size of stable, preformed-plunge-pool energy dissipators, so the extensive Colorado studies had only qualitative usefulness to us.

Furthermore, the limited scour time of 316 min used in this analysis is far from the time required to determine the ultimate and stable scour hole size that was the object of our studies. And finally, many Colorado test channels were so narrow (mostly 12 to 23 pipe diameters) that the sidewalls influenced the scour patterns. Our channels were 72 pipe diameters wide, yet sidewalls affected scour patterns if the dimensionless discharge was high or beaching was extensive--conditions that are not relevant to the application of our research because they exceed our recommendations.

University of Cincinnati

Studies sponsored by the Ohio Department of Highways and the Bureau of Public Roads are reported in four M.S. theses directed by L.M. Laushey (Ofwona 1965, Seaburn 1965, Kappus 1965, and Varga 1966). These theses are the bases for Laushey's (1966) "Design Criteria for Erosion Protection at the Outlet of Culverts" and for three papers presented at the 1967 International Association for Hydraulic Research Congress at Fort Collins, CO (Seaburn and Laushey 1967, Varga and Laushey 1967, Laushey et al. 1967).

Laushey's (1966, p. i) synopsis describes the scope of the tests:

Theoretical and experimental studies were made of dumped rock to control erosion at the outlet of culverts. The variables included full and part-full flow from culverts of different diameters [0.845 inch to 4.06 inch] onto beds of different sizes [5.5 mm to 23.4 mm] and shapes [gravel and spheres]. Experiments [for full-pipe flow] determined the velocity [in the pipe V_o] required to cause incipient motion [V_{oc}] of the bed [$V_{oc} = 3.67 \sqrt{gd^3/D}$; $Q_c = 2.88 \sqrt{gd^3D}$], the size and shape of the ultimate equilibrium hole [$V/D^3 = 2.54(V_o - V_{oc})^2/gd$; for uniform spheres $Z_m = 0.53 V^{1/3}$, and for gravel $Z_m = 0.48 V^{1/3}$], the time rate of progression of erosion [$f(\ln t)$], and the protective effect of submergence [the equations are valid up to $Z_p/D = -0.5$; the bed material is protected by increasing tailwater for $-0.5 \leq Z_p/D \leq -1.0$; and there is no effect for $Z_p > -1.0$] and dense packing of the bed.

The results are presented in dimensionless ratios to make them of interest, or immediate use, to the hydraulic engineer.

Laushey's (1966, p. 14) experiments with elevated pipes demonstrated, for the incipient scour velocity, that "Despite the different free-fall distances between the pipe and the bed, the incipient scour movement of the bed was found to be dependent only on the horizontal momentum."

Laushey's (1966) findings regarding incipient erosion velocities are also presented by Seaburn and Laushey (1967) in dimensionless units. Values of the constant in the equation for V_{OC} are 3.30 for large gravel and 4.28 for spheres and rounded gravel.

Laushey's (1966) findings regarding the magnitude and rate of erosion are also presented by Laushey et al. (1967). Conclusion 2 is of interest because it indicates that an initial large scour hole may not increase much as a result of future storms: "The depths and volumes scoured in short periods of time were large ratios of the ultimate dimensions, in accordance with the logarithmic rate. It might be concluded that one severe storm could erode an appreciable fraction of the ultimate hole."

Varga and Laushey (1967) studied the application of wall jet theory to erosion by submerged jets. They write:

The flow downstream of an outlet can be divided into two broad groups: free and submerged jets. A free jet exists when the tailwater depth is small; then the jet momentum is the primary agent causing scour. With rising tailwater, the jet becomes submerged, and the factors responsible for scour are boundary layer forces in the vicinity of the bed. For equal discharges, the erosion potential of a free jet is much greater than that of a submerged jet

Wall shear stresses were determined by theoretical relationships by assuming that they play the same role in mobilizing the bed particles as the critical tractive stress concept of open channel flow.

The calculated shear stresses, for both sizes of particles, were about 0.4 of the permissible tractive stresses recommended by the U.S. Bureau of Reclamation . . . for canals of non-cohesive stones. The discrepancy can be explained partly by the fact that the calculated wall shear stresses were computed using the average value of the velocity, whereas in turbulent flow peak values might reach 1.5 times the average value. Since shear stresses are proportional to the square of the velocity, instantaneous values with the capacity to initiate erosion could be at least double the average shear stresses. . . .

Soil Conservation Service Design Note No. 6

Using the relationships developed by Seaburn and Laushey (1967) and by Laushey et al. (1967), Culp (1968) derived an equation for the maximum depth of scour and evaluated the constants from the plotted results in the papers referred to. Culp states that his constants "are more conservative than those selected by the authors to represent average results." Culp's equation is

$$Z - Z_{tw} = (0.148 \frac{Q}{\sqrt{Dd}} - 1.82 d\sqrt{D})^{2/3} \quad (\text{II-18})$$

where $(Z - Z_{tw})$ is measured from the level of the downstream channel bed in feet, D is the pipe diameter in feet, d is the riprap diameter in feet, and Q is the discharge in cubic feet per second.

There was insufficient information in the referenced papers to determine the shape and dimensions of the scour hole. Culp used other information available to him and his experience to locate the basin and define its shape. The basin has a horizontal bottom $(Z - Z_{tw})$ long and wide located Z_m below the tailwater level at maximum conduit discharge. The longitudinal center line slope of the banks is 1 on 4 upstream and 1 on 2 downstream. The shape is elliptical upstream and circular downstream. The center of the ellipse and circle is $(Z - Z_{tw})/6$ downstream of the center of the horizontal floor. The common center of the ellipse and circle is located at a distance X from the exit of the horizontal pipe exit, where

$$X = \sqrt{Z_p + D} - \sqrt{\frac{V_o^2}{2g}} \left[\sqrt{\frac{1 + Z_m}{Z_p + D}} + 1 + \frac{Z_m}{2(Z_p + D)} \right] \quad (\text{II-19})$$

In this equation, $(Z_p + D)$ is the distance from the pipe crown to the tailwater surface and V_o is the velocity in the pipe.

Especially considering the limited experiments at Cincinnati, Culp's design has proved to be an excellent guide for SCS use. However, field experience (Blaisdell 1983) shows that the length is short and that the downstream end of the scour hole sometimes erodes.

The experiments reported herein were designed to cover the range of anticipated conditions and provide adequate information for the development of a reliable mathematical model for the design of cantilevered-spillway-outlet plunge-pool energy dissipators. As a result of these experiments, Goon (1986) revised SCS Design Note No. 6. The revision is based on Blaisdell et al. (1981),

Anderson and Blaisdell (1982), and Blaisdell and Anderson (1984). The revised "Riprap Lined Plunge Pool for Cantilever Outlet" is a rectangular pool that circumscribes the ellipse recommended herein (equations X-10 and X-11). The SCS recommended pool depth is 80% of the maximum depth of scour given in this report by equations X-22 and X-23.

Waterways Experiment Station

For estimating the scour at culvert outlets with the invert at the bed level, Bohan (1970) developed generalized equations for the maximum length L_M , width W_M , depth $(Z_m - Z_{tw})$ and volume V_M of scour relative to the pipe diameter D as functions of the Froude number, length of scour time, and tailwater depth. Variables were the discharge Q , scour period in minutes t , and tailwater depth Z_{tw} . The cohesionless bed material had a median diameter of 0.23 mm. Bohan's data were reanalyzed by Fletcher and Grace (1972), and the discharge was expressed in terms of $Q/D^{5/2}$ instead of the Froude number. Fletcher and Grace (1974) present identical and additional information in their appendix A.

Fletcher and Grace (1972; 1974, p. A12 and fig. A13) found that the scour relationships were approximately the same for $Z_{tw} < D/2$ and for $Z_{tw} \geq D/2$, so two sets of equations, identical in form but differing in coefficients and exponents, were used to express the maximum dimensions. In terms of $Q/\sqrt{gD^5}$ and t in min, these equations have the form

$$\frac{Z_m - Z_{tw}}{D} = \frac{W_M}{D} = \frac{L_M}{D} = \frac{V_M}{D^3} = A \left(\frac{Q}{\sqrt{gD^5}} \right)^B t^C \quad (\text{II-20})$$

The coefficients and exponents are:

<u>Dimension</u>	<u>Z_{tw}/D</u>	<u>A</u>	<u>B</u>	<u>C</u>
$(Z_m - Z_{tw})/D$	< 0.5	1.5	0.375	0.10
"	≥ 0.5	1.4	"	"
W_M/D	< 0.5	4.9	0.915	0.15
"	≥ 0.5	3.5	"	"
L_M/D	< 0.5	8.23	0.71	0.125
"	≥ 0.5	14.1	"	"
V_M/D^3	< 0.5	23.5	2.00	0.375
"	≥ 0.5	19.9	"	"

Dimensionless scour hole center line and transverse geometries in terms of the maximum dimensions are presented graphically for each tailwater depth. The deepest scour and the transverse cross section occur at $0.4L_{SM}$ downstream of the culvert outlet.

For $Z_{tw}/D \geq 0.5$ there was zero scour at the culvert outlet. For $Z_{tw}/D < 0.5$ there was scour beneath the culvert exit and, at culvert outlets, a cutoff wall is necessary. However, for cantilevered pipe outlets the scour is provided for by the cantilever of the pipe beyond its supporting bent.

If a horizontal blanket of riprap is used to prevent scour (Fletcher and Grace 1974, p. A12 and fig. A13), the stone size should be

$$\frac{d_{50}}{D} = 0.20 \frac{D}{Z_{tw}} \left(\frac{Q}{\sqrt{gD^5}} \right)^{4/3} \quad (\text{II-21})$$

and the length of riprap protection L_p should be

$$\frac{L_p}{D} = 10 \frac{Q}{\sqrt{gD^5}} + 7 \quad \text{for } \frac{Z_{tw}}{D} < 0.5 \quad (\text{II-22a})$$

and

$$\frac{L_p}{D} = 17 \frac{Q}{\sqrt{gD^5}} \quad \text{for } \frac{Z_{tw}}{D} \geq 0.5 \quad (\text{II-22b})$$

The plan placement of the riprap is given in their figure A14.

If a preformed scour hole is used, the size of riprap can be reduced (Fletcher and Grace 1974, p. A12 and figs. A15 and A16). The proposed preexcavated pool had a bottom $3D$ long by $2D$ wide with 1 on 3 side slopes from the bottom to the original bed level. (Presumably, these side slopes should be extended to above the tailwater surface.) If the depth of the preformed hole is $0.5D$ the coefficient in equation II-21 becomes 0.126, and for a pool depth of $1.0D$ the coefficient is further reduced to 0.083.

Other Studies

Smith and Johnson (1983) report the results of tests using a cantilevered pipe 13 inches in diameter. Various combinations of three dimensionless discharges $Q/\sqrt{gD^5} = 0.53, 0.80$ and 1.06 ; four relative drop heights from the pipe invert to the original bed level $Z/D = 1, 2, 3$ and 4 ; three relative tailwater depths above the original bed level $d_2/D = 0.4, 0.8$ and 1.2 ; and two

relative stone sizes $d_{50}/D = 0.23$ and 0.31 were used to conduct 57 tests. In contrast to the procedure used by many other investigators, but in similarity to ours, Smith and Johnson describe their test procedure as follows: "During each test the rock dune which formed on the downstream side of the scour hole was removed and the discharge sequence repeated until scour was stabilized without the dune present. The philosophy of this approach was to find a depth for the riprap at which no movement would occur, from which recommended dimensions for a stable rock basin or plunge pool could be established."

Smith and Johnson report: "Design criteria were formulated from the stone bed tests, and finally these criteria were verified on tests with the stone layer placed over the [0.35-mm] sand bed." The recommended basin has a flat bottom $D/2$ square and 1 on 2 side slopes. Jet trajectory curves, uncorrected for the flattening of the trajectory below the water surface, give the location of the upstream end of the flat basin floor. Design curves for each discharge tested give, in terms of the pipe diameter, the scour depth below the original bed level as functions of the cantilevered pipe invert elevation and the tailwater depth relative to the original bed elevation. Smith and Johnson further report that "verification tests were run on 8 model rock basins. These were designed according to the [recommended] criteria. Performance met expectations. There was no scour in the sand bed and hence there was no deposition of scoured material. Bank erosion was limited to localized wavewash."

Scour By Two-Dimensional Jets

Three references to scour by two-dimensional jets were discovered after the previous parts of this chapter had been completed. Because they contain material pertinent to our study, they will be discussed briefly. A fourth reference published after the draft of this manuscript had been completed (Nik Hassan and Narayanan 1985) has been discussed under the subheadings "Rate of Scour" and "Maximum Depth of Scour."

Each of these references lists equations developed from model tests or prototype data by numerous authors. The maximum depth of scour below the tailwater surface Z_m is evaluated using the equation

$$Z_m = \frac{C q^x H^y}{d^z} \quad (\text{II-23})$$

Where C is a coefficient, q is the discharge per unit width, H is the fall from the headwater to the tailwater surfaces, d is the bed material size, and x , y and z are exponents.

Locher and Hsu

Based on the publications of seven authors, Locher and Hsu (Novak 1984, ch. 5, subsec. 4.6) discuss erosion at flip buckets and state: "The coefficient C and the exponents . . . x , y and z , summarised in Table 2 [not reproduced here; it is similar to a table presented by Mason and Arumugam (1985)] show that the ultimate scour depth is primarily a function of discharge q . The head H plays only a secondary role and the particle size, d , and lip angle [of the flip bucket], are not particularly significant."

Locher and Hsu (subsec. 5) discuss plunge pools at overfall structures and state: "Axisymmetric jets possess sufficient energy for erosion after penetrating $20D$ into a pool. [Depending on the pipe height, we found the maximum depth of scour to be $7.5D$ or $10.5D$.] . . . in two-dimensional jets . . . erosion can occur at even greater depths up to $40B$, where B is the thickness of the nappe at the entry into the pool." This comment is also found and its source is given in Mason and Arumugam (1985).

Further discussion and references are given by Locher and Hsu (Novak 1984).

Whittaker and Schleiss

The preface to "Scour Related to Energy Dissipators for High Head Structures" (Whittaker and Schleiss 1984) reads:

The following communication deals with scour problems at the toe of dams and weirs and gives a general view of the possibilities of predicting the final depth and form of scours using empirically established formulas and hydraulic model tests.

Thus the authors . . . provide hydraulic engineers with a very valuable state-of-the-art report

The contents are summarized in the abstract:

Background theory is presented on predicting jet trajectories and behavior in air, as well as on the characteristics of a plunging jet in water. The role of model tests in predicting scour is discussed, and some difficulties relating to grain size effects noted. Predicting scour caused by horizontal jets issuing from energy dissipation basins and by plunging jets from free overfall, pressure outlet or ski-jump spillways is then covered in some depth. A large number of different formulae are presented. The accuracy of a number of these is checked in an application to two prototype scour situations - namely Cabora-Bassa and Kariba dams. Some recommendations as to which formulae to use in specific situations are given, as well as some general recommendations for reducing or preventing scour.

This 73-page state-of-the-art publication is recommended for background reading. Only selected items especially pertinent to our study will be mentioned.

With regard to the bed material and grain size effects (pp. 23, 24), Whittaker and Schleiss state:

If the bed material is chosen carefully, good predictive results for scour depth can be obtained by using non-cohesive material

. . . .

. . . Because the eroding jet is more confined than in the non-cohesive case, cohesive material scours more deeply.

Care must be taken in scaling scour values obtained in model tests with non-cohesive material to prototype scales. First, some scour formulae that could be used are dimensionally incorrect

Secondly, there are two grain size limitations that affect scour, one relative and the other absolute. Conceptually, scour formula fall into two groups: those that consider such grain size limitations, and those that do not.

Those formulas that do not consider bed material size in defining the limiting scour depth (p. 26) "reflects the fact that plunging jets reach an effective scouring limit that is much more dependent on jet parameters than on bed material size."

With regard to the several formulas discussed (p. 28), the authors state that "the scour formulae reflect either of two forms for small grain sizes. [Some] equations . . . continue the trend given by larger grain sizes. However, [others] . . . attempt to reflect the limiting grain size It should be noted that a limiting of scour depth with small grain sizes is largely an anticipated trend with little data to substantiate it."

In Whittaker and Schleiss' chapter 5, "Scour by Plunging Jets," the characteristics of a number of empirical equations giving the maximum scour depths for two-dimensional free overfall and ski-jump jets are discussed. For 12 empirical equations, listed are the predicted scour depths based on model tests and the depths evaluated from prototype scale variables. Some of the comparisons are good, while for others the scaled model scour depths are much greater.

Eight scour formulas for plunging jets are given in an appendix. Most of these formulas define the maximum depth of scour below the tailwater level in terms of the height of fall, the discharge per unit width, and the d_{90} size of the bed material.

Mason and Arumugam

Mason and Arumugam's (1985) abstract describes the scope and results of their analyses:

Formulas proposed to date for calculating ultimate scour depth under jets, such as issue from free dam overfalls and flip buckets, are examined. The accuracies of the formulas are evaluated by using each to process sets of scour data from prototypes and models of such prototypes. It is established that scour depth is as adequately calculable using only unit flow q and head drop H as using more complex considerations, but that those formulas most applicable for model purposes are not those best for prototypes. It is demonstrated that where bed particle size d is also considered, the use of the mean particle size d_m is more appropriate than the d_{90} size. Chute friction loss allowances and jet impact angle are also examined in terms of improved accuracy; the relevance of Froude law scaling for this type of scour is verified. Lastly, a new formula for tailwater depth h is presented and shown to give improved accuracy for both models and prototypes.

They list 31 empirical equations which they place in 5 groups:

All the Group I authors seem to have derived their formulas from experiments in which the parameters were varied in turn in order to effect the erosion process. These yielded a fairly constant value for the exponential x of about 0.6, and a value for y , though not so well established, of about 0.2 to 0.3. There is, however more variation in the value of z , ranging from 0 to 0.5, and also concerning which particle size should be taken to characterize the scour process. The majority of authors have adopted the d_{90} size on the basis that smaller particles will be scoured most readily, the ultimate size of hole being governed by the larger particles available in the bed. . . .

The two Group II formulas both supplement the use of q , H and d with the consideration of tailwater depth h

The [three] Group III formulas can, by virtue of the way they were originally expressed, be classed as highly simplified. . . .

The [eight] Group IV formulas comprise those by Russian authors. . . . several of the Group IV formulas contain terms which either depend heavily on subjective judgement or which are poorly defined. . . .

Group V was reserved for formulas developed using time as a parameter. . . . The results of experiments which considered the rate of scour rather than ultimate depth [were] adapted . . . by putting time equal to a sufficiently large number to give expressions for long-term, ultimate scour depth. . . .

Of the 31 equations listed, 6 were not used in the analyses.

In order to compare the remaining 25 formulas . . . , each formula was used to process the 26 sets of prototype and 47 sets of model data to give 73 calculated scour depths. The accuracies of the formulas could then be assessed by comparing these calculated depths with the actual measured depths. The mean value of calculated scour depth divided by measured scour depth . . . was obtained for each formula together with the coefficient of variation V of the results. The statistical analysis of model and prototype data were treated separately in order to isolate possible scale effects.

. . . in all Group I cases, the coefficient lies between about 30% and 50% with, as might be expected, a tendency towards higher values on the prototypes. . . . Interestingly, the best model formulas are noticeably bad for prototypes.

The results of the analyses of . . . Group II formulas are good at model scales For prototypes, however, both are relatively poor.

The Group III formulas . . . results show that neither have much to commend them.

The three Russian formulas, taken as Group IV, for all their complexity, gave generally poorer results than those of any preceding group. At a prototype scale, none of the Group IV formulas would be of any real value.

The Group V equation . . . gave coefficients of variation for the results of 41.89% for models, but 326.79% for prototypes; the latter being principally due to one dramatically high overestimation of prototype scour.

The authors propose a new formula that they claim to be more accurate. It is based on equation II-23 with variable values of the exponents. The improvement appears to be statistical only, improving the coefficient of variation range only from 30% to 50% to an expected 25% for model data and 30% for prototypes. However, their figure 4 shows estimation errors ranging from +100% to -50%.

Quoting from their "Summary and Conclusions":

It is clear from analyses of scour data from prototype dams and model tests of such prototypes that the form of expression [of equation II-23] has been the most convenient and accurate to date for estimating the depth of scour under a free falling jet. It is also clear, however, that the values of the [coefficient and exponents] most appropriate for use in conjunction with prototypes are different from those most appropriate for use with models.

Analyses of other factors affecting scour suggests that allowing for friction loss on the conveying structure improves accuracy in the case of models, but not in the case of prototypes. Allowing for the impact angle of the jet, however, produced inconclusive results. The similarity in accuracy between model and prototype analyses indicates that the concept of an ultimate scour depth is, for all practical purposes, valid. Analyses also showed that for the types of bed material used for model testing this type of scour, the use of the mean particle size d_m gives better accuracy than use of the d_{90} particle size. The validity of using the Froude law for scaling this type of scour was also demonstrated.

III. RESEARCH PLAN

Planning for the study reported here began in early 1948, and a working plan was prepared in April. (Interestingly, this was at about the time the Colorado State University tests were initiated by Doddiah.) A preliminary study of the literature, a proposed design of the experimental equipment, and an outline of the experimental procedure were prepared by University of Minnesota graduate student M.G. Mostofa in the fall and winter of 1949-1950. Planning of a test program was continued in 1950, with input from SCS regional and engineering standards engineers.

In August 1950 research plan SWC-d-9-1-3 was drafted. This plan was followed in all important respects throughout the research, although there were a number of changes in procedure and details during the course of the experiments as a result of experience gained, refinements in needs, and changes in objectives.

The input from SCS indicated that the tests should simulate cantilevered pipes from 12 to 48 inches in diameter, pipe velocities of 10 to 35 ft/s, pipe slopes of 0 to 5%, pipe outlets from 0 to 4 ft above the channel grade, and scour velocities of 1 to 6 ft/s. In dimensionless terms, the combinations of pipe size and velocity give $Q/\sqrt{gD^5} = 0.5$ to 5 and pipe invert heights of $0D$ to $4D$. A study of the tractive forces and velocities required to move various sizes of noncohesive bed material and possible prototype/model scale ratios showed that sands ranging from 0.5 to 8 mm would, in combination with three pipe sizes, represent the range of scour velocities. Specifically, a 1-inch pipe would represent the 12- to 48-inch prototype pipe sizes and prototype scour velocities of 3 to 6 ft/s with length scale ratios ranging from 12 to 48. Similarly, a 3-inch pipe would represent scour velocities of 2 to 4 ft/s with scale ratios of 4 to 16, and a 12-inch pipe would represent scour velocities of 1 to 2 ft/s with scale ratios of 1 to 4.

The research plan prepared in August 1950 was reviewed by L.G. Straub (Director), A.G. Anderson, and E.M. Laursen of the St. Anthony Falls Hydraulic Laboratory. When transmitting the plan to SCS regional engineers E. Freyburger and C.J. Francis and to M.M. Culp (Head), SCS Engineering Standards Unit, Blaisdell wrote:

The plan has been reviewed and discussed with several men here at the laboratory. Their comments are largely confined to laboratory procedures and do not indicate that any major revisions need be made. I am impressed, though, by their admitted ignorance, in spite of years of study in the general field of sediment transportation, of how to tie the laboratory results to your field needs. That the method I have outlined in the working plan will work, is open to question. Nevertheless, those who have reviewed the plan indicate that this is as good an approach as any at this stage of the game.

Research Outline
of 1950

Appendix B, the experimental outline of research plan SWC-d-9-1-3, is quoted in its entirety here. Comments in brackets explain differences between the original plan and how the research was actually performed.

APPENDIX B OF RESEARCH PLAN OF AUGUST 1950

Details of Procedure

The design of this experiment is based on the assumption that the cantilevered outlet will be a satisfactory outlet structure for a range of discharges but that excessive scour will be obtained if the flow exceeds some unknown limit: it will be necessary to determine quantitatively the scour to be anticipated under varying field conditions. The further assumption is made that the stable velocity for the model bed material can be translated into terms of the stable velocity used in the hydraulic design of field channels.

Scour Tests

Tests will be made to determine:

1. The distance from the end of the pipe to:
 - a. the beginning of the scour hole,
 - b. the end of the scour hole, and
 - c. the location of the maximum depth of scour.
2. The width of the scour hole.
3. The depth of the scour hole.
4. The volume of the scour hole. [Although computed, no use was made of this information.]

To achieve these ends, the scour dimensions will be recorded as a contour map. Additional data recorded on these scour hole contour sheets will be:

1. The discharge,
2. The length of the test run,
3. The temperature of the water,
4. The tailwater depth,
5. The height of the pipe above the tailwater level,
6. The diameter of the pipe,
7. The slope of the pipe,

8. The angle at which the jet strikes the water surface [this was not measured],
9. The characteristics of the bed material, and
10. Special notes regarding the experiment.

It is anticipated that the rate of scour will be so rapid that it would be unsafe to design for other than the maximum dimensions of the scour hole. [We still feel the best and safest design will be for the ultimate dimensions.] Therefore, it is not necessary to determine the rate of growth of the scour hole and only its essentially stabilized dimensions will be measured [we did measure the time progress of the scour and projected the scour to its ultimate dimensions]; the tests will be run for a sufficient length of time so that little or no bed material is being removed from the scour hole. [Although the tests were run until there was little bed material movement, movement never completely stopped.]

Initially, at least, the model tests will be made with flat stream beds. This condition is based on the assumption that the scour hole will grow to its ultimate size even if stream banks are used and that the movement of the bed materials out of the scoured area will only lengthen the time for the tests without influencing the final size or form of the scour hole. The tailwater downstream from the model will be at a level $D/2$ below the level of the stream bed and all scour and structure elevation measurements will be referenced to this level. Here D is the diameter of the cantilevered pipe.

The elevation of the invert of the cantilevered pipe above the tailwater level Z will be $0D$, $1D$, $2D$, $4D$, $8D$, $16D$ and $32D$. [The $16D$ and $32D$ pipe heights were not tested.] Most of the initial tests will be run with $Z = D$. The higher values of Z will simulate a pipe cantilevering over a gully head.

The slope of the cantilevered portion of the pipe will be 1%. [This was changed to 0%.] A group of tests will be conducted using slopes of 0% to 20% (sine) to determine the effect of slope on the scour. Slopes to be tested will be 0%, 1%, 5%, 10% and 20%. [The tested range was 0% to 63.5%.]

Tests to determine the effect of the supporting bent and the effect of the downstream slope of the dam on the scour pattern will be made only if it is found that they will fall within the scour hole area. [These tests were found to be unnecessary.]

The tests will cover a little broader range of pipe sizes and discharges than it is anticipated will be required for soil conservation structures. The discharge Q and the pipe diameter D will be combined into the quantity $Q/D^{5/2}$. [This was revised to the fully dimensionless form $Q/\sqrt{gD^5}$.] The tests will cover a range of $Q/D^{5/2}$ from 3 to 30. [$Q/\sqrt{gD^5}$ from 0.53 to 5.3.] The following flows will be used for each model or variation

thereof: $Q/D^{5/2} = 3, 5, 10, 15, 20, 25$ and 30 . [We used $Q/\sqrt{gD^5} = 0.5, 1, 2, 3, 4$ and 5 for the tests used in the analyses presented here.] The effect of low flows with the pipe only partly full will be investigated to determine the effect on the scour pattern of less than the design discharge. [These tests were not made.]

Probably three different sizes of pipe will be used during the study. Initial tests will be made using a setup having $D = 1$ inch. It is anticipated that this size pipe will permit scour determinations for field velocities ranging between 3 and 6 feet per second if the bed material has the range of size mentioned later. Tests will also be made with $D = 3$ inches to cover field velocities in the 2 to 4 feet per second range. A pipe 12 inches in diameter will be used if it proves advisable to conduct tests to cover field velocities in the 1 to 2 foot per second range. [Personnel attending a program review in January 1981 felt the 3-inch and 12-inch pipe tests were not needed. They had confidence that the 1-inch pipe tests would scale up satisfactorily.]

The initial test schedule, consisting of 161 tests, is given in the following table.

Test number and initial schedule

Z	S	D	d	$Q/D^{5/2}$						
				3	5	10	15	20	25	30
D	%	in.	mm.	Test number						
0	1	1	2	1	2	3	4	5	6	7
1				8	9	10	11	12	13	14
2				15	16	17	18	19	20	21
4				22	23	24	25	26	27	28
8				etc.						
16										
32										
1	0	1	2							
	1			8	9	10	11	12	13	14
	5									
	10									
	20									
1	1	1	0.5							
			1	8	9	10	11	12	13	14
			2							
			4							
			8							
		3	0.5							
			1							
			2							
			4							
			8							

The channel in which the tests will be made will have minimum bed dimensions as follows: length $100D$, width $70D$ and depth $12D$. [These channel dimensions proved adequate.] Standard laboratory equipment and methods will be used to conduct the tests and determine the scour hole dimensions.

Bed Materials

Bed materials having several different resistances to scour will be tested for two or three different absolute model sizes. The range of bed material size and model size will be so chosen that the velocities, when stepped up to field conditions, will approximate the range of velocities encountered in the field. The field velocities to be simulated will range from two feet or possibly one foot per second to six feet per second. [All analyses were done using dimensionless parameters, so model scale as such was eliminated as a pertinent parameter.]

The model stream beds, at least for most of the tests, will be composed of uniform sized material. [This procedure was followed.] This will eliminate difficulties that might be traced to sorting and armoring of the scour hole with coarse particles if a graded material were used. [Two nonuniform bed materials were also used.] Uniform size material should also permit a more reliable determination of the settling and stable velocities of the sediment. It is anticipated that the bed materials may be sized in a hydraulic separator. [The hydraulic separator was never developed or used.]

Five different sizes of bed material will be used. The mean diameters of these bed materials will be approximately 0.5 mm, 1 mm, 2 mm, 4 mm and 8 mm. [These sizes of sieved bed materials were those used throughout the test program.] Each of these bed materials will be tested with each pipe size and model variation.

The removal of bed material from the scour hole is largely a process of suspended sediment transportation. The settling velocity of the sediment ω_s is therefore of importance and will be determined for each of the bed materials used. Also of importance is the suspension velocity or some velocity which is characteristic of it. The velocity in the pipe may be taken as this characteristic velocity. The velocity in the pipe is proportional to Q/D^2 . Therefore, the quantity $(Q/D^2)/\omega_s$ may be taken as a measure of the dimensions of the scour hole; $(Q/D^2)/\omega_s$ is a measure of the ratio of the scouring velocity to the stable velocity of the bed material. This quantity will likely prove useful in transferring the laboratory results to field conditions. [The settling velocity was neither determined nor used in the analysis.]

Existing formulas for the transportation of bed sediment make use of the critical tractive force. A critical tractive force τ_c for each of the bed materials used will be determined in a tilting channel. This will permit tying in the present experiments to experiments concerning bed load transportation. [Tests to determine the critical tractive force were not made.]

There may be some question as to whether noncohesive bed materials will scour in the same manner as the cohesive bed materials frequently found in the field. It will likely be desirable to conduct a few tests on stabilized bed materials to answer this question. It is known that the hydraulic laboratory of the U.S. Bureau of Reclamation at Denver, Colorado, has considered this problem and has used stabilized beds composed of lean mixtures of lumnite cement and sand. The specific scheme to be used will be determined after additional study. [No tests of cohesive bed materials were made.]

Determination of Scour Velocity of Bed Material

To adapt the laboratory results to field conditions, the erosivity of the bed materials used must be translated into terms of the scour velocity for the soils at the site of each structure. An intermediate experiment will make this translation possible.

Each of the bed materials used in the laboratory will be placed in a test nozzle and water run over them at increasing velocity until the material just starts to move. This will provide a tie between the settling velocity of the bed material w_s and its scouring velocity v_s . The scour hole parameter can then be written in the form $f[(Q/D^2)/v_s]$. The form of this function will be determined experimentally.

The scour nozzle will be so designed that it can accept undisturbed samples of soil from field locations so the determination of the scour velocity at the location of each outlet can be determined. This will permit an estimation of the ultimate or maximum scour hole dimensions to be expected under field conditions. A safety factor added to the scour velocity will provide the permissible velocity commonly used for design purposes. This safety factor should be determined by the design engineer. [No tests planned under this subheading were made. However, thinking and acting along similar lines, Little et al. (1981) developed a portable flume and tested 11 soils having a plasticity index less than 15.]

Stress and Vibration Tests

Present practice in [SCS] Region III is to use a heavy concrete junction block where the barrel and the cantilever join to absorb vibration and care for the trust forces existing at that point. Information is desired regarding the magnitude of the forces present at the junction block. Tests will be made to determine these forces.

If the pipe is cantilevered too far beyond its supporting bent it will become very flexible and may vibrate excessively when water flows through it. The vibrations may be particularly severe when air is carried through the pipe. The unique facilities available at the St. Anthony Falls Hydraulic Laboratory will permit the making of full scale tests on

cantilevered pipes at heads up to about 20 feet to determine the flexibility of various types of pipe suitable for use in connection with cantilevered spillway outlets. These tests will also check the methods used in the structural design of cantilevered outlets.

The details of these structural tests will be worked out in cooperation with the Engineering Standards Unit and the various interested regional engineering divisions.

[No stress or vibration tests were made.]

**Experimental Outlines
of 1954 to 1968**

The experimental outline was revised to a new form, given the code SWC-e1-3, and approved December 8, 1954. A new code, MINN-W-3, was assigned on December 15, 1958. The outline was further revised in March 1961 and assigned the code Minn-Mi-3. All of these outlines called for the same procedure as that in the 1950 plan.

The leader for all outlines was F.W. Blaisdell. C.L. Anderson and C.A. Donnelly were added in February 1966, and A.R. Robinson was added in April 1968. With the employment of Anderson on January 31, 1966, active preparation for the research began.

The Minn-Mi-3 revision was terminated using code number MI-58-3 in January 1968, and a new plan was submitted.

**Research Outline
of 1968**

A new form of the outline was required, so a revision was made, given the code number MI-65-12, and dated December 17, 1968. Personnel involved were Blaisdell and Anderson.

The experimental plan was much the same in all essentials as the 1950 plan. Deleted were references to the hydraulic separator, the determination of the scour velocity, the scour nozzle, and the stress and vibration tests. Added were tests of the effect of the standard deviation of the bed material. Another addition was the measurement of the progress of scour. This latter addition is because of the realization that scour continues indefinitely and that the rate of scour is needed to determine the ultimate or asymptotic scour dimensions.

In this outline is the first mention of a bed level recorder, and the recording of digital data on punched paper tape and graphical data by an X-Y recorder.

This revision contains the following section:

Responsibilities

Fred W. Blaisdell will guide the study, develop the instrumentation, prepare a comprehensive annotated bibliography, develop the test procedures, perhaps perform some tests, and cooperate in the analyses.

Clayton L. Anderson will supervise the preparation of the test sands, assemble the apparatus, conduct the tests, make the analyses, and prepare or assist in the preparation of the report.

Work Unit/Work
Project Numbers
3504-15070-001
and 3504-20810-001

As a result of administrative changes in the authorizing and recording systems, the project description was briefed to two short paragraphs giving only the objectives and the approach. Space was not available on form AD 421 Research Work Unit/Project Description-Progress Report to go into the detail presented in earlier research outlines.

Research was done under project number 3504-15070-001 from October 19, 1973, and under 3504-20810-001 from April 10, 1979, until the research unit was dissolved and its functions were moved to the Water Conservation Structures Laboratory at Stillwater, OK, after September 30, 1983. Personnel throughout this period were Blaisdell and Anderson. In addition, K. Yalamanchili participated in the experimentation and analysis during 1975.

Impermeable Layer

As a result of a program review on January 14-15, 1981, the recommendation was made to determine the effect on the scour hole geometry of a nonerodible layer at about half the ultimate depth of the plunge pool. Plans for making this determination were informally added to the overall plan and were implemented.

IV. EXPERIMENTAL APPARATUS

Two different channels were used during the course of the experiments. Problems encountered during tests in the first (turbine room at the St. Anthony Falls Hydraulic Laboratory) channel were designed out of the second (main floor) channels.

Turbine Room Channel The turbine room channel was initially selected for the tests because (1) the available head was about 40 ft and small fluctuations in head during long-time tests would have a minor effect on the discharge and (2) directing a stream from a hose onto a bed of concrete sand had shown that a 1-inch stream would scour the sand and that the 7-ft (84D) width of the available channel would be adequate to contain most scour holes without sidewall interference.

The channel, instrumentation design and construction, and sand preparation had been completed or directed by Anderson and Blaisdell by the time A.R. Robinson arrived in June 1967 for a sabbatical year with the Agricultural Research Service at the St. Anthony Falls Hydraulic Laboratory. Anderson had been temporarily reassigned to another project, so Robinson used the channel and apparatus to conduct 45 tests. As noted in his report (1971) on these tests, Robinson screeded an initial channel downstream of his pipe exit. His photographs show that this channel widened excessively. This was due to the deposition in the channel entrance of material scoured from the hole. Such widening would not occur if the scour hole, or more properly the plunge pool, were stable--in a stable pool there would be no scour and no deposit.

Transport Channel

After Robinson's departure in August 1968 and because available personnel were otherwise occupied, long-time test 46 was run from February 10 to April 8, 1970--100,230 minutes or 69.6 days. At the end of this period the downstream channel had widened to almost the full width of the test channel, as shown in figure IV-1.

Obviously, the velocities were sufficient to lift the bed material from the scour hole and deposit the sand in the entrance to the downstream channel. However, the velocities in the channel were not sufficient to readily transport the sand. As a result, a dune formed at the channel entrance. With time, flow around the dune widened the downstream channel. Also, the deposition increased the water level in the scour hole and changed the effective tailwater level indeterminably.

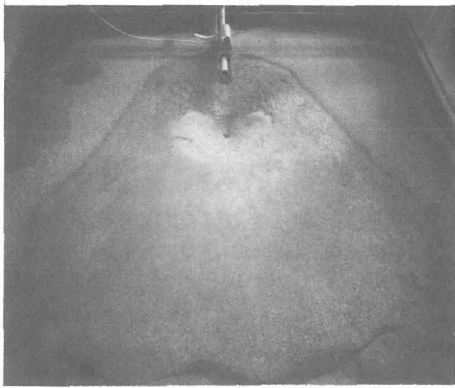


Figure IV-1
Excessively wide and shallow
downstream channel.

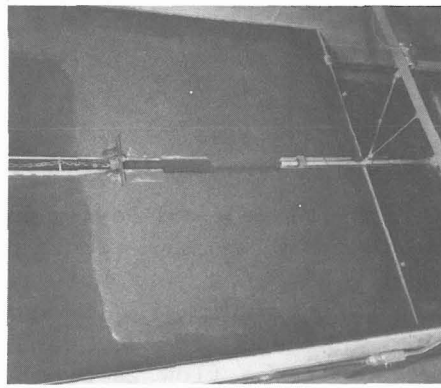


Figure IV-2
Initial screeded channel and
scour transport channel.

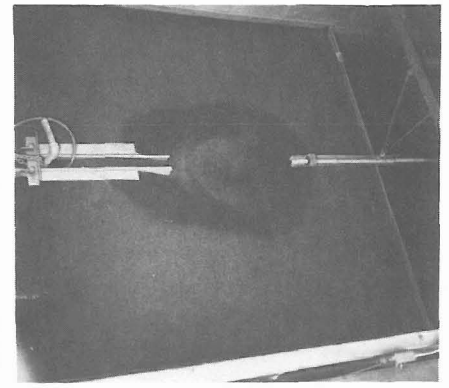


Figure IV-3
Air lift pump removes material
deposited in transport channel.

We wanted to prevent this channel widening, so for run 47, which we ran for 100,000 elapsed minutes between December 12, 1971, and April 8, 1972, we inserted the narrow "transport channel" shown in figure IV-2. The entrance to this channel was located just downstream of the anticipated scour hole.

Figure IV-2 shows transverse lines scribed in the sand at the pipe exit and at the upstream end of the transport channel. Also shown is the initial channel screeded into the sand bed. The chain is connected to a hoist used to pull the transport channel downstream as the scour hole enlarged. Figure IV-3 shows the scour hole after 100,000 minutes--69.4 days. Additional lines scribed across the sand surface show successive positions of the transport channel as the scour hole increased in size. The objectionable downstream channel widening was fully controlled by the transport channel.

However, we found that the eroded bed material would not travel through the transport channel. So we injected air at the base of the pipe shown in the transport channel in figure IV-3, and continuously pumped out a sand-water-air mixture as fast as sand accumulated. Sand pumps were used in the transport channel for all subsequent runs.

Although the transport channel and sand pump solved the downstream channel stability problem, other problems were found. These had to do with mud in the river water and temperature fluctuations. Notes taken during run 46 illustrate these problems.

Water Temperature

When run 46 began on February 10, 1970, the water temperature was 2° Celsius. When the test ended on May 8 the water temperature was 15°. Specifically, from February 10 to 18, the temperature was about 2°; from February 19 to March 4, 4 to 6°; from March 6 to April 24, about 10°; and from April 27 to May 8, about 15°.

Taylor (1971, 1974) and Taylor and Vanoni (1972) ran pairs of experiments in which the temperature differences were 15° Celsius or more--the range of temperatures encountered during run 46. Taylor found that a change in temperature can cause either an increase or a decrease in sediment transport, depending on whether the flow is hydrodynamically smooth or fully rough, and that it can also change the bed form. Taylor states that hydrodynamically smooth flow occurs at boundary Reynolds numbers less than about 13 and that fully rough flow occurs at boundary Reynolds numbers greater than about 200. A discussion on the effect of water temperature, including Taylor's findings, is presented by V.A. Vanoni (1975, subsec. 55, pp. 183-189). J.F. Kennedy (Vanoni 1975, p. 118) remarks that "temperature changes have been found to have a marked effect on alluvial channel roughness, both in laboratory flumes . . . and natural streams To the present time, this effect has not been well elucidated"

We ran four pairs of cantilevered outlet scour tests at different discharges during the period May 1972 to April 1973. Test conditions were the same for each pair except for temperature. The temperature difference in each pair ranged from 9 to 20° Celsius. We compared depth of scour, volume of scour, and the irregularity of the contours (which indicated the presence of dunes in the scour hole). Many of the differences were so small that they were masked by normal experimental randomness. Our conclusion was that temperature *probably* affects the scour, but differently at different discharges.

In view of the uncertainty of the effect of temperature on scour and the large temperature changes that could be expected if we used water taken directly from the Mississippi River in the cantilevered outlet experiments, we decided to control the temperature at a constant 20° Celsius.

Water Turbidity

At the St. Anthony Falls Hydraulic Laboratory, the clearest river water and smallest temperature fluctuations occur during the winter. With spring ice breakup and snowmelt flows, there is an increase in the flow of mud. Much of the mud is organic. Notes taken during run 46 show that the Mississippi River flow at St. Anthony Falls started to increase on April 8, 1970. On March 18 there is the note, "Entire bed has entrapped air. Small bubbles come out when bed is touched." Mud deposits in the channel were noted on April 15. Worm holes were noted in the mud on April 20. At the termination of the run on May 6 the surface was covered with a matted growth which resisted breakup.

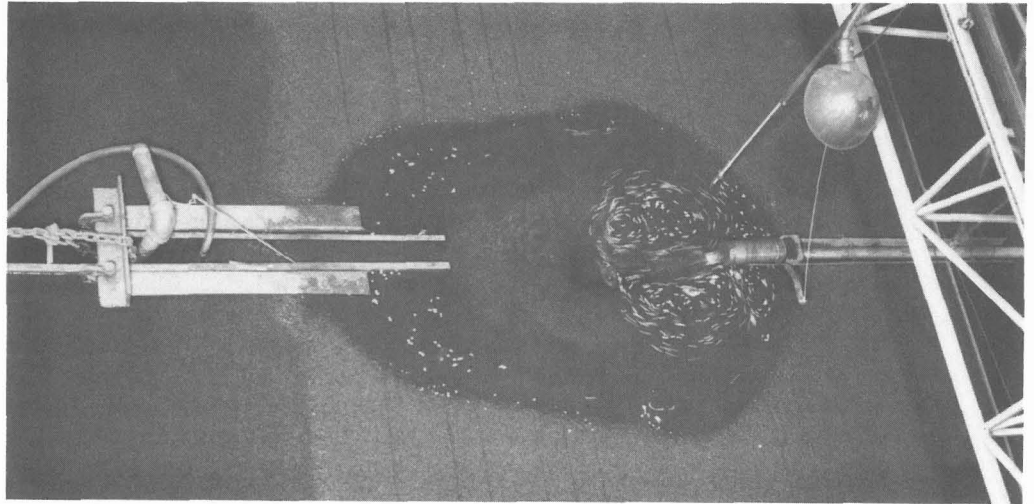


Figure IV-4

Confetti shows low velocity at periphery of scour hole. Mud is deposited on hole periphery and not where scour is still active at hole center after 10^5 minutes (69.4 days).

In figure IV-4, confetti shows circulation in the scour hole. Low velocity reverse currents at the periphery have permitted mud to deposit there, whereas no mud has deposited in the still active, after 69 days, bed where it is affected by jet turbulence. The mud deposit and area of still active bed is also shown in figure IV-3.

To eliminate problems of dirt, aquatic life plugging flow control valves, algal growth changing the bed material erosivity, and their effect on the scour process and progress, we decided to recirculate city water and continuously filter the water to prevent silt and organic matter contamination.

Test Duration

The tests were conducted by allowing scour to take place for increasing intervals and interrupting the scour process to measure its progress. The last scour interval--between 3,162 and 10,000 minutes--was 4.75 days, and the penultimate interval was 1.5 days. After the time-dependent tests, there was also the wait for removal of the bed material suspended by the flow in the scour hole. These could have been periods of inactivity or madework for the operator. We wanted to make better use of the operator's time and expedite the progress of the research. We did this by building two new experimental channels. Thus, while the operator was waiting for one experiment to end, another experiment was begun. This increased the utilization of the apparatus and the efficiency of the operation.

Main Floor Channels

With experience gained in using the turbine room channel, we designed and constructed two new channels especially adapted to the cantilevered outlet scour hole experiment. These channels were designed in 1972, built in 1973, and placed in operation in January 1974. They are identical and are shown in figure IV-5. The flow in the east channel, in the foreground, is from east to west whereas the flow in the west channel, in the background, is from west to east. The space between the two channels contains floodwater piping and operating machinery common to both channels.

The channels are 7 ft wide, the same width as the turbine room channel. Each channel is 20 ft long--sufficiently long to contain a sand bed with an eroded scour hole, a length of transport channel, and a pool upstream of a tailwater level control weir. The test channels are separated by a 5-ft space containing flooding and drainage control valves and piping as well as an eccentric operating mechanism, shown in figure IV-8, that drives the suction pipes shown in figure IV-9. A 5-ft extension of the rails upstream of each channel, shown in the foreground of figure IV-5, supports the cantilevered pipe and control valve carriage. The total length of the test channels and the filter installation, shown in figure IV-7, is about 56 ft. To prevent rust, the channels are lined with stainless steel, the reservoir is of asbestos cement pipe and concrete, the piping is copper and plastic, valves are brass, and all other parts are of nonrusting materials.

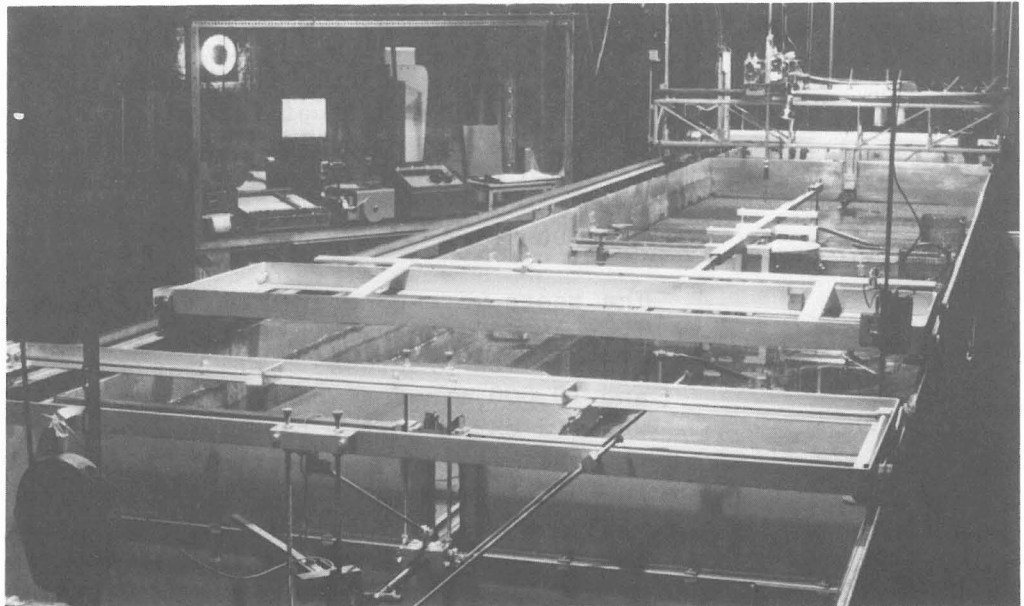


Figure IV-5
Main floor test channels.

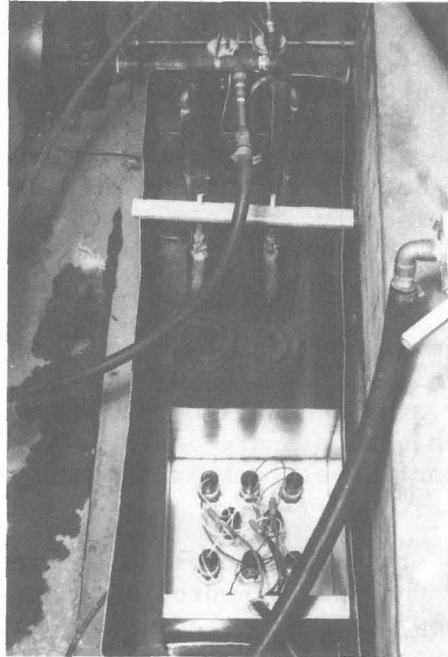


Figure IV-6
Temperature control tank.

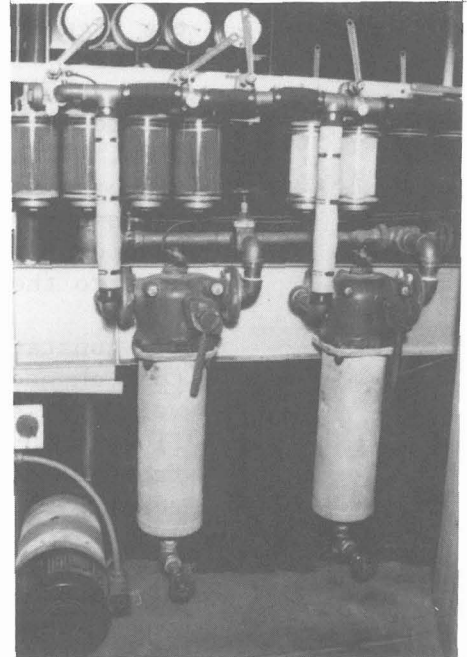


Figure IV-7
Pump, 70- and 10-micron filters,
valves, and pressure gauges.

The supply reservoir is under the channels. The reservoir consists of six 12-inch-diameter asbestos cement pipes encased in concrete and serves as the base for the test channels. Return flow from the channels and constant level tank overflow enters the 12-inch pipe under the right side of the channels shown in figure IV-5. Head boxes at each end are partitioned to divert flow to the adjacent pipe so that flow circulates throughout the reservoir. Flow leaves the reservoir through the 12-inch pipe on the left and enters a 12-inch vertical pipe sump. In the sump is a pump to supply service water for flooding the bed.

From the sump the water enters the temperature control tank shown in figure IV-6. In winter, cold river water circulates around the tank to slightly overcool the test water. The group of eight heaters in the foreground float in the tank to bring the test water to 20° Celsius. In summer, refrigerant passing through the coils at the far end of the tank corrects for the ambient heat and heat generated by the pump. The temperature is sensed in the supply line from the constant level tank just before the water enters the piping to the test channels. The signal goes to a proportional controller which operates the heater controls or refrigerant valves.

From the temperature control tank, the flow enters the pump shown in the lower left corner of figure IV-7. From the pump, the flow passes through one or both of the large 70-micron

filters and is discharged into the header shown at the top of the figure. The header supplies the four pairs of 10-micron filters. The valving is such that any combination or number of filters can be utilized, and filters can be taken out of service for replacement of the filter elements without interrupting the flow. Pressure gauges measure the pressure drop across the filters, and a buildup of pressure indicates when servicing is necessary. Ordinarily, a minimum number of 10-micron filters were used at any one time. From the 10-micron filters, the flow goes to the header which supplies the constant level tank.

The constant level tank is in the ceiling of the floor above the test channel. It can be pressurized with a cover plate and weighted lever arm if additional head is needed for the larger flows when both channels are operating at capacity. Overflow from the constant level tank is returned to the supply reservoir.

The supply line to each channel is a 1-inch copper pipe. Flow is measured by the pressure drop across an elbow in the supply pipe. The elbow was calibrated using differential manometers containing, depending on the pressure difference, Meriam No. 3 fluid or carbon tetrachloride. The calibration indicates the precision of the elbow meters to be within $\pm 2\%$.

From the flow control valve, a hose leads to the three-way valve shown in the center near foreground of figure IV-5. From the three-way valve, a 1-inch copper pipe enters a slot in the upstream end of each test channel. This is the cantilevered pipe. From the side of the three-way valve, a hose leads to a pipe through the channel headwall. This pipe allows the flow to bypass to the tailwater pool at the beginning and end of the run. The bypass line for the west channel can be seen in figure IV-9 at the far side of the channel.

The three-way valve and cantilevered pipe are adjustable in height and slope, and are braced in position. The supports are attached to a movable carriage which is locked in position during a test. The carriage can be moved upstream to move the pipe out of the way during bed preparation and measurement. The opposite end of the far channel in figure IV-5 is identical.

A second carriage rests just beyond the cantilever support carriage. This carriage traverses both channels. On it rests a screed for leveling the sand bed. This carriage also supports an auxiliary point gauge. All carriages are guided by a cable system that ensures their remaining correctly oriented with respect to the channel axis.

Beyond the screed carriage in figure IV-5 is a circular plate. This is the eccentric and its operating mechanism shown in figure IV-8. The eccentric is driven by an electric motor

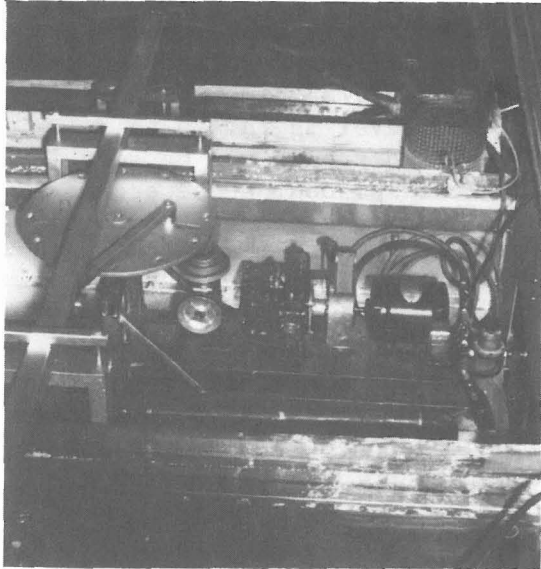


Figure IV-8
Eccentric and variable speed drive
for oscillating suction pipe
support arm.

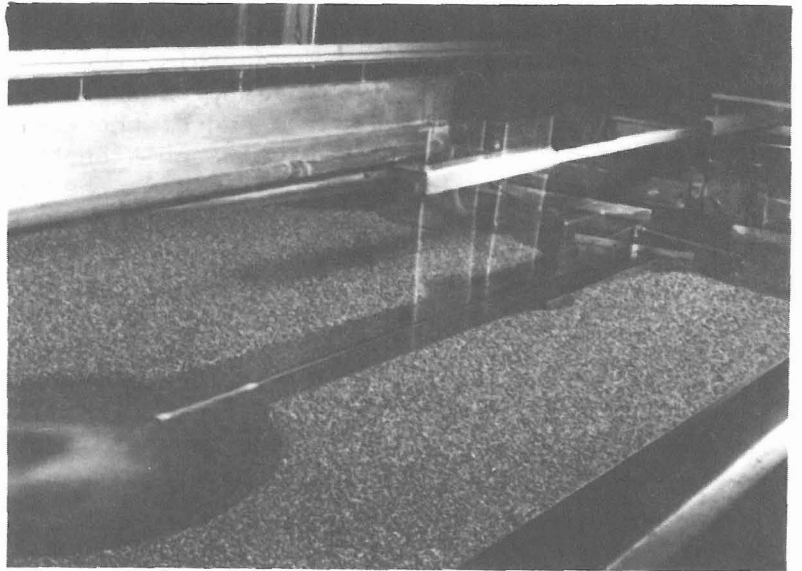


Figure IV-9
Extreme oscillations of suction pipe.

through a hydraulic speed controller and V-belt so its speed can be adjusted. The eccentric drives the longitudinal arms at the center of the channels. These arms oscillate longitudinally and support the suction pipe shown in figure IV-9. The height of the suction pipe can be adjusted so it just clears the bed of the preshaped channel in the bed. Figure IV-9 is a double exposure photograph: The tip of the suction pipe has aluminum paint to show its extreme positions, which can be varied by adjusting the eccentric arm. The position of the end of the oscillating arm is also adjustable. An aspirator at the far end of the suction pipe provides the suction, which can be adjusted by a flow control valve. The aspirator pump takes water from the tailwater pool and the aspirator discharges into the tailwater pool, so there is no change in pool level.

The suction pipe is used to pick up sand eroded from the scour hole and deposited along the entrance to the preformed channel. It was necessary to keep the channel entrance clean and prevent a deposit that would change the tailwater depth in the scour hole. Because this deposit takes place along a length of the preformed channel, an oscillating suction intake was required to pick up the deposit. This device proved completely successful and was used for all of the tests used in the data analysis.

The tailwater level is controlled by an adjustable-height triangular weir. Overflow water discharges into a collection trough and falls into the storage reservoir.

The bed has to be flooded when the bed level measurements are made. To do this, the exit from the tailwater collection trough is plugged and water is fed from the service pump to the downstream end of the test bed. The level is raised to a skimming weir and trough. One weir and trough can be seen in figure IV-5: it is the line that crosses behind the eccentric. The trough is lined with copper screen to catch the confetti used when photographing the flow pattern near the end of each run. From the skimming trough, the excess flow is returned to the reservoir.

The bed material is supported on screens above the channel bottom. This is to facilitate draining the scour hole through the sand bed so that it can be photographed, and to facilitate refilling the scour hole in preparation for the next scour period.

Data Acquisition Apparatus

The data acquisition apparatus is shown in figure IV-5. It includes the bridge at the far end of the channels and the equipment supported by the bridge, and the equipment on the table in the left background.

The bridge and its equipment are shown in figure IV-10. The bridge is supported by L-rails mounted on the channel walls, and the instrument platform on the bridge is supported by transverse cylindrical rails. Both the longitudinal (X) and transverse (Y) motions are motorized and are controlled manually through the handheld control box resting in its cradle at the upper left.

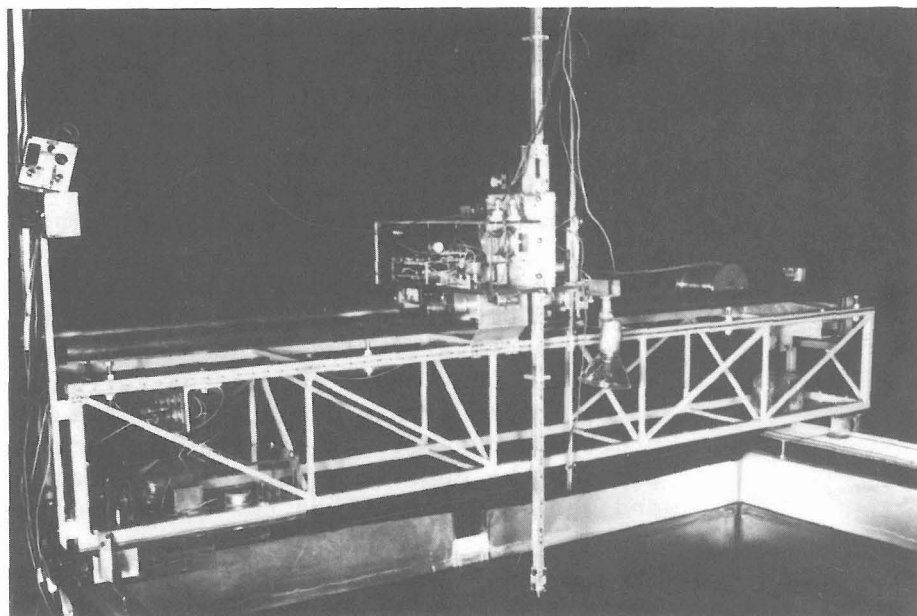


Figure IV-10
Probe bridge and equipment.

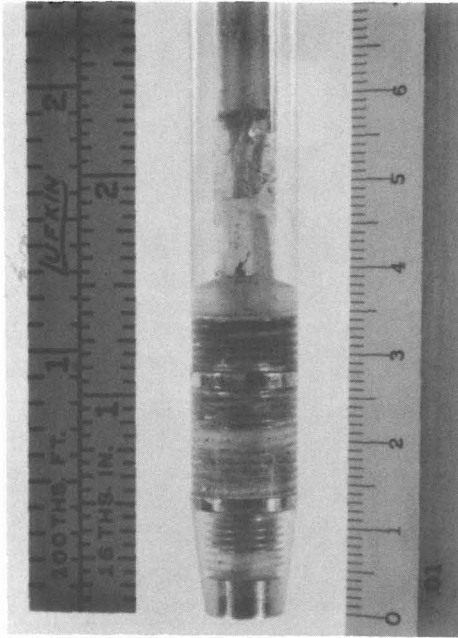


Figure IV-11
Bed level probe.

The vertical (Z) motion is controlled automatically by circuitry which maintains the probe tip at a fixed distance above the submerged sand bed. The electrical conductivity probe, which has been described by Blaisdell (1971), is shown in figure IV-11. It operates on the principle of a Wheatstone bridge. The conductivity across the two ring electrodes, an arm of the Wheatstone bridge, is a measure of the water conductivity. The conductivity between the bottom ring electrode and the button on the probe tip, another arm of the Wheatstone bridge, is affected by the proximity of the bed. The unbalance is sensed and is corrected by a motor which raises or lowers the probe. As a result, the probe follows the vertical profile of the bed as it is traversed, under manual control, across the bed.

All three coordinates of the probe tip were read by mechanical encoders until metal fatigue caused the mechanical encoder fingers to break with increasing frequency. The mechanical encoders were then replaced by optical encoders. The operator initiates each reading as the bed is traversed. At each press of a button on the handheld speed and direction control box, the X-Y-Z coordinates of the probe tip are read by stepping switches and recorded on punched paper tape. In figure IV-12, the control box at the right contains the stepping switches. The tape punch is at the left of the control box. The control box panel is shown in figure IV-13. On the panel are power and function selection switches; run, year, day, and minute dials as well as a button to read this dialed information onto the punched paper tape; and a keyboard to enter supplemental information onto the tape.

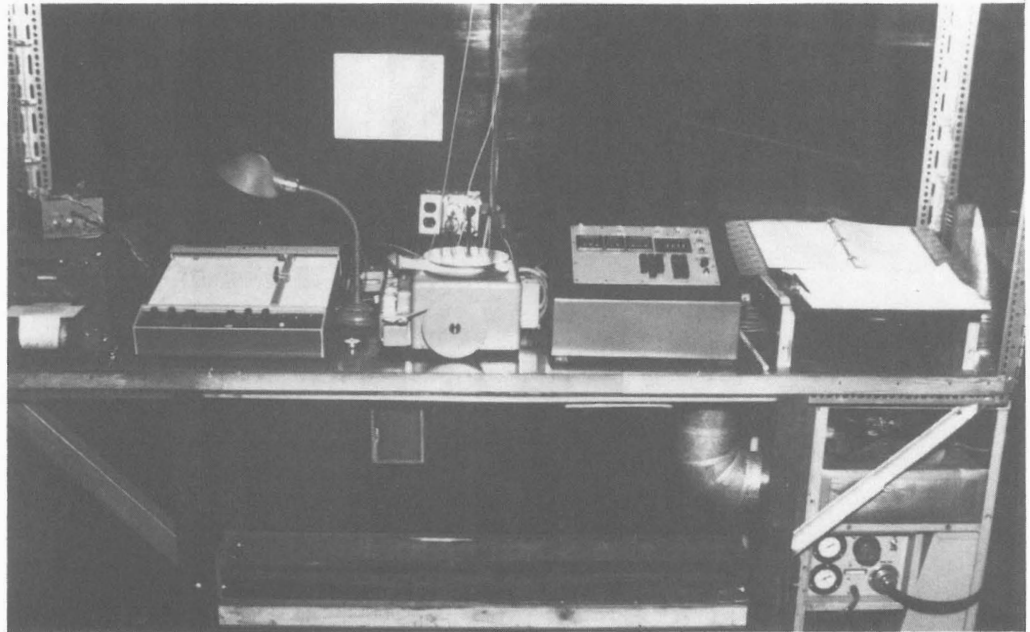


Figure IV-12
Event recorder, X-Y recorder, paper tape punch,
control box, and dehumidifier.

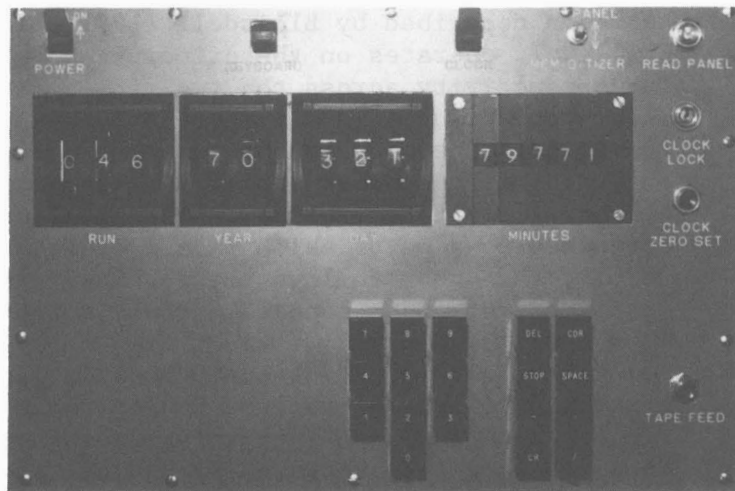


Figure IV-13
Control box panel.

To the left of the punch in figure IV-12 is an X-Y recorder. It is used to simultaneously plot longitudinal (X-Z) and transverse (Y-Z) profiles of the bed being recorded on punched paper tape. The X-Y recorder is driven by potentiometers geared to each of the three coordinates.

At the left end of the instrument table is an event recorder. At the time either three-way valve is operated to turn the flow on or off, the identity of the valve (east or west) and the time are recorded on paper tape.

A dehumidifier is shown in figure IV-12 under the right end of the instrument table. When the instruments are not in use, they are enclosed and the cabinet is pressurized with filtered, dehumidified air.

In addition to the equipment mentioned, an electrical point gauge is supported by the instrument platform. This point gauge, shown in figure IV-10, is used to set and/or read the water level in the scour hole.

Bed Material

The bed material is an important element of the experimental apparatus. Scour of the bed material defines the erosion pattern and the form of the plunge pool. For a stable hole, presumably the scouring or tractive forces are uniform over the entire surface, and the bed material defines this surface. And the size of the scour hole is determined by the resistivity of the bed material, which is measured by its critical tractive force. All of the conclusions and recommendations emanating from this study are based on measurements of the bed material properties and the scour.

To ensure a uniform resistance to scour, all grains should be the same size. Since we used natural sands, our bed materials could not be of uniform size, but the size range should be so small that the bed material would act as if its size were uniform. For absolutely uniform bed material, the geometric standard deviation of sizes σ is 1. However, the practical limit of σ for natural sands, where there is a range of sizes, is 1.10. Little and Mayer (1972, 1976) have shown that for σ less than 1.3 the bed material acts as if it were uniform. Therefore, we prepared our bed materials to meet Little and Mayer's criterion.

We needed a range of uniform sizes to evaluate the effect of bed material size on the scour hole or plunge pool dimensions. We selected 0.5, 1, 2, 4 and 8 mm as the target sizes of uniformly graded bed materials. In addition, to study the effect of armoring, we mixed sands to obtain two larger values of σ having the same $d_{50} = 2$ mm.

All bed materials of the desired sizes were prepared and stored before the tests began. Sieving required two summers because, to ensure accurate sizing, the sand had to be fed to the gently sloping vibrating screens at a very low rate. To secure the needed quantities of each size, 55 tons of commercial sand was sieved.

Five uniform sizes of bed material and two mixtures were prepared. The intended mean, or nominal, size d_{50} and the sieve opening sizes bounding the range of each desired size are given in table IV-1. Also given are the achieved properties of the sands used during the tests.

The size distribution analyses of the bed materials are given in table IV-2 and are plotted on logarithmic probability paper in figure IV-14. The advantage of using logarithmic probability paper is that the distribution of sizes will be a straight line if the distribution is log-normal. Also, the geometric standard deviation of sizes σ can be determined from the $d_{84.1}$, d_{50} and $d_{15.9}$ sizes by the relationships

$$\sigma = \frac{d_{84.1}}{d_{50}} = \frac{d_{50}}{d_{15.9}} = \sqrt{\frac{d_{84.1}}{d_{15.9}}} \quad (\text{IV-1})$$

For additional information on the size-frequency distribution of sediments, see Vanoni (1975, subsec. 15, pp. 36-38).

The specific gravity of the sands was 2.72. However, during the tests some parts of the bottoms of the scour holes were lined with a one- or two-grain layer of magnetic black sand having a specific gravity of 4.1. The magnetic material constituted about 2.6% of the 2-mm bed material.

Table IV-1
Bed material properties

Nominal d_{50} (mm)	Sieve range		Experimental	
	Number	Opening (mm)	d_{50} (mm)	σ
<u>Uniform bed materials</u>				
0.5	45	0.35	0.46	1.24
	25	0.71		
1	14	1.41	0.90	1.24
2	7	2.83	1.84	1.22
4	3-1/2	5.66	3.92	1.23
8	1/2 inch	12.7	7.65	1.26
<u>Graded bed materials</u>				
2	25	0.71	2.00	1.41
	3-1/2	5.66		
2	45	0.35	2.00	1.76
	1/2 inch	12.7		

Table IV-2
Bed material size analyses

Sieve		Mean size (mm)						
Size/No.	Opening (mm)	0.46	0.90	1.84	3.92	7.65	2.00	2.00
		Percent finer						
Size:								
1/2 in	12.7						94.5	
7/16 in	11.2						82.6	99.75
3/8 in	9.51						56.2	99.15
5/16 in	8.00							
No.:								
3	6.35						22.1	98.0
3-1/2	5.66				99.77	3.8	99.90	97.0
4	4.76				82.0	0.05	99.42	93.9
5	4.00				54.9	0.05	97.8	89.7
6	3.36			99.99	23.3	0.05	92.5	82.8
7	2.83			99.7	6.0		88.3	78.1
8	2.38			91.4	0.14		73.5	65.0
10	2.00			66.2	0.10		47.8	50.2
12	1.68			33.7			30.8	33.0
14	1.41		99.95	10.0			17.2	21.7
16	1.19		92.5	0.04			10.7	16.1
18	1.00		74.2				8.2	12.8
20	0.84		45.9				5.0	7.5
25	0.71	99.40	14.6				1.8	3.0
30	0.59	87.2	0.45					
35	0.50	57.0	0.01				0.11	0.15
45	0.350	33.5						0.08
60	0.250	10.1					0.07	
80	0.177	0.01						

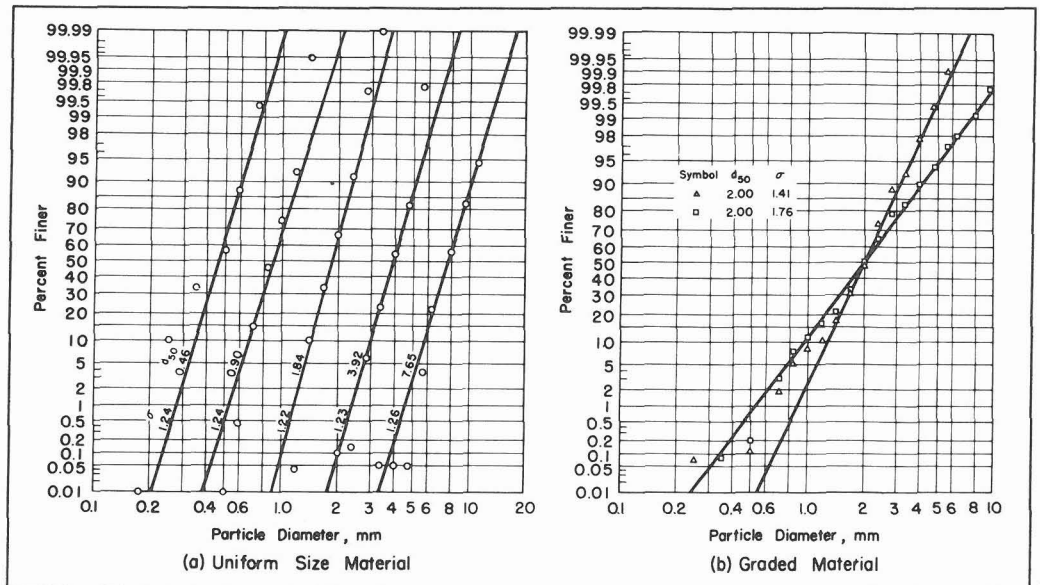


Figure IV-14
Bed material size analyses.

V. EXPERIMENTAL METHODS

There is some mention of the experimental methods in the preceding chapter describing the experimental apparatus. Those explanations are primarily to point out problems encountered during the early tests and to explain the reasons for those parts of the apparatus which we developed to overcome the problems. In this chapter, we will explain the methods we used to acquire the data used to develop the design criteria and equations presented herein.

Bed Preparation

Prior to starting a test, the transport channel was put in place and the bed was somewhat overfilled with the desired bed material. The bed was then flooded. Because the sand was loose and "quick," a tubular concrete vibrator was passed throughout the sand to compact the bed material. The bed was then drained and screeded.

To screed the bed surface, the cantilevered pipe and its carriage were first moved upstream out of the way. The screed carriage was moved to the upstream end of the test bed, and the screed, which is resting on the carriage in figure IV-5, was placed on the carriage cross rail. Stops on the screed supports determined the elevation of the screed bar, which was a half pipe diameter above the tailwater level. The screed carriage and bar were moved downstream along the channel to plane the bed material to an absolutely level surface. This process is shown in figure V-1.

The cantilevered outlet was then moved back into position, the screed bar moved to the end of the cantilevered pipe, and a channel template placed on the screed bar. The stop clamped to the bed screed bar was used to transversely position the channel screed template. This is shown in figure V-2. The channel template was used to screed an exit channel between the cantilevered pipe exit and the transport channel. The upstream end of the exit channel was shaped manually.

Starting a Test

The next step was to set the desired flow rate and bypass the flow to the tailwater pool. The adjustable tailwater level control weir shown at the right in figure IV-9 was set to give the correct tailwater level.

Before any erosion took place, the suction pipe was positioned in the screeded channel at an estimated correct elevation and longitudinal position, and the sand pump was placed in the transport channel. The aspirator pump and the oscillator for the suction were turned on, and the air flow for the sand pump was also turned on and adjusted.

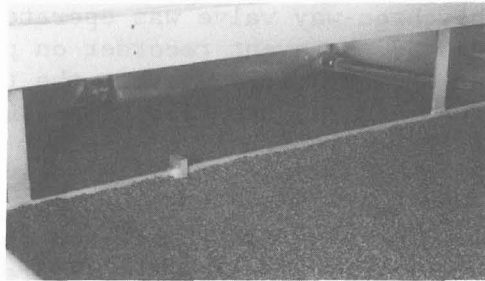


Figure V-1
Screed for leveling bed.

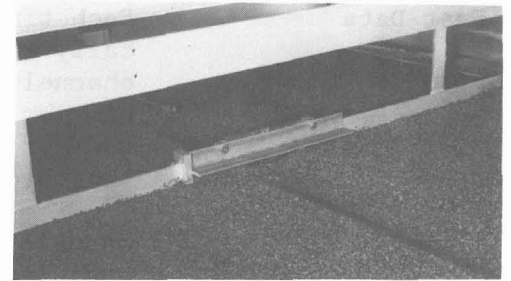


Figure V-2
Initial exit channel screed.

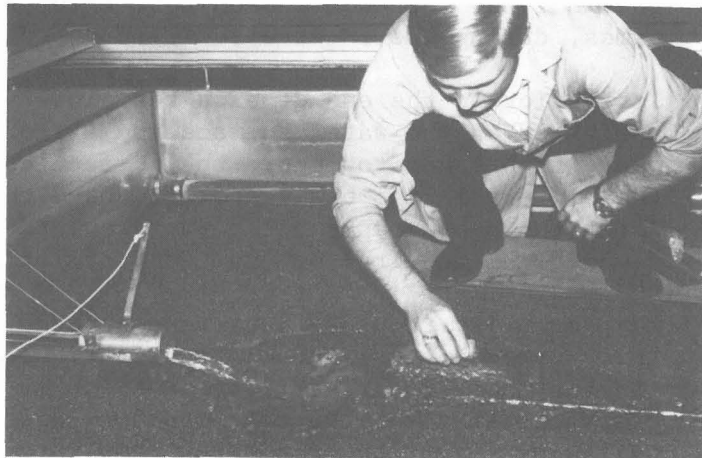


Figure V-3
Channel was manually
cleaned during initial
scour periods.

We digress to say that the scour was stopped and the scour hole was measured each $10^{n/2}$ min from the beginning of the scour period--half each logarithmic cycle in min--on the basis that the scour dimensions increase with logarithmic time. Here n is an integer. The timed measurements actually began at 10 min ($n = 2$) and ended at 10,000 min ($n = 8$).

The initial rate of scour was so rapid that scour periods shorter than 10 min produced holes whose measurements would be of questionable value. Also, the initial rate of erosion was so rapid that manual assistance was needed to keep the channel clear.

We stopped the flow after an initial scour period of $n = -2$ min (6 s) and manually cleaned the channel. This procedure was repeated for $n = -1$ (19 s), $n = 0$ (1 min), and $n = 1$ (3 min 10 s). As the scour period increased, it was also possible to manually clean the channel during the scouring interval. This is shown in figure V-3. The suction pipe, which was initially overwhelmed, was in operation throughout these initial scour periods ($-2 \leq n \leq 2$).

Test Data

Each time the three-way valve was operated, there was automatically recorded by the event recorder on paper tape (a) the test channel (east or west), (b) whether the test period was beginning or ending, and (c) the time. The sum of the elapsed times thus printed is the length of time scour had taken place--the length of the test.

Manually recorded on a data sheet were the date, the clock time and elapsed time, the elbow-meter differential-manometer flow readings, elevations to determine the clearance between the probe and the bed, the tailwater elevation, the water temperature, and appropriate remarks. This information was recorded routinely at the end of each test interval and, for longer test times, during the interval.

Just prior to the end of each test interval, confetti was sprinkled on the water surface and a short-time exposure photograph taken to record the surface currents. After each test interval, the bed was drained and the scour photographed. After the photographs had been taken, the bed was carefully flooded, as required by the bed profiler.

Then manually recorded data were entered on punched paper tape through the control panel shown in figure IV-13. Data included the run number, the year, the consecutive day of the year, the elapsed test time, the dimensionless discharge $Q/\sqrt{gD^5}$, the tailwater elevation, the water temperature, the probe displacement above the sand bed, the test basin (east or west), and the reference bench mark elevation. With this basic information on tape, the next step was to profile the bed.

The first profile was taken on the longitudinal center line. As the probe was traversed along the bed, a button on the handheld control box was pressed to record the X-Y-Z coordinates of the probe on punched paper tape. It was not necessary to stop the traverse to do this. These readings were taken frequently, and particularly before and after any change in the profile.

Simultaneously, a continuous center line profile was recorded by an X-Y recorder. This longitudinal profile was used to select the locations at which 20 or more cross sections would be profiled. Cross sections were taken at the beginning, deepest point and end of the scour hole, and at sufficient intermediate points that the scour hole dimensions could be computed accurately and reliable contours drawn. The maximum interval between cross sections was about 0.2 ft.

After the scour hole had been cross sectioned, the flooded bed was drained, the tailwater reestablished, and the flow again diverted to the scour hole to initiate the next scour interval.

Data Processing

The punched paper data tapes were first read by a Flexowriter to record the data on paper tape. These listings were then checked for consistency, and the tapes were corrected if necessary.

The punched paper tapes were then read by an optical reader and the data transferred onto magnetic tape. The magnetic tape and program decks were processed by the University of Minnesota Computer Center.

The output from the computer center was in two forms: printouts and graphs. Printouts included all of the initial identification data plus the pipe diameter, slope and height above the tailwater, and the bed material size and geometric standard deviation. Also printed out were the recorded X and Z data coordinates of the center line profile, and the recorded Y and Z data coordinates and X location of the deepest cross section profile.

Computed and printed were the scour hole maximum width and its location, the surface area, the volume, the minimum bed elevation and its X and Y coordinates, and other information initially thought desirable but not used in the analyses.

The graphical computer outputs were plots of the center line profiles, deepest cross section profiles, and a contour map of the scour hole. The contours were in terms of the maximum scour hole depth Z_m and were drawn at $0.2Z_m$ intervals. These three plots were primary sources of the data for analyzing the scour hole shape and location. A detailed explanation of the data acquisition for the plots and a detailed description of the plotting procedure and plot analysis are presented in the section "Dimensionless Contour Analysis" in chapter X.

VI. SCOURING PROCESS

The removal of bed material from the scour hole is initiated by the jet plunging through the water and striking the erodible bed. The bed material is first put into suspension. Some of the suspended material recirculates and is deposited in the hole to be picked up again later. Other suspended material is deposited on the downstream slope of the scour hole and is transported up the slope and out of the hole as bed load. If the deposit becomes too steep, the slope becomes unstable and sediment will slide back into the scour hole. However, when the jet is impinging on the bed, parts of the downstream slope can stand at an angle steeper than the angle of repose--nearly vertical sometimes--due to the force of the deflected jet. When the jet is turned off, this unstable downstream slope sloughs back into the scour hole and stabilizes at the angle of repose. Finally, some material placed in suspension by the jet will leave the scour hole in suspension and deposit in the downstream channel.

All these types of sediment entrainment and transport may occur during the development of the scour hole. Initially, the proportion of sand in the water will be very high, and the quantity of sand in motion will be relatively large. As the scour hole approaches its ultimate size, the proportion and quantity of sand in motion will be very low. Eventually, particles may move only infrequently when turbulent bursts strike the bed.

Scour Hole Shape

The scour hole shape changes with the discharge, with the length of time of scour, and with the amount of material suspended in the scour hole. Bed material size in itself does not change the shape.

Variation With Discharge

Photographs showing the scour hole after scour periods of 10,000 min (7 days) for each of six discharges are presented in figure VI-1. The invert of the cantilevered pipe is one pipe diameter above the tailwater surface ($Z_p/D = 1$) and the bed material diameter is 1.84 mm. Confetti and a short time exposure show the flow patterns.

In figure VI-1(a-b), the jet plunges to the bed and rebounds to the surface. The surface boil directs the confetti to the sides of the hole, and there is little or no surface circulation of the confetti. In figure VI-1(c) the scour hole has increased in size, the surface pattern has changed, and there is evidence of reverse flow along the periphery of the upstream half of the scour hole. In figure VI-1(d-f) the scour hole size progressively increases with the flow and the surface currents indicate rapid upstream flow along the sides of the hole. This upstream flow causes beaching, which will be discussed later in detail.

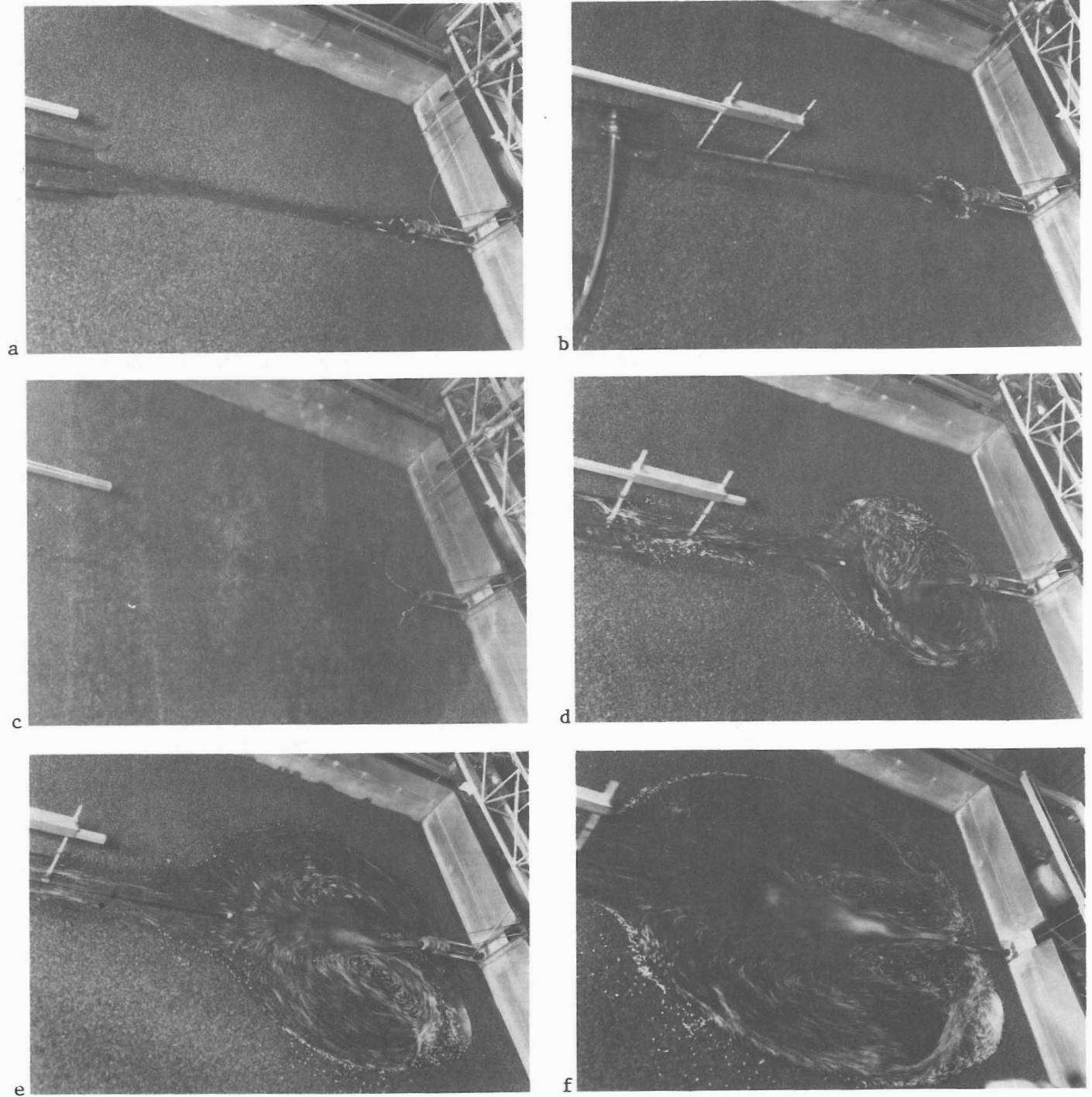


Figure VI-1
 Confetti and short time exposures show flow patterns after
 10,000 minutes (7 days) for six discharges, $Z_p/D = 1$, and $d_{50} =$
 1.84 mm: (a), $Q/\sqrt{gD^5} = 0.5$, run 147; (b), $Q/\sqrt{gD^5} = 1$, run 145;
 (c), $Q/\sqrt{gD^5} = 2$, run 143; (d), $Q/\sqrt{gD^5} = 3$, run 141; (e), $Q/\sqrt{gD^5}$
 = 4, run 139; (f), $Q/\sqrt{gD^5} = 5$, run 137.

The unsymmetrical flow in figure VI-1(d) is not unusual. Although the jet is directed to the left in this 10,000-min picture, the jet was centered or directed to the right at other time periods.

Beaching

In chapter X we determine a "beaching limit." This is the discharge at which the strengths of the reverse currents along the sides of the scour hole are sufficient to erode the bank material. Beach development is discussed below.

The scour holes in figure VI-1(a-c) have sides which stand at about the angle of repose of the bed material. Center line sections and cross sections at the deepest point of these scour holes are shown in figure VI-2(a-c). The contour map of the scour hole shown in figures VI-1(c) and VI-2(c) is presented in figure VI-3 and is typical of nonbeaching scour holes. The contour intervals are in terms of the maximum scour depth.

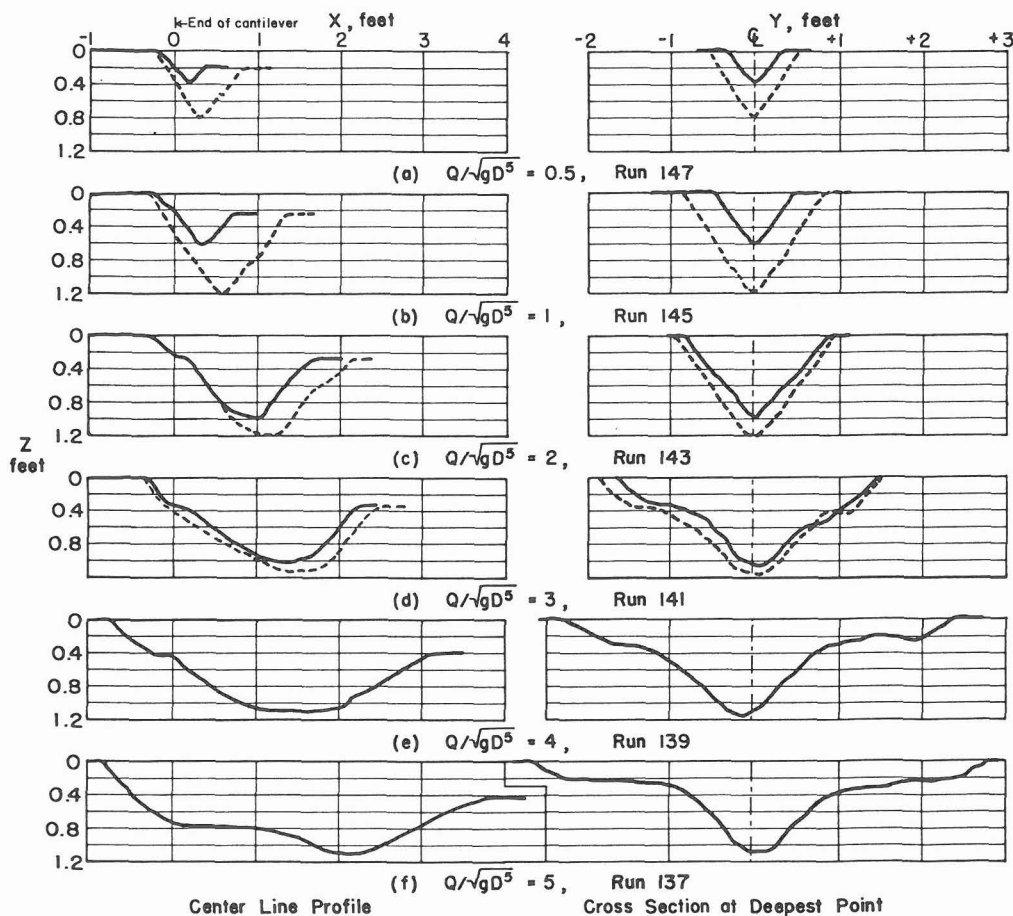


Figure VI-2
Center line profiles and cross sections at deepest point, for $Z_p/D = 1$, $d_{50} = 1.84$ mm, and $t = 10,000$ minutes: time-dependent tests —, suspended-material-removed tests ----.

The scour holes in figure VI-1(d-f) have an angle of repose shape at the bottom, but the side slope flattens and the holes widen near the surface. The widening is caused when the reverse surface currents are strong enough to erode the bank material. Cross sections of these holes are shown in figure VI-2(d-f). The gently sloping surfaces near the scour hole surface we call beaches, and the process of their development we call beaching. The contour map of the scour hole shown in figure IV-1(d) is presented in figure VI-4 and is typical of beached scour holes. The upstream currents on the sides of the beached scour holes are strong enough to transport bed material upstream. The irregular contours on the beaches represent dunes. This transported material eventually reaches the upstream end of the scour hole and is again transported downstream.

This beaching and excessive widening of the scour hole at the surface are, we feel, unacceptable. Therefore, after we had determined the beaching limit, we discontinued testing discharges which exceeded that limit. Furthermore, no attempt was made to develop equations to define the shape of the beached scour holes: our efforts were devoted only to analyzing the nonbeached scour holes.

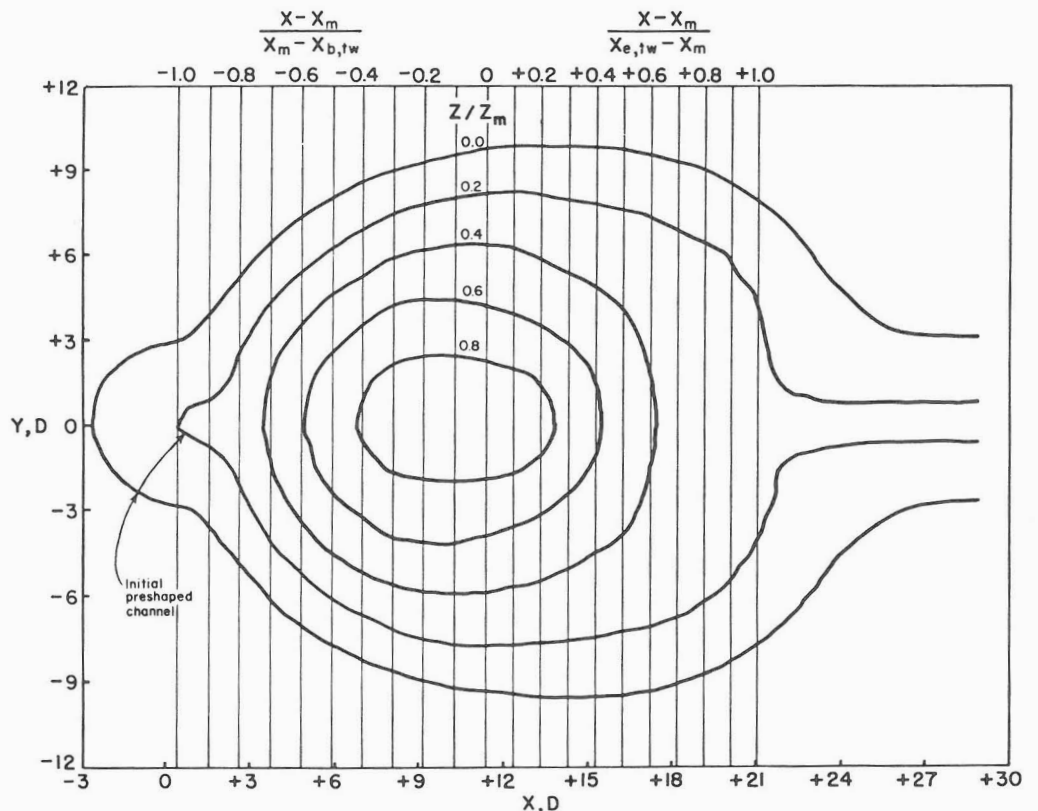


Figure VI-3
Contour plot of run 143, for $Q/\sqrt{gD^5} = 2$, $Z_p/D = 1$, $d_{50} = 1.84$ mm, and $t = 10,000$ minutes.

Suspended-Material-Removed Tests

Material was still suspended in the scour hole at the end of the time-dependent tests, which were usually terminated after 10,000 min. When the flow was diverted to make bed measurements, the suspended material settled out and filled in the bottom of the scour hole. Therefore, the time-dependent measurements did not measure the disturbed depth of the hole.

After the completion of the time-dependent tests, flow was resumed and the suction pipe was extended into the scour hole to remove the suspended material. (Because the suspended-material-removed tests were initiated after the beginning of the test program, they were sometimes run independently of the time-dependent tests.) These suspended-material-removed tests produced scour holes of maximum depth. The resulting scour hole cross section was triangular, with the apex of the triangle well defined. Center line sections and cross sections at the deepest point for the suspended-material-removed tests have been added to figure VI-2(a-d) as dashed lines to show the differences.

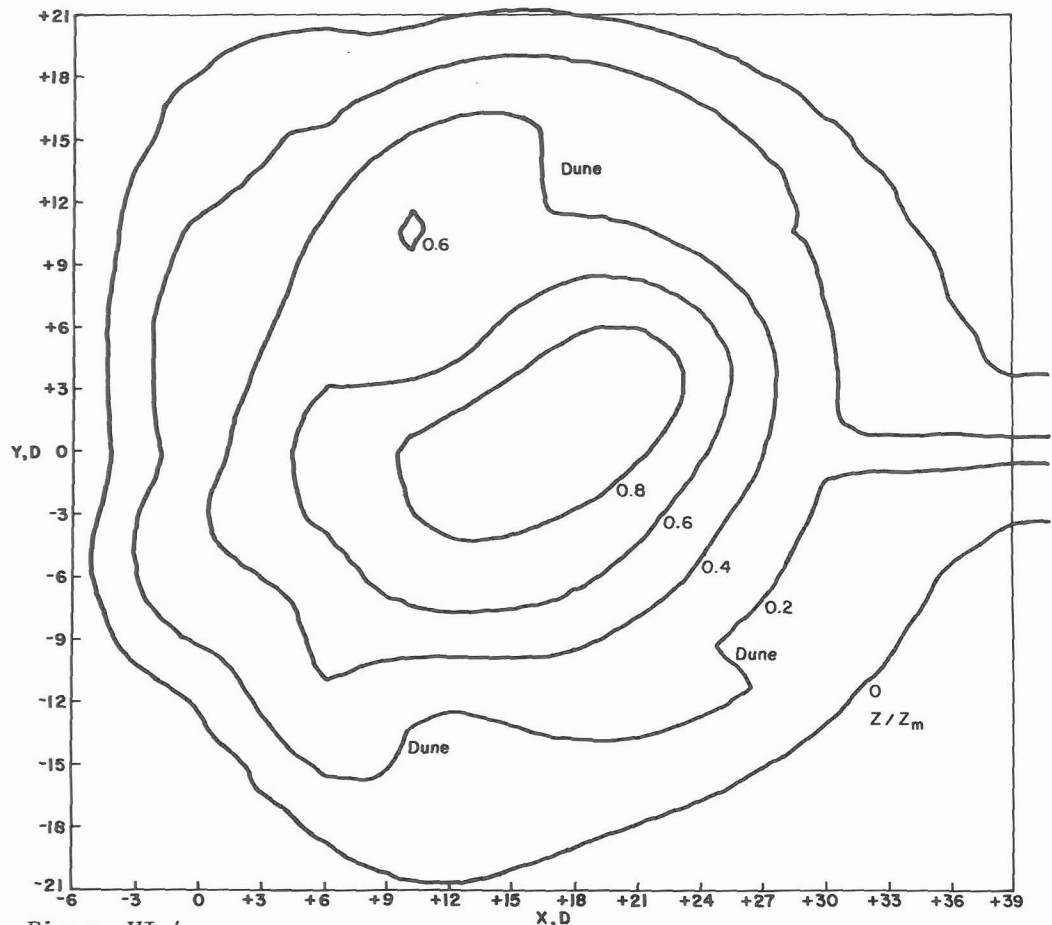


Figure VI-4
Contour plot of run 141, for $Q/\sqrt{gD^5} = 3$, $Z_p/D = 1$, $d_{50} = 1.84$ mm, and $t = 10,000$ minutes.

Progression With Time

The progression of the maximum depth of scour with time is shown in figure VI-5 for the runs discussed in this chapter. It is obvious that the depth--and presumably the other scour hole dimensions--increase exponentially with time. This finding is in agreement with the findings of others.

The time development of scour is discussed in detail in the following chapter.

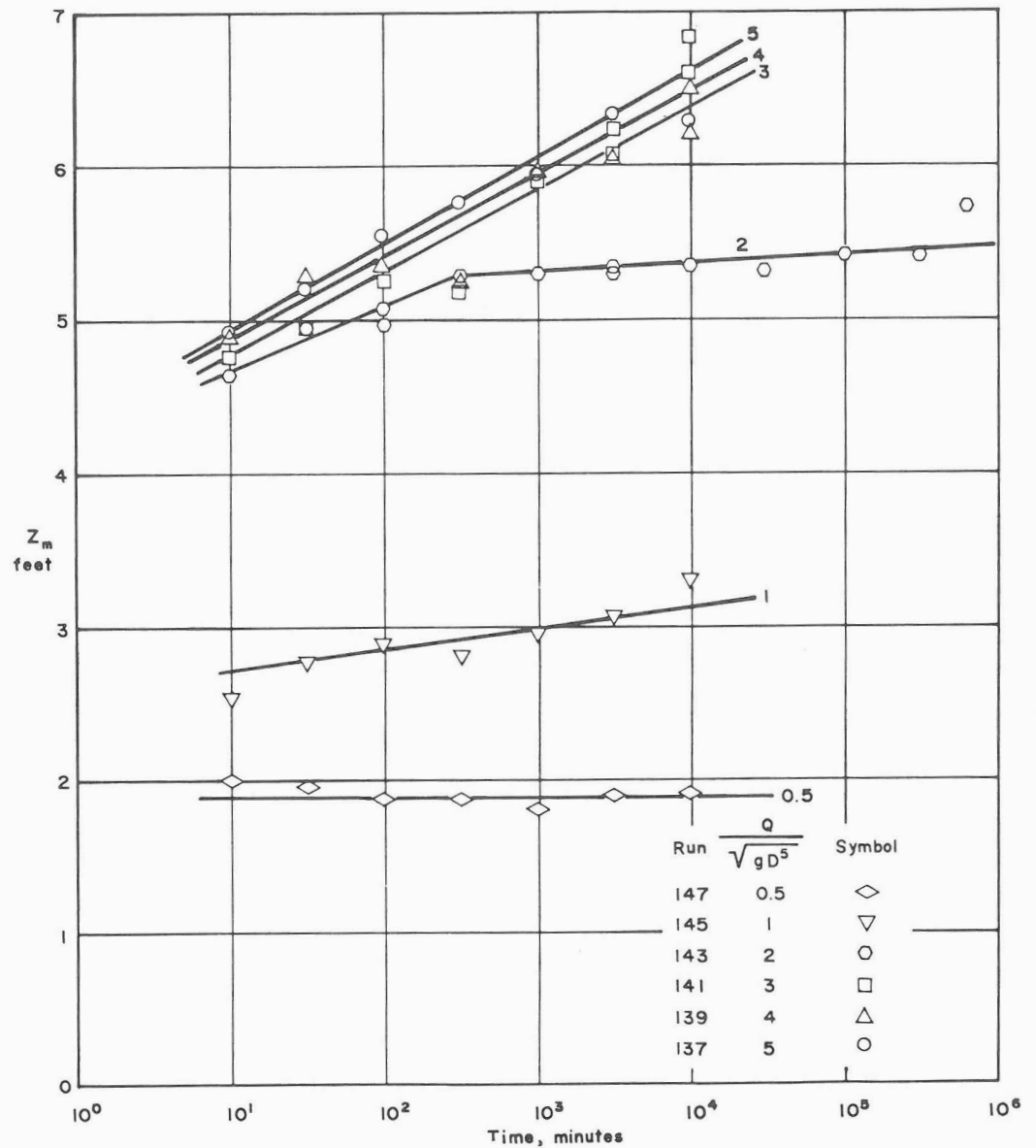


Figure VI-5
Progression of maximum scour depth with time, for $Z_p/D = 1$, and $d_{50} = 1.84$ mm.

Repeatability of Tests

The precision of scour tests is generally less than that of many other hydraulic tests. An indication of the precision of these tests can be gained from three tests that were repeated because flow disturbances damaged the scour hole before all the time interval tests had been completed.

Run 135 ($Q/\sqrt{gD^5} = 5$, $Z_p/D = 1$, $d_{50} = 1.84$ mm) was terminated after 1,000 min because a clogged screen in the exit channel caused the bed to flood. The test was repeated as run 137, shown in figures VI-1(f) and VI-2(f). Comparable data for the measurements at 1,000 min are:

<u>Run</u>	<u>135</u>	<u>137</u>	<u>137/135</u>
Minimum bed elevation	-5.98D	-5.97D	1.00
at X =	24.94D	25.92D	1.04
Maximum width	59.31D	56.99D	0.96
at X =	25.30D	22.92D	0.91
Surface area, ft ²	20.72	19.99	0.96
Volume, ft ³	2.97	2.87	0.97

This is a beached scour hole, and the horizontal dimensions are relatively large. Since $D = 1$ inch, the actual agreement is very good. The relative agreement is within about 4%.

Run 121 ($Q/\sqrt{gD^5} = 5$, $Z_p/D = 0$, $d_{50} = 1.84$ mm) was terminated after 3,162 min because the bed was damaged by flow from a broken hose. The test was repeated as run 123. The comparative tests results at 3,162 min are:

<u>Run</u>	<u>121</u>	<u>123</u>	<u>123/121</u>
Minimum bed elevation	-5.56D	-5.59D	1.01
at X =	23.23D	23.28D	1.00
Maximum width	53.21D	59.46D	1.12
at X =	20.84D	26.44D	1.27
Surface area, ft ²	22.90	23.35	1.02
Volume, ft ³	3.94	3.33	0.85

This again is a beached scour hole. The agreement is excellent for some of the dimensions and not as good for others.

Run 162 ($Q/\sqrt{gD^5} = 2$, $Z_p/D = 0$, $d_{50} = 1.84$ mm, $S = 47.3$) was terminated after 3,162 min because the filters clogged and reduced the flow. The test was repeated as run 164. There were no beaches for these runs, which are compared for $t = 3,162$ min:

<u>Run</u>	<u>162</u>	<u>164</u>	<u>164/162</u>
Minimum bed elevation	-4.47D	-5.01D	1.12
at X =	6.35D	6.87D	1.08
Maximum width	14.67D	17.06D	1.16
at X =	7.46D	7.94D	1.06
Surface area, ft ²	1.50	1.94	1.29
Volume, ft ³	0.209	0.282	1.35

These percentage differences are larger than those cited for the two other repeated tests.

These comparisons give some idea of the repeatability of scour measurements when careful attention is given to controllable variables.

Prototype Similarity

Field trips with SCS personnel have allowed us to observe many field scour holes. Some of these will be cited to show that the scour patterns observed in the laboratory also exist in the field.

Most cantilevered outlets discharge onto cohesive soils. The resulting scour hole banks are frequently vertical or nearly so. Figure VI-6 illustrates this condition. Because we used non-cohesive bed material, our banks stood at the angle of repose.

We have seen two cantilevered outlets that discharge onto sandy soils. They have widened excessively and show the beaching characteristics described earlier. Figure VI-7 shows one of these scour holes, the periphery of which has now been stabilized with riprap. The path of the jet is shown by the air entrained flow. The darker area on either side and downstream of the air entrained flow represents the deep part of the scour hole. The beaches are outside the deep pool; and in the color slide from which this figure was prepared, the beaches are tan-colored sand. In figure VI-8 the end of the deep pool is at the left center. Nearer is the inner edge of the beach and the deposit, which defines the boundary between the upstream and



Figure VI-6
Scour hole at structure No. 1, North Broad River, GA.



Figure VI-7
Scour hole at structure No. 44, Middle Broad River, GA.

downstream currents shown in figure VI-1(e-f). Outside this deposit the erosion by the upstream currents has increased the flow depth, as shown in figure VI-9.

A preshaped pool was provided for a cantilevered outlet in sandy soil at the Cotile Reservoir, Bayou Rapides Watershed, Rapides Parish, LA. Erosion had greatly enlarged the pool, after which the banks were sloped and riprapped as shown in figure VI-10.

The aforementioned two field structures had experienced the same type of beaching we observed during our cantilevered outlet scour studies. As a result of our studies, such excessive enlargement can be anticipated and the plunge pool designed with adequate riprap protection.



Figure VI-8
 Junction of deep pool and beach at downstream end of scour hole shown in figure VI-7.

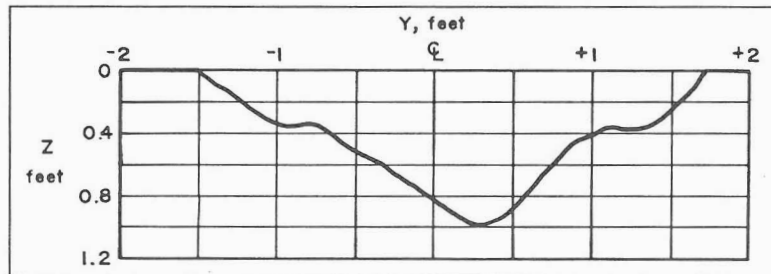


Figure VI-9
 Cross section located 6.4D downstream of cross section in figure VI-2(d) and showing erosion at edge of beach.



Figure VI-10
 Riprapped banks prevent further enlargement of scour hole at Cotile Reservoir's 54-inch-diameter drainage structure in Bayou Rapides Watershed, Rapides Parish, LA.

VII. TIME DEVELOPMENT OF SCOUR

Reference should be made to Blaisdell et al. (1981) for a detailed discussion of the time development of scour and the ultimate scour dimensions. However, pertinent points from that paper as they apply to the present analysis will be summarized here.

Among Laursen's (1952) four general characteristics of local scour, presented in chapter II under "General Principles," the last three are pertinent to the progression of scour: (2) the rate of scour will decrease as the flow section is enlarged, (3) there is a limiting extent of scour, and (4) this limit is approached asymptotically. Also presented in chapter II, under "Rate of Scour," are Anderson's (Vanoni 1975, pp. 50-52) comments on the several different functions that, instead of a single function, describe the progression of scour. For all of the functions mentioned, the scour increases with time and without limit. A typical semilogarithmic plot of progression of scour for a range of discharges is shown in figure VI-5. Mentioned under the same heading is Thomas' (1971) theoretical equation that has the exponential form

$$V_{Z_m} = \frac{a}{bt} \quad (\text{VII-1})$$

where $V_{Z_m} = Z_m/t$ is the average velocity by which the scour depth increases, Z_m is the maximum scour depth, t is the elapsed scour time, and a and b are constants.

Because the functions mentioned by Anderson and Thomas do not approach an asymptotic limit, the equations indicate that scour will increase without limit and, thus, do not conform to Laursen's fourth characteristic. To circumvent this difficulty, Blaisdell et al. (1981) used Thomas' velocity of scour idea to develop a hyperbolic logarithmic velocity-of-scour method of plotting the data. The method, which allows the scour progress to be defined and the asymptotic (ultimate) depth of scour to be computed, was used for the analyses presented in this report. To explain this method and its use, we quote, with changes in symbols and figure and equation numbering, from the section "Hyperbolic Logarithmic Velocity-of-Scour Method" in Blaisdell et al. (1981):

To define the relationship between the logarithm of the average velocity of scour and the logarithm of time, the writers looked for a mathematical curve having a shape similar to the experimental curves of Thomas' plots of $\log V_{Z_m}$ versus $\log t$, and having an asymptote from which the ultimate depth of scour could be computed. Such a curve is a limb of a vertically-oriented hyperbola with the origin of the hyperbola offset on the y-axis.

The general form for the equation for the hyperbola shown in Fig. VII-1 is

$$\frac{(y - y_0)^2}{A^2} - \frac{x^2}{B^2} = 1 \quad (\text{VII-2})$$

in which A = the semitransverse axis; and B = the semiconjugate axis of the hyperbola. We have defined y and x in dimensionless units when applying Eq. VII-2 to data from our research on scour at cantilevered pipe spillway or culvert outlets. Our definitions of y and x are:

$$y = \log \frac{Z_m/D_p}{V_{p1}t/D_p} = \log \frac{Z_m}{D_p} - \log \frac{V_{p1}t}{D_p} \quad (\text{VII-3})$$

$$x = \log \frac{V_{p1}t}{D_p} \quad (\text{VII-4})$$

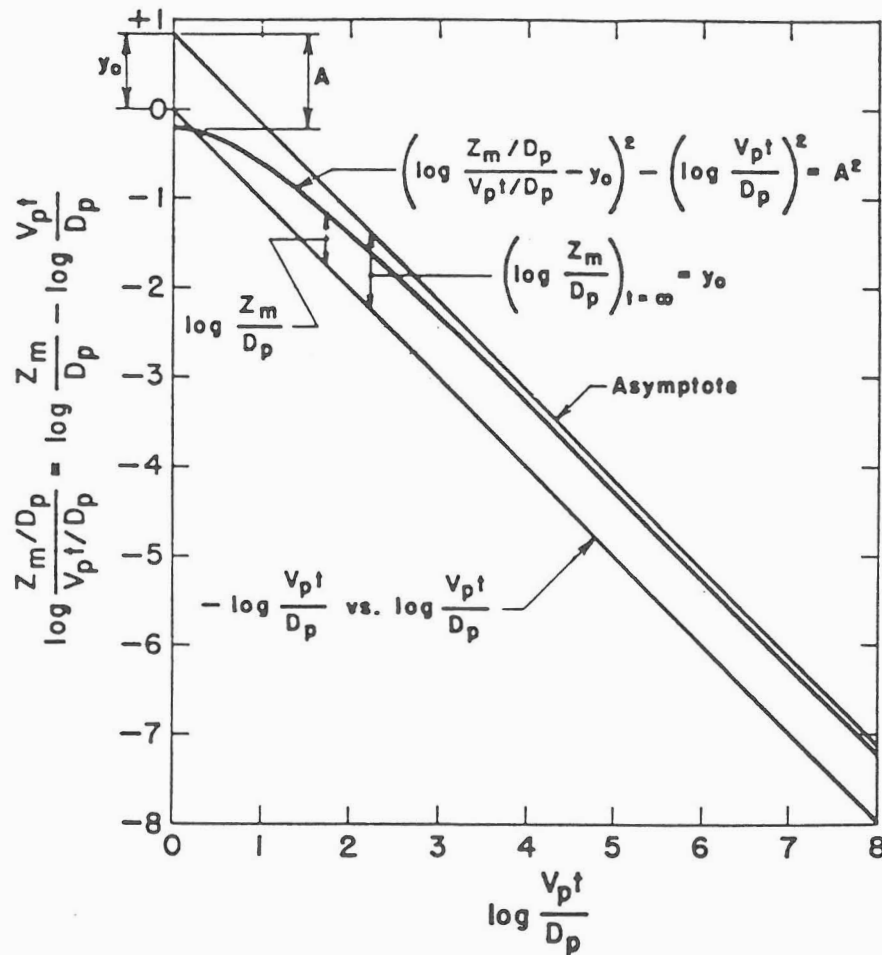


Figure VII-1
General form of the hyperbola.

in which Z_m = the maximum depth of scour measured from the tailwater surface; V_p and D_p = the jet velocity and diameter at the point where the jet plunges into the tailwater surface; and t = the time from the beginning of scour. Because $\log V_p t/D_p$ appears on both axes, the hyperbola is rectangular, $A = B$, Eq. VII-2 becomes

$$(y - y_0)^2 - x^2 = A^2 \quad (\text{VII-5})$$

and

$$A = \sqrt{(y - y_0)^2 - x^2} \quad (\text{VII-6})$$

The writers have evaluated A by assuming values for y_0 and using experimental values y and x to compute A . The best value of A is that value for which the standard error of estimate, σ , is a minimum. The procedure we used is:

1. Plot experimental values of y and x and estimate the asymptote. Extrapolate the asymptote to $x = 0$. The distance on the y -axis between the origin and the asymptote at $x = 0$ is an initial value of y_0 .
2. Use the data to compute values of A . (A should be a constant.)
3. Compute the standard error, σ , of A .
4. Assume another value of y_0 and repeat steps 2 and 3.
5. Repeat step 4 until the minimum value of σ is found. (The best fit values of y_0 and A are those for which σ is a minimum.)
6. Compute $Z_m/D_p = \text{antilog } y_0$. (This is the asymptotic value of Z_m/D_p --the value of Z_m/D_p at $t = \infty$.)

Fig. VII-2 is a typical plot of data obtained by the writers. There it will be noted that the data, which covers scour periods ranging from 600 sec ($\log V_p t/D_p = 4.60$) to 1.90×10^7 sec ($\log V_p t/D_p = 9.10$) by 0.5 increments of the logarithm plus a scour period of 3.74×10^7 sec ($\log V_p t/D_p = 9.40$), are far to the right of $x = 0$ and approach the asymptote of the hyperbola. The equation of the hyperbola of best fit is

$$(y - 0.844)^2 - x^2 = (1.0641)^2 \quad (\text{VII-7})$$

and the ultimate or asymptotic value of the scour depth is

$$\frac{Z_m}{D_p} = \text{antilog } y_0 = \text{antilog } 0.844 = 6.98 \quad (\text{VII-8})$$

(Experimental data for the 3.74×10^7 sec scour period did not become available until after Eq. VII-7 had been evaluated. However, this omission affects only the numerical values in Eq. VII-7. The omission of the last data point does not affect the sense of the hyperbolic logarithmic velocity-of-scour analytical method)

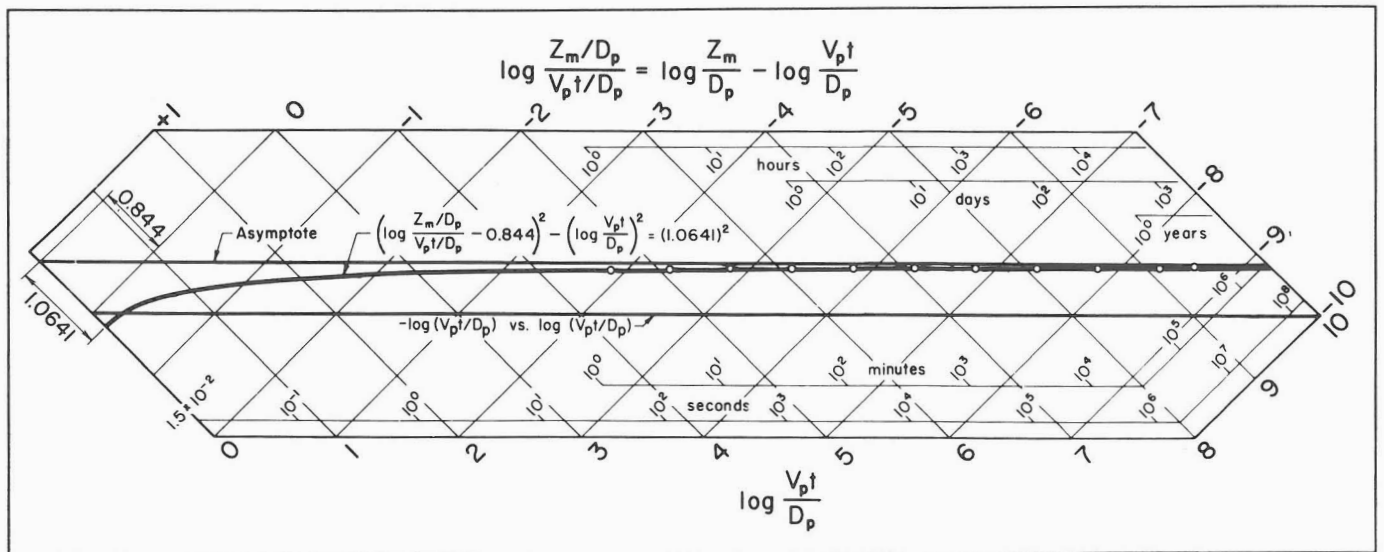


Figure VII-2
 Typical hyperbolic logarithmic plot of cantilevered pipe spillway scour progression.

VIII. JET PROPERTIES

The jet issuing from the cantilevered pipe plunges into the tailwater and attacks the stream bed. The point at which the jet impinges on the scoured bed is assumed, a priori, as the center of the scour hole. Equations will therefore be developed here defining the path and properties of the jet between the pipe exit and the bed of the scour hole.

Jet Trajectory

The general case of a jet discharging into air and subsequently plunging into a pool is shown in figure VIII-1. The horizontal distance from the pipe exit to the point of impingement on the scoured bed X_j is composed of the free-fall distance to the point where the jet plunges into the tailwater surface X_p plus the horizontal distance the jet travels below the tailwater surface. These distances are computed separately and then combined.

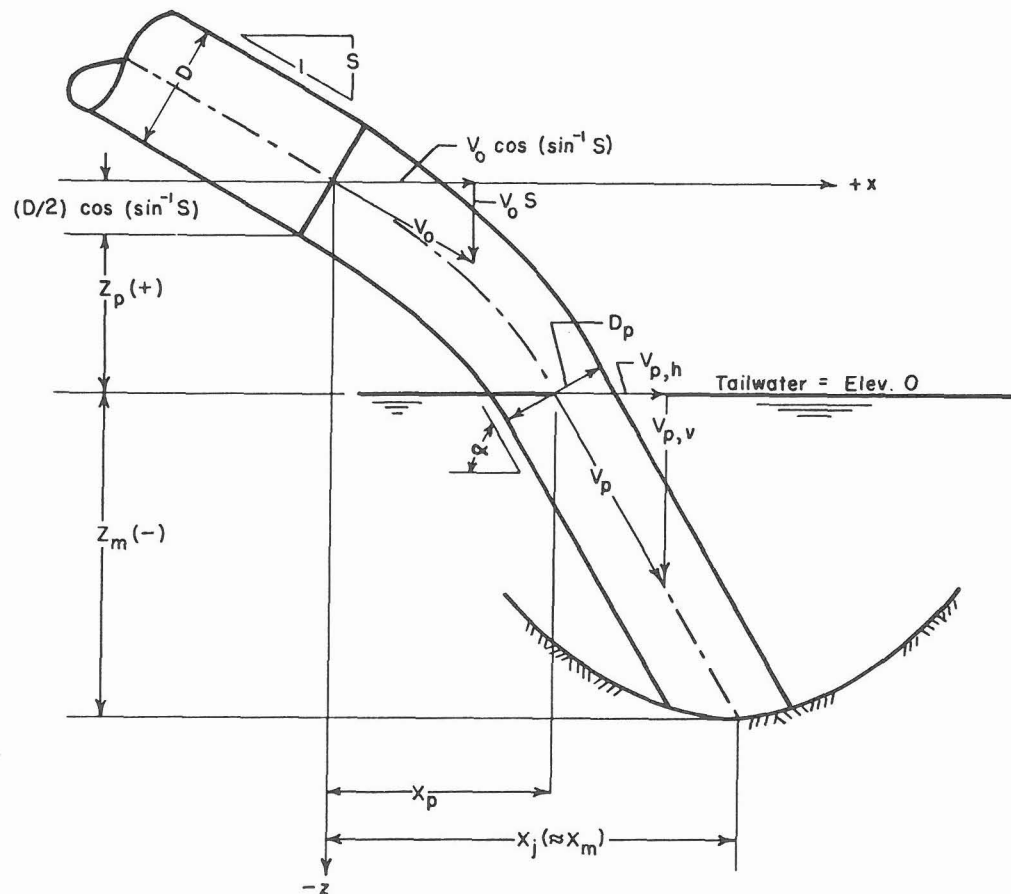


Figure VIII-1
Jet trajectory.

As shown in figure VIII-1, the pipe has a diameter D and a slope S , S being the sine of the pipe inclination. In accordance with open channel usage, S is considered to be positive if the slope falls in the direction of flow. The velocity of efflux is V_o . The origin of the jet coordinates x and z are at the center line of the pipe exit $Z_p + (D/2) \cos(\sin^{-1} S)$ above the tailwater surface, Z_p being the elevation of the pipe invert above the tailwater surface.

The freely falling jet leaves the pipe with a horizontal velocity of $V_o \cos(\sin^{-1} S)$ and a vertical velocity of $V_o S$. The horizontal velocity remains constant, but in air the vertical velocity accelerates under the force of gravity g . The coordinates of the free-falling jet at any time t are

$$x = V_o t \cos(\sin^{-1} S) \quad (\text{VIII-1a})$$

and

$$z = - V_o S t - \frac{gt^2}{2} \quad (\text{VIII-1b})$$

When equation VIII-1a is solved for t , t is substituted in equation VIII-1b, and the resulting equation is solved for x , the equation of the free-falling-jet trajectory is obtained:

$$x = (- V_o S + \sqrt{V_o^2 S^2 - 2gz}) \frac{V_o}{g} \cos(\sin^{-1} S) \quad (\text{VIII-2})$$

Equation VIII-2 is used to compute the distance from the pipe exit to the point where the jet plunges into the tailwater X_p . To compute this distance, $- [Z_p + (D/2) \cos(\sin^{-1} S)]$ is substituted for z , and x becomes X_p . The resulting equation for the distance from the pipe exit to the plunge point is

$$X_p = \left\{ - V_o S + \sqrt{V_o^2 S^2 + 2g[Z_p + (D/2) \cos(\sin^{-1} S)]} \right\} \frac{V_o}{g} \cos(\sin^{-1} S) \quad (\text{VIII-3})$$

(The sign change under the radical shifts the vertical origin from the pipe center line to the tailwater surface.)

The jet is not under the influence of gravity below the tailwater surface, so the jet continues at the angle at which the jet enters the tailwater. At and below the tailwater surface the horizontal velocity of the jet $V_{p,h}$ is identical to the horizontal velocity at the pipe exit. This horizontal plunge velocity $V_{p,h}$ is

$$V_{p,h} = V_o \cos(\sin^{-1} S) \quad (\text{VIII-4})$$

The vertical velocity at and below the tailwater surface is the square root of the sum of the squares of the vertical velocity at the pipe exit $V_o S$ and the velocity increase due to the free fall height $\{2g[Z_p + (D/2) \cos(\sin^{-1} S)]\}^{1/2}$. Therefore, the vertical component of the plunge velocity $V_{p,v}$ is

$$V_{p,v} = \sqrt{(V_o S)^2 + 2g[Z_p + (D/2) \cos(\sin^{-1} S)]} \quad (\text{VIII-5})$$

and the angle of inclination of the submerged jet α is

$$\alpha = \tan^{-1} \frac{V_{p,v}}{V_{p,h}} \quad (\text{VIII-6})$$

The depth of scour below the tailwater surface is Z_m (Z_m is negative below the tailwater surface). Therefore, below the tailwater surface the jet travels a horizontal distance of $-Z_m/\tan \alpha$. Adding this distance to the distance from the pipe exit to the plunge point, the horizontal distance from the pipe exit to the bottom--and center--of the scour hole as defined by the jet X_j is

$$X_j = X_p - \frac{Z_m}{\tan \alpha} \quad (\text{VIII-7})$$

Plunge Velocity and Diameter

The jet velocity accelerates and its average diameter decreases until the jet plunges into the tailwater. As a result, it is the jet plunge velocity and plunge diameter that govern the scour. These quantities are used in subsequent analyses, so they will be defined here.

The jet plunge velocity V_p can be obtained from equations VIII-4 and VIII-5. It is

$$V_p = \sqrt{V_{p,h}^2 + V_{p,v}^2} \quad (\text{VIII-8})$$

The jet plunge diameter D_p comes from the equation of continuity. It is

$$D_p = D \sqrt{V_o/V_p} \quad (\text{VIII-9})$$

This concludes the presentation of information used in the analyses which follow.

IX. DATA SUMMARY

The test run numbers and parameters for the runs used in the analyses which follow are listed in table IX-1 for convenience of reference. Beaching occurred for those run numbers listed to the right and above the lines in the table.

A summary of each test condition and resulting observations are presented in table IX-2. Most values listed are non-dimensionalized by the pipe diameter D or the observed maximum scour depth Z_m .

The summary is arranged in (a) major groups of seven pipe elevations relative to the tailwater elevation, five bed material sizes, and one uniform bed material and size distribution and (b) minor groups of five pipe slopes, two bed material size distributions, and a fixed bed. There is also one step hydrograph test. Within each group there is a range of discharges and lengths of time of scour.

The following paragraphs explain the table IX-2 column headings or the data beneath the headings:

The test run numbers in column 1 do not necessarily indicate the order in which the tests were made. Three digit run numbers (XXX) identify the time-dependent tests for the times listed in column 3 and four digit run numbers (LXXX) identify the suspended-material-removed tests.

The dimensionless discharge $Q/\sqrt{gD^5}$ listed in column 2 is a form of the Froude number that is appropriate for quantifying the discharge of a full-flowing pipe.

Column 3 gives the length of time from the beginning of each run to each bed measurement. Infinity (∞) is used to indicate the time to the ultimate scour condition as computed using the asymptotic velocity-of-scour method described in chapter VII. The time for the LXXX runs is from the beginning of the run--sometimes a continuation of the time-dependent tests, but more often a completely separate test. The completely separate tests are identified in table IX-2 as beginning at time zero. The continuation tests began with the time and scour at the end of the time-dependent tests.

In column 4, the distance from the pipe exit to the upstream end of the scour hole is symbolized by X_b . A negative value indicates that the upstream end of the scour hole is upstream of the pipe exit. The additional subscript t_w in column 4, as well as in columns 6, 8, 9, 10 and 11, indicates that the measurement point is to the intersection with the tailwater surface of the projected scour hole slope.

Table IX-1
Test schedule and test numbers

Z_p (D)	S (%)	D (in)	d (mm)	σ	$Q/\sqrt{gD^5}$							
					0.5	1	2	2.5	3	3.5	4	5
<u>Time-Dependent Tests</u>												
Effect of pipe height												
-2	0	1	1.84	1.22	109	111	113		115		117	119
-1					105	103	101		99		97	107
0					133	131	129		127		125	123
0												¹ 121
+1					147	145	143	173	141	175	139	137
+1												¹ 135
+2					159	157	155		153		151	149
+4					144	146	148		150		152	154
+8					161	163	165		167		169	171
+1	As above, fixed bed				179	181	183	185	187			
Effect of standard deviation of bed material												
+1	0	1	1.84	1.22	147	145	143		141		139	137
												¹ 135
			2.00	1.41	168	170	172		174		176	178
			2.00	1.76	180	182	184		186		188	190
Effect of bed material size												
+1	0	1	0.46	1.24	132	134	136		138		140	142
			0.90	1.24	120	122	124		126		128	130
			1.84	1.22	147	145	143		141		139	137
												¹ 135
			3.92	1.23	118	116	114		112		110	108
			7.65	1.26	102	100	98		96		104	106
Effect of pipe slope												
+1	0	1	1.84	1.22	147	145	143		141		139	137
+1												¹ 135
0	34											166
+1	43						156					
+1	64						160					
+1	78						158					
0	47						¹ 162					
0	47						164					

Table IX-1--Continued
 Test schedule and test numbers

Z_p (D)	S (%)	D (in)	d (mm)	σ	$Q/\sqrt{gD^5}$							
					0.5	1	2	2.5	3	3.5	4	5
<u>Suspended-Material-Removed Tests</u>												
Effect of pipe height												
-2	0	1	1.84	1.22				1113				
-1								1101				
0					1133	1131	1129					
+1					1147	1145	1143	1173	1141	1175		
+2					1159	1157	1155					
+4					1144	1146	1148					
+8					1161	1163	1165					
+1	As above, fixed bed				1179	1181	1183	1185				
Effect of standard deviation of bed material												
+1	0	1	1.84	1.22	1147	1145	1143		1141			
			2.00	1.41	1168	1170	1172		1174			
			2.00	1.76	1180	1182	1184					
Effect of bed material size												
+1	0	1	0.46	1.24	1132	1134						
			0.90	1.24	1120	1122	1124					
			1.84	1.22	1147	1145	1143		1141			
			3.92	1.23	1118	1116	1114		1112	1110		
			7.65	1.26	1102	1100	1098		1096	1104	1106	
					1177	composite scour for all $Q/\sqrt{gD^5}$						
Effect of pipe slope												
+1	0	1	1.84	1.22	1147	1145	1143		1141			
0	34										1166	
+1	43						1156					
+1	64						1160					
+1	78						1158					
0	47						1164					

Beaching occurred for those run numbers listed to the right and above the lines in the table.

¹ Test 121 interrupted by jet from sand pump which severely damaged bed; test 135 scour altered by flooding of bed caused by clogged screen in basin outlet; and test 162 altered by reduced flow due to clogged filters.

In column 5, X_m is the distance from the pipe exit to the point of maximum scour hole depth as listed on the computer printout.

In column 6, X_e is the distance from the pipe exit to the projected downstream end of the scour hole.

In column 7, Z_m is the maximum depth of the scour hole below the water surface as listed on the computer printout. Z_m is always negative. The value of Z_m/D , sometimes listed when the duration of the run is ∞ , is an asymptotic value computed by the hyperbolic logarithmic velocity-of-scour method described in chapter VII.

In column 8, W_m is the projected width of the scour hole at the location of the maximum depth X_m .

In columns 9, 10 and 11, the values represent the maximum dimensions of the scour hole in terms of the maximum depth. They are always negative because Z_m is negative. Dimensional values of the scour hole maximum dimensions become positive when the negative nondimensional values are multiplied by the negative dimensional value of Z_m . The values in columns 9, 10 and 11 also are an indication of the slopes of the scour hole ends and sides.

In column 12 are notes regarding the absence or presence of beaching as described in chapters VI and X plus, for the fixed bed tests, whether or not the fixed bed described in chapter X was exposed in the scour hole.

The nondimensionalized experimental data listed in table IX-2 are used in the analyses presented in chapter X. Much additional data acquired during the tests, not necessary for the analyses presented here, are not presented. These data include notes taken during the tests, punched paper tapes digitizing the X-Y-Z coordinates of the scour hole surface, X-Y plots of the scour hole sections, flow-with-confetti and drained-bed photographs of each scour hole, computer printouts of certain scour hole data and computed dimensions, computer plots of the scour hole contours at $0.2Z_m$ intervals, and computer plots of the longitudinal center line section and the cross section at the location of the maximum scour hole depth.

Table IX-2

Summary of experimental data ($d_{50} = 1 \text{ inch} = 0.0833 \text{ ft} = 25.4 \text{ mm}$)

Run	$\frac{Q}{\sqrt{gd^5}}$	Time Minutes	$\frac{X_{b,tw}}{D}$	$\frac{X_m}{D}$	$\frac{X_{e,tw}}{D}$	$\frac{Z_m}{D}$	$\frac{W_{m,tw}}{D}$	$\frac{X_m - X_{b,tw}}{Z_m}$	$\frac{X_{e,tw} - X_m}{Z_m}$	$\frac{W_{m,tw}}{2Z_m}$	Beaching
(1)	(2)	(3)	(4)	(5)	(6)	(7)	(8)	(9)	(10)	(11)	(12)
			$\frac{Z}{D} = -2$	$d_{50}/D = 0.0724$	$(d_{50} = 1.84 \text{ mm})$	$\sigma = 1.22$	$S = 0$				
109	0.5	--	No scour, no data taken.								
111	1	100	-3.77	5.47	?	-2.903	11.61	Too little scour to		None.	
		316	-3.72	7.61	?	-2.959	9.93	obtain meaningful		"	
		1000	-3.70	6.46	?	-3.057	10.08	data.		"	
		3162	-3.72	6.84	?	-3.167	11.21	"		"	
		10000	-3.78	6.79	29.32	-3.345	11.75	"		"	
113	2	10	-4.00	5.97	?	-3.327	13.05	-3.00	--	-1.96	None.
		31	-4.33	8.38	?	-3.462	16.02	-3.67	--	-2.31	"
		100	-4.63	7.50	?	-3.695	16.31	-3.28	--	-2.21	"
		316	-5.44	8.88	31.62	-3.977	18.59	-3.60	-5.72	-2.34	"
		1000	-5.15	8.60	34.09	4.486	21.32	-3.07	-5.68	-2.38	"
		3162	-5.50	9.76	31.77	-4.671	20.51	-3.27	-4.71	-2.20	"
		10000	-5.05	11.85	34.03	-5.045	25.51	-3.35	-4.40	-2.53	"
1113	7290	-5.60	12.33	36.51	-5.086	23.55	-3.53	-4.75	-2.32	" , slight contour irregularity.	
115	3	10	-5.87	10.09	?	-3.658	15.45	-4.36	--	-2.11	One side.
		31	-5.05	9.81	?	-3.910	17.94	-3.80	--	-2.29	" "
		100	-4.48	11.02	?	-4.204	18.79	-3.69	--	-2.23	Some, $Z/Z_m = 0$ to -0.4.
		316	-5.09	13.72	35.50	-5.008	23.05	-3.76	-4.35	-2.30	" , " 0 to -0.5.
		1000	-3.19	16.69	41.72	-5.278	21.83	-3.77	-4.74	-2.07	Strong, " 0 to -0.4.
		3162	-4.29	15.48	43.49	-5.849	26.44	-3.38	-4.79	-2.26	" , " 0 to -0.4.
		10000	-3.87	16.14	46.27	-6.474	30.15	-3.09	-4.65	-2.32	" one side, 0 to -0.4.
117	4	10	-4.23	11.24	?	-4.161	18.26	-3.71	--	-2.19	Some, $Z/Z_m = 0$ to -0.5.
		31	-3.88	11.24	?	-4.738	19.94	-3.19	--	-2.10	Strong, -0.5.
		100	-3.72	13.77	45.20	-4.928	22.53	-3.55	-6.38	-2.28	" one side, " -0.3.
		316	-4.79	14.76	48.03	-5.413	23.77	-3.61	-6.15	-2.20	" both sides, " -0.4.
		1000	-3.95	19.05	49.73	-6.020	25.05	-3.82	-5.10	-2.08	" both sides, " -0.35.
		3162	-4.73	19.65	49.46	-6.603	32.40	-3.69	-4.51	-2.45	" " " -0.35.
		10000	-6.30	21.41	49.40	-7.156	34.83	-3.87	-3.91	-2.43	" " " -0.3.
119	5	10	-4.70	12.45	?	-4.738	21.91	-3.62	--	-2.31	Some
		31	-6.08	12.62	42.98	-4.941	23.04	-3.78	-6.14	-2.33	Strong, $Z/Z_m = 0$ to -0.6.
		100	-8.50	16.91	44.61	-5.677	23.28	-4.48	-4.88	-2.05	" " " 0 to -0.4.
		316	-9.36	17.24	44.40	-6.137	26.82	-4.33	-4.42	-2.18	" " " 0 to -0.4.
		1000	-10.36	22.07	58.38	-6.573	29.00	-4.93	-5.22	-2.05	" " " 0 to -0.4.
		3162	-10.98	23.28	58.96	-7.653	37.78	-4.48	-4.66	-2.47	" " " 0 to -0.3.
		10000	-11.42	23.23	56.54	-8.143	45.87	-4.25	-4.09	-2.82	" " " 0 to -0.4.

Table IX-2--Continued

Summary of experimental data ($d_{50} = 1 \text{ inch} = 0.0833 \text{ ft} = 25.4 \text{ mm}$)

Run	$\frac{Q}{\sqrt{gd^5}}$	Time Minutes	$\frac{X_{b,tw}}{D}$	$\frac{X_m}{D}$	$\frac{X_{e,tw}}{D}$	$\frac{Z_m}{D}$	$\frac{W_{m,tw}}{D}$	$\frac{X_m - X_{b,tw}}{Z_m}$	$\frac{X_{e,tw} - X_m}{Z_m}$	$\frac{W_{m,tw}}{2Z_m}$	Beaching
(1)	(2)	(3)	(4)	(5)	(6)	(7)	(8)	(9)	(10)	(11)	(12)
			$Z_p/D = -1$	$d_{50}/D = 0.0724$	$(d_{50} = 1.84 \text{ mm})$		$\sigma = 1.22$	$S = 0$			
105	0.5	1000		13.06		-1.674	Visual observation indicates no scour.				
103	1	10	+2.09	7.61	?	-1.955	8.01	-2.82	--	-2.04	None.
		31	+2.38	5.20	?	-1.969	7.81	-1.43	--	-1.98	"
		100	+2.75	6.51	?	-2.018	7.91	-1.86	--	-1.96	"
		316	+2.53	6.40	?	-2.116	8.05	-1.83	--	-1.90	"
		1000	+2.33	8.88	42.37	-2.245	8.31	-2.92	-14.92	-1.85	"
		3162	+2.30	8.93	39.52	-2.349	8.64	-2.82	-13.02	-1.84	"
		10000	+2.28	10.03	30.31	-2.484	9.22	-3.12	-8.16	-1.85	"
101	2	10	-2.00	11.24	41.41	-2.552	11.21	-5.19	-11.82	-2.20	"
		31	-2.00	10.64	25.87	-2.901	12.71	-4.36	-5.25	-2.19	"
		100	-2.00	11.85	29.79	-3.171	14.69	-4.37	-5.66	-2.31	"
		316	-3.50	12.45	30.18	-3.490	17.06	-4.57	-5.08	-2.44	"
		1000	-2.95	12.23	30.82	-3.994	19.63	-3.80	-7.71	-2.46	"
		3162	-2.60	12.23	32.05	-4.521	22.13	-3.28	-4.38	-2.45	"
		10000	-2.82	10.03	32.47	-4.693	24.18	-2.74	-4.78	-2.58	"
		∞				-14.22					
1101		12630	-2.68	13.69	37.47	-5.131	23.43	-3.19	-4.63	-2.28	Irregular right contour.
99	3	10	-3.52	10.03	31.57	-3.405	13.96	-3.98	-6.32	-2.05	Strong, $Z/Z_m = 0$ to -0.45.
		31	-3.50	11.85	32.02	-3.767	17.48	-4.07	-5.35	-2.32	" " " -0.35.
		100	-2.84	13.88	33.37	-4.073	19.88	-4.10	-4.78	-2.44	" " " -0.35.
		316	-3.20	14.98	34.72	-4.466	19.72	-4.07	-4.42	-2.21	" " " -0.45.
		1000	-3.10	16.08	40.58	-5.012	23.50	-3.83	-4.89	-2.34	" " " -0.4.
		3162	-3.25	17.29	43.62	-5.552	25.72	-3.70	-4.74	-2.32	" " " -0.3.
		10000	-3.48	19.65	46.23	-5.663	27.82	-4.08	-4.69	-2.46	" " " -0.4.
97	4	10	-4.66	10.69	40.70	-3.859	15.86	-3.98	-7.78	-2.05	Strong, $Z/Z_m = 0$ to -0.4.
		31	-3.90	16.63	39.23	-3.926	18.56	-4.73	-5.23	-2.36	" " " -0.45.
		100	-3.70	13.66	41.13	-4.595	21.69	-3.78	-5.98	-2.36	" " " -0.4.
		316	-5.22	16.03	43.00	-5.294	22.92	-4.01	-5.09	-2.16	" " " -0.6.
		1000	-4.61	19.65	47.28	-5.485	26.77	-4.42	-5.04	-2.44	" " " -0.3.
		3162	-3.23	20.37	48.65	-5.926	31.76	-3.98	-4.77	-2.68	" " " -0.3.
		10000	-3.40	19.65	48.98	-6.393	37.59	-2.60	-4.59	-2.94	" " " -0.6.
		12342	-4.06	23.28	59.86	-6.288	37.95	-2.94	-3.94	-2.04	Considerable, " -0.4.
107	5	10	-3.33	17.73	30.95	-4.472	20.68	-4.71	-2.96	-2.31	Strong, $Z/Z_m = 0$ to -0.4.
		31	-3.93	13.61	46.95	-4.208	21.97	-4.17	-7.92	-2.61	" " " -0.4.
		100	-6.21	12.45	63.23	-4.172	23.93	-4.47	-12.17	-2.87	" " " -0.5.
		316	-7.74	17.24	58.71	-4.724	22.11	-5.29	-8.78	-2.34	" " " -0.3.
		1000	-7.98	14.82	51.96	-5.626	37.70	-4.05	-6.60	-3.35	" " " -0.7.
		3162	-7.00	20.86	53.16	-6.859	33.86	-4.06	-4.71	-2.47	" " " -0.45.
		10000	-5.98	23.23	67.46	-7.694	39.17	--	--	-2.54	" " " -0.5.

Run	$\frac{Q}{\sqrt{gb^5}}$	Time Minutes	$\frac{X_{b,tw}}{D}$	$\frac{X_m}{D}$	$\frac{X_{e,tw}}{D}$	$\frac{Z_m}{D}$	$\frac{W_{m,tw}}{D}$	$\frac{X_m - X_{b,tw}}{Z_m}$	$\frac{X_{e,tw} - X_m}{Z_m}$	$\frac{W_{m,tw}}{2Z_m}$	Beaching
(1)	(2)	(3)	(4)	(5)	(6)	(7)	(8)	(9)	(10)	(11)	(12)
			$Z_p/D = 0$	$d_{50}/D = 0.0724$	$(d_{50} = 1.84 \text{ mm})$	$\sigma = 1.22$	$S = 0$				
133	0.5	10	-0.96	1.89	4.84	-1.465	5.39	-1.94	-2.01	-1.84	None.
		31	-1.18	1.72	5.07	-1.826	5.64	-1.59	-1.84	-1.54	"
		100	-1.18	2.11	5.16	-1.755	6.49	-1.87	-1.74	-1.85	"
		316	-1.11	1.81	5.14	-1.846	6.46	-1.58	-1.80	-1.75	"
		1000	-1.25	1.81	4.83	-1.787	6.60	-1.71	-1.69	-1.85	"
		3162	-1.27	1.55	4.63	-1.763	6.49	-1.60	-1.75	-1.84	"
		10000	-1.36	1.64	4.82	-1.798	6.54	-1.67	-1.77	-1.82	"
		∞				-2.04					
1133		9960	-1.74	3.22	8.50	-3.431	10.49	-1.45	-1.54	-1.53	"
131	1	10	-0.28	3.22	6.75	-2.219	7.50	-1.58	-1.59	-1.69	None.
		31	-0.56	3.30	7.50	-2.486	8.18	-1.55	-1.69	-1.64	"
		100	-0.73	3.30	7.51	-2.611	9.02	-1.54	-1.61	-1.73	"
		316	-0.90	3.22	7.73	-2.714	9.28	-1.52	-1.66	-1.71	"
		1000	-1.08	3.69	8.19	-2.749	9.47	-1.74	-1.64	-1.72	"
		3162	-1.11	3.60	9.17	-2.980	9.75	-1.58	-1.87	-1.64	"
		10000	-1.29	4.03	8.98	-3.420	11.49	-1.56	-1.45	-1.68	"
		∞				-6.17					
1131		11225	-1.41	6.60	15.38	-5.242	16.29	-1.53	-1.67	-1.55	"
129	2	10	+0.47	10.06	16.47	-3.790	12.55	-2.46	-1.64	-1.61	None.
		31	+0.19	9.42	17.90	-3.750	13.83	-2.46	-2.26	-1.84	"
		100	+0.49	10.02	18.52	-4.139	14.89	-2.30	-2.05	-1.80	"
		316	+0.08	11.26	19.66	-4.453	16.64	-2.51	-1.89	-1.87	"
		1000	+0.12	10.57	19.35	-4.642	16.52	-2.25	-1.89	-1.78	"
		3162	-0.08	10.62	19.57	-4.697	17.19	-2.28	-1.90	-1.83	"
		10000	-0.46	11.26	20.49	-4.870	17.58	-2.41	-1.90	-1.80	"
		∞				-7.80					
1129		8520	-0.01	16.26	30.87	-7.307	20.63	-2.23	-2.00	-1.41	"
127	3	10	-0.23	13.66	23.26	-3.777	15.00	-3.68	-2.54	-1.98	Considerable, $Z/Z_m = 0$ to -0.3.
		31	-0.14	15.48	26.08	-4.200	16.05	-3.72	-2.52	-1.91	" " -0.4.
		100	-0.21	15.53	29.25	-4.348	17.07	-3.62	-3.16	-1.96	" " -0.4.
		316	-0.05	14.82	32.30	-4.378	17.54	-3.40	-3.99	-2.00	" " -0.35.
		1000	-0.90	15.31	33.72	-5.109	18.25	-3.17	-3.60	-1.79	" " -0.35.
		3162	-2.08	17.24	36.19	-5.765	19.68	-3.35	-3.29	-1.71	" " -0.35.
		10000	-1.92	16.03	36.42	-6.403	23.38	-2.80	-3.18	-1.82	" " -0.3.
125	4	10	-0.32	17.29	27.24	-4.298	16.45	-4.10	-2.32	-1.91	Strong, $Z/Z_m = 0$ to -0.4.
		31	-1.27	17.84	29.69	-4.544	19.03	-4.20	-2.61	-2.09	Very strong " " -0.45.
		100	-2.93	19.60	34.00	-4.795	17.78	-4.70	-3.00	-1.85	" " -0.4.
		316	-3.40	20.31	37.55	-5.274	19.10	-4.50	-3.27	-1.81	" " -0.4.
		1000	-3.91	20.86	41.43	-5.428	20.33	-4.56	-3.79	-1.87	" " -0.4.
		3162	-4.72	22.29	47.18	-5.495	25.75	-4.92	-4.53	-2.34	" " -0.4.
		10000	-4.62	20.81	54.94	-5.949	30.97	-4.27	-5.74	-2.60	" " -0.4.

Table IX-2--Continued
 Summary of experimental data ($d_{50} = 1 \text{ inch} = 0.0833 \text{ ft} = 25.4 \text{ mm}$)

Run	$\frac{Q}{\sqrt{gD^5}}$	Time Minutes	$\frac{X_{b,tw}}{D}$	$\frac{X_m}{D}$	$\frac{X_{e,tw}}{D}$	$\frac{Z_m}{D}$	$\frac{W_{m,tw}}{D}$	$\frac{X_m - X_{b,tw}}{Z_m}$	$\frac{X_{e,tw} - X_m}{Z_m}$	$\frac{W_{m,tw}}{2Z_m}$	Beaching (12)
(1)	(2)	(3)	(4)	(5)	(6)	(7)	(8)	(9)	(10)	(11)	(12)
123	5	10	+0.40	21.47	32.39	-4.778	17.62	-4.41	-2.28	-1.84	Very strong, $Z/Z_m = 0$ to -0.5.
		31	-1.72	22.68	34.31	-5.152	20.08	-4.74	-2.26	-1.95	" " " " -0.4.
		100	-4.66	22.07	33.62	-4.722	21.19	-5.66	-2.44	-2.24	" " " " -0.4.
		316	-5.71	22.68	43.10	-5.373	22.56	-5.28	-3.80	-2.10	" " " " -0.3.
		1000	-6.70	23.23	45.06	-5.398	23.37	-5.54	-4.04	-2.16	" " " " -0.3.
		3162	-8.00	23.28	58.24	-5.594	25.86	-5.59	-6.25	-2.31	" " " " -0.4.
		10000	-8.60	23.28	64.86	-5.692	27.20	-5.60	-7.30	-2.39	" " " " -0.35.
121	5	10	-0.95	19.05	28.67	-4.207	20.58	-4.75	-2.29	-2.44	Very strong, $Z/Z_m = 0$ to -0.4.
		31	-1.08	21.36	34.51	-4.980	23.12	-4.51	-2.64	-2.32	" " " " -0.4.
		100	-3.27	22.90	36.61	-5.305	22.70	-4.93	-2.58	-2.14	" " " " -0.35.
		316	-5.12	22.07	37.02	-5.385	22.47	-5.05	-2.78	-2.09	" " " " -0.3.
		1000	-6.38	23.23	45.34	-5.354	23.57	-5.53	-4.13	-2.20	" " " " -0.35.
		3162	-7.52	23.23	49.16	-5.557	28.56	-5.53	-4.67	-2.57	" " " " -0.5.
		--			No data, scour hole damaged during test.						
			$\frac{Z_p}{D} = 1$	$d_{50}/D = 0.0724$	$(d_{50} = 1.84 \text{ mm})$		$\sigma = 1.22$	$S = 0$			
147	0.5	10	-0.65	1.18	5.32	-1.992	5.95	-1.23	-1.76	-1.49	None.
		31	-0.91	1.81	5.13	-1.965	6.22	-1.38	-1.69	-1.58	"
		100	-1.11	1.81	5.28	-1.878	6.28	-1.55	-1.85	-1.67	"
		316	-1.05	1.81	5.09	-1.898	6.20	-1.51	-1.73	-1.63	"
		1000	-0.79	1.76	5.18	-1.831	6.40	-1.39	-1.87	-1.75	"
		3162	-1.33	1.76	5.28	-1.902	6.35	-1.62	-1.85	-1.67	"
		10000	-1.04	1.72	5.15	-1.918	6.35	-1.44	-1.79	-1.66	"
∞						-2.23					
1147		7180	-2.50	3.13	9.94	-4.367	11.92	-1.29	-1.56	-1.36	"
145	1	10	-0.88	3.43	8.04	-2.522	7.72	-1.71	-1.83	-1.53	"
		31	-0.85	3.52	8.72	-2.782	8.20	-1.57	-1.87	-1.47	"
		100	-0.88	3.69	8.85	-2.892	8.63	-1.58	-1.78	-1.49	"
		316	-1.02	3.82	9.00	-2.821	9.10	-1.72	-1.84	-1.61	"
		1000	-1.50	3.69	8.86	-2.950	9.25	-1.76	-1.75	-1.57	"
		3162	-1.39	3.56	9.06	-3.076	9.30	-1.61	-1.79	-1.51	"
		10000	-1.32	3.77	9.55	-3.320	10.15	-1.53	-1.74	-1.53	"
∞						-4.83					
1145		17135	-3.50	6.68	16.74	-6.850	18.81	-1.49	-1.47	-1.37	"

Run	$\frac{Q}{\sqrt{gD^5}}$	Time Minutes	$\frac{X_b, tw}{D}$	$\frac{X_m}{D}$	$\frac{X_e, tw}{D}$	$\frac{Z_m}{D}$	$\frac{W_m, tw}{D}$	$\frac{X_m - X_b, tw}{Z_m}$	$\frac{X_e, tw - X_m}{Z_m}$	$\frac{W_m, tw}{2Z_m}$	Beaching
(1)	(2)	(3)	(4)	(5)	(6)	(7)	(8)	(9)	(10)	(11)	(12)
143	2	10	+1.50	9.63	18.48	-4.643	14.00	-1.75	-1.91	-1.51	None.
		31	+1.55	10.27	19.45	-4.942	15.00	-1.76	-1.86	-1.52	"
		100	+1.30	10.40	19.60	-5.091	15.80	-1.79	-1.81	-1.55	"
		316	+0.92	10.92	20.25	-5.299	17.50	-1.89	-1.76	-1.66	"
		1000	+0.62	11.39	20.95	-5.334	18.20	-2.02	-1.79	-1.70	"
		3162	+0.30	11.13	20.70	-5.350	18.65	-2.02	-1.79	-1.74	"
		10000	+0.42	11.34	21.08	-5.362	19.80	-2.04	-1.82	-1.85	"
		31623	-1.18	11.73	21.28	-5.338	20.65	-2.41	-1.79	-1.93	"
		100000	-1.80	11.56	21.40	-5.460	21.10	-2.45	-1.80	-1.93	"
		316228	-2.36	11.90	21.48	-5.425	21.73	-2.63	-1.76	-2.00	Possibly.
		304670									None.
		623896	-2.64	11.98	21.38	-5.743	22.98	-2.55	-1.64	-2.00	"
∞				-6.32						"	
1143		7320	-0.50	13.01	27.88	-7.014	21.70	-1.93	-2.12	-1.55	"
173	2.5	10	+1.68	10.96	21.42	-4.709	16.50	-1.97	-2.22	-1.75	None.
		31	+1.32	12.80	21.49	-4.921	18.55	-2.33	-1.77	-1.88	"
		100	+0.28	11.51	22.79	-5.149	20.10	-2.18	-2.19	-1.95	"
		316	-1.20	11.64	23.78	-5.616	22.60	-2.29	-2.16	-2.01	Some irregularity one side.
		1000	-1.14	11.26	23.90	-5.687	23.40	-2.18	-2.22	-2.06	More irregularity one side.
		3162	-0.87	11.47	23.68	-5.644	23.73	-2.19	-2.16	-2.10	Irregularity both sides.
		10000	--	12.45	--	-6.017	--	Probe data not good.			
∞				-8.97							
1173		12963	-1.87	12.88		-6.504		-2.27	-2.05	-2.05	Irregularity one side.
141	3	10	+2.37	12.45	23.25	-4.765	19.90	-2.12	-2.27	-2.09	None.
		31	+1.62	14.25	24.77	-4.965	18.55	-2.54	-2.12	-1.87	"
		100	+0.50	14.25	25.40	-5.267	19.95	-2.61	-2.12	-1.89	"
		316	-1.87	13.61	25.33	-5.185	23.20	-2.98	-2.26	-2.24	"
		1000	-3.08	15.45	28.00	-5.919	21.40	-3.13	-2.12	-1.81	One side, $Z/Z_m = 0$ to -0.4 .
		3162	-5.95	14.93	30.32	-6.237	32.10	-3.35	-2.47	-2.57	Both sides, " " -0.4 .
		10000	-5.23	16.90	32.30	-6.842	33.25	-3.23	-2.25	-2.43	One side, " " -0.4 .
		∞				-14.55					
1141		12511	-4.65	16.60	31.17	-6.464	28.26	-3.29	-2.25	-2.19	Strong, both sides.
175	3.5	10	--	15.23	--	-4.772	--	Contour map not read.			Irregularity one side.
		31	--	14.93	--	-5.322	--				" " "
		100	--	15.11	--	-5.604	--				" " " "
		316	--	15.36	--	-5.510	--				" " " "
		1000	--	18.31	--	-5.930	--				" " " "
		3162	--	20.02	--	-6.637	--				" " " "
		10000	--	20.37	--	-6.877	--				" " " "
∞				-12.71							
1175		44223	--	19.47	--	-6.795	--				" " " "

Table IX-2--Continued

Summary of experimental data ($d_{50} = 1 \text{ inch} = 0.0833 \text{ ft} = 25.4 \text{ mm}$)

Run	$\frac{Q}{\sqrt{gD^5}}$	Time Minutes	$\frac{X_{b,tw}}{D}$	$\frac{X_m}{D}$	$\frac{X_{e,tw}}{D}$	$\frac{Z_m}{D}$	$\frac{W_{m,tw}}{D}$	$\frac{X_m - X_{b,tw}}{Z_m}$	$\frac{X_{e,tw} - X_m}{Z_m}$	$\frac{W_{m,tw}}{2Z_m}$	Beaching
(1)	(2)	(3)	(4)	(5)	(6)	(7)	(8)	(9)	(10)	(11)	(12)
139	4	10	+2.50	16.39	27.50	-4.863	20.85	-2.86	-2.28	-2.14	One side, $Z/Z_m = 0$ to -0.35.
		31	+1.32	17.50	29.20	-5.318	23.02	-3.04	-2.20	-2.16	" " " " -0.35.
		100	+1.10	15.66	29.57	-5.267	29.80	-2.76	-2.64	-2.83	" " " " -0.35.
		316	+1.65	18.44	34.70	-5.279	22.70	-3.18	-3.08	-2.15	Both sides, " " -0.35.
		1000	+0.65	18.61	35.98	-5.982	22.05	-3.00	-3.90	-1.84	" " " " -0.2.
		3162	-7.30	19.04	39.20	-6.049	22.90	-4.35	-3.33	-1.89	" " " " -0.2.
		10000	-5.65	21.35	42.10	-6.512	30.25	-4.15	-3.19	-2.32	" " " " -0.2.
137	5	10	+2.20	22.08	34.50	-4.930	20.60	-4.03	-2.52	-2.09	Strong, $Z/Z_m = 0$ to -0.4.
		31	-2.25	23.10	36.90	-5.224	23.80	-4.85	-2.64	-2.28	" " " " -0.3.
		100	-3.75	24.47	36.85	-5.570	23.40	-5.07	-2.22	-2.10	" " " " -0.35.
		316	-6.05	24.34	43.50	-5.782	24.30	-5.26	-3.31	-2.10	" " " " -0.3.
		1000	-8.5	25.92	42.30	-5.970	24.50	-5.76	-2.83	-2.05	" " " " -0.25.
		3162	-9.10	24.94	45.50	-6.324	26.90	-5.38	-3.25	-2.13	" " " " -0.2.
		10000	-10.2	25.88	49.70	-6.257	24.35	-5.77	-3.81	-2.02	" " " " -0.25.
135	5	10	+1.00	20.37	34.40	-4.494	23.02	-4.31	-3.12	-2.56	Strong, $Z/Z_m = 0$ to -0.3.
		31	+0.41	23.57	35.39	-5.209	22.22	-4.45	-2.27	-2.13	" " " " -0.35.
		100	-2.00	25.45	40.39	-5.656	22.76	-4.85	-2.64	-2.01	" " " " -0.25.
		316	-5.61	25.67	42.88	-5.707	23.88	-5.48	-3.02	-2.09	" " " " -0.25.
		1000	-8.06	24.94	45.38	-5.978	26.75	-5.52	-3.42	-2.24	" " " " -0.25.
		--	Screen clogged, bed flooded, scour altered, repeated as Run 137.								
			$Z_p/D = 2$	$d_{50}/D = 0.0724$	$(d_{50} = 1.84 \text{ mm})$		$\sigma = 1.22$	$S = 0$			
159	0.5	10	-0.80	2.15	6.15	-1.682	5.81	-1.75	-2.38	-1.73	None.
		31	-0.87	2.15	6.10	-1.713	5.87	-1.76	-2.31	-1.71	"
		100	-1.10	2.23	6.05	-1.752	6.13	-1.90	-2.18	-1.75	"
		316	-0.93	2.02	6.65	-2.004	6.22	-1.47	-2.31	-1.55	"
		1000	-0.93	2.28	7.08	-2.707	7.75	-1.19	-1.77	-1.43	"
		3162	-1.47	2.49	7.92	-2.970	8.82	-1.33	-1.83	-1.48	"
		10000	-1.62	2.66	8.05	-3.362	9.53	-1.27	-1.60	-1.42	"
1159		9790	-6.13	4.29	15.03	-7.529	20.66	-1.38	-1.43	-1.37	"
		11037	-6.50	4.71	16.50	-8.051	22.13	-1.39	-1.46	-1.37	"
157	1	10	-0.49	3.47	9.32	-2.361	8.16	-1.68	-2.48	-1.73	None.
		31	-0.21	3.43	9.47	-2.699	8.90	-1.35	-2.24	-1.65	"
		100	-0.39	3.60	8.98	-2.652	9.04	-1.50	-2.03	-1.70	"
		316	-0.82	3.65	9.46	-3.033	9.54	-1.47	-1.92	-1.57	"
		1000	-0.79	3.95	9.50	-3.096	9.84	-1.53	-1.79	-1.59	"
		3162	-0.88	3.77	10.20	-3.257	10.46	-1.43	-1.97	-1.61	"
		10000	-0.96	4.03	10.51	-3.574	10.74	-1.40	-1.81	-1.50	"
1157	7245				6.76						
			-6.61	8.48	23.51	-9.936	27.49	-1.38	-1.52	-1.51	"

Run	$\frac{Q}{\sqrt{gD^5}}$	Time Minutes	$\frac{X_{b,tw}}{D}$	$\frac{X_m}{D}$	$\frac{X_{e,tw}}{D}$	$\frac{Z_m}{D}$	$\frac{W_{m,tw}}{D}$	$\frac{X_m - X_{b,tw}}{Z_m}$	$\frac{X_{e,tw} - X_m}{Z_m}$	$\frac{W_{m,tw}}{2Z_m}$	Beaching
(1)	(2)	(3)	(4)	(5)	(6)	(7)	(8)	(9)	(10)	(11)	(12)
155	2	10	+2.17	8.78	17.88	-4.301	12.84	-1.54	-2.12	-1.49	None.
		31	+2.21	9.25	17.30	-4.651	14.02	-1.51	-1.73	-1.51	"
		100	+1.84	9.16	18.72	-4.894	14.85	-1.50	-1.95	-1.26	"
		316	+1.53	10.23	19.34	-4.961	16.25	-1.75	-1.84	-1.64	"
		1000	+1.42	10.40	19.55	-5.000	17.09	-1.80	-1.83	-1.71	"
		3162	+1.06	10.66	20.18	-5.389	18.30	-1.78	-1.77	-1.70	"
		10000	+0.29	11.26	21.53	-5.832	19.36	-1.88	-1.76	-1.66	"
		∞				-7.93					
1155		13091	-0.86	16.86	33.70	-10.168	29.39	-1.45	-1.74	-1.66	"
153	3	10	+2.84	15.06	25.12	-5.027	20.05	-2.43	-2.00	-1.99	None.
		31	+2.54	14.59	26.42	-5.400	21.67	-2.23	-2.19	-2.01	"
		100	+2.14	14.72	26.83	-5.731	22.37	-2.20	-2.11	-1.95	"
		316	+1.19	15.79	26.96	-5.782	22.93	-2.53	-1.93	-1.98	A little on right.
		1000	+1.35	16.13	27.18	-5.903	22.87	-2.50	-1.87	-1.94	" " " "
		3162	-0.16	16.43	27.42	-6.088	23.62	-2.72	-1.81	-1.94	Considerable on right.
		10000	-0.90	17.50	29.49	-5.742	25.00	-3.20	-2.09	-2.18	" " "
151	4	10	+3.71	18.95	30.50	-5.495	21.69	-2.74	-2.14	-1.97	On right.
		31	+4.29	18.31	30.06	-5.569	21.38	-2.52	-2.11	-1.92	" "
		100	+5.46	19.25	32.32	-5.781	24.78	-2.39	-2.26	-2.14	" "
		316	+1.13	19.04	35.46	-6.044	24.90	-2.96	-2.72	-2.06	Strong both sides.
		1000	-4.24	24.21	39.86	-6.602	24.22	-4.31	-2.37	-1.84	" " "
		3162	-3.55	20.54	40.77	-6.685	25.96	-3.60	-3.03	-1.94	" " "
		--			Test terminated.						
149	5	10	+9.07	22.97	35.86	-5.523	26.86	-2.52	-2.33	-2.43	Strong.
		31	+7.08	22.80	36.88	-5.821	32.91	-2.70	-2.42	-2.83	"
		100	-3.29	25.67	42.16	-6.112	22.79	-4.74	-2.70	-1.86	"
		316	-4.26	26.86	44.53	-6.524	24.50	-4.78	-2.71	-1.88	"
		1000	-5.50	27.81	48.37	-6.756	26.28	-4.93	-3.04	-1.94	"
		3162	-7.24	28.06	48.28	-6.806	28.81	-5.19	-2.97	-2.12	"
		--			Test terminated.						
			$Z_p/D = 4$	$d_{50}/D = 0.0724$	$(d_{50} = 1.84 \text{ mm})$			$\sigma = 1.22$	$S = 0$		
144	0.5	10	-0.34	2.29	6.78	-1.266	4.93	-2.08	-3.55	-1.95	None.
		31	-0.44	2.29	6.31	-1.344	5.09	-2.03	-2.99	-1.89	"
		100	-0.58	3.02	7.04	-1.478	5.80	-2.44	-2.72	-1.96	"
		316	-0.88	3.28	6.26	-1.376	5.85	-3.02	-2.16	-2.12	"
		1000	-0.82	2.29	6.59	-1.368	5.99	-2.27	-3.14	-2.19	"
		3162	-0.86	2.29	6.98	-1.599	6.30	-1.97	-2.93	-1.97	"
		10000	-0.98	2.80	7.99	-2.196	7.68	-1.72	-2.36	-1.75	"
		∞				-2.61					
1144		8193	-8.40	5.10	18.88	-9.771	26.28	-1.38	-1.41	-1.34	"

Table IX-2--Continued
 Summary of experimental data ($d_{50} = 1 \text{ inch} = 0.0833 \text{ ft} = 25.4 \text{ mm}$)

Run	$\frac{Q}{\sqrt{gd^5}}$	Time Minutes	$\frac{X_{b,tw}}{D}$	$\frac{X_m}{D}$	$\frac{X_{e,tw}}{D}$	$\frac{Z_m}{D}$	$\frac{W_{m,tw}}{D}$	$\frac{X_m - X_{b,tw}}{Z_m}$	$\frac{X_{e,tw} - X_m}{Z_m}$	$\frac{W_{m,tw}}{2Z_m}$	Beaching	
(1)	(2)	(3)	(4)	(5)	(6)	(7)	(8)	(9)	(10)	(11)	(12)	
146	1	10	+0.59	4.30	9.92	-2.224	8.06	-1.67	-2.53	-1.81	None.	
		31	+0.23	4.17	9.81	-2.393	8.51	-1.65	-2.36	-1.78	"	
		100	-0.09	4.26	9.84	-2.448	8.98	-1.78	-2.28	-1.83	"	
		316	-0.32	4.39	10.01	-2.604	9.30	-1.81	-2.16	-1.78	"	
		1000	-0.78	4.39	10.99	-3.359	11.10	-1.54	-1.96	-1.65	"	
		3162	-1.36	4.60	11.02	-3.331	11.51	-1.79	-1.93	-1.73	"	
		10000	-1.57	4.99	11.25	-3.182	11.51	-2.06	-1.97	-1.81	"	
		∞				-6.03						"
1146		11610	-6.95	8.05	24.62	-10.658	29.45	-1.41	-1.56	-1.38	"	
148	2	10	+3.41	9.30	14.73	-3.763	12.19	-1.56	-1.44	-1.62	None.	
		31	+2.62	9.56	16.97	-4.144	13.21	-1.67	-1.79	-1.59	"	
		100	+3.00	9.90	15.62	-4.215	14.09	-1.64	-1.36	-1.67	"	
		316	+2.43	9.95	17.30	-4.580	16.20	-1.64	-1.60	-1.77	"	
		1000	+2.29	10.54	17.46	-4.980	17.05	-1.66	-1.39	-1.71	"	
		3162	+1.75	10.84	20.80	-5.326	17.69	-1.71	-1.87	-1.66	"	
		10000	+0.18	10.80	20.56	-5.294	18.71	-2.01	-1.84	-1.77	"	
		∞				-10.21						"
1148		9780	-0.10	18.06	34.60	-10.391	31.00	-1.75	-1.59	-1.49	"	
150	3	10	+5.39	16.36	26.65	-5.232	19.31	-2.10	-1.97	-1.85	None.	
		31	+5.05	17.17	27.60	-5.522	20.75	-2.19	-1.89	-1.88	"	
		100	+4.62	17.34	28.66	-5.671	22.32	-2.24	-2.00	-1.97	Little.	
		316	+3.90	17.51	28.10	-5.954	20.46	-2.28	-1.78	-1.72	"	
		1000	+3.54	17.98	29.15	-6.217	23.02	-2.32	-1.80	-1.85	On left.	
		3162	+2.66	18.41	29.29	-6.127	23.16	-2.57	-1.78	-1.89	" "	
		10000	+0.65	19.14	30.29	-6.378	24.35	-2.90	-1.75	-1.91	" "	
												" "
152	4	10	+6.29	22.65	32.47	-5.687	22.31	-2.88	-1.73	-1.96	Some left, little right.	
		31	+6.37	22.60	34.21	-5.915	22.09	-1.74	-1.96	-1.87	Same, but more.	
		100	+5.43	23.37	35.14	-6.194	26.38	-2.90	-1.90	-2.13	Severe on left.	
		316	+4.45	23.29	37.45	-6.543	30.24	-2.88	-2.16	-2.31	Strong both sides.	
		1000	-3.80	24.44	40.59	-7.427	28.42	-3.80	-2.17	-1.91	Strong.	
		3162	-6.01	24.10	42.91	-7.427	28.88	-4.05	-2.53	-1.94	"	
												"
												"
											Test terminated.	
154	5	10	+12.49	27.39	39.30	-5.942	23.39	-2.51	-2.00	-1.97	Strong both sides.	
		31	+9.81	26.66	41.14	-6.288	27.71	-2.68	-2.30	-2.20	Severe.	
		100	+11.22	27.05	41.33	-6.496	31.88	-2.44	-2.20	-2.45	"	
		316	+0.20	30.04	47.53	-6.948	28.22	-4.29	-2.52	-2.03	"	
		1000	+3.79	27.56	46.63	-7.254	32.44	-3.28	-2.63	-2.24	"	
		3162	-3.74	32.31	54.30	-8.044	30.68	-4.48	-2.73	-1.91	"	
												"
												"
											Test Terminated.	

Run	$\frac{Q}{\sqrt{gD^5}}$	Time Minutes	$\frac{X_{b,tw}}{D}$	$\frac{X_m}{D}$	$\frac{X_{e,tw}}{D}$	$\frac{Z_m}{D}$	$\frac{W_{m,tw}}{D}$	$\frac{X_m - X_{b,tw}}{Z_m}$	$\frac{X_{e,tw} - X_m}{Z_m}$	$\frac{W_{m,tw}}{2Z_m}$	Beaching
(1)	(2)	(3)	(4)	(5)	(6)	(7)	(8)	(9)	(10)	(11)	(12)
			$Z_p/D = 8$		$d_{50}/D = 0.0724$		$(d_{50} = 1.84 \text{ mm})$		$\sigma = 1.22$	$S = 0$	
161	0.5	10	-0.25	2.58	6.30	-1.352	5.32	-2.09	-2.75	-1.97	None.
		31	-0.73	4.24	7.79	-1.262	5.96	-3.94	-2.81	-2.36	"
		100	+0.05	2.41	8.22	-1.694	6.32	-1.39	-3.42	-1.86	"
		316	-1.05	3.99	7.82	-1.481	7.14	-3.40	-2.59	-2.41	"
		1000	-1.40	3.47	8.06	-1.379	7.49	-3.53	-3.33	-2.72	"
		3162	-0.59	2.66	7.99	-1.501	7.19	-2.16	-3.55	-2.40	"
		10000	-0.66	3.77	8.19	-1.548	7.56	-2.86	-2.86	-2.44	"
		∞				-2.16					
1161		8880	-7.00	5.14	17.97	-8.691	24.46	-1.40	-1.48	-1.41	"
163	1	10	+0.51	5.96	11.05	-2.192	9.30	-2.49	-2.32	-2.12	None.
		31	+0.61	5.36	11.42	-2.389	9.75	-1.99	-2.54	-2.04	"
		100	-0.09	5.61	11.51	-2.746	10.31	-2.08	-2.15	-1.88	"
		316	-0.21	4.93	12.18	-3.080	11.09	-1.67	-2.35	-1.80	"
		1000	-0.55	5.48	11.89	-2.958	11.88	-2.04	-2.17	-2.01	"
		3162	-0.83	5.14	11.71	-2.829	11.96	-2.11	-2.32	-2.11	"
		10000	-0.19	5.27	13.05	-3.453	12.90	-1.58	-2.25	-1.87	"
		∞				-7.74					
1163		8940	-4.55	8.95	23.22	-9.783	27.06	-1.38	-1.46	-1.38	"
		12779	-3.36	6.51	16.50	-5.876	16.69	-1.68	-1.70	-1.42	"
		16700	-3.49	6.47	17.51	-6.233	18.17	-1.60	-1.77	-1.46	"
165	2	10	+4.91	11.13	20.41	-3.869	13.70	-1.61	-2.40	-1.77	None.
		31	+4.42	10.92	20.87	-3.995	14.11	-1.63	-2.49	-1.76	"
		100	+4.50	12.07	22.45	-4.694	16.88	-1.61	-2.21	-1.80	"
		316	+4.21	12.20	21.47	-4.639	17.32	-1.72	-2.00	-1.87	"
		1000	+3.76	11.56	21.66	-4.839	17.50	-1.61	-2.09	-1.81	"
		3162	+3.49	12.45	22.56	-5.236	19.02	-1.71	-1.93	-1.82	"
		----	Test terminated.								----
		∞				-10.00					
1165		7450	-0.14	17.50	35.98	-10.458	32.23	-1.69	-1.77	-1.54	"
		9975	+2.78	15.11	31.92	-8.263	27.36	-1.49	-2.03	-1.66	"
167	3	10	+9.26	19.25	30.57	-5.341	19.01	-1.87	-2.12	-1.78	None.
		31	+8.71	19.04	32.38	-5.707	21.81	-1.81	-2.34	-1.91	"
		100	+8.23	20.24	32.54	-6.198	24.83	-1.94	-1.98	-2.00	"
		316	+7.48	21.09	32.95	-6.810	22.75	-2.00	-1.74	-1.67	"
		1000	+6.73	21.09	34.31	-7.097	24.72	-2.02	-1.86	-1.74	Right.
		3162	+6.27	21.52	34.48	-7.179	25.83	-2.12	-1.80	-1.80	Strong right, none left.
		10000	+5.30	22.03	34.97	-6.956	27.11	-2.40	-1.86	-1.95	" " " "
		15820	+3.28	23.83	38.11	-8.259	28.07	-2.49	-1.73	-1.70	----

Table IX-2--Continued
 Summary of experimental data ($d_{50} = 1 \text{ inch} = 0.0833 \text{ ft} = 25.4 \text{ mm}$)

Run	$\frac{Q}{\sqrt{gD^5}}$	Time Minutes	$\frac{X_{b,tw}}{D}$	$\frac{X_m}{D}$	$\frac{X_{e,tw}}{D}$	$\frac{Z_m}{D}$	$\frac{W_{m,tw}}{D}$	$\frac{X_m - X_{b,tw}}{Z_m}$	$\frac{X_{e,tw} - X_m}{Z_m}$	$\frac{W_{m,tw}}{2Z_m}$	Beaching	
(1)	(2)	(3)	(4)	(5)	(6)	(7)	(8)	(9)	(10)	(11)	(12)	
169	4	10	+12.35	26.14	38.40	-5.946	24.15	--	--	-2.03	Slight left.	
		31	+12.20	26.31	39.71	-6.484	23.54	--	--	-1.82	More left.	
		100	+10.64	27.42	40.25	-6.912	23.56	--	--	-1.70	Strong left.	
		316	+10.32	25.92	41.21	-6.948	25.56	--	--	-1.84	" "	
		1000	+9.97	28.62	42.20	-7.207	28.80	--	--	-2.00	" "	
		3162	+8.98	28.40	42.58	-7.560	31.32	--	--	-2.07	" "	
		--	Flow failure damaged scour hole.								--	
171	5	10	--	32.81	--	-6.484	--	--	--	--	Asymmetrical.	
		31	--	33.06	--	-6.731	--	--	--	--	One side.	
		100	--	33.28	--	-7.175	--	--	--	--	Both sides.	
		316	--	34.05	--	-7.592	--	--	--	--	--	
		1000	--	34.09	--	-7.741	--	--	--	--	--	
		--	Flow failure damaged scour hole.								--	
			$Z_p/D = 1 \quad d_{50}/D = 0.0724 \quad (d_{50} = 1.84 \text{ mm}) \quad \sigma = 1.22 \quad S = 0.428$									
156	2	10	-0.79	5.41	14.59	-3.975	11.50	-1.56	-2.31	-1.45	None.	
(Corresponds to Run 155)		31	-0.56	5.63	14.43	-4.183	12.25	-1.48	-2.10	-1.46	"	
		100	-1.15	5.88	15.45	-4.364	12.46	-1.61	-2.19	-1.43	"	
		316	-0.94	5.88	14.75	-4.266	12.71	-1.60	-2.08	-1.48	"	
		1000	-1.18	6.27	16.34	-4.823	14.18	-1.54	-2.09	-1.47	"	
		3162	-2.29	6.23	15.42	-4.749	14.74	-1.79	-1.94	-1.55	"	
		10000	-1.45	6.95	16.94	-5.310	16.25	-1.58	-1.88	-1.53	"	
		∞				-8.32						
1156	2	12778	-2.70	10.93	24.69	-8.369	23.11	-1.63	-1.64	-1.38		
			$Z_p/D = 1 \quad d_{50}/D = 0.0724 \quad (d_{50} = 1.84 \text{ mm}) \quad \sigma = 1.22 \quad S = 0.635$									
160	2	10	-1.59	3.40	11.34	-3.123	10.05	-1.60	-2.54	-1.61	None.	
(Corresponds to Run 148)		31	-2.44	3.19	11.84	-3.292	10.92	-1.71	-2.63	-1.81	"	
		100	-2.19	3.40	12.09	-3.394	11.30	-1.65	-2.56	-1.66	"	
		316	-2.24	4.09	13.01	-4.081	12.05	-1.55	-2.18	-1.48	"	
		1000	-2.40	3.87	12.92	-3.892	12.93	-1.61	-2.32	-1.66	"	
		3162	-2.59	3.87	13.68	-4.234	13.61	-1.52	-2.32	-1.61	"	
		10000	-2.61	3.75	13.58	-3.944	13.70	-1.61	-2.49	-1.74	"	
		∞				-7.82						
1160		12980	-5.27	9.39	24.43	-9.791	28.28	-1.50	-1.54	-1.44	"	
			$Z_p/D = 1 \quad d_{50}/D = 0.0724 \quad (d_{50} = 1.84 \text{ mm}) \quad \sigma = 1.22 \quad S = 0.782$									
158	2	10	-2.53	2.33	10.16	-2.506	9.98	-1.94	-3.12	-1.99	None.	
(Corresponds to Run 165)		31	-2.59	3.57	10.10	-2.977	10.93	-2.07	-2.19	-1.84	"	
		100	-2.89	1.65	9.65	-2.907	10.95	-1.56	-2.75	-1.88	"	
		316	-2.79	4.26	10.05	-2.919	11.37	-2.42	-1.98	-1.95	"	
		1000	-3.26	1.99	10.48	-2.985	11.61	-1.76	-2.84	-1.94	"	
		3162	-3.39	2.16	10.36	-3.202	12.05	-1.73	-2.56	-1.88	"	
		10000	-3.34	2.85	10.91	-3.339	12.35	-1.85	-2.41	-1.85	"	
		∞				5.20						
1158		18493	-8.40	6.44	20.95	-9.748	27.80	-1.52	-1.49	-1.42	"	

Run	$\frac{Q}{\sqrt{gD^3}}$	Time Minutes	$\frac{X_{b,tw}}{D}$	$\frac{X_m}{D}$	$\frac{X_{e,tw}}{D}$	$\frac{Z_m}{D}$	$\frac{W_{m,tw}}{D}$	$\frac{X_m - X_{b,tw}}{Z_m}$	$\frac{X_{e,tw} - X_m}{Z_m}$	$\frac{W_{m,tw}}{2Z_m}$	Beaching
(1)	(2)	(3)	(4)	(5)	(6)	(7)	(8)	(9)	(10)	(11)	(12)
			$Z_p/D = 0 \quad d_{50}/D = 0.0724 \quad (d_{50} = 1.84 \text{ mm}) \quad \sigma = 1.22 \quad S = 0.473$								
162	2	10	-1.71	5.97	12.08	-4.099	11.95	-1.87	-1.49	-1.10	None.
(Corresponds to Run 143)		31	-1.61	5.84	13.01	-4.162	12.22	-1.79	-1.72	-1.47	"
		100	-1.79	6.10	13.21	-4.401	12.79	-1.79	-1.62	-1.45	"
		316	-1.87	6.31	13.64	-4.586	13.60	-1.78	-1.60	-1.48	"
		1000	-1.99	6.10	13.90	-4.390	13.99	-1.84	-1.78	-1.58	"
		3162	-2.16	6.40	13.90	-4.511	14.34	-1.90	-1.66	-1.59	"
		10000	Scour hole damaged. Test repeated as Run 164.								
164	2	10	-1.40	5.93	12.17	-4.036	11.99	-1.82	-1.55	-1.48	None.
(Corresponds to Run 143)		31	-1.90	6.18	12.20	-4.244	12.89	-1.90	-1.42	-1.52	"
		100	-2.02	6.23	13.49	-4.315	13.22	-1.91	-1.68	-1.53	"
		316	-1.95	6.44	16.12	-5.309	16.27	-1.58	-1.82	-1.53	"
		1000	-2.39	6.05	15.22	-5.038	16.85	-1.68	-1.82	-1.67	"
		3162	-2.45	6.87	14.40	-5.006	16.89	-1.86	-1.50	-1.69	"
		10000	-2.85	8.32	18.93	-6.357	20.32	-1.76	-1.67	-1.60	"
		∞				-8.57					"
1164		13143	-3.92	11.48	26.94	-9.220	26.46	-1.67	-1.68	-1.43	"
			$Z_p/D = 0 \quad d_{50}/D = 0.0724 \quad (d_{50} = 1.84 \text{ mm}) \quad \sigma = 1.22 \quad S = 0.342$								
166	3	10	-1.11	11.36	22.10	5.893	17.71	-2.08	-1.80	-1.48	None.
(Corresponds to Run 141)		31	-0.58	11.78	23.03	-6.030	19.11	-2.05	-1.87	-1.58	"
		100	-0.85	12.68	23.72	-6.368	20.52	-2.12	-1.73	-1.61	"
		316	-0.96	12.64	24.98	-6.674	21.58	-2.04	-1.85	-1.62	"
		1000	-1.27	13.49	24.93	-6.772	22.97	-2.18	-1.69	-1.70	"
		3162	-3.19	12.13	24.79	-6.921	23.40	-2.21	-1.83	-1.69	"
		10000	-5.24	12.94	25.55	-7.047	25.78	-2.58	-1.79	-1.83	"
		∞				-9.51					"
1166		14400	-4.04	15.12	34.30	-9.301	28.82	-2.06	-2.06	-1.55	"
			$Z_p/D = 1 \quad d_{50}/D = 0.0181 \quad (d_{50} = 0.46 \text{ mm}) \quad \sigma = 1.24 \quad S = 0$								
132	0.5	10	-1.07	2.38	6.24	-1.847	7.63	-1.87	-2.09	-2.06	None.
		31	-1.39	2.76	6.53	-1.961	8.19	-2.12	-1.92	-2.09	"
		100	-1.73	2.38	6.91	-2.090	8.72	-1.97	-2.17	-2.09	"
		316	-1.88	2.38	7.21	-2.283	8.97	-1.86	-2.12	-1.97	"
		1000	-2.01	2.21	7.21	-2.310	9.37	-1.83	-2.16	-2.03	"
		3162	-2.22	2.38	7.49	-2.467	9.76	-1.86	-2.07	-1.98	"
		10000	-3.14	2.80	9.82	-3.618	12.07	-1.64	-1.94	-1.69	"
		∞				-4.37					"
1132		32690	-12.08	6.27	25.68	-11.784	36.97	-1.56	-1.65	-1.57	"

Table IX-2--Continued
 Summary of experimental data ($d_{50} = 1 \text{ inch} = 0.0833 \text{ ft} = 25.4 \text{ mm}$)

Run	$\frac{Q}{\sqrt{gD^5}}$	Time Minutes	$\frac{X_{b,tw}}{D}$	$\frac{X_m}{D}$	$\frac{X_{e,tw}}{D}$	$\frac{Z_m}{D}$	$\frac{W_{m,tw}}{D}$	$\frac{X_m - X_{b,tw}}{Z_m}$	$\frac{X_{e,tw} - X_m}{Z_m}$	$\frac{W_{m,tw}}{2Z_m}$	Beaching
(1)	(2)	(3)	(4)	(5)	(6)	(7)	(8)	(9)	(10)	(11)	(12)
134	1	10	-0.77	4.13	10.00	-2.845	10.49	-1.72	-2.06	-1.84	None.
		31	-1.36	4.30	11.21	-3.320	11.98	-1.70	-2.08	-1.80	"
		100	-1.92	4.17	11.46	-3.539	12.33	-1.72	-2.06	-1.74	"
		316	-2.05	4.22	11.34	-3.779	12.70	-1.66	-1.88	-1.68	"
		1000	-2.25	4.69	12.80	-3.964	13.45	-1.75	-2.04	-1.70	"
		3162	-2.86	4.77	12.99	-4.113	14.33	-1.86	-2.00	-1.74	"
		10000	-3.65	5.03	13.79	-4.368	15.70	-1.99	-2.00	-1.80	"
		∞				-7.74					
1134		28559	-10.26	11.01	32.73	-13.367	39.99	-1.59	-1.62	-1.50	"
136	2	10	+1.23	9.82	20.12	-4.553	14.70	-1.89	-2.26	-1.61	None.
		31	+0.23	10.80	22.00	-4.992	17.65	-2.12	-2.24	-1.77	"
		100	-0.30	12.08	23.63	-5.574	19.77	-2.22	-2.07	-1.77	Slight, $Z/Z_m = 0$ to -0.15.
		316	-0.89	12.30	25.32	-6.139	20.89	-2.15	-2.12	-1.70	" " -0.2.
		1000	-0.83	13.54	26.99	-6.575	22.81	-2.18	-2.04	-1.73	Yes, " " -0.25.
		3162	-0.64	12.90	27.90	-6.866	23.98	-1.87	-2.18	-1.75	Strong, " " -0.3.
		10000	-1.89	13.15	28.26	-7.007	25.28	-2.15	-2.16	-1.80	" " -0.25.
138	3	10	+2.57	13.71	24.05	-4.376	17.92	-2.54	-2.36	-2.05	Strong, $Z/Z_m = 0$ to -0.4.
		31	+0.59	14.78	26.90	-4.745	20.70	-2.99	-2.55	-2.18	" " " -0.3.
		100	-1.92	16.83	29.90	-5.393	21.40	-3.48	-2.42	-1.98	" " " -0.3.
		316	-4.12	18.45	31.59	-6.139	26.78	-3.68	-2.14	-2.18	" " " -0.3.
		1000	-6.00	14.78	37.23	-6.862	25.78	-3.03	-3.27	-1.88	" " " -0.3.
		3162	-7.45	20.76	40.38	-7.765	32.94	-3.50	-2.53	-2.12	" " " -0.3.
		--			Test terminated.						
140	4	10	+4.58	17.77	27.83	-4.741	24.65	-2.78	-2.12	-2.60	Strong, $Z/Z_m = 0$ to -0.2.
		31	+3.82	18.71	32.40	-5.063	22.72	-2.94	-2.70	-2.24	" " " -0.3.
		100	+4.90	21.36	34.98	-5.460	20.83	-3.01	-2.49	-1.91	" " " -0.3.
		247	-7.08	24.48	40.28	-5.825	21.30	-5.42	-2.71	-1.83	" " " -0.3.
		--			Test terminated.						
142	5	10	+1.05	23.03	37.70	-4.792	21.62	-4.59	-3.06	-2.26	Strong, $Z/Z_m = 0$ to -0.5.
		31	-3.13	24.61	43.24	-5.319	20.78	-5.22	-3.50	-1.95	" " " -0.4.
		70	-7.70	27.05	42.97	-5.542	22.52	-6.27	-2.87	-2.03	" " " -0.4.
		--			Test terminated.						
			$Z_p/D = 1$	$d_{50}/D = 0.0354$	$(d_{50} = 0.90 \text{ mm})$	$\sigma = 1.24$	$S = 0$				
120	0.5	10	-0.63	2.81	7.42	-2.357	7.86	-1.46	-1.96	-1.67	None.
		31	-0.87	2.76	7.68	-2.517	8.48	-1.44	-1.95	-1.68	"
		100	-1.40	2.92	8.33	-2.670	9.15	-1.62	-2.03	-1.71	"
		316	-1.42	2.87	7.81	-2.658	9.36	-1.61	-1.86	-1.76	"
		1000	-1.48	2.59	7.65	-2.493	9.34	-1.63	-2.03	-1.87	"
		3162	-1.65	2.87	8.80	-3.180	10.24	-1.42	-1.86	-1.61	"
		10000	-1.88	2.87	8.48	-3.045	10.56	-1.56	-1.84	-1.73	"
		∞				-5.18					
1120		12971	-11.63	6.87	22.68	-11.815	34.08	-1.57	-1.34	-1.44	"

Run	$\frac{Q}{\sqrt{gD^5}}$	Time Minutes	$\frac{X_{b,tw}}{D}$	$\frac{X_m}{D}$	$\frac{X_{e,tw}}{D}$	$\frac{Z_m}{D}$	$\frac{W_{m,tw}}{D}$	$\frac{X_m - X_{b,tw}}{Z_m}$	$\frac{X_{e,tw} - X_m}{Z_m}$	$\frac{W_{m,tw}}{2Z_m}$	Beaching
(1)	(2)	(3)	(4)	(5)	(6)	(7)	(8)	(9)	(10)	(11)	(12)
122	1	10	-1.19	3.69	9.40	-3.026	9.78	-1.61	-1.89	-1.62	None.
		31	-1.10	3.69	10.00	-3.259	10.68	-1.47	-1.94	-1.64	"
		100	-1.29	3.80	10.12	-3.253	10.85	-1.56	-1.94	-1.67	"
		316	-1.42	3.80	10.51	-3.480	11.40	-1.50	-1.93	-1.64	"
		1000	-1.45	4.13	11.65	-3.787	11.86	-1.47	-1.98	-1.56	"
		3162	-1.91	4.13	11.56	-3.885	12.11	-1.55	-1.91	-1.56	"
		10000	-1.95	4.30	11.83	-4.051	12.55	-1.54	-1.86	-1.55	"
		∞				-6.62					
1122		10300	-7.12	9.86	26.12	-11.025	31.78	-1.54	-1.47	-1.44	"
124	2	10	+1.10	10.07	19.78	-4.557	14.88	-1.97	-2.13	-1.63	Slight, $Z/Z_m = 0$ to -0.2 .
		31	+0.78	10.20	20.68	-4.938	16.16	-1.90	-2.12	-1.64	" " " -0.2 .
		100	+0.35	11.14	21.02	-5.193	17.74	-2.08	-1.90	-1.71	" " " -0.3 .
		316	-0.95	10.54	20.62	-5.326	18.02	-2.16	-1.89	-1.69	" " " -0.3 .
		1000	-1.25	11.44	21.98	-5.759	20.08	-2.20	-1.83	-1.74	Little, " " " -0.4 .
		3162	-2.10	11.27	22.33	-5.747	22.30	-2.33	-1.92	-1.94	" " " -0.4 .
		10000	-2.82	12.21	23.79	-5.837	21.53	-2.57	-1.98	-1.84	Yes, " " " -0.3 .
		∞				-8.81					
1124		27038	-3.27	16.83	33.83	-9.569	32.03	-2.10	-1.78	-1.68	--
126	3	10	+2.04	12.60	23.34	-4.486	17.85	-2.35	-2.39	-1.99	Yes, $Z/Z_m = 0$ to -0.3 .
		31	+1.21	13.45	23.85	-4.800	19.77	-2.55	-2.17	-2.06	" " " -0.3 .
		100	-2.72	14.01	23.44	-4.317	17.00	-3.88	-2.18	-1.96	Strong, " " " -0.5 .
		316	-7.63	14.91	27.84	-5.240	21.59	-4.30	-2.47	-2.06	" " " -0.5 .
		1000	-4.29	11.96	31.40	-5.852	25.32	-2.78	-3.32	-2.16	" " " -0.4 .
		3162	-11.98	20.76	35.97	-6.905	30.53	-4.74	-2.30	-2.21	" " " -0.5 .
		6000	-14.42	19.95	37.95	-7.506	31.52	-4.58	-2.40	-2.10	" " " -0.5 .
		10000	-14.33	21.02	45.25	-8.075	31.52	-4.38	-3.00	-1.95	" " " -0.4 .
128	4	10	-1.22	19.14	30.72	-4.514	17.07	-4.51	-2.56	-1.89	Wide + much upstream, $Z/Z_m = 0$ to -0.5 .
		31	-3.88	19.65	33.30	-4.930	17.18	-4.77	-2.77	-1.74	Very wide 0 contour, " " " -0.6 .
		100	-8.55	21.53	33.75	-5.283	20.49	-5.69	-2.31	-1.94	" " " " " " -0.35 .
		316	-14.50	22.26	38.27	-5.837	21.43	-6.30	-2.74	-1.84	" " " " " " -0.4 .
		1000	-17.84	24.74	42.62	-5.786	22.52	-7.36	-3.09	-1.95	" " " " " " -0.3 .
		3162	-20.90	25.55	51.04	-6.308	25.22	-7.36	-3.44	-2.00	" " " " " " -0.25 .
		--	Test terminated.								
		--									
130		10	-3.63	23.63	37.45	-4.733	18.52	-5.76	-2.92	-1.96	Very wide 0 & -0.2 contours, $Z/Z_m = 0$ to -0.6 .
		31	-3.32	24.61	41.88	-5.401	22.28	-5.17	-3.20	-2.06	" " " " " " -0.4 .
		100	-8.26	26.32	42.64	-5.833	23.35	-5.93	-2.80	-2.00	" " " " " " -0.5 .
		316	-6.26	23.76	43.84	-6.014	25.12	-4.99	-3.34	-2.09	" " " " " " -0.4 .
		--	Test terminated.								
		--									

Table IX-2--Continued

Summary of experimental data ($d_{50} = 1 \text{ inch} = 0.0833 \text{ ft} = 25.4 \text{ mm}$)

Run	$\frac{Q}{\sqrt{gD^5}}$	Time Minutes	$\frac{X_{b,tw}}{D}$	$\frac{X_m}{D}$	$\frac{X_{e,tw}}{D}$	$\frac{Z_m}{D}$	$\frac{W_{m,tw}}{D}$	$\frac{X_m - X_{b,tw}}{Z_m}$	$\frac{X_{e,tw} - X_m}{Z_m}$	$\frac{W_{m,tw}}{2Z_m}$	Beaching
(1)	(2)	(3)	(4)	(5)	(6)	(7)	(8)	(9)	(10)	(11)	(12)
			$Z_p/D = 1$		$d_{50}/D = 0.1543$		$(d_{50} = 3.92 \text{ mm})$		$\sigma = 1.23$	$S = 0$	
118	0.5	10	-0.49	1.88	3.71	-1.192	3.62	-1.99	-1.54	-1.52	
		31	-0.26	1.82	3.84	-1.413	3.88	-1.47	-1.43	-1.37	
		100	-0.56	2.04	4.07	-1.518	4.53	-1.71	-1.34	-1.49	
		316	-0.38	2.15	4.97	-1.812	5.03	-1.39	-1.56	-1.39	
		1000	-0.66	2.04	4.72	-1.683	5.30	-1.60	-1.59	-1.57	
		3162	-0.39	1.99	4.78	-1.763	5.27	-1.35	-1.58	-1.49	
		10000	-0.55	2.10	5.20	-1.916	5.91	-1.38	-1.62	-1.54	
		∞				-3.57					
1118		37568	-2.86	3.05	9.78	-4.760	12.45	-1.24	-1.41	-1.31	
116	1	10	-0.05	3.64	7.17	-2.303	6.41	-1.60	-1.53	-1.39	
		31	+0.05	3.86	7.18	-2.561	7.09	-1.49	-1.30	-1.38	
		100	-0.13	3.86	7.82	-2.794	7.61	-1.43	-1.42	-1.36	
		316	-0.38	4.02	8.49	-2.935	8.63	-1.50	-1.52	-9.47	
		1000	-0.62	3.86	8.28	-2.868	8.80	-1.56	-1.54	-1.53	
		3162	-0.29	3.97	8.01	-2.818	8.68	-1.51	-1.43	-1.54	
		10000	-0.60	3.91	8.43	-2.757	8.81	-1.64	-1.64	-1.60	
		∞				-3.93					
1116		31681	-3.40	7.20	18.05	-7.399	20.12	-1.43	-1.47	-1.36	
114	2	10	+2.98	9.41	12.92	-4.052	11.00	-1.59	-0.87	-1.36	
		31	+2.52	9.90	13.85	-4.426	11.94	-1.67	-0.89	-1.35	
		100	+2.12	10.40	15.71	-4.659	12.49	-1.78	-1.14	-1.34	
		316	+2.45	10.51	14.18	-4.629	13.13	-1.74	-0.79	-1.42	
		1000	+1.83	10.45	15.88	-4.616	13.10	-1.87	-1.18	-1.42	
		3162	+1.34	10.01	16.81	-4.776	13.34	-1.81	-1.42	-1.40	
		10000	+1.07	10.84	17.88	-4.825	14.28	-2.02	-1.46	-1.48	
		∞				-6.22					
1114			-2.21	13.65	26.93	-7.746	21.68	-2.05	-1.71	-1.00	
112	3	10	+3.58	12.54	21.25	-4.395	15.58	-2.04	-1.98	-1.77	
		31	+3.43	13.97	23.88	-4.807	17.40	-2.19	-2.06	-1.81	
		100	+3.23	14.58	24.77	-5.107	18.93	-2.22	-2.00	-1.76	
		316	+3.26	13.97	25.00	-5.359	19.91	-2.00	-2.06	-1.86	
		1000	+1.89	14.14	27.23	-5.549	21.09	-2.21	-2.36	-1.90	
		3162	+1.86	13.59	27.36	-5.721	21.60	-2.05	-2.41	-1.89	
		10000	+0.74	14.14	29.73	-5.929	23.43	-2.26	-2.63	-1.98	
		∞				-9.53					
1112		11490	+0.21	14.72	29.39	-6.245	25.17	-2.32	-2.35	-2.02	

Run	$\frac{Q}{\sqrt{gb^5}}$	Time Minutes	$\frac{X_{b,tw}}{D}$	$\frac{X_m}{D}$	$\frac{X_{e,tw}}{D}$	$\frac{Z_m}{D}$	$\frac{W_{m,tw}}{D}$	$\frac{X_m - X_{b,tw}}{Z_m}$	$\frac{X_{e,tw} - X_m}{Z_m}$	$\frac{W_{m,tw}}{2Z_m}$	Beaching
(1)	(2)	(3)	(4)	(5)	(6)	(7)	(8)	(9)	(10)	(11)	(12)
110	4	10	+6.00	17.88	28.91	-4.690	18.38	-2.53	-2.35	-1.96	None.
		31	+4.72	18.37	30.32	-4.899	22.02	-2.79	-2.44	-2.25	"
		100	+4.89	17.33	32.70	-5.083	22.04	-2.45	-3.02	-2.17	"
		316	+3.99	18.59	34.53	-5.224	23.31	-2.79	-3.05	-2.23	"
		1000	+2.92	17.77	34.96	-5.383	23.43	-2.76	-3.19	-2.18	"
		3162	+2.68	18.04	35.28	-5.494	24.98	-2.80	-3.14	-2.27	"
		10000	+1.42	18.48	36.40	-5.794	26.82	-2.94	-3.09	-2.31	"
	∞				-8.05						
1110			+1.12	18.31	34.78	-6.194	28.22	-2.78	-2.66	-2.28	"
108	5	10	+6.10	23.21	33.74	-5.071	23.08	-3.37	-2.08	-2.28	None.
		31	+5.11	22.38	36.19	-5.163	23.80	-3.34	-2.67	-2.30	"
		100	+5.93	22.05	36.62	-5.286	25.05	-3.05	-2.76	-2.37	"
		316	+4.11	21.72	38.95	-5.758	25.50	-3.06	-2.99	-2.21	"
		1000	+2.58	23.15	38.30	-5.654	27.42	-3.64	-2.68	-2.42	"
		3162	+3.38	22.00	40.84	-5.942	27.92	-3.13	-3.17	-2.35	"
		10000	+3.05	21.83	41.80	-5.954	28.71	-3.15	-3.35	-2.41	"
	--		$Z_p/D = 1$	$d_{50}/D = 0.3012$		$(d_{50} = 7.65 \text{ mm})$	$\sigma = 1.26$	$S = 0$			
102	0.5	--	No scour. Stones vibrated in place.								
100	1	10	-1.13	3.97	6.17	-1.506	4.34	-3.39	-1.46	-1.44	None.
		31	-1.08	3.86	5.98	-1.475	4.37	-3.35	-1.44	-1.48	"
		100	-1.09	3.58	6.18	-1.807	4.41	-2.58	-1.44	-1.22	"
		316	-1.25	3.58	6.02	-1.782	5.10	-2.71	-1.37	-1.43	"
		1000	-1.05	3.58	6.98	-1.770	5.49	-2.62	-1.92	-1.55	"
		3162	-1.21	3.86	5.81	-1.985	5.73	-2.68	-1.03	-1.51	"
			--	Test terminated.							
	∞				-3.27						
1100		23053	-1.11	4.24	9.15	-3.058	8.82	-1.75	-1.61	-1.44	"
98	2	10	+0.84	9.02	12.80	-3.341	8.17	-2.45	-1.13	-1.22	None
		31	+2.91	9.02	12.84	-3.457	8.59	-1.77	-1.10	1.24	"
		100	+2.45	8.20	13.05	-3.426	9.58	-1.68	-1.42	-1.40	"
		316	+2.14	8.36	13.59	-3.390	9.82	-1.83	-1.54	-1.45	"
		1000	+2.22	8.91	14.25	-3.629	9.96	-1.84	-1.47	-1.37	"
		3162	+1.68	9.63	13.15	-3.531	10.61	-2.25	-1.00	-1.50	"
		10000	+1.27	8.20	13.56	-3.561	10.82	-1.95	-1.50	-1.52	"
	∞				-4.12						
1098		41162	+1.27	10.87	21.81	-3.650	16.40	-1.70	-1.94	-1.45	"

Table IX-2--Continued
 Summary of experimental data ($d_{50} = 1 \text{ inch} = 0.0833 \text{ ft} = 25.4 \text{ mm}$)

Run	$\frac{Q}{\sqrt{gD^5}}$	Time Minutes	$\frac{X_{b,tw}}{D}$	$\frac{X_m}{D}$	$\frac{X_{e,tw}}{D}$	$\frac{Z_m}{D}$	$\frac{W_{m,tw}}{D}$	$\frac{X_m - X_{b,tw}}{Z_m}$	$\frac{X_{e,tw} - X_m}{Z_m}$	$\frac{W_{m,tw}}{2Z_m}$	Beaching		
(1)	(2)	(3)	(4)	(5)	(6)	(7)	(8)	(9)	(10)	(11)	(12)		
96	3	10	+3.31	13.20	19.55	-4.390	12.01	-2.35	-1.45	-1.37	None.		
		31	+2.58	12.76	18.86	-4.328	12.80	-2.35	-1.41	-1.48	"		
		100	+3.67	13.81	21.42	-4.531	13.59	-2.24	-1.68	-1.50	"		
		316	+1.40	12.49	20.93	-4.568	13.29	-2.43	-1.85	-1.45	"		
		1000	+0.19	12.71	21.90	-4.752	14.79	-2.63	-1.93	-1.56	"		
		3162	+0.25	11.39	21.70	-4.641	14.53	-2.40	-2.22	-1.56	"		
		10000	-0.48	12.21	23.69	-4.813	14.69	-2.64	-2.38	-1.53	"		
		∞					-5.70					"	
1096		28136	+2.36	13.31	29.89	-5.871	20.15	-1.87	-2.82	-1.72	"		
104	4	10	+6.50	18.26	26.67	-4.641	15.52	-2.53	-1.81	-1.67	None.		
		31	+5.18	17.44	28.88	-4.825	15.69	-2.54	-2.37	-1.62	"		
		100	+5.13	16.50	29.01	-4.795	16.12	-2.37	-2.61	-1.68	"		
		316	+4.44	18.97	30.25	-4.844	17.42	-3.00	-2.33	-1.80	"		
		1000	+3.25	16.56	30.05	-4.973	16.89	-2.68	-2.71	-1.70	"		
		3162	+3.35	16.45	31.68	-4.979	17.50	-2.63	-3.06	-1.76	"		
		10000	+2.59	16.83	32.48	-5.095	18.09	-2.79	-3.07	-1.78	"		
		∞					-5.93					"	
1104		11337	+3.66	17.84	33.47	-5.207	18.23	-2.72	-3.00	-1.75	"		
106	5	10	+3.91	22.77	33.90	-4.856	16.90	-3.88	-2.29	-1.74	None.		
		31	+6.41	22.60	34.82	-5.169	18.00	-3.13	-2.36	-1.74	"		
		100	+5.94	22.22	35.55	-4.991	18.65	-3.26	-2.67	-1.87	"		
		316	+7.25	20.35	37.22	-5.249	17.71	-2.50	-3.21	-1.69	"		
		1000	+7.05	20.51	37.63	-5.286	18.32	-2.55	-3.24	-1.73	"		
		3162	+6.82	21.06	35.38	-5.366	18.62	-2.65	-2.67	-1.73	"		
		10000	+4.96	20.18	39.45	-5.163	18.53	-2.95	-3.73	-1.79	"		
		∞					-6.27					"	
1106		8517	+4.00	20.02	39.53	-5.152	19.25	-3.11	-3.79	-1.87	"		
1177	0.5 to 5.0	Step hydrograph test											
		183000	-5.65	14.25	43.80	6.781	23.03	2.94	4.36	1.70	None.		
			$Z_p/D = 1$	$d_{50}/D = 0.0787$		$(d_{50} = 2.00 \text{ mm})$		$\sigma = 1.41$	$S = 0$				
168	0.5	10	-0.79	1.82	5.17	-1.564	5.05	-1.67	-2.14	-1.61	None.		
		31	-0.86	1.44	4.87	-1.630	5.19	-1.41	-2.10	-1.59	"		
		100	-1.26	1.78	5.32	-1.862	6.13	-1.63	-1.90	-1.65	"		
		316	-1.44	1.86	5.58	-1.909	6.18	-1.73	-1.95	-1.62	"		
		1000	-1.51	2.03	5.76	-2.007	6.56	-1.76	-1.86	-1.63	"		
		3162	-1.57	1.99	5.32	-2.023	6.95	-1.76	-1.65	-1.72	"		
		--		Test terminated.									
		∞						-2.09				"	
1168		3224	-2.08	2.85	8.20	-3.319	9.50	-1.49	-1.61	-1.43	"		

Run	$\frac{Q}{\sqrt{gb^5}}$	Time Minutes	$\frac{X_{b,tw}}{D}$	$\frac{X_m}{D}$	$\frac{X_{e,tw}}{D}$	$\frac{Z_m}{D}$	$\frac{W_{m,tw}}{D}$	$\frac{X_m - X_{b,tw}}{Z_m}$	$\frac{X_{e,tw} - X_m}{Z_m}$	$\frac{W_{m,tw}}{2Z_m}$	Beaching
(1)	(2)	(3)	(4)	(5)	(6)	(7)	(8)	(9)	(10)	(11)	(12)
170	1	10	-1.07	2.93	7.35	-2.447	7.80	-1.63	-1.81	-1.59	None.
		31	-1.14	3.02	8.07	-2.443	8.12	-1.70	-2.07	-1.66	"
		100	-1.64	3.36	8.02	-2.435	8.30	-2.05	-1.91	-1.70	"
		316	-1.18	3.32	8.23	-2.643	8.73	-1.70	-1.86	-1.65	"
		1000	-1.57	3.19	7.82	-2.702	9.09	-1.76	-1.71	-1.68	"
		3162	-1.64	3.66	8.91	-3.052	9.98	-1.74	-1.72	-1.63	"
		10000	-1.98	3.75	9.19	-2.993	10.47	-1.91	-1.82	-1.75	"
		∞				-4.79					
1170		10140	-2.01	4.64	12.19	-4.403	12.54	-1.51	-1.71	-1.42	"
172	2	10	+1.39	8.96	16.84	-4.096	13.01	-1.85	-1.92	-1.59	None.
		31	+1.65	9.52	17.70	-4.505	14.24	-1.75	-1.82	-1.58	"
		100	+1.29	9.13	17.47	-4.391	14.76	-1.79	-1.90	-1.68	"
		316	+0.55	9.77	16.81	-4.438	15.68	-2.08	-1.59	-1.77	"
		1000	+0.65	10.20	17.41	-4.548	16.78	-2.10	-1.59	-1.84	"
		3162	-0.43	10.50	18.92	-4.701	17.59	-2.33	-1.79	-1.87	"
		10000	-0.15	10.80	19.58	-4.898	18.82	-2.24	-1.79	-1.92	"
		∞				-5.87					
1172		12745	-0.44	11.91	25.72	-6.131	19.82	-2.01	-2.25	-1.62	"
174	3	10	--	12.81	--	-4.175	Contour map not read.			Yes, unsymmetrical.	
		31	--	14.95	--	-4.454	"	"	"	"	"
		100	--	12.34	--	-5.067	"	"	"	"	"
		316	--	13.41	--	-4.866	"	"	"	"	"
		1000	--	11.48	--	-5.063	"	"	"	"	"
		3162	--	12.92	--	-5.051	"	"	"	"	"
		--	Test terminated. Operation problems.								
1174		11093	--	14.69	--	-5.715	"	"	"	"	"
176	4	--	Not tested.								
178	5	--	Not tested.								

Table IX-2--Continued
 Summary of experimental data ($d_{50} = 1 \text{ inch} = 0.0833 \text{ ft} = 25.4 \text{ mm}$)

Run	$\frac{Q}{\sqrt{gD^5}}$	Time Minutes	$\frac{X_{b,tw}}{D}$	$\frac{X_m}{D}$	$\frac{X_{e,tw}}{D}$	$\frac{Z_m}{D}$	$\frac{W_{m,tw}}{D}$	$\frac{X_m - X_{b,tw}}{Z_m}$	$\frac{X_{e,tw} - X_m}{Z_m}$	$\frac{W_{m,tw}}{2Z_m}$	Beaching
(1)	(2)	(3)	(4)	(5)	(6)	(7)	(8)	(9)	(10)	(11)	(12)
			$Z_p/D = 1$	$d_{50}/D = 0.0787$	$(d_{50} = 2.00 \text{ mm})$	$\sigma = 1.76$	$S = 0$				
180	0.5	10	-0.77	1.74	4.62	-1.658	5.51	-1.51	-1.74	-1.66	None.
		31	-1.04	2.12	5.37	-1.854	6.25	-1.70	-1.75	-1.69	"
		100	-1.15	1.69	5.49	-1.776	6.48	-1.60	-2.14	-1.82	"
		316	-1.19	1.86	5.41	-1.819	6.62	-1.68	-1.95	-1.82	"
		1000	-1.27	1.69	5.92	-1.795	6.59	-1.65	-2.36	-1.84	"
		3162	-1.36	1.74	5.18	-1.772	6.73	-1.75	-1.94	-1.90	"
		10000	-1.29	2.03	5.62	-1.953	7.30	-1.70	-1.84	-1.87	"
		∞				-2.08					
1180		29692	-3.68	3.70	12.15	-5.121	15.20	-1.44	-1.65	-1.48	"
182	1	10	-1.01	3.79	8.32	-2.590	8.67	-1.85	-1.75	-1.67	None.
		31	-1.54	3.32	7.58	-2.570	8.93	-1.89	-1.66	-1.74	"
		100	-1.52	3.79	8.78	-2.998	9.99	-1.77	-1.66	-1.67	"
		316	-1.97	3.62	8.41	-2.912	10.33	-1.92	-1.64	-1.77	"
		1000	-2.11	3.53	8.49	-2.896	10.39	-1.95	-1.71	-1.79	"
		3162	-2.41	3.66	8.19	-2.872	10.59	-2.11	-1.58	-1.84	"
		10000	-2.45	3.75	8.33	-2.802	10.84	-2.21	-1.64	-1.93	"
		∞				-3.53					
1182		22940	-3.97	6.01	17.62	-6.615	20.06	-1.51	-1.76	-1.52	"
184	2	10	+1.73	8.92	15.68	-3.886	13.24	-1.85	-1.74	-1.70	None.
		31	+1.61	8.75	17.03	-4.043	14.14	-1.77	-2.05	-1.75	"
		100	+1.02	9.48	16.30	-4.113	15.02	-2.06	-1.66	-1.83	"
		316	+0.77	9.48	16.93	-4.431	15.65	-1.97	-1.68	-1.77	"
		1000	-0.04	9.82	17.27	-4.290	17.19	-2.30	-1.74	-2.00	"
		3162	-0.24	9.52	16.33	-4.298	17.76	-2.27	-1.58	-2.07	"
		10000	-2.39	9.52	16.79	-4.274	18.27	-2.79	-1.70	-2.14	"
		∞				-5.06					
1184		22621	-2.40	13.41	28.18	-6.658	22.90	-2.38	-2.22	-1.72	"
186	3	10	+1.22	12.68	21.69	-4.310	18.79	-2.66	-2.09	-2.18	Yes, unsymmetrical.
		31	--	12.72	--	-4.722	17.80	Contour map not read.			" "
		100	--	14.35	--	-4.977	--	" "	" "	" "	" "
		316	--	13.37	--	-5.056	--	" "	" "	" "	" "
		1000	--	11.40	--	-5.177	--	" "	" "	" "	" "
		3162	--	13.54	--	-5.417	--	" "	" "	" "	" "
		10000	--	14.18	--	-5.590	--	" "	" "	" "	" "
188	4	--	Not tested.								
190	5	--	Not tested.								

Run	$\frac{Q}{\sqrt{gD^5}}$	Time Minutes	$\frac{X_{b,tw}}{D}$	$\frac{X_m}{D}$	$\frac{X_{e,tw}}{D}$	$\frac{Z_m}{D}$	$\frac{W_{m,tw}}{D}$	$\frac{X_m - X_{b,tw}}{Z_m}$	$\frac{X_{e,tw} - X_m}{Z_m}$	$\frac{W_{m,tw}}{2Z_m}$	Beaching
(1)	(2)	(3)	(4)	(5)	(6)	(7)	(8)	(9)	(10)	(11)	(12)
Horizontal fixed bed at $(Z_{m,u}/D)_{\text{computed}} = -0.5$											
$Z_p/D = 1 \quad d_{50}/D = 0.0724 \quad (d_{50} = 1.84 \text{ mm}) \quad \sigma = 1.22 \quad S = 0$											
179	0.5	11	-0.89	1.76	5.06	-1.862	5.96	-2.63	-3.32	-1.60	None. Bed not exposed.
		31	-1.09	1.76	5.38	-1.725	5.97	-2.90	-3.57	-1.73	" " " "
		100	-1.20	1.76	5.48	-1.686	5.90	-3.09	-3.59	-1.75	" " " "
		316	-1.22	1.76	5.11	-1.721	5.98	-3.18	-3.15	-1.74	" " " "
		1000	-1.29	1.68	5.80	-2.102	6.44	-3.32	-3.77	-1.53	" " " "
		3162	-1.39	1.64	5.59	-2.028	6.60	-3.48	-3.50	-1.63	" " " "
		9970	-1.52	1.64	5.90	-2.173	6.99	-3.67	-3.75	-1.61	" " " "
1179		14203	-3.29	1.72	11.44	-3.276	12.59	-7.01	-7.72	-1.92	" Fixed bed exposed.
181	1	10	-0.69	4.18	8.37	-2.833	8.22	-4.42	-4.64	-1.45	None. Bed not exposed.
		31	-1.14	3.35	9.22	-3.159	9.14	-5.04	-5.32	-1.45	" " " "
		100	-1.44	3.47	8.97	-3.225	9.30	-5.51	-4.90	-1.44	" Bed exposed w/flow.
		316	-1.25	3.73	9.83	-3.524	10.53	-5.47	-5.61	-1.49	" " " " "
		1000	-1.61	3.56	9.62	-3.473	10.65	-5.96	-5.27	-1.53	" " " " "
		3162	-1.52	3.52	9.55	-3.414	10.72	-6.00	-5.07	-1.57	" " " " "
		10000	-1.54	3.56	9.14	-3.382	11.10	-6.14	-4.54	-1.64	" " " " "
1181		22809	-2.78	4.42	11.58	-3.689	15.98	-9.98	-7.38	-2.17	" Fixed bed exposed.
183	2	10	+1.62	8.39	13.77	-3.677	11.16	-7.14	-5.01	-1.52	None. Bed not exposed.
		31	+1.43	11.26	17.80	-3.803	15.42	-7.63	-8.74	-2.03	" Fixed bed exposed.
		100	+0.78	13.52	20.78	-3.866	17.44	-8.54	-11.46	-2.26	" " " "
		316	+0.41	13.78	20.92	-3.865	18.14	-9.14	-11.37	-2.35	" " " "
		1000	-0.41	14.93	22.45	-3.901	18.97	-10.16	-12.70	-2.43	" " " "
		3162	-0.68	15.83	23.31	-3.893	20.50	-10.61	-13.38	-2.63	" " " "
		10012	-0.33	15.45	23.55	-3.897	21.21	-10.42	-13.46	-2.72	" " " "
1183		54322	-0.60	15.79	27.27	-3.920	25.02	-13.60	-14.27	-3.19	" " " "
185	2.5	10	+1.70	13.99	23.31	-3.881	17.99	-9.54	-12.07	-2.32	None. Fixed bed exposed.
		31	+1.41	14.81	23.22	-3.893	19.80	-10.13	-11.68	-2.54	" " " "
		100	-0.24	15.66	25.17	-3.885	22.61	-12.04	-13.37	-2.91	" " " "
		327	-1.36	14.68	27.45	-3.913	27.49	-13.39	-15.42	-3.51	" " " "
		1000	-1.19	15.40	29.79	-3.928	27.82	-13.41	-17.57	-3.54	" " " "
		3162	-1.98	15.58	30.87	-3.912	30.34	-14.37	-18.48	-3.88	" " " "
		10000	-4.17	15.58	33.32	-3.904	33.55	-16.72	-20.77	-4.30	" " " "
1185		31462	-4.60	13.97	36.08	-3.912	36.91	-19.78	-21.90	-4.72	" " " "
187	3	10	+1.69	14.51	22.34	-3.889	20.78	-11.74	-8.91	-2.67	None. Fixed bed exposed.
		31	+0.09	15.28	27.09	-3.908	26.71	-13.62	-13.38	-3.42	" " " "
		100	+0.00	14.29	30.29	-3.904	31.87	-13.95	-16.34	-4.08	" " " "

X. ANALYSES OF TEST RESULTS

Analyses of the experimental data can begin now that the introductory information has been presented. Not all experimental data were used in the analyses, as explained under the immediately following subhead "Beaching Limit." Determination of the beaching limit and the data to be included in the analyses was the first analytical step. The second step was to develop equations to define the shape of the contours. Using suitable parameters, it was found possible to collapse all scour hole contours into a single dimensionless pattern. The third step was to evaluate the parameters in the dimensionless contour equations: the coordinates of the x and y axes of the scour hole, the distance to the maximum scour depth, and the ultimate and time-dependent scour depths. The fourth step was to compare the computed and experimental scour holes to determine how well the equations represented the data. Finally, the effect of a nonerodible layer on the scour was analyzed.

Beaching Limit

Two general shapes of scour hole are described in chapter VI: (1) a scour hole having the general shape of an inverted cone with side slopes approximating the angle of repose of the bed material (figure VI-2(a-c)), and (2) a scour hole with a conical bottom but with beaches near the top of the hole (figure VI-2(d-f)). When these beaches existed, the beach slopes were relatively flat, flow over the beaches was in an upstream direction, and dunes formed and moved upstream on the beaches. When beaches formed, the surface of the scour hole was very wide--excessively wide, we feel.

The desirable scour hole--and plunge pool--shape is felt to be of the nonbeaching conical form. Therefore, the conditions separating the beaching from the nonbeaching scour holes were sought. The criteria are developed in this section of this report.

Listed in table IX-2 are the test parameters and notes concerning beaching. The beaching notes are based on an inspection of the computer-generated plots of the scour hole dimensionless contours and on cross section profiles. A typical nonbeaching contour plot is shown in figure VI-3 and a typical plot with beaches is shown in figure VI-4. Small irregularities in the contours near the top of the scour hole indicate that beaching is imminent. Large irregularities in the upper contours indicate that the beaching is extensive and that there are dunes on the beaches. The cross section profiles shown in figure VI-2 also indicate beaching if the side slopes, which are at the approximate angle of repose of the bed material near the bottom of the scour hole, become relatively flat near the top of the scour hole.

The data of table IX-2 are plotted in figure X-1. Interpretation of figure X-1 requires explanation because of the way the data are plotted. Each box represents--collapses to--a single point on the plot and provides beaching data for one or more test runs. The data points for each run are arranged horizontally, each data point corresponding to a cumulative time interval in the test, as explained more fully in the following paragraph. The shading of the data points indicates the absence (open circles), degree (partially darkened circles), and presence (solid circles) of beaching.

The abscissa is in terms of relative discharge $Q/\sqrt{gD^5}$. Each box along the abscissa represents a single relative discharge. Distributed horizontally in each box is the time from the beginning of the test run in minutes expressed in exponential form. For example, $n = 1$ represents 10 min, $n = 2$ represents 100 min, $n = 2.5$ represents 316 min, and so forth. R indicates a run in which the suspended material was removed.

The ordinate is in terms of relative bed material size d_{50}/D . Each box along the ordinate represents a single bed material size. Distributed vertically within the boxes for $d_{50}/D = 0.0724$ ($d_{50} = 1.84$ mm) are relative cantilevered pipe heights Z_p/D . Other bed material sizes were tested only for $Z_p/D = +1$. The paired pipe slopes alongside the $Q/\sqrt{gD^5} = 2$ and 3 boxes for $d_{50}/D = 0.0724$ indicate comparison runs: the upper of each pair having a zero pipe slope and varying pipe height, and the lower having a zero or plus one pipe height and a pipe slope producing the same angle of entry of the jet into the pool surface. Plotted in the $d_{50}/D = 0.0787$ boxes are data for two gradations of bed material, $\sigma = 1.41$ and 1.76.

From an inspection of figure X-1, the approximate nonbeaching limits of $Q/\sqrt{gD^5}$ for each bed material size can be read. These limits are plotted in figure X-2. The equation of the line of best fit that represents the beaching limit--the minimum size of bed material that will not beach at a given discharge--is

$$\frac{d_{50}}{D} \geq -0.04 + 0.04 \frac{Q}{\sqrt{gD^5}} \quad (X-1)$$

No beaching limit was obtained for the tests using $d_{50}/D = 0.3012$ (7.65 mm) bed material: the arrow indicates that the data point should be located somewhere to the right of the actual plotted location.

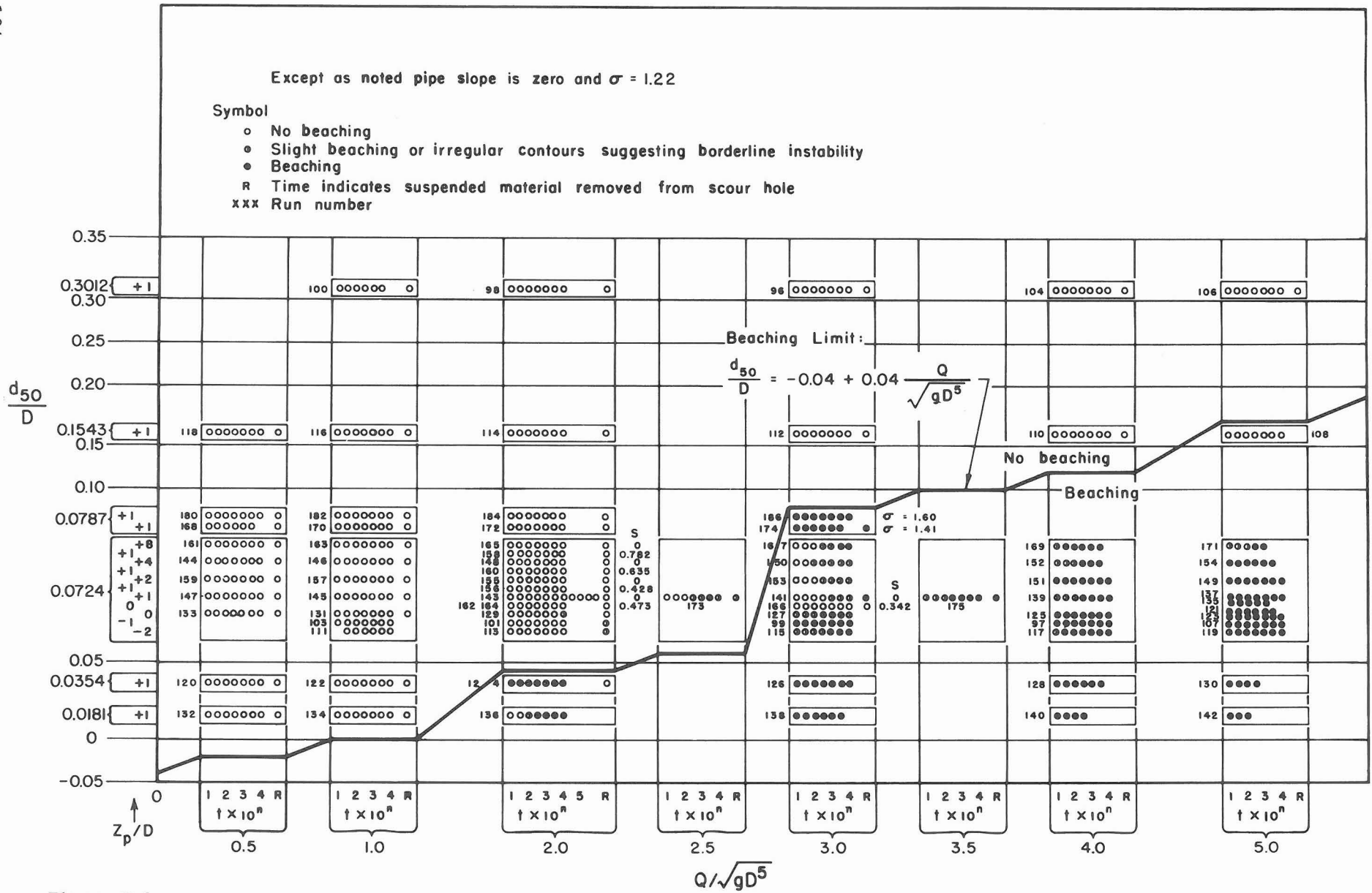


Figure X-1
Scour hole beaching.

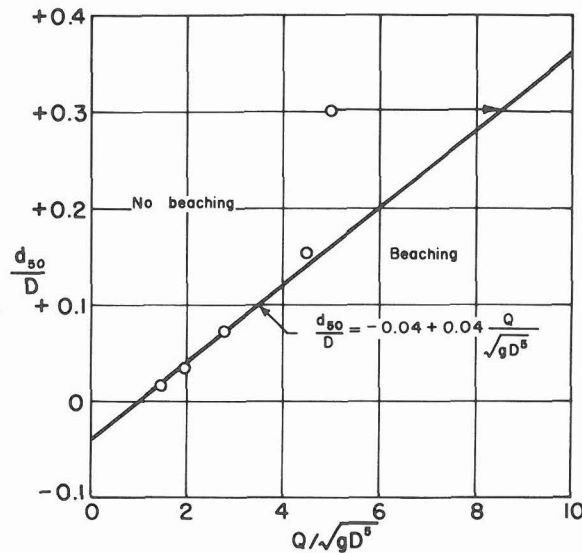


Figure X-2
Beaching limit.

Equation X-1 is plotted in figure X-1. It can be noted that all beaching data and almost all borderline data are covered by the curve representing the equation. The conclusion is that equation X-1 adequately represents the beaching limit.

When equation X-1 is solved for the dimensionless discharge,

$$\frac{Q}{\sqrt{gD^3}} \leq 1.0 + 25 \frac{d_{50}}{D} \tag{X-2}$$

After this limiting discharge was determined, most tests were run at or below the limiting discharge given by equation X-2. Also, because beaching is associated with an excessively wide scour hole and, thus, was felt to be unacceptable, only the nonbeaching data were used in subsequent analyses. The test runs on which subsequent analyses were made are listed in table X-1.

Dimensionless Contour Analysis

There are numerous steps between taking the initial measurements of the scour hole shape and plotting the dimensionless and normalized contour map. Development of procedures for plotting the contour map and evaluation of the parameters and equations that normalize and describe the contour pattern in dimensionless units were the primary objectives of this study. Evaluation of these items provides the basis for proportioning plunge pool energy dissipators. In this section the steps that led to the contour maps will be described in some detail. During this process, the pertinent parameters will become apparent. This section will conclude with the development of equations that mathematically describe the contours.

Table X-1
Nonbeaching runs used in analyses

		$Q/\sqrt{gD^5}$						
		0.5	1	2	2.5	3	4	5
Pipe Height ($d_{50} = 1.84$ mm, $d_{50}/D = 0.0724$, $\sigma = 1.22$, $S = 0$)								
	Z_p/D							
	-2							
	-1				101			
	0	133	131	129				
	+1	147	145	143	173			
	+2	159	157	155				
	+4	144	146	148				
	+8	161	163	165				

Pipe Slope ($d_{50} = 1.84$ mm, $d_{50}/D = 0.0724$, $\sigma = 1.22$)								
	S	Z_p/D						
	0.473	0		164				
	0	+1		143				
	0.428	+1		156				
	0	+2		155				
	0.635	+1		160				
	0	+4		148				
	0.782	+1		158				
	0	+8		165				

Bed Material Size ($Z_p/D = +1$, $S = 0$)								
	d_{50}	d_{50}/D	σ					
	0.46 mm	0.0181	1.24	132	134			
	0.90 mm	0.0354	1.24	120	122			
	1.84 mm	0.0724	1.22	147	145	143		
	3.92 mm	0.1543	1.23	118	116	114	112	110
	7.65 mm	0.3012	1.26		100	98	96	104
								106

Standard Deviation of Bed Material ($d_{50} = 2.00$ mm, $d_{50}/D = 0.0787$, $Z_p/D = +1$, $S = 0$)								
		σ						
		1.22	147	145	143			
		1.41	168	170	172			
		1.76	180	182	184			

Time-dependent runs have the listed 3-digit Nos. (XXX);
suspended-material-removed runs have 4-digit Nos. (LXXX).

The initial measurements were made in a manner to facilitate subsequent computations. First, a center line profile of the bed was simultaneously recorded digitally on punched paper tape and graphically by an X-Y recorder. The stationing and elevation of the beginning and end of the scour hole and the point of maximum depth of scour were noted on the X-Y recorder chart. Then, the about 20 cross sections required to adequately define the contours were taken at approximately uniform intervals along the scour hole, making certain that one of the cross sections was taken through the point of maximum scour depth. Each cross section profile was recorded on the X-Y recorder chart, and X, Y and Z coordinates of points along each cross section were read onto punched paper tape at frequent intervals, making sure that points close to and on both sides of any change in the bed slope were recorded.

The punched paper tape data were fed into a computer to grid the data for a plotting program. No satisfactory gridding program was discovered in 1975 when computer plotting of the scour hole contours was initiated, so a gridding program was written that was especially adapted to the manner in which the data were acquired. The first gridding step was to interpolate linearly along cross sections to determine the elevations at grid lines. The second gridding step was to interpolate along grid lines to determine the elevations at grid intersections. Using the gridded data, the University of Minnesota Computer Center's CNTOUR plotting program was used to generate a plot tape. A PLOTPAC program plotted a contour map, a center line profile, and a cross section at the point of deepest scour on a 30-inch-wide Calcomp plotter. This large plotter was used because information was scaled from the plots. (Near the end of the test program the Calcomp plotter was replaced with a 14-inch-wide Varian electrostatic plotter on which the same scale was used in plotting contour maps. When the width of the map exceeded the plotter width, the map was plotted in halves and spliced along its center line.) Initially contours were plotted in terms of the pipe diameter. However, to facilitate normalization, analyses, and comparisons, all contour maps used in this analysis were plotted in terms of the maximum depth of scour. Contours at the water surface ($0.0Z_m$) and $0.2Z_m$, $0.4Z_m$, $0.6Z_m$ and $0.8Z_m$ were plotted. Here Z_m is the maximum depth of scour below the tailwater surface. Example plots are shown in figures VI-3 and VI-4.

The distances from the center of the scour hole--distance X_m from the pipe exit--to the beginning ($X_m - X_b$), to the end ($X_e - X_m$), and to the sides at the deepest point ($W_m/2$) were chosen as normalizing parameters for the scour hole contours. Accurately taking these dimensions from the sections proved difficult due to scour hole irregularities. Because of its indefiniteness,

the downstream end of the scour hole proved especially difficult to determine. The precision and consistency of the readings were improved by projecting the slopes of the scour hole to the water surface; these distances from the point of deepest scour are designated $(X_m - X_{b,tw})$, $(X_{e,tw} - X_m)$ and $(W_{m,tw}/2)$ and were used for all subsequent analyses.

The contour map was analyzed after the limits of the scour hole had been determined. First, the center of the scour hole was located on the contour map. Then, as shown in figure VI-3, cross sections were drawn each tenth of the distance from the scour hole center to both the upstream and downstream ends of the hole. Upstream of the scour hole center--the origin for the contour pattern--these distances are in terms of $(X - X_m)/(X_m - X_{b,tw})$ and are negative. Downstream of the center these distances are in terms of $(X - X_m)/(X_{e,tw} - X_m)$ and are positive. At each of the 21 cross sections, the distance Y from the center line to each contour intersection was scaled and recorded.

For each cross section and contour, the two values of Y were summed without regard to sign and divided by $W_{m,tw}$ to give the average distance from the center line to the contour. For the time-dependent data, scanning the tabulation for each run showed that the values of $2Y/W_{m,tw}$ for all seven test times were in reasonable agreement, so they were averaged. For the suspended-material-removed data, only a single value of $2Y/W_{m,tw}$ was available for each intersection.

With normalized, dimensionless values of the contours now available, the contours were plotted and compared. Figure X-3 is an example plot. Similar plots were prepared for all test runs for both the time-dependent and suspended-material-removed tests. These plots were used to develop and verify the equation defining the contours.

In developing a geometrical representation of the contours, it was assumed that the adopted curves should substantially circumscribe the plotted data to ensure that the recommended shape would not scour. By trial it was found that an ellipse best fitted the time-dependent data. Although a circle better fitted much of the suspended-material-removed data, an ellipse was also satisfactory. Independent evaluations of the fit by Anderson and Blaisdell were almost identical: They agreed that elliptical equations satisfactorily represented both the time-dependent and suspended-material-removed contours.

In the general equation for an ellipse,

$$\frac{x^2}{a^2} + \frac{y^2}{b^2} = 1 \quad (X-3)$$

the x-axis is defined by

$$x_{us} = \frac{X - X_m}{X_m - X_{b,tw}} \quad (X-4a)$$

for the upstream half of the ellipse, by

$$x_{ds} = \frac{X - X_m}{X_{e,tw} - X_m} \quad (X-4b)$$

for the downstream half of the ellipse, and the y-axis is defined by

$$y = \frac{2Y}{W_{m,tw}} \quad (X-5)$$

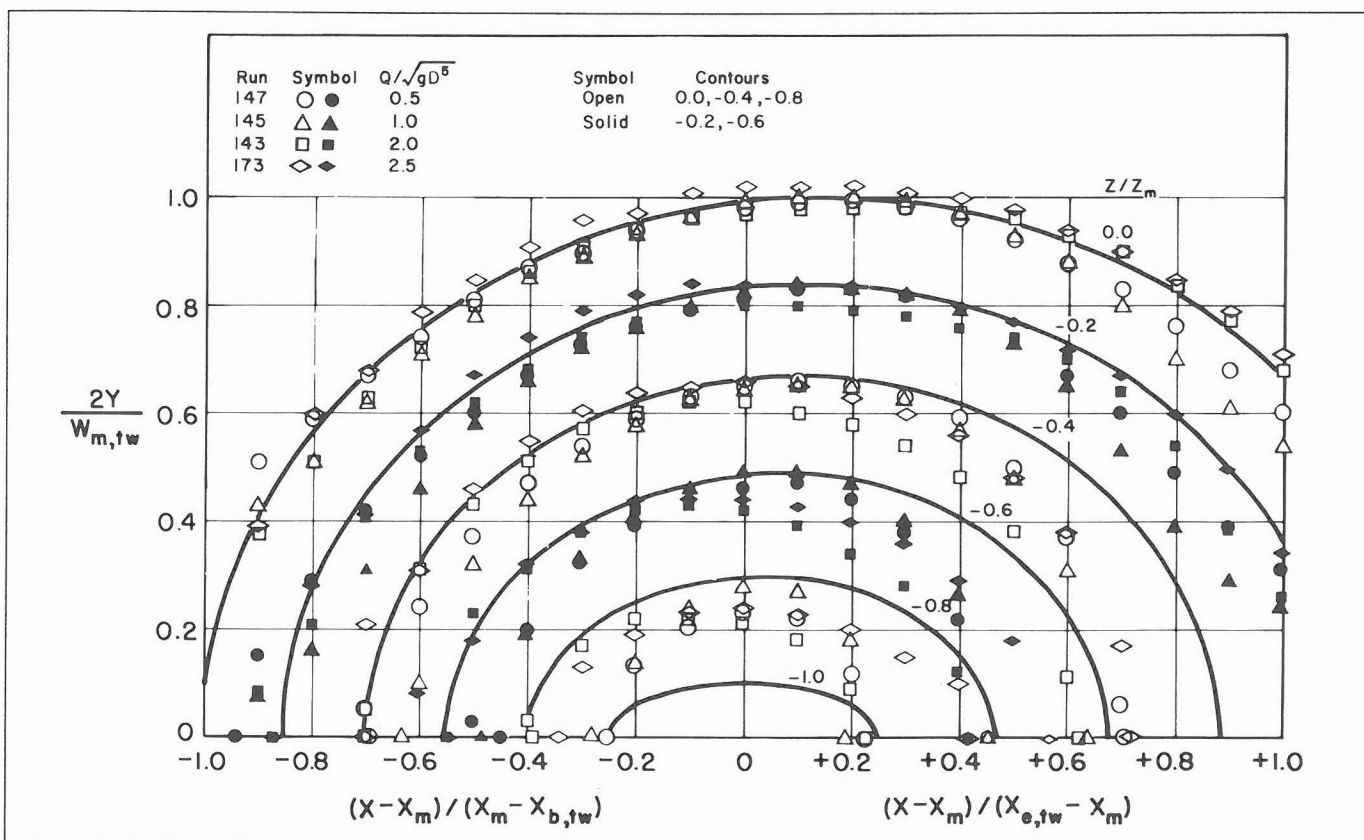


Figure X-3
 Example of average normalized dimensionless time-dependent contour data, for $d_{50} = 1.84$ mm, $d_{50}/D = 0.0724$, $\sigma = 1.22$, $Z_p/D = +1$, and $S = 0$.

The coefficients a and b were determined by inspection of the extremities of the ellipses and adjustment to constants of the first and second differences, respectively, between contour values. The adopted values of these coefficients are, for the x-axis

$$a = 1.15 - 0.90 \frac{Z}{Z_m} \quad (X-6)$$

and, for the y-axis,

$$b = 1.00 - 0.775 \frac{Z}{Z_m} - 0.125 \left(\frac{Z}{Z_m}\right)^2 \quad (X-7)$$

However, inspection of the contour data plots showed that the centers of the ellipses shifted downstream with increase in the contour elevation. The zero correction 0_{corr} to the value of X_m to locate the center of each elliptical contour is

$$0_{\text{corr}} = 0.15\left(1 - \frac{Z}{Z_m}\right) \quad (X-8)$$

Substituting the values given in equations X-4 through X-8 into equation X-3 and solving for the x parameters, the equation for the contours reads

$$\begin{aligned} \frac{X - X_m}{X_m - X_{b,tw}} &= \frac{X - X_m}{X_{e,tw} - X_m} \\ &= 0.15\left(1 - \frac{Z}{Z_m}\right) \mp \left(1.15 - 0.90 \frac{Z}{Z_m}\right) \times \\ &\quad \sqrt{1 - \left[\frac{2Y/W_{m,tw}}{1.00 - 0.775(Z/Z_m) - 0.125(Z/Z_m)^2} \right]^2} \end{aligned} \quad (X-9)$$

Equation X-9 has been plotted in figure X-3. There it can be seen that the equation substantially circumscribes the contour data. The fit of all other data was generally in similar agreement with equation X-9.

Parameter Evaluation Use of the equation for the contours representing the scour hole shape requires that the parameters in the equation be evaluated. The parameters are the scour hole axes coordinates--the upstream ($X_m - X_{b,tw}$) and downstream ($X_{e,tw} - X_m$) half-length parameters and the half-width ($W_{m,tw}/2$) parameter,--the distance from the pipe exit to the maximum scour depth (X_m), and the maximum scour depth (Z_m). This evaluation will be done in the following three subsections.

Scour Hole Axes Coordinates

The magnitudes of the scour hole axes coordinates determine the maximum dimensions of the scour hole. These dimensions are given by the length and width parameters $(X_m - X_{b,tw})$, $(X_{e,tw} - X_m)$, and $(W_{m,tw}/2)$. These parameters are related to the maximum scour depth Z_m , and the ratios of the parameter lengths to the scour depth are a rough approximation of the scour hole side slopes. These ratios were used in the analyses of the experimental data.

Initially, the ratios for each time of test were plotted against time. Inspection showed, however, that the variation with time was erratic and that there was no detectable consistent trend to the variation. Therefore, for subsequent analyses, values of the ratios for all times of scour were averaged. Further initial analyses showed that these ratios varied with the dimensionless discharge $Q/\sqrt{gD^5}$.

The experimental data are plotted in figures X-4 through X-7. For easier identification, the data are spread out in groups of $Q/\sqrt{gD^5}$, each group representing a single point on the abscissa. For convenience, the spread in each constant discharge group in figures X-4 and X-6 are plotted according to pipe height, and the spread in figures X-5 and X-7 according to sediment particle size. The data in figures X-4 and X-5 are for the half-length parameters, and the data in figures X-6 and X-7 are for the half-width parameter. Because the upstream and downstream half-length data seemed to fall together, they were plotted on the same figure. The open symbols represent averages of the time-dependent observations; the solid symbols, single observations of the observed suspended-material-removed dimensions.

There is considerable scatter to some of the data. Some scatter is to be expected because of the nature of the experiments, but what is reasonable is not known. Scour was absent or negligible for the two lowest discharges when the pipe was submerged ($Z_p/D = -1$ and -2), so no data are plotted for the lowest submerged pipe discharges. For the submerged pipe and discharge of 2, the jet was supported by the tailwater and the scour hole was very long in comparison to the other holes. Obviously, the curve as drawn does not represent this condition. The values for the time-dependent tests also are high for the lowest discharge (0.5) and two highest pipes. The reason eludes us.

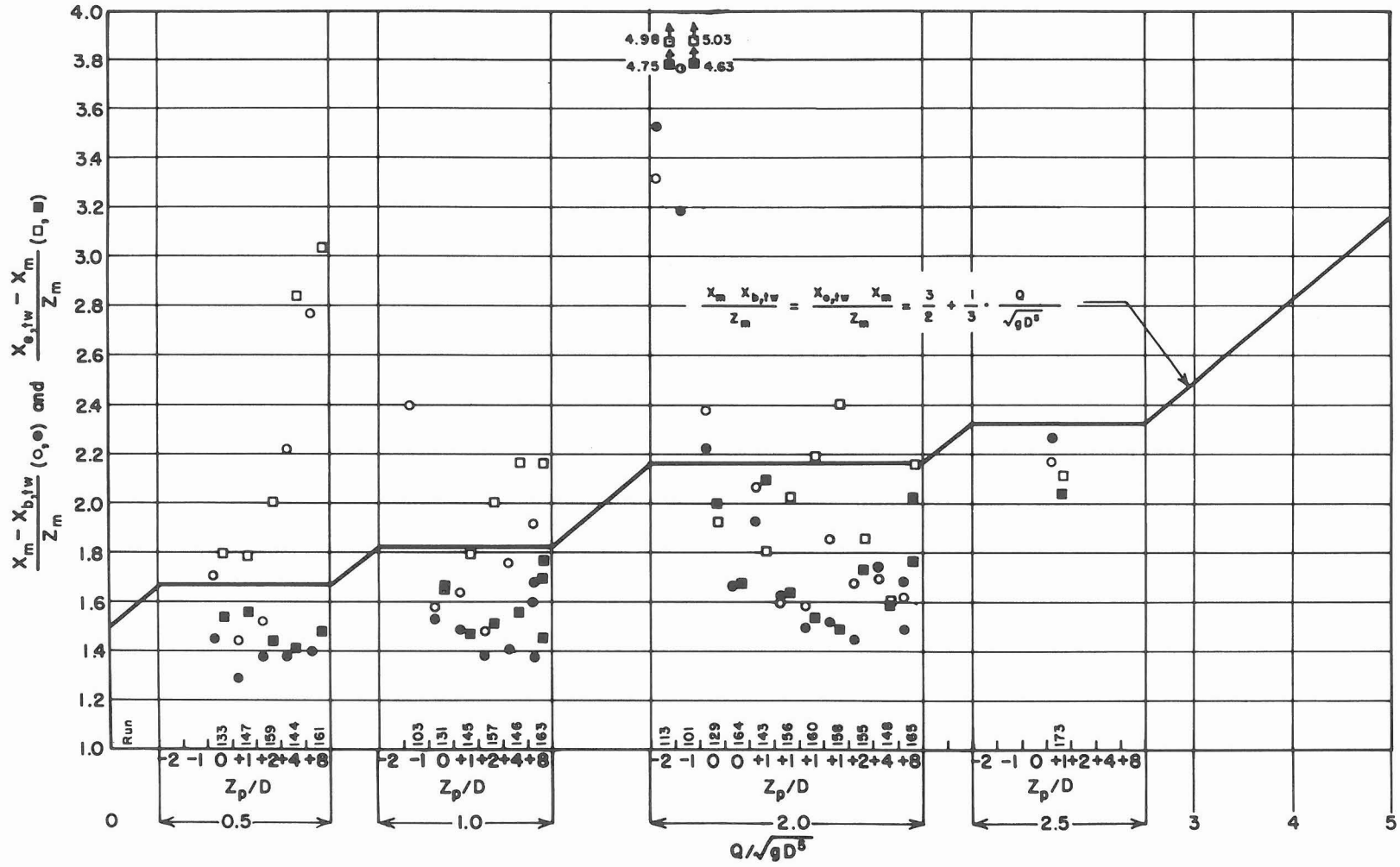


Figure X-4
 Center line scour hole axis coordinates, for pipe height data,
 $d_{50}/D = 0.0724$, and $d_{50} = 1.84$ mm: open symbols = time-
 dependent data, solid symbols = suspended-material-removed data.

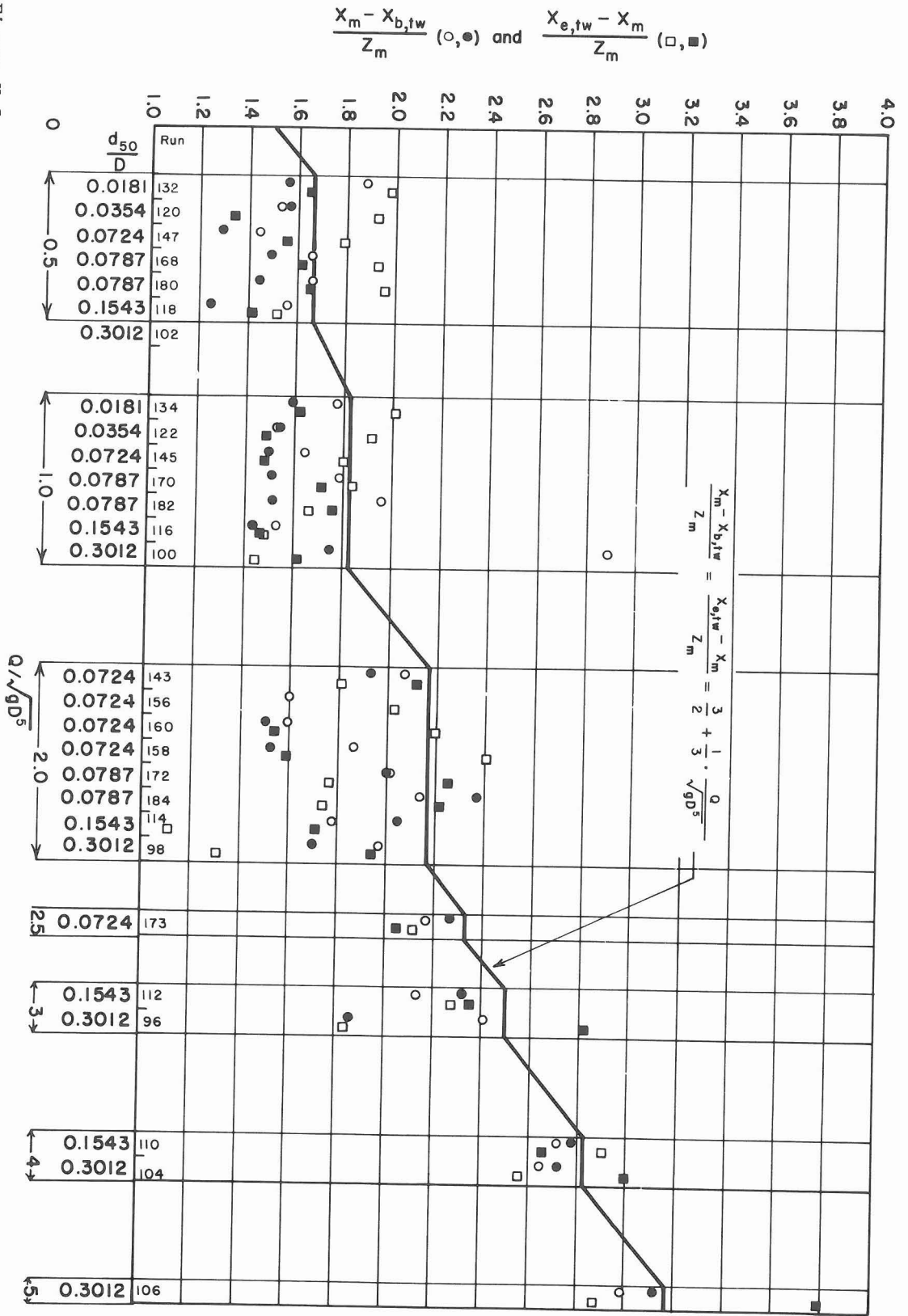


Figure X-5
 Center line scour hole axis coordinates, for sediment size data,
 and $Z_p/D = +1$: open symbols = time-dependent data, solid symbols
 = suspended-material-removed data.

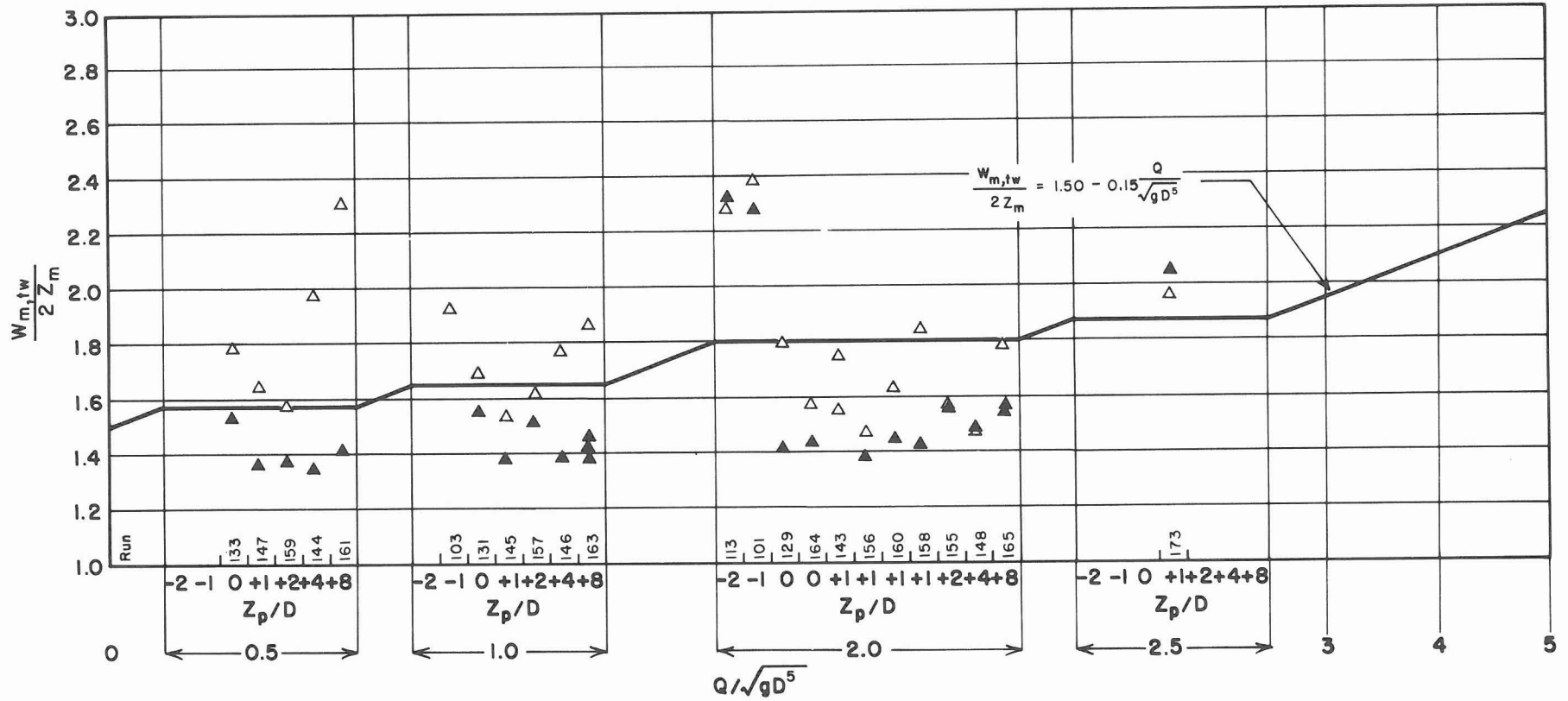
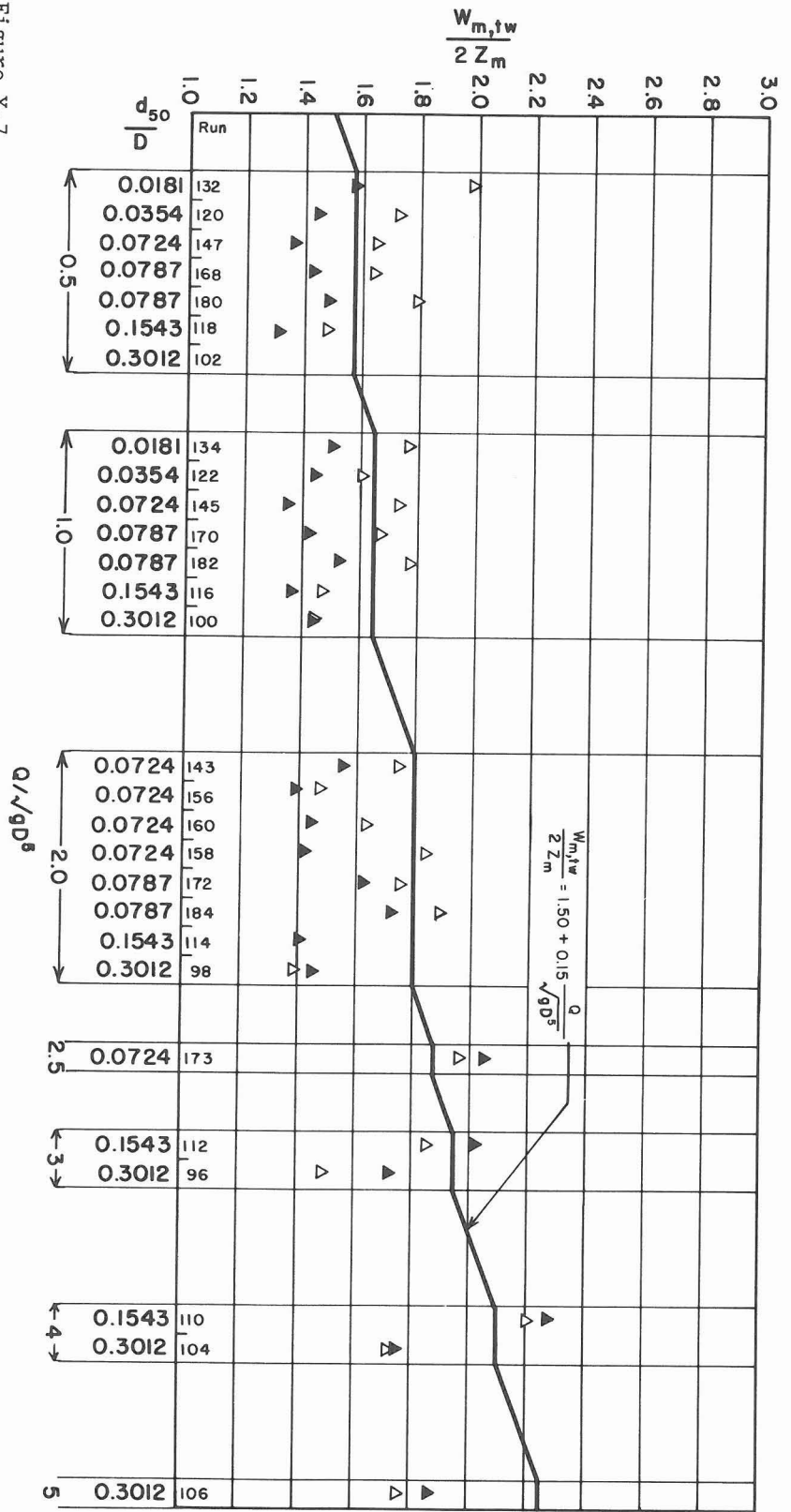


Figure X-6
 Width scour hole axis coordinates, for pipe height data, $d_{50}/D = 0.0724$, and $d_{50} = 1.84$ mm: open symbols = time-dependent data, solid symbols = suspended-material-removed data.



The curves shown in the figures are suggested as being reasonable representations of the results. They are drawn as approximate, sufficiently conservative envelopes of the data. The equation for the upstream and downstream half-lengths of the scour hole is

$$\frac{X_m - X_{b,tw}}{Z_m} = \frac{X_{e,tw} - X_m}{Z_m} = \frac{3}{2} + \frac{1}{3} \frac{Q}{\sqrt{gD^5}} \quad (X-10)$$

and that for the half-width is

$$\frac{W_{m,tw}}{2Z_m} = 1.5 + 0.15 \frac{Q}{\sqrt{gD^5}} \quad (X-11)$$

Distance to Maximum Scour Depth

As described in the section on the jet trajectory and shown in figure VIII-1, the distance from the pipe exit to the point where the scour depth is maximum, X_m , is related to the trajectory of the jet issuing from the pipe. Therefore, in the following analysis the distance to the maximum scour depth is expressed as a ratio of the computed jet trajectory length X_j . It was anticipated, a priori, that the ratio X_m/X_j would be in the vicinity of 1.0.

An important point that was kept in mind throughout the analysis is that the distance to the maximum scour depth determines the location of the center of the scour hole and, in the case of a plunge pool energy dissipator, the location of the plunge pool relative to the pipe exit. If the plunge pool is located too far upstream, the jet will attack and erode the downstream end of the pool. This has happened in some plunge pools designed on the basis of earlier criteria. On the other hand, if the plunge pool is located too far downstream, the jet may strike the upstream slope and subject the upstream end of the plunge pool to intensive attack and erosion, thereby endangering the dam. Determining the proper value of X_m is therefore important.

For oblique jets impinging on a solid surface, Beltaos (1976) had found that the stagnation point was not at the projected center line of the jet but was removed from the center line by a distance s . In an attempt to better define the location of the center of the scour hole, the distance X_m was corrected by s . The corrected distance $(X_m + s)/X_j$ was then compared with the uncorrected distance X_m/X_j . The comparison was made for each run on the averages of the ratios for all length-of-scour times. The standard deviations for both ratios were low; the probable error of the average indicated that either average would define the location of the scour hole center within about one pipe

diameter. Therefore, averages were used for subsequent analyses. The subsequent comparisons showed that the standard deviations of the corrected and uncorrected ratios were almost identical. This indicates that both ratios have the same precision. It follows that either ratio will satisfactorily predict the distance to the maximum scour depth. As a result, only the simpler X_m/X_j ratio was used in subsequent analyses.

The distance to the maximum depth of scour was analyzed first by computing X_j based on the observed depth of scour. After equations had been developed for the maximum scour depth Z_m , the distance to the maximum scour depth was reanalyzed using the recommended-equation value of the maximum scour depth to compute X_j . The objective was to determine the effect on X_m of using the recommended-equation values instead of observed values of Z_m . The results of these analyses are presented in the following subsections.

Distance based on observed scour depth. Early plots of incomplete data indicated that X_m/X_j varied with $Q/\sqrt{gD^5}$ when Z_m in the equation

$$X_j = X_p - \frac{Z_m}{\tan \alpha} \quad (\text{VIII-7})$$

is based on the observed scour depth. This variation was confirmed by a well-defined relationship obtained when the suspended-material-removed data were plotted. The variation was eliminated by multiplying the observed value of $Z_m/\tan \alpha$ by $\sin \alpha$. Multiplying by $\sin \alpha$ can be considered a modification to correct Z_m for the vertical component of the plunge velocity -- the component of the plunge velocity that determines the depth of scour. And it can be shown that the plunge velocity is related to the relative discharge for which a correction is indicated. Therefore, to compensate for the effect of discharge, the equation used to compute the jet impingement length is

$$X_j = X_p - Z_m \frac{\sin \alpha}{\tan \alpha} \quad (\text{X-12a})$$

The inverts of some pipes were at or below the tailwater level; that is, Z_p/D was zero or negative. For these high-tailwater conditions the jet was partially or wholly supported by the tailwater and the equation for the jet trajectory was invalid. For purposes of analysis, it was assumed that

$$\text{for } \frac{Z_p}{D} < +1, \text{ use } \frac{Z_p}{D} = +1 \quad (\text{X-12b})$$

Average values of X_m/X_j based on the observed values of Z_m for all the time-dependent data and observed values for the suspended-material-removed data are plotted in figures X-8 through X-11. For each discharge, the figures show the variation of X_m/X_j with, respectively, (1) pipe height, (2) sediment size, (3) sediment size distribution, and (4) jet impingement angle for four combinations of pipe slope and pipe height. In figure X-9, beaching existed for those runs labeled "B," and the data are not plotted.

The range in X_m/X_j is from about 0.9 to 1.3. No explanation is available as to why the data for $Q/\sqrt{gD^5} = 1$ fall below the other data, but the difference appears to be real.

The submerged pipe height data in each group in figure X-8 are separated by a dashed line to indicate that the jet was partially or wholly supported and that different scour criteria

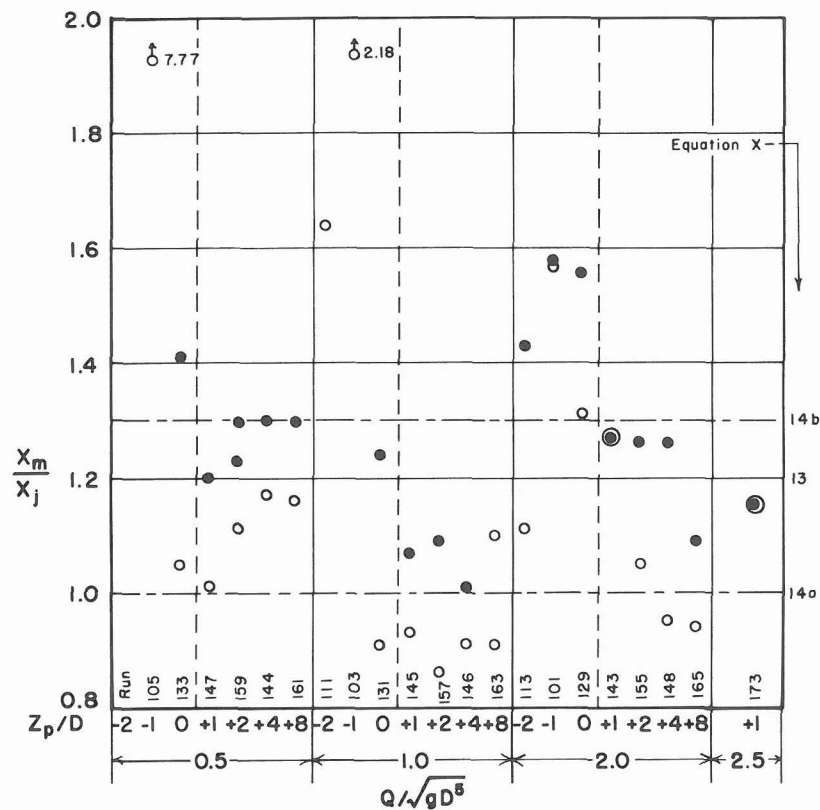


Figure X-8
Distance to observed maximum scour depth in terms of computed jet trajectory length based on observed maximum scour depth, for pipe height data, $d_{50}/D = 0.0724$, and $d_{50} = 1.84$ mm: open symbols = time-dependent data, solid symbols = suspended-material-removed data.

probably apply. For example, there was no observable scour for $Q/\sqrt{gD^5} = 0.5$ when $Z_p/D = -2$ and -1 . For $Q/\sqrt{gD^5} = 1$ and similar pipe heights, there was little scour and the scour hole was shallow making difficult the determination of X_m . The same comment applies for $Q/\sqrt{gD^5} = 2$ and $Z_p/D = -2$, while for $Z_p/D = -1$, X_m was reasonably well defined. In general, the data available to determine X_m/X_j when the pipe is submerged are limited because there was little or no scour at high pipe submergences and low discharges.

Considerable randomness in the data is apparent in all plots. As a result, if there is any trend with any variable, the trend is lost in the experimental variation. Therefore, it is concluded that the ratio X_m/X_j is a constant with respect to relative discharge $Q/\sqrt{gD^5}$ (figures X-8 through X-11), relative pipe height Z_p/D (figure X-8), relative sediment size d_{50}/D (figure X-9), geometric sediment size distribution σ over the limited range tested (figure X-10), and jet impingement angle α (figure X-11).

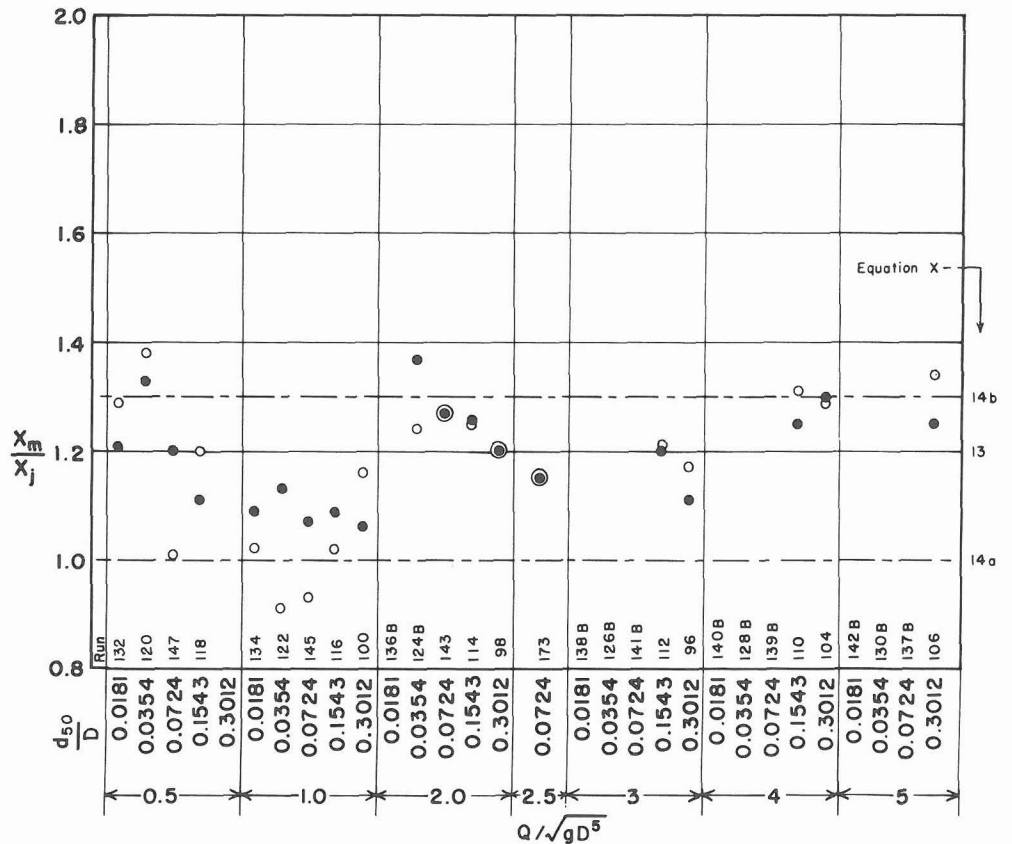


Figure X-9
Distance to observed maximum scour depth in terms of computed jet trajectory length based on observed maximum scour depth, for sediment size data, and $Z_p/D = +1$: open symbols = time-dependent data, solid symbols = suspended-material-removed data.

Either of two criteria may be used to define X_m/X_j : (1) an average value, recognizing that the ends of the elliptic scour hole or plunge pool may be subject to attack that may erode material or (2) a low envelope value of X_m/X_j for the upstream half of the elliptical hole and a high envelope value for the downstream half, joining the two halves with straight parallel sides. For alternative (1), the suggested average distance to the center of the scour hole or plunge pool $X_{m,a}$ is

$$\frac{X_{m,a}}{X_j} = 1.2 \quad (X-13)$$

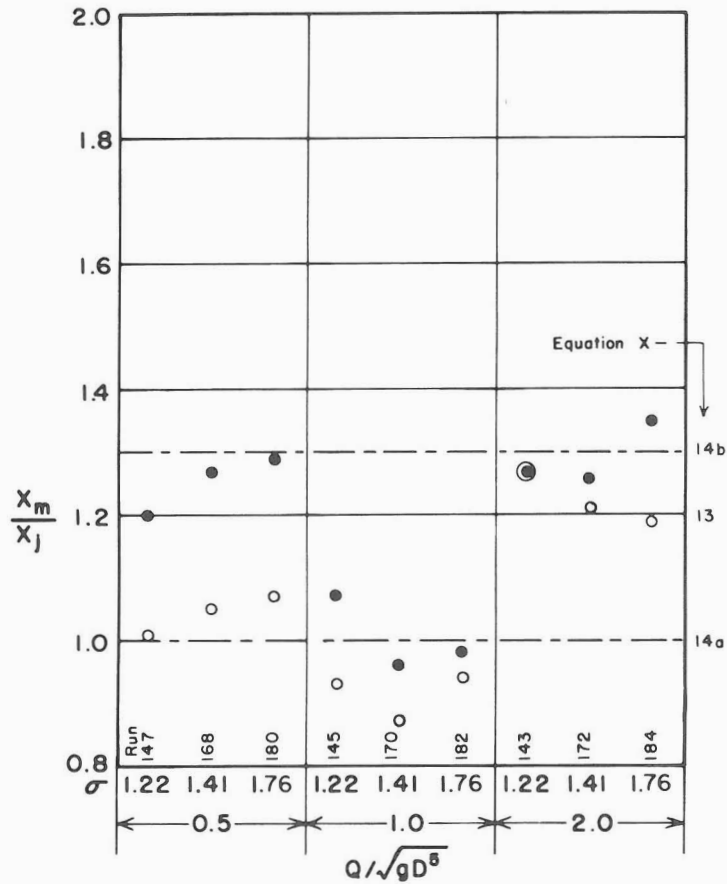


Figure X-10
 Distance to observed maximum scour depth in terms of computed jet trajectory length based on observed maximum scour depth, for sediment size distribution data, $\sigma = 1.22$, $d_{50}/D = 0.0724$, and $d_{50} = 1.84$ mm; and $\sigma = 1.41$ and 1.76 , $d_{50}/D = 0.0787$, and $d_{50} = 2.00$ mm: open symbols = time-dependent data, solid symbols = suspended-material-removed data.

For alternative (2), the suggested distance to the center of the upstream semiellipse $X_{m,b}$ is

$$\frac{X_{m,b}}{X_j} = 1.0 \quad (\text{X-14a})$$

the suggested distance to the center of the downstream semiellipse $X_{m,e}$ is

$$\frac{X_{m,e}}{X_j} = 1.3 \quad (\text{X-14b})$$

and the length of the parallel-sided center section $X_{m,c}$ is

$$\frac{X_{m,c}}{X_j} = 0.3 \quad (\text{X-14c})$$

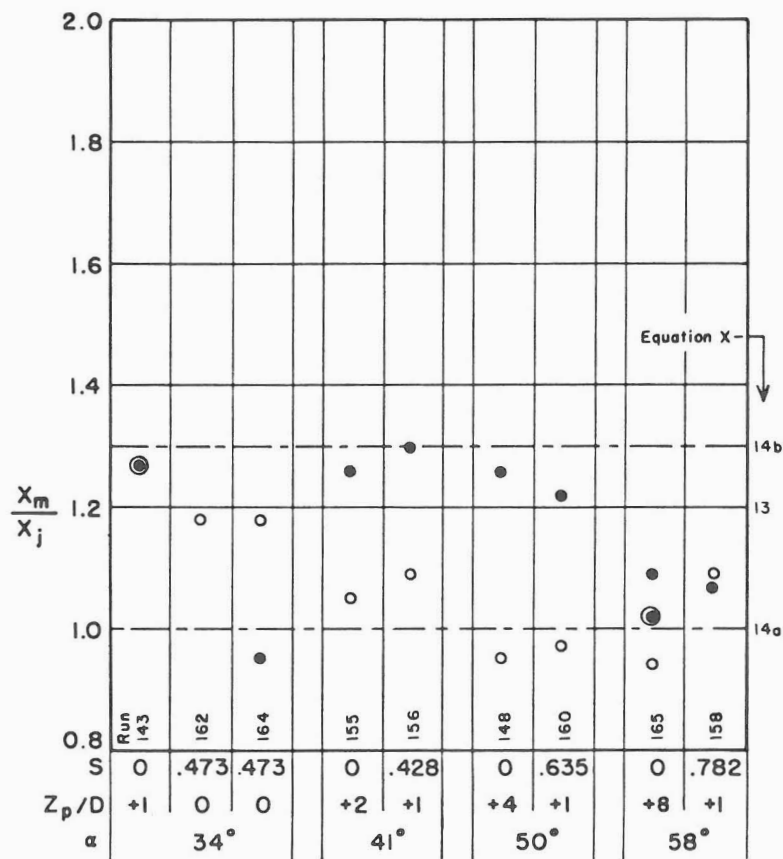


Figure X-11
Distance to observed maximum scour depth in terms of computed jet trajectory length based on observed maximum scour depth, for jet impingement angle data, $d_{50}/D = 0.0724$, $d_{50} = 1.84$ mm, and $Q/\sqrt{gD^5} = 2$: open symbols = time-dependent data, solid symbols = suspended-material-removed data.

Lines representing these equations have been plotted on figures X-8 through X-11.

Distance based on computed scour depth. The equations recommended for computing the ultimate depth of scour $Z_{m,u}$, developed later in the section "Maximum Scour Depth," are:

For $Z_p/D \leq 1$,

$$\frac{Z_{m,u}}{D} = - 7.5[1 - e^{-0.6(F_d - 2)}] \quad (X-22)$$

and for $Z_p/D > 1$,

$$\frac{Z_{m,u}}{D} = - 10.5[1 - e^{-0.35(F_d - 2)}] \quad (X-23)$$

Equations X-22 and X-23 represent an envelope of the observed values of Z_m/D . As a result, most of the computed absolute values--remember that the maximum scour depth Z_m is a negative number--of Z_m/D will exceed the observed absolute values of Z_m/D . Because Z_m appears in equation X-12, most of the values of X_j based on the computed values of Z_m will exceed the values of X_j based on the observed values of Z_m . Therefore the values of X_m/X_j based on the computed values of Z_m will be different from the values of X_m/X_j based on the observed values of Z_m . Since in practice the location of the maximum scour depth (and the location of the plunge pool) will be based on the computed value of Z_m , X_m/X_j based on computed values of Z_m will be investigated in this subsection and an equation will be developed to evaluate X_m/X_j based on computed values of Z_m .

For the time-dependent tests, Z_m/D was computed using equations X-22 or X-23 and the logarithm of this value, y_o , inserted into the equation

$$\frac{Z_m}{D} = - \text{antilog} (x + y_o - \sqrt{x^2 + a^2}) \quad (X-15)$$

to compute the maximum scour depth at any time. In equation X-15, $x = \log(tV_p/D_p)$ and a is defined by equation X-27. X_j was computed by the equation

$$X_j = X_p - \frac{Z_m}{\tan \alpha} \quad (\text{VIII-7})$$

Then the observed value of X_m at each test time was divided by the value of X_j based on the computed maximum scour depth at that time. The resulting values of X_m/X_j for all test times were averaged and plotted in figure X-12. For the suspended-material-removed tests, equations X-22 and X-23 were again used to compute Z_m/D , equation VIII-7 was used to compute X_j , and the observed value of X_m was divided by X_j . These values of X_m/X_j are plotted in figure X-13.

Figures X-12 and X-13 show that the values of X_m/X_j decrease with increasing discharge for both the time-dependent and the suspended-material-removed tests. The two plots are similar, and, because the data appeared to be representable by an exponential relation, the data were plotted on a semilogarithmic grid. A least squares analysis was made to derive the relation

$$\frac{X_m}{X_j} = 1.15 e^{-0.15 Q/\sqrt{gD^5}} \quad (X-16)$$

expressing the distance to the location of the maximum depth as a function of both the dimensionless discharge and the ratio of the maximum depth of scour to the jet trajectory distance. This relation is plotted in both figures X-12 and X-13.

The limits of X_m/X_j are also defined on the plots. The upper limit of X_m/X_j , with one high outlier from the time-dependent results, is defined by

$$\frac{X_m}{X_j} = 2.09 e^{-0.26 Q/\sqrt{gD^5}} \quad (X-17)$$

and the lower limit, with three low outliers from the suspended-material-removed results, is expressed by

$$\frac{X_m}{X_j} = 0.80 e^{-0.086 Q/\sqrt{gD^5}} \quad (X-18)$$

Figure X-13 shows more scatter for the suspended-material-removed results than for the time-dependent results shown in figure X-12. Therefore, the limits are more conservative for the time-dependent results.

Equations X-16, X-17 and X-18 converge at $X_m/X_j = 0.5$ and $Q/\sqrt{gD^5} = 5.5$. Since no data were obtained for $Q/\sqrt{gD^5} > 5$ and there was only one test at $Q/\sqrt{gD^5} = 5$, equation X-15 presumably should not be extrapolated beyond $Q/\sqrt{gD^5} = 5.5$. In practice this apparently will not be a limitation because seldom will $Q/\sqrt{gD^5}$ exceed 2.5 (Blaisdell 1983).

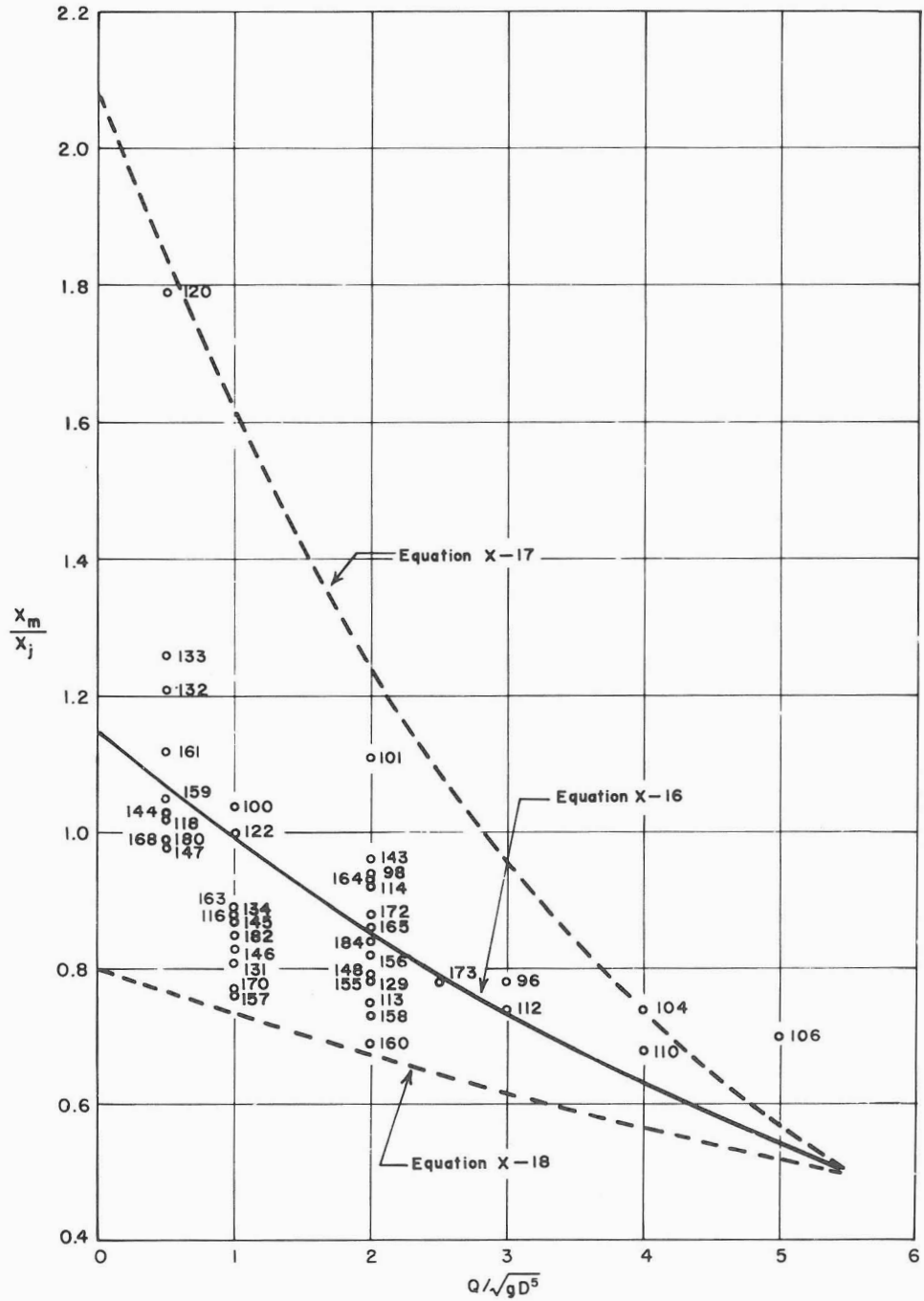


Figure X-12
Location of maximum depth of scour for time-dependent tests.

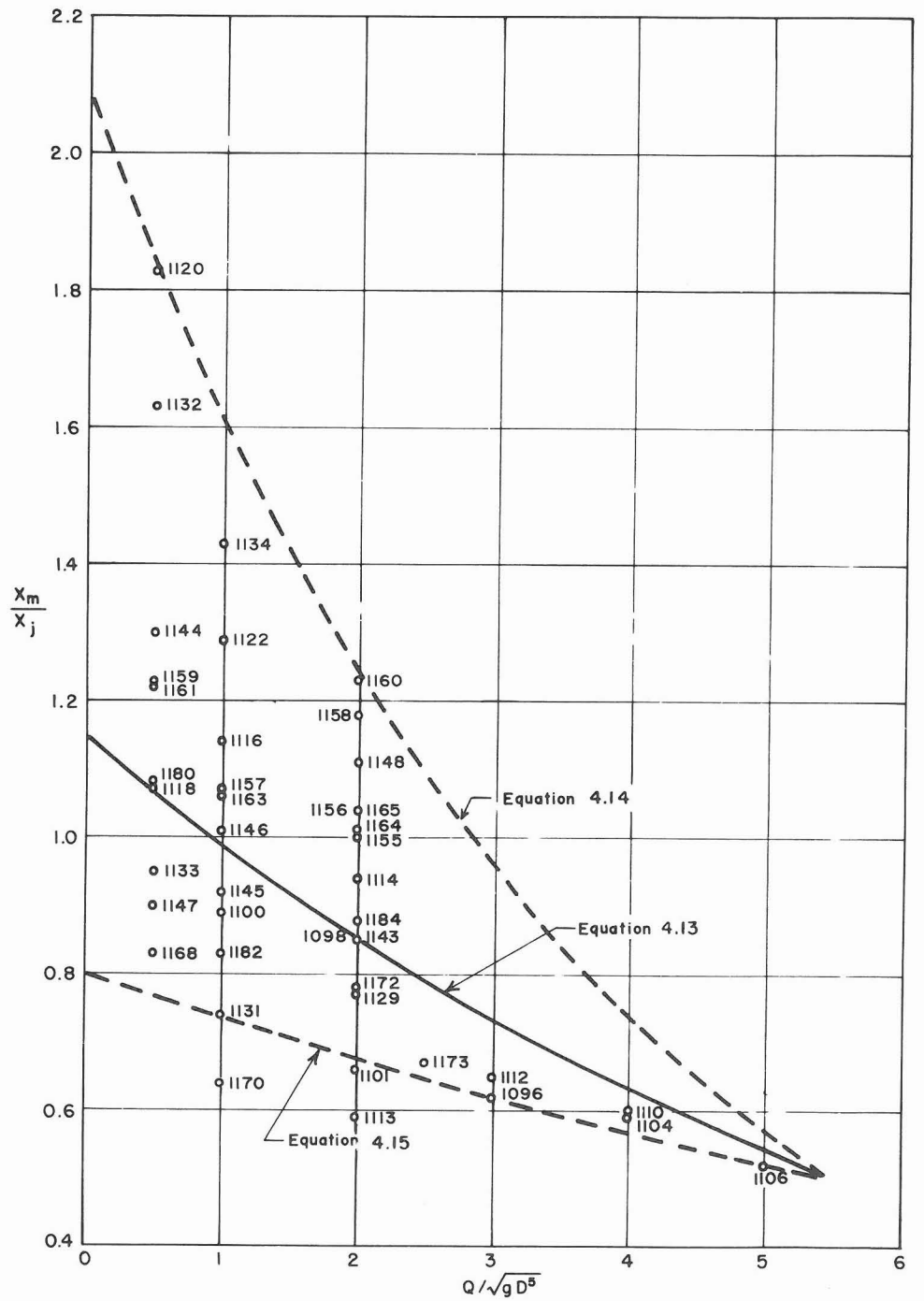


Figure X-13
Location of maximum depth of scour for suspended-material-removed tests.

When $Q/\sqrt{gD^5} \leq 2$ there is a range of values of X_m/X_j for each discharge because of the variety of conditions, such as pipe height and slope and bed material size and size distribution. However, the values of X_m/X_j computed by equation X-15 represent mean values that are recommended for the design of plunge pool energy dissipators.

Comparison of results. A comparison of equation X-16 with equation X-13 or equation X-14 shows a difference in trend of X_m/X_j with $Q/\sqrt{gD^5}$. The variation in X_m/X_j with $Q/\sqrt{gD^5}$ was noted when discussing the "Distance based on observed scour depth" and was taken into account through the addition of $\sin \alpha$ to obtain equation X-12, which was used in the initial analysis of the data. However, the computed value of Z_m and equation VIII-7 (uncorrected for the variation with $Q/\sqrt{gD^5}$) were used to compute X_j when analyzing the distance based on the computed scour depth. Therefore, the variation of X_m/X_j with $Q/\sqrt{gD^5}$ appears in equation X-16 and the trend is expected.

The important point is how well use of equation X-16, together with other recommended relationships, represents the test results. A comparison of experimental contour maps with their respective computed contour maps showed that for 28 of the 40 conditions tested, the locations of the maximum depth agreed within $\pm 1D$. This comparison therefore supports the recommendation that equation X-16 be used to locate the scour hole and plunge pool with respect to the pipe outlet.

Maximum Scour Depth

Except for the maximum depth of the scour hole Z_m , all the terms in the equations that define the scour hole now have been evaluated. Because the maximum scour hole depth is included, either directly or indirectly, in the equations for (1) the scour hole contours, equation X-9, (2) the scour hole axes coordinates, equations X-10 and X-11, and (3) the distance to the maximum scour hole depth, equation X-16, a relationship to quantitatively evaluate Z_m is essential. Relationships for both the suspended-material-removed ultimate $Z_{m,u,smr}$ and the time-dependent ultimate $Z_{m,u,td}$ maximum scour depths will be developed in this section.

Ultimate maximum scour depth. The scour data used to develop the relationship describing the ultimate maximum depth of scour $Z_{m,u}$ are the asymptotic scour hole depths computed for each set of time-dependent scour data by the hyperbolic logarithmic velocity-of-scour method described in chapter VII plus the maximum scour hole depth data from the suspended-material-removed tests listed in table X-1.

In an initial analysis of the data, no evidence was found of a direct relationship between the discharge and the scour depth. However, as a result of further study and despite considerable scatter of the data, the ultimate scour hole depth was found to be related to the densimetric Froude number

$$F_d = \frac{V_p}{\sqrt{gd_{50}(\rho_s - \rho)/\rho}} \quad (X-19)$$

a dimensionless parameter which includes both the jet and the bed material properties. Here g is the acceleration due to gravity, d_{50} is the mean size of the bed material, and ρ and ρ_s are the densities of the fluid and bed material respectively.

The observed values of the ultimate maximum scour hole depth relative to the pipe diameter $Z_{m,u}/D$ were plotted as a function of the densimetric Froude number. The suspended-material-removed data for a range of pipe heights and pipe slopes are plotted in figure X-14 and for a range of bed material sizes and size distributions are plotted in figure X-15. Similar plots for the asymptotic scour hole depths derived from the time-dependent data analysis are plotted in figures X-16 and X-17.

To ensure that the recommended equation defining the ultimate scour hole depth would be conservative, that is, predict dimensions of a plunge pool that would not scour, the curve to represent the data in figures X-14 through X-17 was drawn to envelop almost all of the data points. The curve, first drawn for the suspended-material-removed data and later found to fit the asymptotic time-dependent data with equal or greater conservatism, was first represented by the relation

$$\frac{Z_{m,u}}{D} = - 11 \log (F_d - 1) \quad (X-20)$$

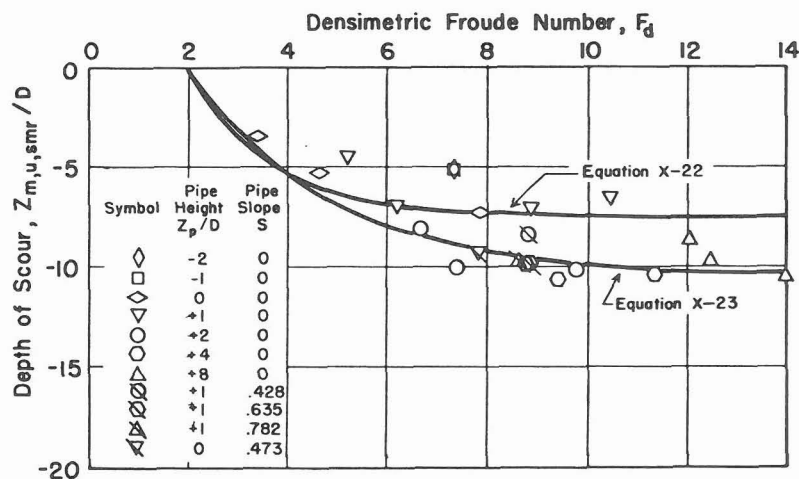


Figure X-14
Observed ultimate maximum scour depths for pipe heights and pipe slopes with suspended material removed.

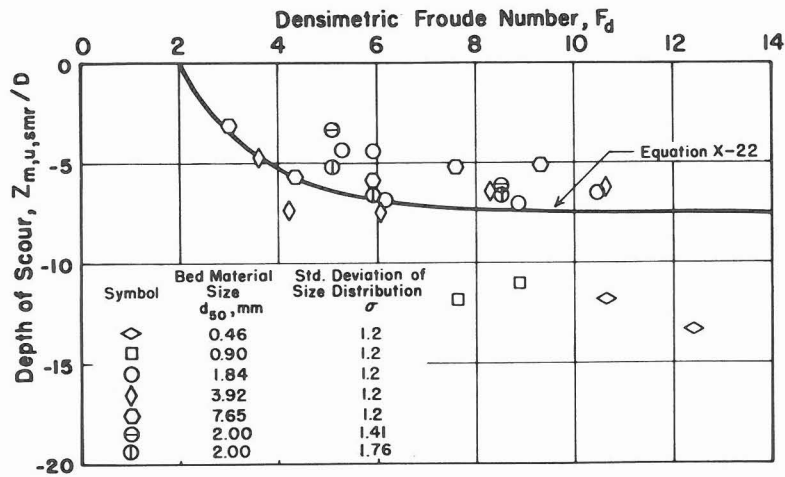


Figure X-15
Observed ultimate maximum scour depths for bed material sizes and size distributions with suspended material removed and $Z_p/D = 1$.

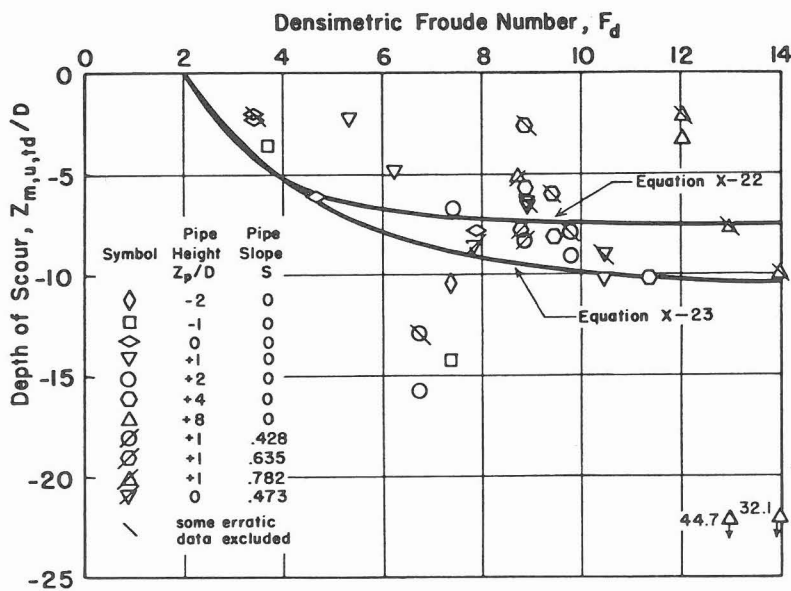


Figure X-16
Computed ultimate maximum depths from time-dependent tests of pipe heights and pipe slopes, for $d_{50}/D = 0.0724$.

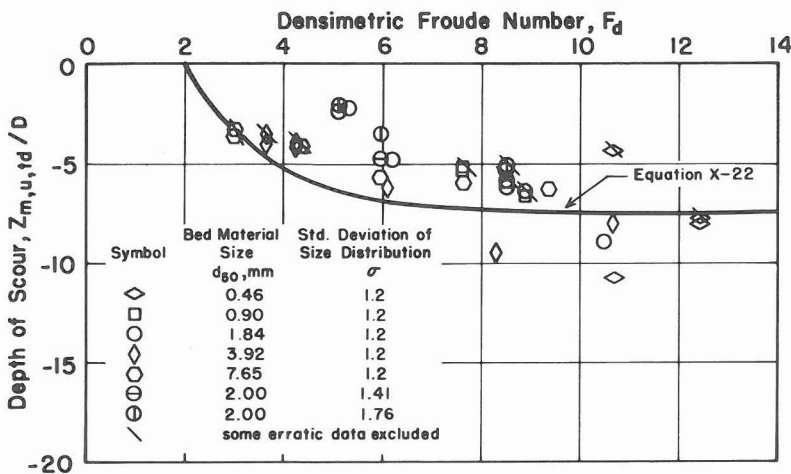


Figure X-17
Computed ultimate maximum depths from time-dependent tests of bed material sizes and size distributions, for $Z_p/D = 1$.

Subsequent examination of the suspended-material-removed data in figure X-15 showed that for a relative pipe height of $Z_p/D = 1$, the observed relative depth $Z_{m,u}/D$ was below -7.5 for only those tests with mean bed material sizes of 0.46 and 0.90 mm. Figure X-14 showed that the observed relative depths for $Z_p/D \leq 1$ were -7.5 or less while the relative depths for $Z_p/D > 1$ were -10.5 or less.

Rather than use the logarithmic function with limits for each range of pipe height, functions asymptotic to $Z_{m,u}/D = -7.5$ and -10.5, respectively, were sought to represent the relative scour depth.

The exponential relation

$$\frac{Z_{m,u}}{D} = -A[1 - e^{-k(F_d - c)}] \quad (X-21)$$

is asymptotic to A and, with the proper coefficients, closely approximates the logarithmic curve defined by equation X-20 for low densimetric Froude numbers. A review of typical field conditions indicated that, in practice, densimetric Froude numbers will generally be less than 6--less than half the range of densimetric Froude numbers covered by the test data--so similarity at the low F_d numbers is desirable. Using the asymptotic limits discussed above for A and deriving k and c from the plotted data, the following relationships were established for the two ranges of pipe height:

For $Z_p/D \leq 1$,

$$\frac{Z_{m,u}}{D} = -7.5[1 - e^{-0.6(F_d - 2)}] \quad (X-22)$$

and for $Z_p/D > 1$,

$$\frac{Z_{m,u}}{D} = -10.5[1 - e^{-0.35(F_d - 2)}] \quad (X-23)$$

These curves are plotted on figures X-14 through X-17 as applicable to the data presented on each figure. Computed values of the ultimate relative scour hole depths are listed in table X-2 to permit ready comparison with the corresponding suspended-material-removed and time-dependent asymptotic scour depths also listed in table X-2.

Table X-2
 Summary of relative scour-hole-depth data for
 nonbeaching scour holes

Run	$\frac{Q}{\sqrt{gd^5}}$	$\frac{z_p}{D}$	$\frac{d_{50}}{D}$	σ	S	F_d	$\frac{z_{m,u}}{D}$			$^3\alpha$	Time, Minutes ³	
							¹ Equation	² smr	³ td		Begin	End
113	2	-2	0.0724	1.22	0	7.37	-7.20	-5.09	-10.45	2.23	0	7290
101	2	-1	"	"	"	7.37	-7.20	-5.13	-14.22	2.72	0	12630
133	0.5	0	"	"	"	3.43	-4.32	-3.43	-2.04	1.32(0.82)	0	9960
131	1	"	"	"	"	4.68	-6.00	-5.24	-6.17	2.04	0	11225
129	2	"	"	"	"	7.91	-7.28	-7.31	-7.80	1.76	0	8520
147	0.5	1	"	"	"	5.34	-6.49	-4.37	-2.23	0.90	0	7180
145	1	"	"	"	"	6.22	-6.90	-6.85	-4.83	1.63	0	17135
143	2	"	"	"	"	8.91	-7.38	-7.01	-6.32	1.16(1.05)	0	7320
173	2.5	1	"	"	"	10.48	-7.45	-6.50	-8.97	1.84(1.64)	10000	12963
159	0.5	2	"	"	"	6.72	-8.49	-8.05	-12.91	3.33(3.09)	0	11037
157	1	"	"	"	"	7.44	-8.94	-9.94	-6.76	2.12	0	7245
155	2	"	"	"	"	9.80	-9.82	-10.17	-7.93	1.80(1.58)	0	13091
144	0.5	4	"	"	"	8.87	-9.55	-9.77	-2.61	2.78(1.80)	0	8193
146	1	"	"	"	"	9.43	-9.72	-10.65	-6.03	2.42(2.12)	0	11610
148	2	"	"	"	"	11.38	-10.11	-10.39	-10.21	2.09	0	9780
161	0.5	8	"	"	"	12.07	-10.19	-8.69	-2.16	1.88(1.58)	0	8880
163	1	"	"	"	"	12.48	-10.23	-9.78	-7.74	4.06(2.41)	0	12779
165	2	"	"	"	"	14.02	-10.34	-10.46	-10.00	3.30(2.08)	0	9975
156	2	1	"	"	0.428	8.86	-7.38	-8.37	-8.32	3.07(1.80)	10000	12778
160	2	1	"	"	0.635	8.80	-7.37	-9.79	-7.82	----(2.00)	10000	12980
158	2	1	"	"	0.782	8.73	-7.37	-9.75	-5.20	----(1.17)	10000	18493
162	2	0	"	"	0.473	7.85	-7.28	-9.22	-8.57	----(1.79)	10000	13143
132	0.5	1	0.0181	1.24	0	10.68	-7.46	-11.78	-4.37	2.91(1.90)	0	32690
134	1	"	"	"	"	12.44	-7.49	-13.37	-7.74	2.06(1.96)	0	28559
120	0.5	"	0.0354	1.24	"	7.63	-7.24	-11.82	-5.18	1.89(1.82)	0	12971
122	1	"	"	"	"	8.89	-7.38	-11.02	-6.62	1.82	0	10300
118	0.5	"	0.1543	1.23	"	3.66	-4.72	-4.76	-3.57	2.24(2.07)	0	37568
116	1	"	"	"	"	4.26	-5.57	-7.40	-3.93	1.48(1.43)	0	31681
114	2	"	"	"	"	6.10	-6.86	-7.75	-6.22	1.26(1.29)	0	20009
112	3	"	"	"	"	8.31	-7.33	-6.25	-9.53		0	11490
110	4	"	"	"	"	10.66	-7.46	-6.19	-8.05		0	14088
100	1	"	0.3012	1.26	"	3.05	-3.50	-3.06	-3.27	1.93(1.80)	0	23053
098	2	"	"	"	"	4.37	-5.69	-5.65	-4.12	0.94	0	41162
096	3	"	"	"	"	5.95	-6.80	-5.87	-5.70	1.08	0	28136
104	4	"	"	"	"	7.63	-7.24	-5.21	-5.93	0.99(1.04)	0	11337
106	5	"	"	"	"	9.36	-7.41	-5.15	-6.27	1.03	0	8517
168	0.5	"	0.0787	1.41	"	5.12	-6.35	-3.32	-2.09	0.65	31621	3224
170	1	"	"	"	"	5.96	-6.80	-4.40	-4.79	1.74	10000	10140
172	2	"	"	"	"	8.54	-7.35	-6.13	-5.87	1.30(1.19)	10000	12745
180	0.5	"	0.0787	1.76	"	5.12	-6.35	-5.12	-2.08	1.23(0.87)	10000	29692
182	1	"	"	"	"	5.96	-6.80	-6.62	-3.53	----(1.06)	10000	22940
184	2	"	"	"	"	8.54	-7.35	-6.66	-5.06	1.13(1.01)	10000	22621

¹Computed using equations X-21 and X-22.

²Suspended-material-removed tests.

³Time-dependent tests (some erratic data excluded).

The differences between the observed and computed relative ultimate scour hole depths for the suspended-material-removed tests are plotted as solid squares in figure X-18 for the pipe height and pipe slope tests and in figure X-19 for the sediment size and sediment size distribution tests. The computed depths are those defined by equations X-22 and X-23.

Positive values of $[(Z_{m,u}/D)_{\text{observed}} - (Z_{m,u}/D)_{\text{computed}}]$ indicate a greater-than-observed computed depth and are considered to be conservative. Some conservatism is desirable to ensure that the predicted scour hole depth will be greater than the observed depth. Although there is considerable scatter to the suspended-material-removed data plotted in figures X-18 and X-19, the computed depth is conservative for 24 of the 42 cases investigated; and the average difference for the ultimate relative scour hole depth is close to zero, with a rather large standard deviation. Discounting the data from the two finest bed materials, the mean of the differences for the ultimate case becomes positive (conservative), the standard deviation is decreased by more than a pipe diameter, and two-thirds of the individual differences are conservative.

Based on this analysis of the suspended-material-removed and time-dependent experimental data, equations X-22 and X-23 are recommended for defining the ultimate maximum scour depth $Z_{m,u}$.

Maximum time-dependent depth. The computed depth at any time is derivable from the hyperbolic technique discussed in chapter VII. Expressed in simplest form, the depth at any time is defined by the relationship

$$\frac{Z_m}{D} = - \text{antilog} (x + y_o - \sqrt{x^2 + a^2}) \quad (\text{X-24})$$

where

$$y_o = \log \frac{-Z_{m,u}}{D} \quad (\text{X-25})$$

(in which $Z_{m,u}/D$ is computed from equations X-22 and X-23),

$$x = \log \frac{tV_p}{D_p} \quad (\text{X-26})$$

(in which t is the time in seconds, V_p is the jet plunge velocity, and D_p is the diameter of the jet at the plunge point), and

a is the semimajor axis of the hyperbola.

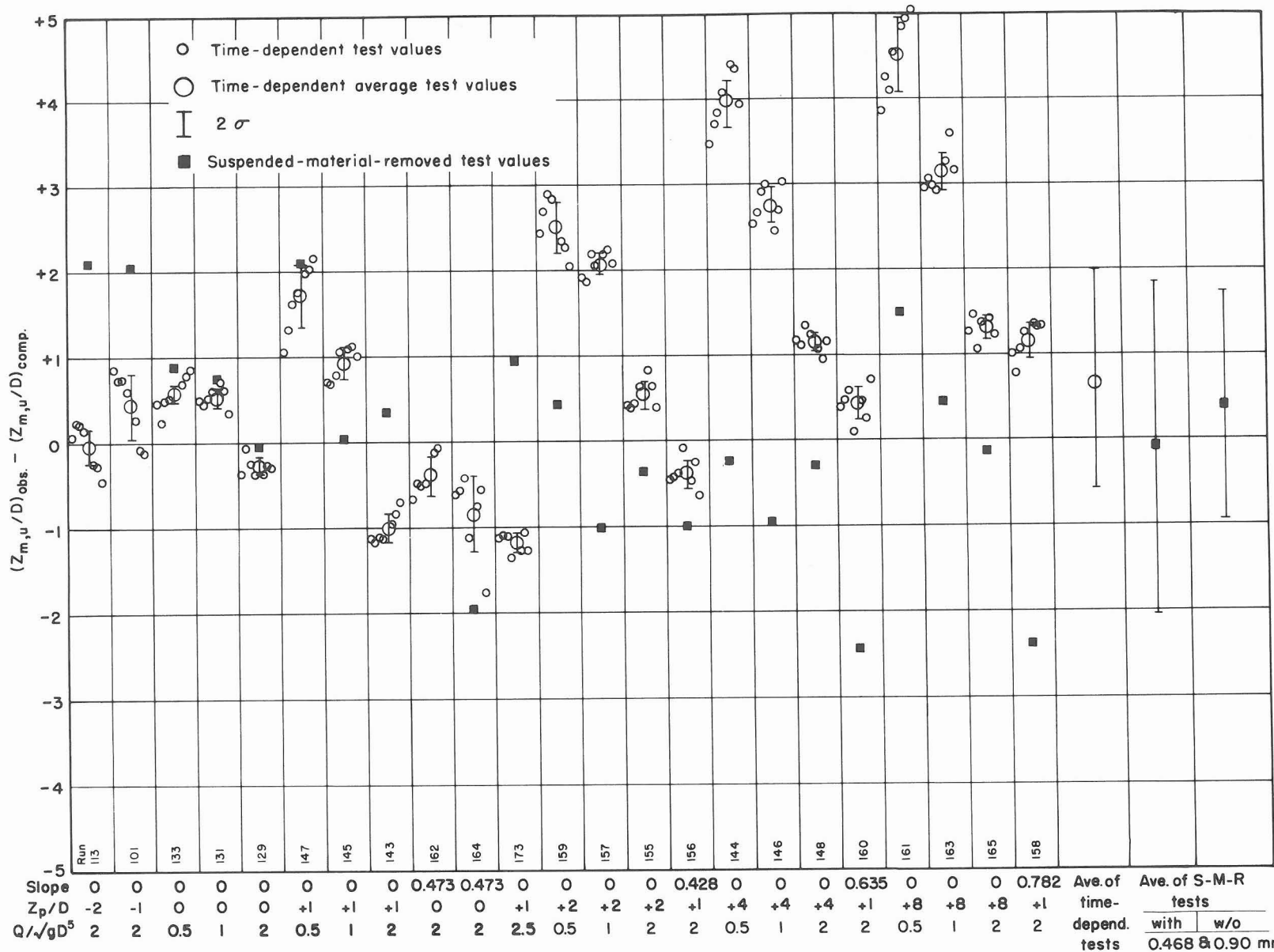


Figure X-18
 Difference in depth of scour, observed minus computed, for pipe height and slope tests.

Ave. of time-depend. tests	Ave. of S-M-R tests	
	with	w/o
	0.468	0.90 mm

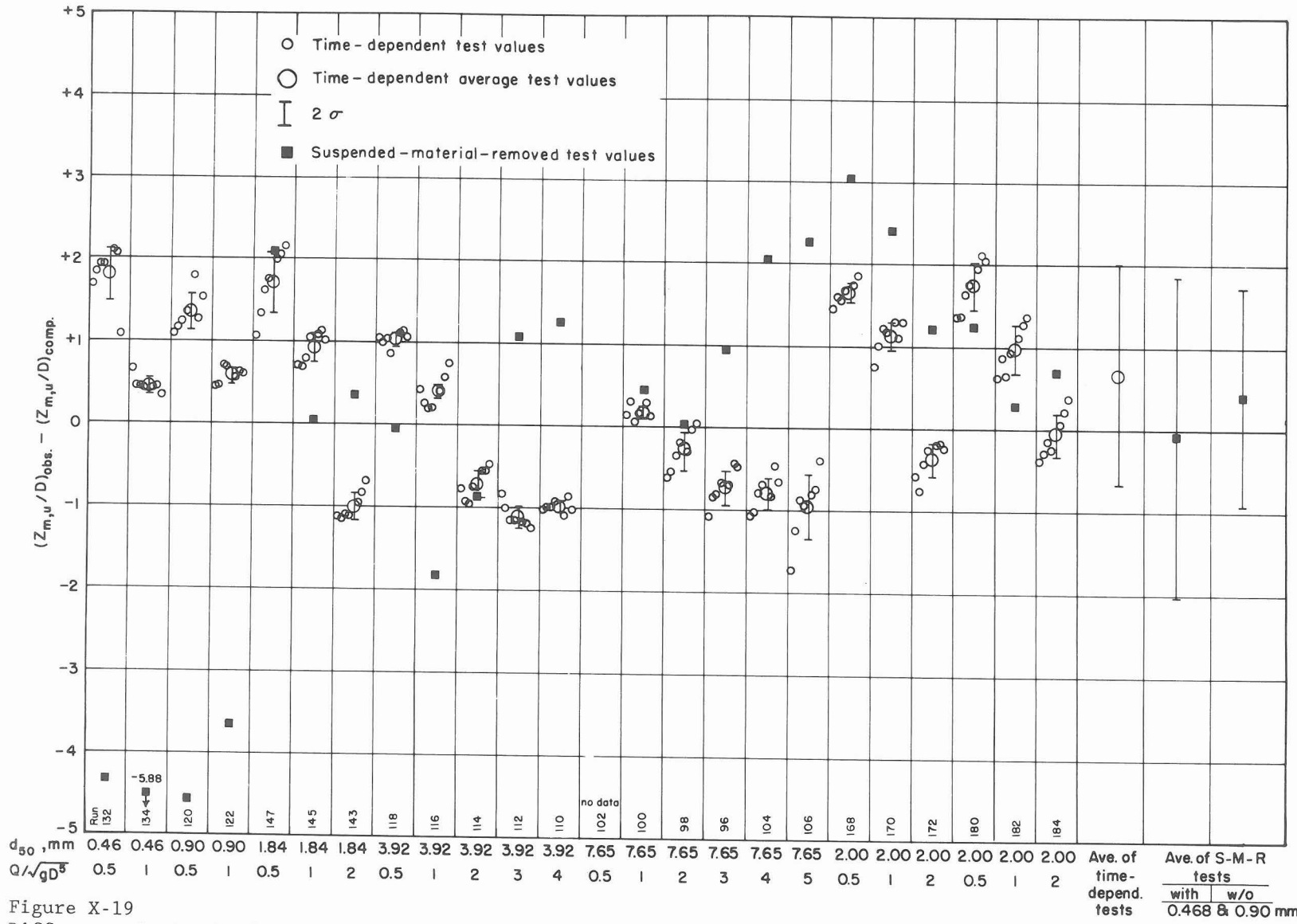


Figure X-19
 Difference in depth of scour, observed minus computed, for sediment size and distribution tests.

The hyperbolic semiaxis parameter a is plotted against the densimetric Froude number in figures X-20 and X-21. Although there is a great deal of scatter, with few exceptions the constant

$$a = 1.75 \quad (X-27)$$

was found to represent the data as well as or better than the constant initially developed in this study by Blaisdell,

$$a = 1.2 + F_d/15$$

or the constant developed later by Anderson

$$a = \frac{a_{d_{50}} \times a_{Z_p}}{11.9 F_d - 0.92} \quad (X-28)$$

where

$$a_{d_{50}} = [2.0 + 0.034 \left(\frac{d_{50}}{D}\right)^{-2.16}] \times F_d(1.1 - 0.984 d_{50}/D)^{-0.274} \quad (X-29)$$

and

$$a_{Z_p} = 5 e^{0.867 Z_p/D} F_d^{-0.535(1 + Z_p/D)^{0.781}} \quad (X-30)$$

Using equations X-24 to X-27, the depths were computed for all times for each of the test runs and compared to the observed depth for each test. The differences $[(Z_m/D)_{obs} - (Z_m/D)_{comp}]$ are plotted as small open circles for individual test times in figures X-18 and X-19. The average for each run is plotted as a large open circle, and the range of standard deviations for each run is indicated. The differences are within ± 1 for about one-half of the tests, the remainder ranging up to an ultra-conservative +4 for the 4D and 8D pipe heights with the minimum discharge. The differences for individual times of scour within a run generally varied from 1/2 to 1; but commonly, the computed depth became more conservative with time. The mean of all the differences was +0.67, indicating significant conservatism.

Based on the above analysis of the progression of scour with time, equations X-24, X-26, X-25 and X-27 are recommended for determining the scour at any time.

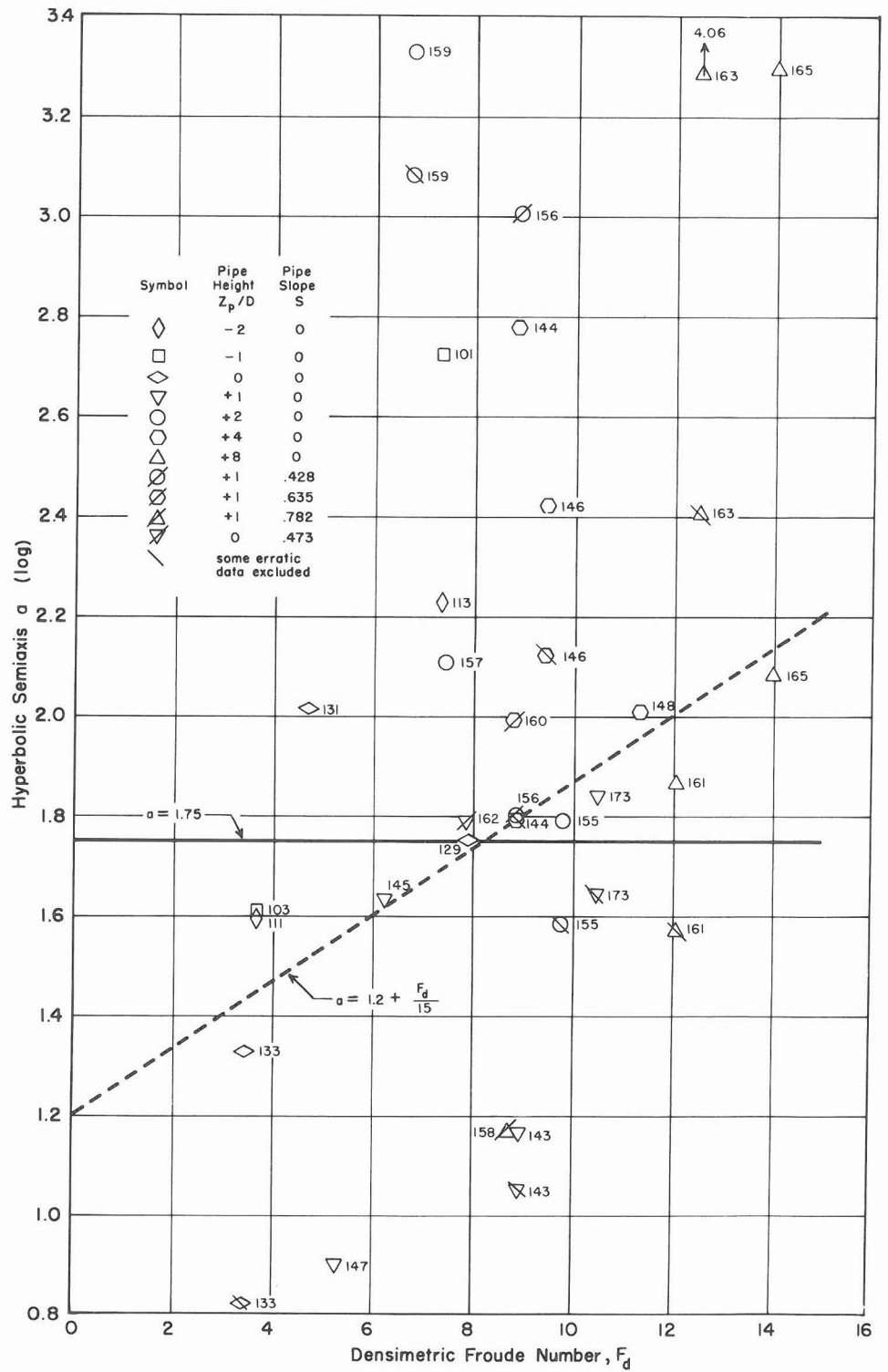


Figure X-20
 Hyperbolic semiaxis from time-dependent tests of pipe heights and pipe slopes, for $d_{50}/D = 0.0724$.

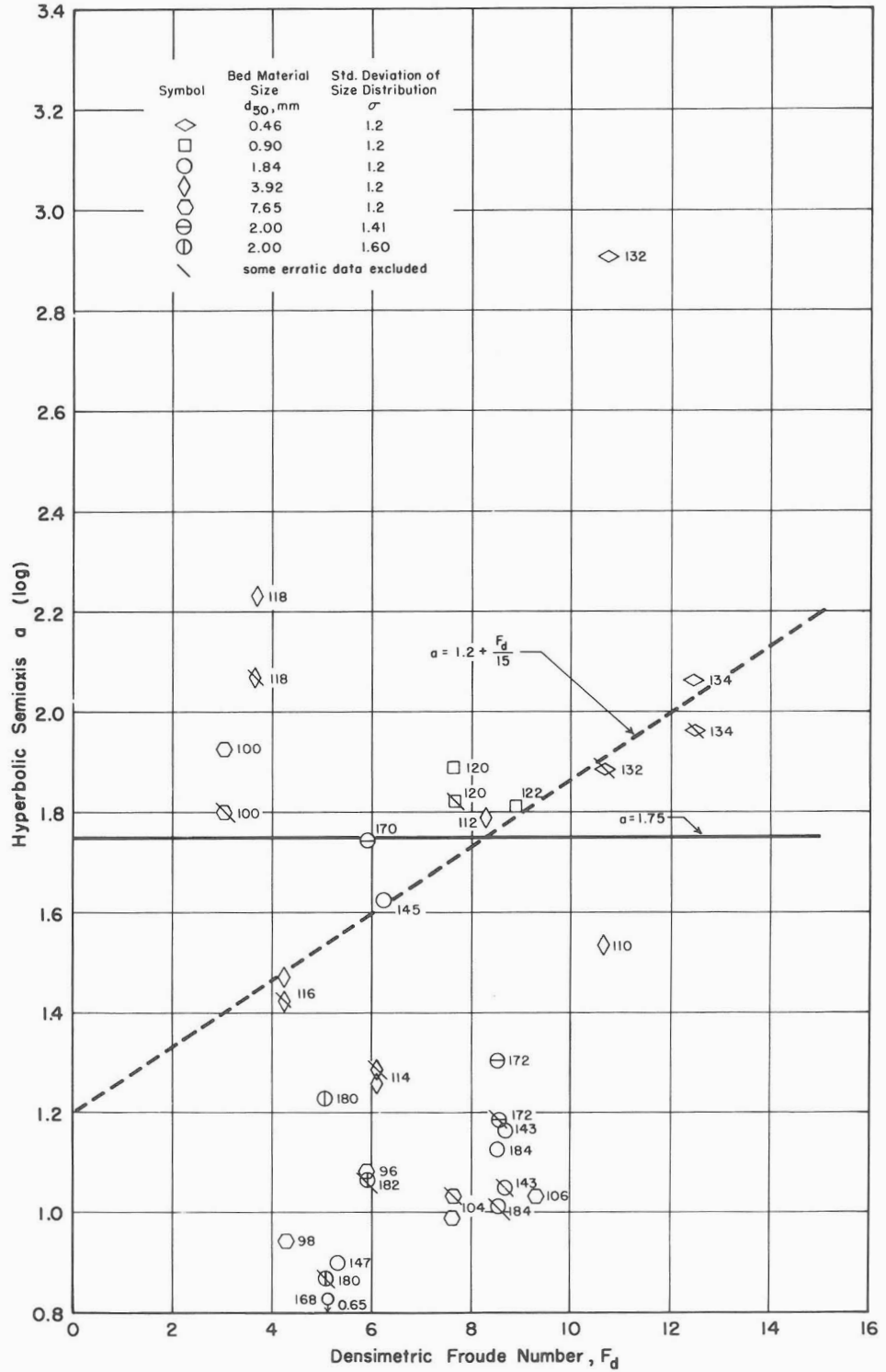


Figure X-21
Hyperbolic semiaxis from time-dependent tests of bed material sizes and size distributions, for $Z_p/D = 1$.

Comparison of Computed and Experimental Scour Holes

The critical test of how well the computed scour holes represented the observed experimental scour holes could be made only after the analysis of the experimental data had been completed. Until that time the possibility had existed that the computed scour holes would be excessively large because, to be conservative, many of the curves for which equations were developed enveloped the data and multiple envelopments could result in computed scour holes that are ultraconservative. The test of the fit of the computed scour holes to the observed experimental scour holes is made in this section.

Comparison Criteria

Only half of the 80 tests could be used in the comparison. Test conditions for the other half exceeded the limiting criteria established for beaching and had not been used in establishing the equations.

The equations used to compute the scour hole parameters are

1. For Z_m , equations X-22, X-23, X-24 and X-27 and equations VIII-8, VIII-9, VIII-4 and VIII-5 with $t = 10,000$ min (6.9 days) and 1,000,000 min (1.9 years);
2. for F_d , equation X-19;
3. for X_m , equation X-16;
4. for X_j , equation VIII-7;
5. for $X_{b,tw}$, $X_{e,tw}$ and $W_{m,tw}$, equations X-10 and X-11;
6. for the contours, equation X-9; and
7. for the beaching limit, equation X-2.

These are the equations recommended for use in the design of plunge pool energy dissipators or for estimating the size of holes that will be scoured in noncohesive soils.

Two computation times were used in the comparisons. For the time-dependent tests, only the 10,000-min experimental scour holes were used and these observed scour holes were compared with the 10,000-min computed scour holes. A time of scour of 1 million min (1.90 years) was used to compute the scour holes that were compared with the experimental suspended-material-removed scour hole tests.

Scour Hole Comparisons

To make the comparisons, contour maps of the computed scour holes were computer generated to the same scale as that used for the contour maps computer generated from the experimental data. The two contour maps for each scour hole were physically compared as to (a) the relative size of the scour hole as indicated by the maximum surface width, this width being the best defined dimension; (b) the relative shape of the scour hole, where "circular" may mean that the shape is less elliptical rather than truly circular; (c) the relative location of the scour hole with respect to the pipe exit; and (d) the maximum depth of the scour hole. The range of magnitude of the differences was also evaluated. A summary of the comparisons is presented in table X-3.

Table X-3
Comparison of computed and experimental scour hole parameters

Percentage of scour holes in which:									
(a) Computed scour hole is:									
Narrower (unconservative) by:					Wider (conservative) by:				
>10D	>5D-10D	2D-5D	<2D	Total	>10D	>5D-10D	2D-5D	<2D	Total
Time-dependent tests									
0	2	18	15	35	0	2	33	30	65
Suspended-material-removed tests									
5	5	5	5	20	5	25	40	10	80
(b) Shape is:									
							Circular	Elliptical	
Time-dependent tests							58	42	
Suspended-material-removed tests							55	45	
(c) Computed scour hole is located too far:									
Upstream by:						Downstream by:			
(Unconservative)						(Conservative)			
>1D	≤1D	Total	>1D	≤1D	Total	>1D	≤1D	Total	
12	20	32	18	50	68				
28	20	48	20	32	52				
(d) Computed scour hole is:									
Shallower by:						Deeper by:			
(Unconservative)						(Conservative)			
>1D	≤1D	Total	>1D	≤1D	Total	>1D	≤1D	Total	
8	30	38	15	48	62				
18	15	32	28	40	68				

Summary of Comparisons

Summarizing the results of the comparisons of the computed and experimental scour holes,

1. The degree of conservatism was identical for the time-dependent and suspended-material-removed tests despite random differences in the magnitude of the conservatism.
2. With regard to scour hole size,
 - (a) About 70% of the computed scour holes were larger than the experimental scour holes; that is, about 70% of the scour holes were conservative with regard to size.
 - (b) Ninety-six percent of the time-dependent and 60% of the suspended-material-removed experimental scour hole widths were within $\pm 5D$ of the computed widths.
3. With regard to scour hole shape, only a small percentage of the experimental holes were more circular than elliptical. Because a circle is an ellipse with equal axes, the elliptical contour shape defined by equation X-9 seems to be a reasonably correct representation of the scour hole shape.
4. With regard to the location of the scour hole,
 - (a) An average of about 60% of the computed scour holes were located downstream of the observed location. Because some field riprapped plunge pools have scoured at the downstream end, field experience indicates that locating the plunge pool downstream of its observed location, as will occur for an indicated 60% of the experimental holes, is desirable.
 - (b) On average, about 60% of the experimental scour holes were located within $\pm 1D$ of the computed location.
5. With regard to the scour hole depth,
 - (a) An average of 65% of the computed scour holes were deeper than the experimental scour holes. This indicates conservatism with regard to scour hole depth.
 - (b) Two-thirds of the computed scour hole depths are within $\pm 1D$ of the experimental depths.

Overall, these comparisons show that, although some scour holes can be expected to exceed the dimensions predicted by the recommended equations, on the average the recommended equations will predict the scour hole and plunge pool dimensions with a moderate degree of conservatism.

Effect of Nonerrodible Layer

In the field, a rock ledge or other nonerrodible layer may limit the depth of the scour hole. This concern was expressed during a program review on January 15-16, 1981. A part of the report of that review "related to the effect of non-errodible layers on the size and shape of the scour hole. There was broad agreement that the presence of a non-errodible layer could lead to gross changes in the lateral extent of the scour hole. [However, the tests reported in the following section showed this assumption to be incorrect.] A limited investigation of the effect of a non-errodible layer located at one-half the ultimate depth of the scour hole formed in uniform material is recommended." Such an investigation was conducted and the results of the tests follow.

Test Program

As recommended, the investigation was limited. For all tests the bed material size was 1.84 mm, the pipe height $Z_p/D = 1.0$, and the nonerrodible layer was a plywood surface located at $Z_{m,u}/D = -0.5$. Discharges $Q/\sqrt{gD^5} = 0.5, 1.0, 2.0, 2.5$ and 3.0 were used, although the test with the last discharge was terminated after 100 min because expected beaching occurred. Both a time-dependent test, with a full complement of times, and a suspended-material-removed test were conducted for each discharge.

Test Results

The observed contour data were compared with the contour equations developed for full-depth scour holes. The comparisons showed that the tests logically fell into two groups (table IX-2, odd numbered runs 179-187 and 1179-1185): (1) those tests in which the scour was not influenced by the presence of the fixed bed, and (2) those tests in which the scour exposed the fixed bed.

Time-dependent tests with discharges $Q/\sqrt{gD^5} = 0.5$ and 1.0 (and 2 for test times of 10 and 31 min) fall into the first group. For $Q/\sqrt{gD^5} = 0.5$ the bed was never exposed during these tests. For $Q/\sqrt{gD^5} = 1.0$ the fixed bed was exposed during the longer time-dependent tests, but the fixed bed was covered when the flow stopped. For both flows the fixed bed was exposed after the suspended-material-removed tests.

All other time-dependent tests and all suspended-material-removed tests fall into the second group. The following results were obtained in the group-2 time-dependent tests: For $Q/\sqrt{gD^5} = 2.0$, scour reached the fixed bed shortly after 31 min of testing; and for $Q/\sqrt{gD^5} = 2.5$ and 3.0 , the fixed bed was exposed before the first reading at 10 min.

The results of these comparisons follow the section headed "Definitions."

Definitions

$(Z_m/D)_{\text{obs}}$ is the depth to the bottom of the scour hole or to the fixed bed if the fixed bed was exposed by the scour.

$Z_{m,u}/D$ is the ultimate depth of scour given by equation X-22.

When the agreement is said to be "satisfactory," the data for the fixed bed tests are considered to agree with contour equation X-9 developed from the full depth scour holes as well as did the data used to develop the equation. Typical agreement of the fixed bed data with the equation is shown in figure X-22.

Contours are conservative when the data fall within the contours and are unconservative when the data fall outside and require a higher (less negative) Z_m/D contour to be conservative.

The observed contour elevations are based on the maximum observed depth of scour. Because the fixed bed was located at $-0.5(Z_{m,u}/D)$, the observed -1.0 fixed bed contour corresponds to the -0.5 ultimate scour hole contour when the bed is exposed. Therefore, to obtain corresponding contours for comparison when the fixed bed is exposed, each -0.2 plotted-contour-data elevation increment was multiplied by 0.5 to obtain the computed equation X-9 contour based on the ultimate scour depth. Both the $(Z_{m,u}/D)_{\text{obs}}$ and $(Z_{m,u}/D)$ contour elevations are listed for the following comparisons, the latter values for later use in the analyses.

Contour Comparisons

Data for these comparisons are shown in figure X-22, but only for the 0.0 , -0.4 and -0.8 contours.

Data for contour $(Z_m/D)_{\text{obs}} = 0.0$ [$(Z_{m,u}/D) = 0.0$]. Although the upstream data fall outside the computed curve by a maximum of about 0.04 and $0.11(2Y/W_{m,tw})$, respectively, for $Q/\sqrt{gD^5} = 0.5$ and 1.0 , figure X-22 shows that the agreement of the observed data with the equation curve for the 0.0 contour is generally satisfactory.

Data for contour $(Z_m/D)_{\text{obs}} = -0.2$ [$(Z_{m,u}/D) = -0.1$]. The data for the upstream half of this contour agree satisfactorily with the computed -0.2 contour, falling outside a maximum of $0.04(2Y/W_{m,tw})$.

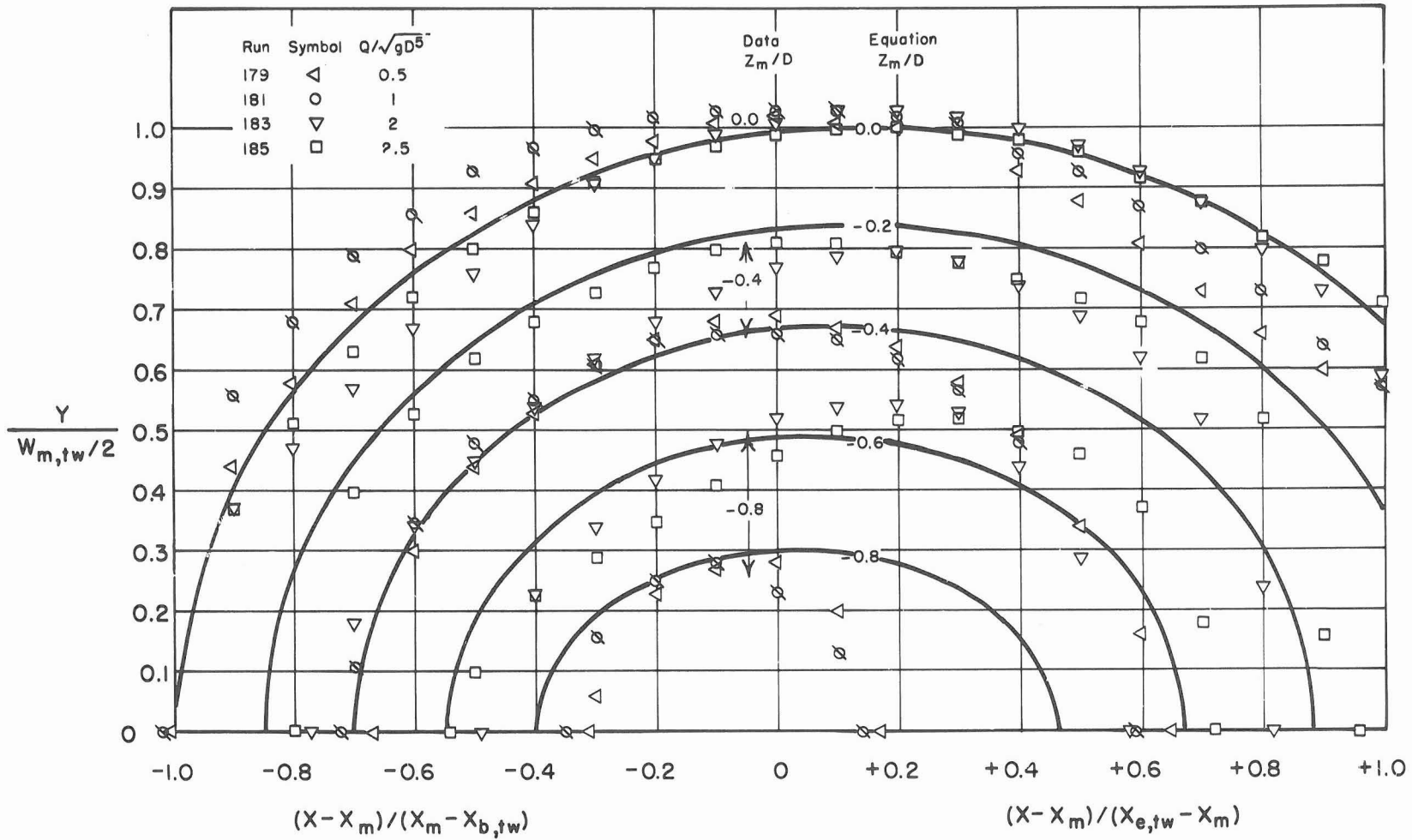


Figure X-22
 Average normalized contours for fixed bed tests, with $d_{50} = 1.84$ mm,
 and $Z_p/D = +1.0$.

For the downstream half of this contour, the $Q/\sqrt{gD^5} = 0.5$ and 1.0 data fall increasingly safely inside, and the $Q/\sqrt{gD^5} = 2.0$ and 2.5 data fall increasingly outside the computed -0.2 contour with distance downstream. Eventually, the data for the two highest discharge rates approach the -0.1 contour.

Data for contour $(Z_m/D)_{\text{obs}} = -0.4$ [$(Z_{m,u}/D) = -0.2$]. As can be seen in figure X-22, for the upstream half of the contour and for $Q/\sqrt{gD^5} = 0.5, 1.0$ and 2.0 the data follow the -0.4 contour while for $Q/\sqrt{gD^5} = 2.5$ the data follow the -0.2 contour.

For the downstream half, the $Q/\sqrt{gD^5} = 0.5$ and 1.0 fall well within the -0.4 contour and the $Q/\sqrt{gD^5} = 2.0$ and 2.5 fall slightly within the -0.2 contour.

Data for contour $(Z_m/D)_{\text{obs}} = -0.6$ [$(Z_{m,u}/D) = -0.3$]. The $Q/\sqrt{gD^5} = 0.5$ and 1.0 data follow the -0.6 computed contour for the upstream half and are increasingly within the -0.6 computed contour for the downstream half.

The $Q/\sqrt{gD^5} = 2.0$ and 2.5 upstream data begin at the computed -0.5 contour, converge to the -0.4 contour at the hole mid-length, and follow the -0.4 contour for the downstream half.

Data for contour $(Z_m/D)_{\text{obs}} = -0.8$ [$(Z_{m,u}/D) = -0.4$]. As can be seen in figure X-22, the $Q/\sqrt{gD^5} = 0.5$ and 1.0 data follow the computed -0.8 contour for the upstream half and fall well within that contour for the downstream half.

The $Q/\sqrt{gD^5} = 2.0$ and 2.5 data fall within the computed -0.6 contour for the upstream half and approach the computed -0.5 contour in the downstream half.

Conclusions

The preceding comparisons lead to the following conclusions:

1. Because for $Q/\sqrt{gD^5} = 0.5$ and 1.0 the test conditions agree with those used to develop the contour equations, the observed data contours agree with the equation contours. This was expected.
2. Because for $Q/\sqrt{gD^5} = 2.0$ and 2.5 the fixed bed was exposed, the equation contours based on the depth to the fixed bed do not define the observed contours. However, the equation contours based on the computed ultimate depth do adequately and conservatively define the observed contours.

Recommendation

To determine the scour hole contours when there is a fixed bed--rock ledge or other erosion-resistant surface--exposed in the scour hole, these findings, although based on limited tests, suggest that the fixed bed contours be based on the computed ultimate scour hole depth. With this procedure, some *computed* scour hole contours will be *below* the fixed bed. The contours above the fixed bed will then define the scour hole shape down to the fixed bed and the area of the fixed bed that will be exposed.

XI. COMPOSITE SCOUR HOLE (AND PLUNGE POOL)

The discharge was constant for those tests used to develop the mathematical model of the scour hole and for the design of plunge pool energy dissipators. However, in nature there will be a range of discharges; consequently, plunge pool energy dissipators must be designed to accommodate the anticipated discharge range.

For the maximum anticipated discharge, the scour hole may be of maximum depth and may be located farthest downstream. While lesser discharges may scour to a lesser depth, the jet may erode the upstream slope of the larger discharge scour hole and, as a result, the upstream limit of the scour hole may be located farther upstream. To prevent damage to a plunge pool energy dissipator, the constructed pool must circumscribe the scours computed for the entire range of discharges. A single test was performed to check the validity of this design procedure.

Description of Test

The bed material selected for this "hydrograph" test was the largest used during the cantilevered outlet scour hole test program-- $d_{50} = 7.65$ mm, $d_{50}/D = 0.3012$. This size was selected because lack of beaching at any discharge made it possible to use the widest range of discharges. Discharges used to produce a step hydrograph were $Q/\sqrt{gD^5} = 0.5, 1, 2, 3, 4$ and 5 . The pipe was horizontal and its invert was one pipe diameter above the tailwater level-- $S = 0$ and $Z_p/D = 1.0$.

The log of the test was lost during transfer of the St. Anthony Falls Hydraulic Laboratory project in Minneapolis, MN, to the Water Conservation Structures Laboratory in Stillwater, OK. The computer printout, a computer-generated contour map, some notes, and fallible memory are the basis of this summary of the test.

The total elapsed time of the test was 183,000 min--127 days. During that period the maximum discharge scoured a hole, then a lesser discharge scoured the upstream slope. This scoured material was deposited in the larger hole, and was subsequently swept out by a larger discharge (see figure XI-1 for a scour hole reflecting this sequence of events under field conditions) or was removed by suction as in the suspended-material-removed tests. Repeated periodic variation of the discharge over the 0.5-5.0 range eventually produced a scour hole in which there was no further apparent scour and no material in suspension. This hole was then measured and a contour map plotted.

Test Results

The composite scour hole test is listed in table IX-1 as run 1177. The contour map is plotted in terms of dimensionless maximum scour depth in figure XI-2 and the longitudinal section is shown in figure XI-3, both as dots. The maximum depth of scour is 24% greater than that for the test with a single discharge rate of 5 but is only 92% of the computed ultimate



Figure XI-1
Smaller discharge has scoured the upstream end and deposited the material in the hole scoured by a larger discharge. Crooked Creek Watershed, Houston County, MN.

scour depth. Because the angle of impingement was greater for a discharge rate of 3 than of 5, the combination of impingement angle and discharge rate caused the maximum depth of scour to occur at a discharge rate of 3. As a result, the observed maximum depth of scour for a discharge rate of 3 was 100% of the computed ultimate scour depth.

The composite test maximum scour hole depth is located about six pipe diameters upstream of the single maximum flow location. As expected, the contour map and cross section (not shown herein) show no evidence of beaching.

Comparison with Computed Contours

Contour maps were computer generated and plotted for discharges of $Q/\sqrt{gD^5} = 1, 2, 3, 4$ and 5 and times of 10,000 and 1,000,000 min (6.9 days and 1.9 years). The equations used for computing these contours were subsequently modified so are not those presently advocated; but they do, on average, give approximately the same maximum scour depths as do the recommended equations. These time-dependent maximum scour depths for the 1.9-year period range from 67% to 81% of the ultimate scour depths. It would have been desirable to compare contours computed for the ultimate depth; but because of the transfer of the project from Minnesota to Oklahoma, plotting the ultimate scour depth contours was not practical. However, comparisons based on the scour anticipated in 1.9 years demonstrate the feasibility of the procedure for predicting plunge pool dimensions, that is, if contours based on the scour after 1.9 years circumscribe the observed contours--and they do--then contours based on the greater ultimate maximum scour depth will be larger and will also circumscribe the observed contours.

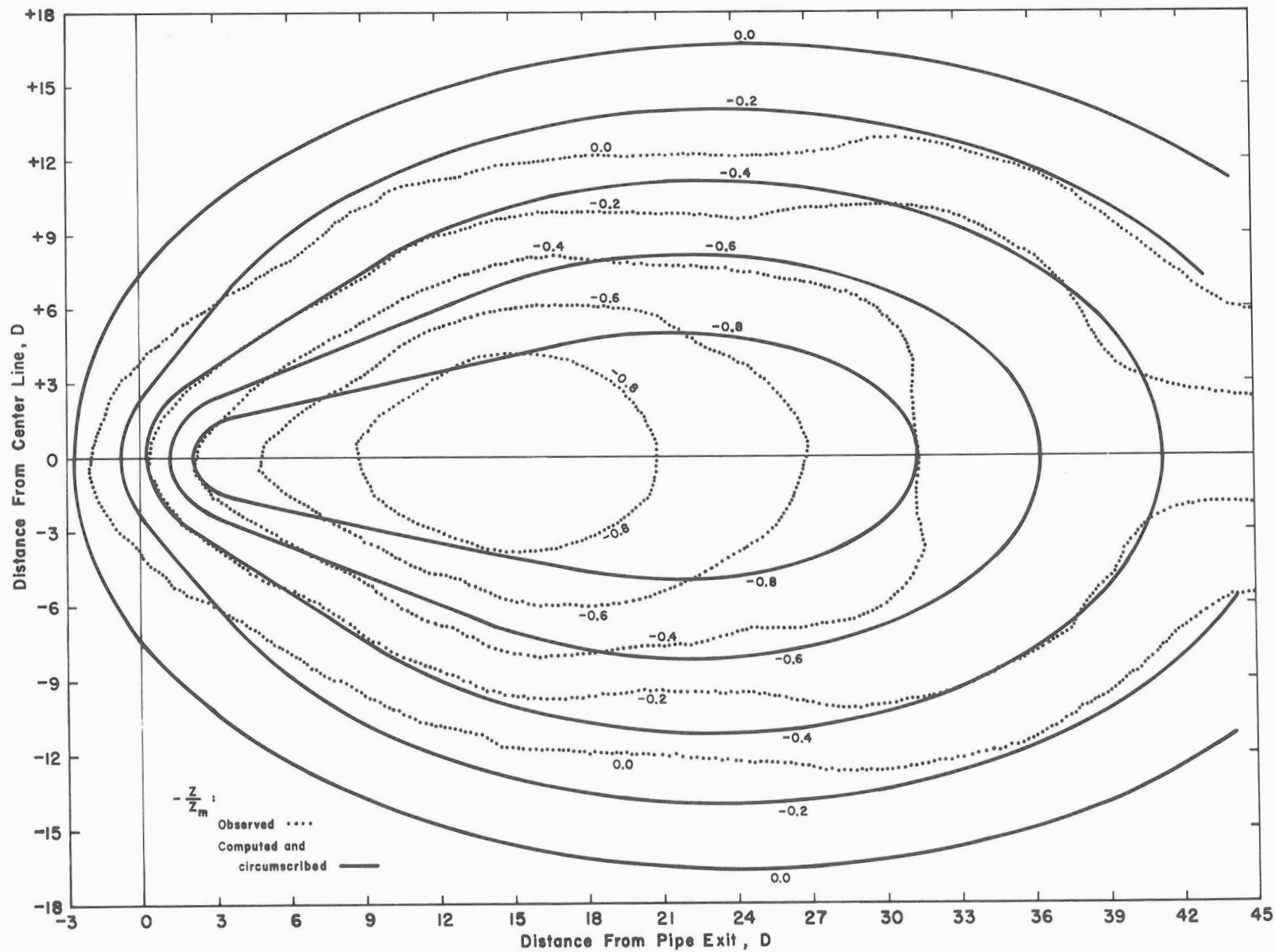


Figure XI-2
 Observed and computed circumscribed composite contours, with
 depth expressed in dimensionless units.

Starting with the contours computed for the maximum discharge, those contours which circumscribe the observed contours were traced on figure XI-2. Of the contours computed for $Q/\sqrt{gD^3} = 5$, only the 0.0 computed contour circumscribes the complete observed contour. Other computed contours for $Q/\sqrt{gD^3} = 5$ fall within the observed contours at the upstream end of the scour hole. However, computed contours for lesser discharges do circumscribe both the observed and higher discharge contours and were also traced on figure XI-2. They were used to draw the circumscribed computed contour, and then erased to clarify the figure.

Except for the 0.0 contour, the computed contour for $Q/\sqrt{gD^3} = 1$ determined the upstream end of the plunge pool, the contour for $Q/\sqrt{gD^3} = 5$ determined the downstream end of the plunge pool, and tangents to both circumscribed all other computed contours. The solid contour lines in figure XI-2 indicate the principle of the method proposed to develop the actual shape of the plunge pool.

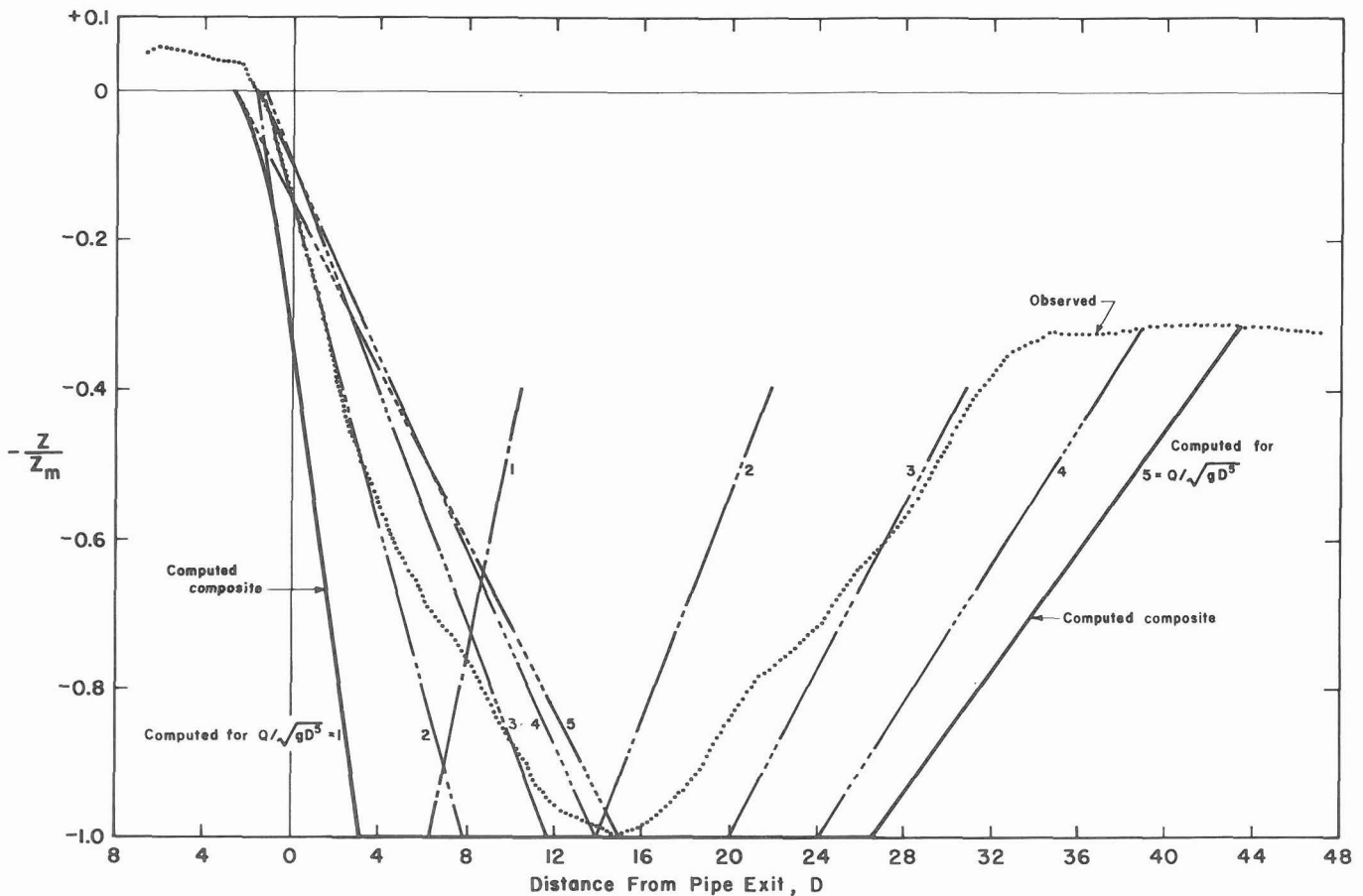


Figure XI-3
Observed and computed composite longitudinal profiles, with depth expressed in dimensionless depth units.

These solid lines circumscribe both the observed and the largest contours computed for all discharges. However, these contours are distorted because they are based on the composite dimensionless maximum depths. Because of the transfer from Minnesota to Oklahoma, plotting an undistorted contour map was not practical. However, an undistorted longitudinal profile was computed and is plotted in figure XI-4 for comparison with the distorted longitudinal profile plotted in figure XI-3.

The locations of the contours scaled from the computed contour maps for all discharges are plotted in figure XI-3. A circumscribed longitudinal section is also plotted as a solid line

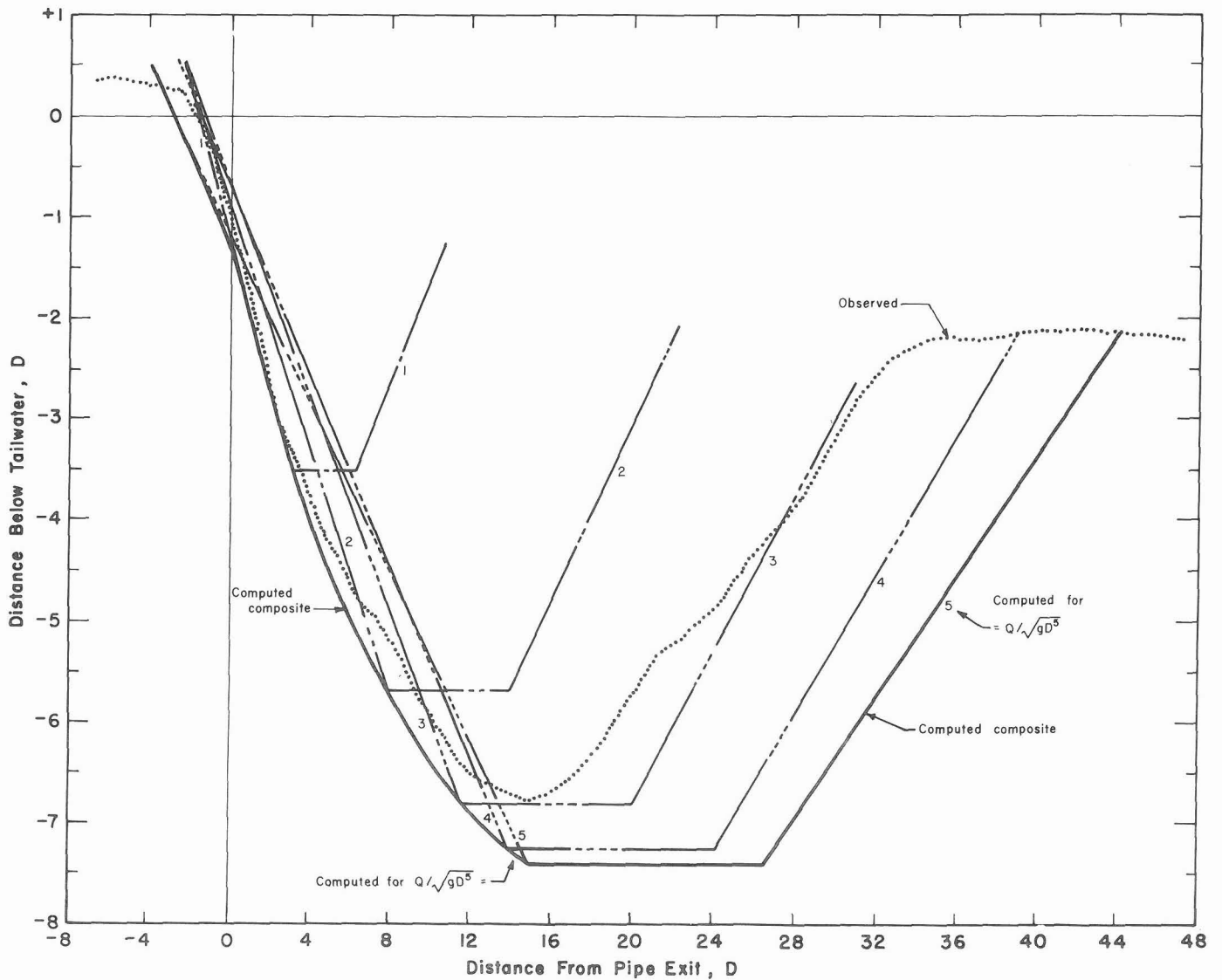


Figure XI-4
Observed and computed longitudinal profiles in terms of pipe diameters.

to show the shape of the distorted longitudinal profile. The longitudinal section shows that the shape of the upstream end of the plunge pool is largely controlled by the lowest discharges while the downstream end is controlled by the largest discharge.

The elevations in figures XI-2 and XI-3 are expressed in terms of the maximum depth of the hole. The maximum computed depth varies with the discharge, is not at the same elevation as is shown in figure XI-3, and the scour hole bottom, shown to be horizontal in figure XI-3, is not horizontal over its entire length. Like the composite contours in figure XI-2, the shape of the computed profile in figure XI-3 is distorted.

In figure XI-4 the longitudinal section depths are plotted in terms of the pipe diameter; and, except for the exaggerated scale of the ordinate, the shape of the computed composite profile is not distorted. The depths are those for a maximum depth based on $Z_{m,u}$; depths based on $Z_{m,t}$ did not circumscribe the bottom of the composite observed depth. The downstream end of the plunge pool is again determined by the computed shape for the maximum discharge. However, the actual--and undistorted--upstream slope shown in figure XI-4 is a curve defined by every discharge.

Suggested Design Procedure

Based on logic and verified by a single step-hydrograph test, the suggested procedure for determining the plunge pool size and shape is to (1) use the computed ultimate maximum scour hole depth to compute separate contour maps for discharges covering the complete range of anticipated discharges and (2) develop the design contour, circumscribing all of the contours computed for each elevation for the complete range of discharges.

XII. PLUNGE POOL ENERGY DISSIPATOR DESIGN PROCEDURE

The procedure, equations, and criteria for designing plunge pool energy dissipators are summarized and assembled in this chapter for convenience of reference and use. This chapter is written as a design guide.

The primary design equations are dimensionless. Thus, any dimensionally consistent system of units can be used to determine the plunge pool dimensions.

Only a few quantities need be known before beginning a design. Among these are the discharge Q and pipe diameter D , which are combined with the acceleration of gravity g to give the dimensionless discharge parameter $Q/\sqrt{gD^5}$; the pipe invert height above the tailwater level Z_p ; and the median sediment or riprap diameter d_{50} , which must meet minimum design criteria but which may be varied if the designer wishes to determine the effect of riprap size on the plunge pool dimensions. Most of the design parameters are defined in figure VIII-1 and are not defined in the text. Note especially that the scour depths Z , Z_m and $Z_{m,u}$ are always negative.

Limiting Discharge

The shape of the scour hole is related to the discharge and bed material size. The desirable scour hole or plunge pool shape is that of an inverted cone having side slopes approximating the submerged angle of repose of the bed material. An undesirable scour hole also has a conical bottom but with excessive widening or beaches near the top of the hole. The relation which ensures that the scour hole will not have a beach is

$$\frac{Q}{\sqrt{gD^5}} \leq 1.0 + 25 \frac{d_{50}}{D} \quad (\text{X-2})$$

The following equations for the scour hole or plunge pool dimensions are valid only if this limiting discharge is not exceeded.

Jet Computations

The jet issuing from the pipe with a velocity V_o determines the location and dimensions of the plunge pool. The jet equations needed for the plunge pool design are:

The horizontal velocity of the jet $V_{p,h}$ expressed in terms of the velocity at which the jet plunges into the tailwater,

$$V_{p,h} = V_o \cos(\sin^{-1} S) \quad (\text{VIII-4})$$

the vertical velocity $V_{p,v}$ at the plunge point,

$$V_{p,v} = \sqrt{(V_o S)^2 + 2g[Z_p + (D/2)\cos(\sin^{-1} S)]} \quad (\text{VIII-5})$$

and the jet velocity at the plunge point,

$$V_p = \sqrt{V_{p,h}^2 + V_{p,v}^2} \quad (\text{VIII-8})$$

Design note: The jet is partially or wholly supported by the tailwater and the equation for the jet trajectory is invalid if $Z_p \leq 0$. Therefore,--following: (a) the explanation preceding equation X-12b, (b) equation 12b, and (c) the data presented in figure X-8 verifying this procedure--assume for design purposes that for $Z_p < +D$, that $Z_p = +D$.

Because the vertical velocity increases between the pipe exit and the tailwater surface, the jet diameter at the plunge point is

$$D_p = D\sqrt{V_o/V_p} \quad (\text{VIII-9})$$

The path of the jet determines the location of the plunge pool. The path is a parabola between the pipe exit and the tailwater surface, so the horizontal distance to the plunge point is

$$X_p = \left\{ -V_o S + \sqrt{V_o^2 S^2 + 2g[Z_p + (D/2) \cos(\sin^{-1} S)]} \right\} \left\{ \frac{V_o}{g} \cos(\sin^{-1} S) \right\} \quad (\text{VIII-3})$$

After the jet enters the tailwater, gravity no longer affects the jet trajectory, so the jet continues tangent to the parabolic slope at the tailwater surface. The angle of this slope is

$$\alpha = \tan^{-1} \frac{V_{p,v}}{V_{p,h}} \quad (\text{VIII-6})$$

The jet continues at this slope until impinging on the bed. So the horizontal distance the jet travels from the pipe exit to the point of impingement on the bed is

$$X_j = X_p - \frac{Z_m}{\tan \alpha} \quad (\text{VIII-7})$$

Because the scour hole depth Z_m is not known, X_j cannot be computed yet.

Densimetric
Froude Number

The densimetric Froude number,

$$F_d = \frac{V_p}{\sqrt{gd_{50}(\rho_s - \rho)/\rho}} \quad (\text{X-19})$$

is a parameter used to measure the ability of the jet to mobilize the bed material. This parameter is the ratio of the jet plunge velocity V_p to a characteristic sediment velocity based on the sediment or riprap size d_{50} , the sediment density ρ_s , and the fluid density ρ . The maximum depth of the scour hole or plunge pool is related to F_d , increasing as F_d increases.

Ultimate Maximum
Scour Hole or
Plunge Pool Depth

To remove any possibility of ambiguity, the term "ultimate maximum scour hole depth $Z_{m,u}$ " needs the following definition. As scour progresses, material is suspended in the bottom of the scour hole. Flow from the hole removes some of the suspended material, but other material is recirculated in suspension. For completely stable holes, there will be no material in suspension, so we inserted a suction line and removed the suspended material. The result was a much deeper hole. The equations presented in this section are for the depth of the ultimate maximum or completely stable hole--a hole or plunge pool in which bed material or riprap will not be eroded.

The equations for the ultimate maximum scour hole depths are:

For $Z_p/D \leq 1$

$$\frac{Z_{m,u}}{D} = - 7.5[1 - e^{-0.6(F_d - 2)}] \quad (X-22)$$

and for $Z_p/D > 1$

$$\frac{Z_{m,u}}{D} = - 10.5[1 - e^{-0.35(F_d - 2)}] \quad (X-23)$$

These equations indicate that the bed material will not scour if $F_d \leq 2$. The upper limit of applicability is not known; the experimental data extend only to $F_d = 14$.

Scour Hole Location

Now equation VIII-7 can be used to compute the jet length. This gives the *approximate* location of the maximum depth. The *actual* location of the maximum depth, that is, the location of the center of the scour hole or plunge pool, was found to average

$$\frac{X_m}{X_j} = 1.15 e^{-0.15 Q/\sqrt{gD^5}} \quad (X-16)$$

where X_m is the distance from the pipe exit to the center of the scour hole or plunge pool.

Scour Hole Shape

The scour hole shape is that of an ellipse. The equation defining the scour hole contours is

$$\begin{aligned} \frac{X - X_m}{X_m - X_{b,tw}} &= \frac{X - X_m}{X_{e,tw} - X_m} \\ &= 0.15\left(1 - \frac{Z}{Z_m}\right) \mp \left(1.15 - 0.90 \frac{Z}{Z_m}\right) \times \\ &\quad \sqrt{1 - \left[\frac{2Y/W_{m,tw}}{1.00 - 0.775(Z/Z_m) - 0.125(Z/Z_m)^2} \right]^2} \end{aligned} \quad (X-9)$$

The values of Z_m and X_m are given by equations X-22, X-23 and X-16. The distances from the center of the hole at X_m to the water surface contour at the upstream end $X_{b,tw}$, the downstream end $X_{e,tw}$, and the width $W_{m,tw}$ can be obtained from

$$\frac{X_m - X_{b,tw}}{Z_m} = \frac{X_{e,tw} - X_m}{Z_m} = \frac{3}{2} + \frac{1}{3} \frac{Q}{\sqrt{gD^5}} \quad (X-10)$$

and

$$\frac{W_{m,tw}}{2Z_m} = 1.5 + 0.15 \frac{Q}{\sqrt{gD^5}} \quad (X-11)$$

The remaining variables are X , Y and Z . Z is the elevation of the scour hole or plunge pool contour. $Z = 0$ at the tailwater surface and $Z = Z_m$ at the bottom of the hole or pool. When a value of Z is selected, the contour equation is expressed in terms of X and Y measured from axes originating at the center of the hole or pool. Solution of this equation for a range of values of Z gives the size and shape of the pipe spillway plunge pool energy dissipator for the selected discharge, pipe size, pipe height, and bed material or riprap size.

Time Progression of Scour

The ultimate limit of scour is approached asymptotically. The hyperbolic logarithmic equation defining the depth progression is

$$\frac{Z_m}{D} = - \text{antilog} (x + y_0 - \sqrt{x^2 + a^2}) \quad (X-24)$$

where

$$y_o = \log \frac{-Z_{m,u}}{D} \quad (X-25)$$

is computed with the aid of equation X-22 or X-23,

$$x = \log \frac{tV_p}{D_p} \quad (X-26)$$

is computed with the aid of equations VIII-8 and VIII-9, and the logarithm of the hyperbola semiaxis is

$$a = 1.75 \quad (X-27)$$

Because the scour hole or plunge pool location and shape are functions of Z_m/D , the variation of these dimensions with time t in seconds can now be computed.

Agreement of
Equations With
Experimental Holes

To ensure that the design plunge pools would not erode, the several equations were evaluated to envelop most of the experimental data. Multiple envelopments could have resulted in ultraconservative computed plunge pool sizes. To check on the degree of conservatism, equation values of the scour hole widths, depths, and locations were compared with the experimental values.

For the scour holes in which the suspended material was completely removed, these comparisons show that 83% of the observed depths were less than or within one pipe diameter of the computed depths, 85% of the observed widths were less than or within two pipe diameters of the computed widths, and 72% of the computed locations were further downstream or within one pipe diameter of the observed location. The conclusion is that, although some scour holes and plunge pools can be expected to exceed the dimensions predicted by the design equations, on the average the design equations will predict the scour hole and plunge pool dimensions with a moderate degree of conservatism.

Composite
Plunge Pool
Energy Dissipator

At every elevation the constructed plunge pool contours must circumscribe the contours computed for the complete range of discharges anticipated during the life of the structure. For the maximum anticipated discharge, the scour hole will have the maximum size and maximum depth, and will be located farthest downstream from the spillway outlet: The anticipated maximum discharge can, therefore, be expected to determine the downstream dimensions (and possibly the maximum depth) of a plunge pool energy dissipator. However, at a lesser discharge the jet may attack the upstream slope of the larger discharge scour hole. Therefore, a less-than-maximum discharge may determine the

upstream dimensions. To summarize: Each constructed plunge pool energy dissipator contour must circumscribe all contours computed for that elevation for the entire range of anticipated discharges.

The contours for each discharge may be computed by substituting into equation X-9 the values computed using equation X-10 and X-11. Z_m is obtained from equation X-22 or X-23 and equation X-19. Assumed values of Z in equation X-9 should cover the range $0.0 \leq Z \leq Z_m$.

The resulting contour coordinates at each contour elevation and discharge are in terms of Z_m . To determine the circumscribing dimensions and the design dimensions of the plunge pool energy dissipator, Z_m needs to be converted into dimensional units. This can be done by inserting the known dimensional value of D into equation X-22 or X-23.

Effect of Nonerodible Layer

The effect of a horizontal rock ledge or other nonerodible layer on the scour hole dimensions was evaluated in a single test series by placing a plywood sheet at half the maximum depth computed using the maximum nonbeaching discharge for the bed material used. A full range of flows was tested.

The observed contours were compared with the equation contours developed for the full-depth scour holes. The comparisons logically fall into two groups:

1. For low flows the scour did not reach and was not influenced by the fixed bed. These test conditions agree with those used to develop the contour equations. As expected, the observed contours agree with the equation contours.
2. The higher flows scoured to and exposed the fixed bed. Although the equation contours based on the depth to the fixed bed did not define the observed contours, the equation contours based on the computed maximum depth do adequately and conservatively define the observed contours.

To determine the scour hole contours when there is a fixed bed exposed in the scour hole, these findings, although based on limited tests, suggest that the fixed bed contours be based on the computed ultimate scour hole depth. With this procedure, some *computed* scour hole contours will be *below* the fixed bed. The contours above the fixed bed then define the scour hole shape down to the fixed bed and the area of the fixed bed that will be exposed.

XIII. EXAMPLES OF APPLICATION OF RESULTS

Computations will be made in this section to show in both familiar and dimensionless units of measurement the magnitudes of the plunge pool or scour hole depths below tailwater and distances from the pipe exit to the center that can be expected for a range of practical applications.

Example Values

Discharge. Data listed by Blaisdell (1983, table 2) were analyzed to obtain an idea of the range of discharges used in practice throughout the United States. For $Q/\sqrt{gD^5}$ a single minimum value of 0.31 and a single maximum value of 2.94 are listed. Other values fall in the range 0.54 to 2.49. Fifty-four percent of the relative discharges are in the range 1.5 to 2.0 and 30% in the range 2.0 to 2.5. Because $Q/\sqrt{gD^5} = 0.5$ is the lowest dimensionless discharge at which the pipe remained full during the study reported here, this will be the minimum discharge used as an example. $Q/\sqrt{gD^5} = 2.0$ will be selected as a typical value; and $Q/\sqrt{gD^5} = 3.0$ as the possible maximum dimensionless discharge used in practice.

Pipe size. Farm ponds might use pipes 12 inches or smaller in diameter. Upstream flood control reservoir spillways might use pipes of up to 72 inches or larger in diameter. To cover this range, example computations will be made for pipe diameters of 12, 24, 36 and 72 inches.

Pipe height. Ordinarily the invert of the pipe will be close to the tailwater level, so a pipe height of $Z_p/D = 1$ will be used in the example computations. Because pipes discharging surface drainage into gullies may discharge well above the tailwater level, a relative pipe height of 5 will be used to illustrate the effect of higher heights on the scour hole dimensions.

Pipe slope. Only one pipe slope S will be used--1%. Since pipe height has a similar effect as pipe slope on the angle at which the jet enters the tailwater, the higher pipe will also indicate the effect of pipe slope.

Scour time. Two times of scour duration will be used as examples. The ultimate maximum depth of scour represents a completely stable scour hole or plunge pool. The corresponding experimental condition is the scour obtained for the suspended-material-removed tests, which were run until there was no observable sediment movement. In the example, equations X-22 and X-23 will be used to compute $Z_{m,u}$, the ultimate maximum scour depth for completely stable holes. During the time-dependent tests there was some sediment in suspension at the end of each time and scour was still taking place, albeit slowly--apparently at a logarithmic time increment. To compute the maximum scour depth $Z_{m,t}$ for this condition, a time increment $t = 10,000$ min (6.94 days) was selected. For this time, some further increase

in scour hole or plunge pool size can be anticipated. Eventually there will be no further removal of sediment from the scour hole, and a balance will be achieved between the sediment eroded and the sediment deposited from suspension.

Riprap size. The size of bed material or riprap will affect the size of the scour hole or riprapped plunge pool. Since the required thickness of the riprap increases in proportion to its size and since the volume of riprap required is determined by both riprap thickness and plunge pool size, there will likely be an optimum combination of riprap and plunge pool sizes. Therefore, plunge pool dimensions will be computed for bed material or riprap sizes of 3, 6, 12, 18 and 36 inches.

Beaching Limit

Equation X-2 is used to compute the discharge below which no beaching will occur. These dimensionless discharges are listed in table XIII-1 for the ranges of variables used in the example. Because the maximum dimensionless discharge used in the example is 3, beaching is anticipated only for the 3-inch riprap, 72-inch pipe, and dimensionless discharge of 3. The equations defining the plunge pool or scour hole dimensions are not applicable to this beaching condition.

Interestingly, equation X-2 indicates beaching will not occur for any size bed material when $Q/\sqrt{gD^5} \leq 1$.

Jet Computations

Certain jet dimensions are needed for use in the computations. The densimetric Froude number given by equation X-19 requires knowledge of the jet plunge velocity V_p --the velocity at which the jet enters the tailwater. Equations VIII-8, -4 and -5 are used to compute V_p . The distance to the center of the scour hole requires X_j --given by equation VIII-7, which in turn requires both the distance to the plunge point X_p given by equation VIII-3, and the angle α at which the jet enters the tailwater given by equation VIII-6. The jet plunge diameter D_p used in computing the time-dependent maximum scour depth is given by equation VIII-9. The jet properties V_p , D_p , X_p and α are listed in table XIII-2 for the conditions of the example.

Plunge Pool (or Scour Hole) Dimensions

The results of the computations are listed in table XIII-3. Equations X-22 and X-23 are used to compute the ultimate and completely stable depth $Z_{m,u}$. To compute the time-dependent depth of scour $Z_{m,t}$, equations X-24 and X-27 and equations VIII-8, -9, -4 and -5 are used. The distance to the center of the pool or hole X_m is computed using equations X-16 and VIII-7, the values of Z_m just computed, and the values of X_p and α listed in table XIII-2.

Table XIII-1
 Values of $Q/\sqrt{gD^5}$ below which
 beaching will not occur, as
 calculated using equation X-2

d_{50} in	D - inches			
	12	24	36	72
3	7.2	4.1	3.1	2.0
6	13.5	7.2	5.2	3.1
12	26.0	13.5	9.3	5.2
18	38.5	19.8	13.5	7.2
36	76.0	38.5	26.0	13.5

Table XIII-2
 Jet dimensions for example calculations, with $S = 0.01$

D in	$Z_p = 1D$				$Z_p = 5D$				
	V_p ft/s	D_p ft	X_p ft	α deg.	V_p ft/s	D_p ft	X_p ft	α deg.	Z_p ft
$Q/\sqrt{gD^5} = 0.5$									
12	10.47	0.59	1.10	69.8	19.15	0.43	2.11	79.1	5
24	14.80	1.17	2.20	69.8	27.09	0.87	4.21	79.1	10
36	18.13	1.76	3.30	69.8	33.18	1.30	6.32	79.1	15
72	25.64	3.52	6.59	69.8	46.92	2.61	12.64	79.1	30
$Q/\sqrt{gD^5} = 2.0$									
12	17.47	0.91	4.35	34.2	23.72	0.78	8.38	52.5	5
24	24.70	1.82	8.69	34.2	33.54	1.56	16.76	52.5	10
36	30.25	2.73	13.04	34.2	41.08	2.34	25.14	52.5	15
72	42.79	5.46	26.08	34.2	58.09	4.68	50.28	52.5	30
$Q/\sqrt{gD^5} = 3.0$									
12	23.79	0.95	6.47	24.4	28.69	0.87	12.57	41.0	5
24	33.64	1.91	12.94	24.4	40.58	1.74	25.05	41.0	10
36	41.20	2.86	19.41	24.4	49.70	2.61	37.57	41.0	15
72	58.27	5.73	38.83	24.4	70.28	5.21	75.14	41.0	30

Some computed positive values of $Z_{m,u}/D$ are listed for information only. Of course, such indicated buildup of bed material is not possible; positive computed values of $Z_{m,u}$ actually indicate there is no scour.

Various comparisons of the depths are possible. Within each group of constant pipe size, pipe height, and discharge, the decrease of depth with increasing riprap size is readily apparent. Comparisons between groups with the same discharge and pipe size will show the effect of pipe height. And the effect of discharge can be found by comparing groups having the same pipe size and pipe height.

In table XIII-3 some of the depths computed for the time-dependent condition with $t = 10,000$ min increase with increase in size of the riprap. This is, of course, illogical. The trend is most noticeable for the larger pipe sizes and larger relative discharges. This illogical trend did not occur for the (unlisted) time-dependent depths computed for $t = 10^{90}$ min and for the $Z_{m,u}$ depths.

An examination of the illogical values of $Z_{m,t}$ in table XIII-3 shows that they are associated with F_d values greater than about 8. In the discussion in chapter X following equation X-21 we noted that in practice generally $F_d < 6$, so these illogical values--if F_d is the correct parameter to separate them--may have no practical significance. In any case, if the plunge pool size is based on $Z_{m,u}$ there is no anomaly.

It should be kept in mind that scour is still active, albeit perhaps slowly, for the time-dependent condition and that the smaller depths for $t = 10,000$ min as compared with the $Z_{m,u}$ depths indicate that the time-dependent depths can be expected to scour further. The additional scour and the degree of damage to the time-dependent plunge pool is probably indicated by the difference between the time-dependent and ultimate depths.

Because the lengths and widths of the pools or holes are proportional to the values of Z_m , example magnitudes can be readily computed by entering values for $Q/\sqrt{gD^5}$ and Z_m in equations X-10 and X-11.

Table XIII-3

Examples of plunge pool (or scour hole) dimensions computed for $Q/\sqrt{gD^5} = 0.5, 2.0$ and 3.0 , $S = 0.010$, and $t = 10,000$ minutes

D	d_{50}	Z_p	Q	F_d	$Z_{m,u}$	$Z_{m,t}$	$X_{m,u}$	$X_{m,t}$	$\frac{Z_{m,u}}{D}$	$\frac{Z_{m,t}}{D}$	$\frac{X_{m,u}}{D}$	$\frac{X_{m,t}}{D}$
in	in	ft	ft ³ /s		ft	ft	ft	ft				
$Q/\sqrt{gD^5} = 0.5$												
12	3	1	2.8	2.87	-3.1	-2.2	2.4	2.0	-3.06	-2.23	2.37	2.05
	6			2.03	-0.1	-0.1	1.2	1.2	-0.14	-0.11	1.23	1.21
	12			1.44	0	---	---	---	+3.02	---	---	---
	18			1.17	0	---	---	---	+4.82	---	---	---
	36			0.83	0	---	---	---	+7.64	---	---	---
24	3	2	16.0	4.06	-10.6	-7.4	6.5	5.3	-5.32	-3.72	3.26	2.63
	6			2.87	-6.1	-4.4	4.7	4.1	-3.06	-2.21	2.37	2.04
	12			2.03	-0.3	-0.2	2.5	2.4	-0.14	-0.10	1.23	1.21
	18			1.66	0	---	---	---	+1.70	---	---	---
	36			1.17	0	---	---	---	+4.82	---	---	---
36	3	3	44.2	4.98	-18.7	-12.7	10.9	8.5	-6.24	-4.22	3.62	2.82
	6			3.52	-13.5	-9.5	8.8	7.3	-4.49	-3.18	2.93	2.42
	12			2.49	-5.7	-4.2	5.8	5.2	-1.90	-1.39	1.92	1.72
	18			2.03	-0.4	-0.3	3.7	3.6	-0.14	-0.10	1.23	1.21
	36			1.44	0	---	---	---	+3.02	---	---	---
72	3	6	250.1	7.04	-42.8	-26.6	23.8	17.5	-7.14	-4.43	3.97	2.91
	6			4.98	-37.5	-25.1	21.7	16.9	-6.24	-4.18	3.62	2.81
	12			3.52	-26.9	-18.9	17.6	14.4	-4.49	-3.15	2.93	2.41
	18			2.87	-18.4	-13.2	14.2	12.2	-3.06	-2.19	2.37	2.03
	36			2.03	-0.8	-0.6	7.4	7.3	-0.14	-0.10	1.23	1.21
12	3	5	2.8	5.26	-7.1	-4.9	3.7	3.3	-7.14	-4.94	3.71	3.26
	6			3.72	-4.7	-3.4	3.2	3.0	-4.74	-3.44	3.22	2.95
	12			2.63	-2.1	-1.6	2.7	2.6	-2.08	-1.55	2.67	2.57
	18			2.15	-0.5	-0.4	2.4	2.3	-0.52	-0.40	2.36	2.33
	36			1.52	0	---	---	---	+1.93	---	---	---
24	3	10	16.0	7.44	-17.9	-11.4	8.2	6.8	-8.93	-5.70	4.08	3.42
	6			5.26	-14.3	-9.8	7.4	6.5	-7.14	-4.90	3.71	3.25
	12			3.72	-9.5	-6.8	6.4	5.9	-4.75	-3.42	3.22	2.95
	18			3.04	-6.4	-4.7	5.8	5.5	-3.19	-2.34	2.90	2.73
	36			2.15	-1.1	-0.8	4.7	4.7	-0.52	-0.40	2.36	2.33
36	3	15	44.2	9.11	-28.9	-17.2	12.7	10.3	-9.63	-5.75	4.22	3.43
	6			6.44	-24.8	-16.3	11.8	10.1	-8.28	-5.44	3.94	3.36
	12			4.55	-18.6	-13.0	10.6	9.4	-6.20	-4.34	3.52	3.14
	18			3.72	-14.2	-10.2	9.7	8.8	-4.75	-3.40	3.22	2.94
	36			2.63	-6.2	-4.6	8.0	7.7	-2.08	-1.54	2.67	2.56
72	3	30	250.1	12.88	-61.6	-31.2	26.1	19.9	-10.27	-5.20	4.35	3.31
	6			9.11	-57.8	-34.1	25.3	20.5	-9.63	-5.69	4.22	3.41
	12			6.44	-49.7	-32.4	23.7	20.1	-8.28	-5.39	3.94	3.35
	18			5.26	-42.9	-29.1	22.3	19.4	-7.14	-4.84	3.71	3.24
	36			3.72	-28.5	-20.3	19.3	17.6	-4.75	-3.38	3.22	2.94

Table XIII-3--Continued
 Examples of plunge pool (or scour hole) dimensions
 computed for $Q/\sqrt{gD^5} = 0.5, 2.0$ and $3.0, S = 0.010,$
 and $t = 10,000$ minutes

D	d_{50}	Z_p	Q	F_d	$Z_{m,u}$	$Z_{m,t}$	$X_{m,u}$	$X_{m,t}$	$\frac{Z_{m,u}}{D}$	$\frac{Z_{m,t}}{D}$	$\frac{X_{m,u}}{D}$	$\frac{X_{m,t}}{D}$
in	in	ft	ft ³ /s		ft	ft	ft	ft				
$Q/\sqrt{gD^5} = 2.0$												
12	3	1	11.3	4.80	-6.1	-4.2	11.3	9.0	-6.10	-4.20	11.34	8.97
	6			3.39	-4.2	-3.1	9.0	7.5	-4.24	-3.06	9.02	7.53
	12			2.40	-1.6	-1.2	5.7	5.2	-1.59	-1.18	5.70	5.18
	18			1.96	0	----	----	----	+0.19	----	----	----
	36			1.38	0	----	----	----	+3.35	----	----	----
24	3	2	64.2	6.78	-14.1	-9.0	25.1	18.7	-7.07	-4.52	12.56	9.36
	6			4.80	-12.2	-8.3	22.7	17.8	-6.10	-4.17	11.34	8.92
	12			3.39	-8.5	-6.1	18.0	15.0	-4.24	-3.04	9.02	7.50
	18			2.77	-5.5	-4.0	14.3	12.5	-2.77	-2.02	7.17	6.23
	36			1.96	0	----	----	----	+0.19	----	----	----
36	3	3	176.8	8.30	-22.0	-13.2	38.6	27.6	-7.33	-4.40	12.88	9.21
	6			5.87	-20.3	-13.3	36.5	27.8	-6.77	-4.44	12.18	9.26
	12			4.15	-16.3	-11.3	31.5	25.3	-5.44	-3.78	10.51	8.44
	18			3.39	-12.7	-9.1	27.1	22.5	-4.24	-3.02	9.02	7.49
	36			2.40	-4.8	-3.5	17.1	15.5	-1.59	-1.17	5.70	5.17
72	3	6	1000.3	11.75	-44.9	-23.1	78.4	51.1	-7.48	-3.85	13.07	8.52
	6			8.31	-44.0	-26.1	77.3	54.9	-7.33	-4.35	12.88	9.15
	12			5.87	-40.6	-26.4	73.1	55.3	-6.77	-4.40	12.18	9.21
	18			4.80	-36.6	-24.7	68.0	53.1	-6.10	-4.12	11.34	8.86
	36			3.39	-25.5	-18.0	54.1	44.8	-4.24	-3.00	9.02	7.46
12	3	5	11.3	6.51	-8.3	-5.5	12.6	10.7	-8.33	-5.49	12.59	10.73
	6			4.60	-6.3	-4.4	11.2	10.0	-6.28	-4.40	11.25	10.02
	12			3.26	-3.7	-2.7	9.6	8.9	-3.73	-2.72	9.58	8.92
	18			2.66	-2.2	-1.6	8.6	8.2	-2.16	-1.60	8.55	8.19
	36			1.88	0	----	----	----	+0.45	----	----	----
24	3	10	64.2	9.21	-19.3	-11.4	26.9	21.8	-9.66	-5.72	13.46	10.88
	6			6.51	-16.7	-10.9	25.2	21.4	-8.33	-5.44	12.59	10.70
	12			4.60	-12.6	-8.7	22.5	20.0	-6.28	-4.36	11.25	10.00
	18			3.76	-9.7	-6.9	20.6	18.8	-4.83	-3.44	10.30	9.39
	36			2.66	-4.3	-3.2	17.1	16.4	-2.16	-1.59	8.55	8.18
36	3	15	176.8	11.28	-30.3	-16.4	41.2	32.1	-10.09	-5.47	13.74	10.72
	6			7.97	-27.6	-17.1	39.5	32.5	-9.20	-5.67	13.16	10.85
	12			5.64	-22.7	-15.2	36.3	31.3	-7.56	-5.06	12.08	10.45
	18			4.60	-18.8	-13.0	33.7	29.9	-6.28	-4.34	11.25	9.98
	36			3.26	-11.2	-8.1	28.7	26.7	-3.73	-2.70	9.58	8.90
72	3	30	1000.3	15.95	-62.5	-27.1	83.7	60.6	-10.42	-4.52	13.96	10.09
	6			11.28	-60.6	-32.4	82.4	64.0	-10.09	-5.40	13.74	10.67
	12			7.97	-55.2	-33.7	79.0	64.9	-9.20	-5.61	13.16	10.81
	18			6.51	-50.0	-32.2	75.5	63.9	-8.33	-5.36	12.59	10.65
	36			4.60	-37.7	-25.9	67.5	59.8	-6.28	-4.31	11.25	9.96

Table XIII-3--Continued
 Examples of plunge pool (or scour hole) dimensions
 computed for $Q/\sqrt{gD^5} = 0.5, 2.0$ and $3.0, S = 0.010,$
 and $t = 10,000$ minutes

D	d_{50}	Z_p	Q	F_d	$Z_{m,u}$	$Z_{m,t}$	$X_{m,u}$	$X_{m,t}$	$\frac{Z_{m,u}}{D}$	$\frac{Z_{m,t}}{D}$	$\frac{X_{m,u}}{D}$	$\frac{X_{m,t}}{D}$
in	in	ft	ft ³ /s		ft		ft	ft	ft			
					$Q/\sqrt{gd^5} = 3.0$							
12	3	1	17.0	6.53	-7.0	-4.6	16.1	12.2	-7.00	-4.59	16.07	12.16
	6			4.62	-5.9	-4.1	14.3	11.4	-5.94	-4.14	14.35	11.44
	12			3.27	-4.0	-2.9	11.2	9.4	-3.99	-2.90	11.19	9.43
	18			2.67	-2.5	-1.8	8.7	7.7	-2.47	-1.83	8.74	7.70
	36			1.89	0	---	---	---	+0.54	----	----	----
24	3	2	96.2	9.24	-14.8	-8.7	33.4	23.6	-7.40	-4.35	16.71	11.78
	6			6.53	-14.0	-9.1	32.1	24.2	-7.00	-4.54	16.07	12.09
	12			4.62	-11.9	-8.2	28.7	22.8	-5.94	-4.11	14.35	11.39
	18			3.77	-9.8	-7.0	25.4	20.8	-4.91	-3.49	12.68	10.38
	36			2.67	-4.9	-3.6	17.5	15.4	-2.47	-1.82	8.74	7.68
36	3	3	265.2	11.31	-22.4	-12.0	50.5	33.7	-7.47	-4.01	16.82	11.23
	6			8.00	-21.9	-13.4	49.6	35.9	-7.30	-4.46	16.54	11.96
	12			5.66	-20.0	-13.3	46.6	35.7	-6.66	-4.43	15.52	11.91
	18			4.62	-17.8	-12.3	43.0	34.1	-5.94	-4.09	14.35	11.36
	36			3.26	-12.0	-8.6	33.6	28.1	-3.99	-2.87	11.19	9.38
72	3	6	1500.0	16.00	-45.0	-19.3	101.2	59.6	-7.50	-3.21	16.87	9.94
	6			11.31	-44.8	-22.1	100.9	66.9	-7.47	-3.69	16.82	11.15
	12			8.00	-43.8	-26.5	99.2	71.3	-7.30	-4.42	16.54	11.89
	18			6.53	-42.0	-26.9	96.4	71.9	-7.00	-4.48	16.07	11.98
	36			4.62	-35.6	-24.3	86.1	67.8	-5.94	-4.06	14.35	11.31
12	3	5	17.0	7.88	-9.2	-5.8	16.9	14.0	-9.16	-5.76	16.92	14.05
	6			5.57	-7.5	-5.1	15.5	13.5	-7.49	-5.10	15.51	13.48
	12			3.94	-5.2	-3.7	13.6	12.3	-5.17	-3.70	13.55	12.31
	18			3.22	-3.6	-2.7	12.3	11.4	-3.64	-2.66	12.26	11.43
	36			2.27	-1.0	-0.7	10.0	9.8	-0.96	-0.72	9.99	9.79
24	3	10	96.2	11.14	-20.1	-11.1	35.4	27.7	-10.07	-5.54	17.69	13.86
	6			7.88	-18.3	-11.4	33.8	28.0	-9.16	-5.71	16.92	14.00
	12			5.57	-15.0	-10.1	31.0	26.9	-7.49	-5.06	15.51	13.45
	18			4.55	-12.4	-8.6	28.8	25.7	-6.20	-4.32	14.41	12.83
	36			3.22	-7.3	-5.3	24.5	22.8	-3.64	-2.64	12.26	11.42
36	3	15	265.2	13.64	-31.0	-15.2	53.7	40.4	-10.32	-5.07	17.90	13.47
	6			9.65	-29.3	-17.0	52.3	41.9	-9.78	-5.67	17.44	13.97
	12			6.82	-25.7	-16.5	49.2	41.5	-8.56	-5.51	16.41	13.83
	18			5.57	-22.5	-15.1	46.5	40.3	-7.49	-5.03	15.51	13.43
	36			3.94	-15.5	-11.0	40.6	36.8	-5.17	-3.66	13.55	12.28
72	3	30	1500.5	19.29	-62.9	-23.1	108.2	74.6	-10.48	-3.86	18.03	12.44
	6			13.64	-61.9	-30.0	107.4	80.4	-10.32	-5.00	17.90	13.40
	12			9.65	-58.7	-33.6	104.6	83.5	-9.78	-5.60	17.44	13.92
	18			7.88	-54.9	-33.7	101.5	83.6	-9.16	-5.62	16.92	13.93
	36			5.57	-44.9	-29.9	93.0	80.4	-7.49	-4.99	15.51	13.40

XIV. CONCLUSIONS

There are two major conclusions resulting from these tests:

1. The beaching limit discharge--that discharge greater than which beaching can be expected and below which beaches will not develop--is

$$\frac{Q}{\sqrt{gD^5}} \leq 1.0 + 25 \frac{d_{50}}{D} \quad (\text{X-2})$$

2. The procedures presented in chapter XII can, with a moderate degree of conservatism, be used to determine the size, shape, location, and riprap to be used for stable cantilevered pipe outlet plunge pool energy dissipators.

REFERENCES

- Abt, S.R. 1980. Scour at culvert outlets in cohesive material. Ph.D. thesis. 157 pp. [On file at the Colorado State University, Fort Collins.]
- Abt, S.R.; Kloberdanz, R.L.; and Mendoza, C. 1984. Unified culvert scour determination. *Journal of Hydraulic Engineering* 110(10):1475-1479.
- Abt, S.R., and Ruff, J.F. 1981. Estimating local scour in cohesive material. In Proceedings of the Specialty Conference Water Forum '81, San Francisco, CA, August 10-14, 1981. American Society of Civil Engineers. pp. 860-867.
- Abt, S.R., and Ruff, J.F. 1982. Estimating culvert scour in cohesive material. *Journal of the Hydraulics Division* 108(HY1):25-34.
- Abt, S.R.; Ruff, J.F.; and Doehring, F.K. 1985. Culvert slope effects on outlet scour. *Journal of Hydraulic Engineering* 111(HY10):1363-1367.
- Anderson, A.G.; Paintal, A.S.; and Davenport, J.T. 1970. Tentative design procedure for riprap-lined channels. National Academy of Sciences--National Academy of Engineering, National Research Council, Highway Research Board, National Cooperative Highway Research Program Report 108, 75 pp.
- Anderson, C.L., and Blaisdell, F.W. 1982. Plunge pool energy dissipator for pipe spillways. In Proceedings of the Conference Applying Research to Hydraulic Practice, Jackson, MS, August 17-20, 1982. American Society of Civil Engineers, pp. 289-297.
- Beltaos, S. 1976. Oblique impingement of circular turbulent jets. *Journal of Hydraulic Research* 14(1):17-36.
- Blaisdell, F.W. 1971. Discussion of "Automatic Device for Plotting Profiles of Hydraulic Models," by Y.J. Kingma, *Journal of Hydraulic Research* 9(3):467-475.
- Blaisdell, F.W. 1983. Analysis of scour observations at cantilever outlets. U.S. Department of Agriculture Misc. Pub. No. 1427, 14 pp.
- Blaisdell, F.W.; Anderson, C.L.; and Hebaus, G.G. 1981. Ultimate dimensions of local scour. *Journal of the Hydraulics Division* 107(HY3):327-337.

- Blaisdell, F.W., and Anderson, C.L. 1984. Pipe spillway plunge pool design equations. In Proceedings of the Conference Water for Resources Development, Coeur d'Alene, ID, August 14-17, 1984. American Society of Civil Engineers, pp. 390-396.
- Blinco, P.H., and Simons, D.B. 1973. Measurement of instantaneous boundary shear stress. In Proceedings of the 21st Annual Hydraulics Division Specialty Conference, Montana State University, Bozeman, August 15-17, 1973. American Society of Civil Engineers, pp. 43-54.
- Bohan, J.P. 1970. Erosion and riprap requirements at culvert and storm-drain outlets. U.S. Army Engineer Waterways Experiment Station Research Report H-70-2, Vicksburg, MS, 18 pp, 2 tables, 4 photographs, 20 plates.
- Cola, R. 1965. Energy dissipation of a high velocity vertical jet entering a basin. In Proceedings, 11th Congress of the International Association for Hydraulic Research, Leningrad, U.S.S.R., vol. 1, paper 1.52.
- Culp, M.M. 1968. Armored scour hole for cantilever outlet. U.S. Department of Agriculture, Soil Conservation Service Design Note No. 6, 3 pp, 7 dwg.
- Davis, C.V., and Sorensen, E.K., Ed. 1969. Spillways and stream-bed protection works. In Handbook of Applied Hydraulics, 3d ed., McGraw Hill Book Co., New York, p. 20-38.
- Doddiah, Doddiah. 1949. Comparison of scour caused by hollow and solid jets of water. M.S. thesis. 156 pp. [On file at the Colorado Agricultural and Mechanical College, Fort Collins.]
- Doddiah, Doddiah; Albertson, M.L.; and Thomas, R.K. 1953. Scour from jets. In Proceedings, Fifth Congress of the International Association for Hydraulic Research, Minneapolis, MN, September 1-4, 1953, pp. 161-169.
- Fletcher, B.P., and Grace, J.L., Jr. 1972. Practical guidance for estimating and controlling erosion at culvert outlets. U.S. Army Engineer Waterways Experiment Station Misc. Paper H-72-5, Vicksburg, MS, 11 pp. 4 tables, 23 figures.
- Fletcher, B.P., and Grace, J.L., Jr. 1974. Practical guidance for design of lined channel expansions at culvert outlets. U.S. Army Engineer Waterways Experiment Station Technical Report H-74-9, Vicksburg, MS, 91 pp.
- Goon, H.J. 1986. Riprap lined plunge pool for cantilever outlet. U.S. Department of Agriculture, Soil Conservation Service Design Note No. 6 (Second edition), 15 pp.

Hallmark, D.E. 1955. Scour at the base of a free overfall. M.S. thesis. [On file at the Colorado Agricultural and Mechanical College, Fort Collins.]

Hartung, F., and Haustler, F. 1973. Scours, stilling basins and downstream protection under free jets. Transactions, 11th International Congress on Large Dams, vol. II, question 41, reply 3, Madrid, Spain, June 1973. pp. 39-56.

Iwagaki, Y.; Smith, G.L.; and Albertson, M.L. 1958. Analytical study of the mechanics of scour for three-dimensional jet. Colorado State University Research Foundation Report No. CER60GLS9, Fort Collins, 66 pp.

Kappus, U. 1965. Hydraulics of box culverts. M.S. thesis. [On file at the University of Cincinnati, Cincinnati, OH.]

Karaki, S.S., and Haynie, R.M. 1963. Mechanics of local scour: Part II--Bibliography. Colorado State University Report CER63SSK46, Fort Collins, 51 pp.

Kloberdanz, R.L. 1982. Localized culvert scour in noncohesive bed material. M.S. thesis. 98 pp. [On file at the Colorado State University, Fort Collins.]

Laursen, E.M. 1952. Observations on the nature of scour. In Proceedings of Fifth Hydraulic Conference, Bulletin 34, University of Iowa, Iowa City, June 9-11, 1952, pp. 179-197.

Laushey, L.M. 1966. Design criteria for erosion protection at the outlet of culverts. University of Cincinnati Research Foundation, Cincinnati, OH, 44 pp.

Laushey, L.M.; Kappus, U.; and Ofwona, M.P. 1967. Magnitude and rate of erosion at culvert outlets. In Proceedings, 12th Congress of the International Association for Hydraulic Research, Colorado State University, Fort Collins, September 11-14, 1967, pp. 338-345.

Little, W.C., and Mayer, P.G. 1972. The role of sediment gradation on channel armoring. Georgia Institute of Technology, School of Civil Engineering in cooperation with Environmental Resources Center, ERC-0672, Atlanta, 104 pp.

Little, W.C., and Mayer, P.G. 1976. Stability of channel beds by armoring. Journal of the Hydraulics Division 102(HY11):1647-1661.

Little, W.C.; Grissinger, E.H.; and Murphey, J.B. 1981. Erodibility of streambank materials of low cohesion. Transactions, American Society of Agricultural Engineers 24(3):624-630.

- Mason, P.J.; and Arumugam, K. 1985. Free jet scour below dams and flip buckets. *Journal of Hydraulic Engineering* 111(2):220-235. Discussions: 113(9):1192-1205.
- Mendoza, C.; Abt, S.R.; and Ruff, J.F. 1983. Headwall influence on scour at culvert outlets. *Journal of Hydraulic Engineering* 109(HY7):1056-1060.
- Mendoza-Cabrales, C. 1980. Headwall influence on scour at culvert outlets. M.S. thesis. 186 pp. [On file at the Colorado State University, Fort Collins.]
- Nik Hassan, N.M.K., and Narayanan, Rangaswami. 1985. Local scour downstream of an apron. *Journal of Hydraulic Engineering* 111(11):1371-1385.
- Novak, P., ed. 1984. *Developments in hydraulic engineering--2*. Elsevier Applied Science Publishers, London and New York, 243 pp.
- Ofwona, P. 1965. Time progression of erosion at culvert outlets. M.S. thesis. [On file at the University of Cincinnati, Cincinnati, OH.]
- Opie, T.R. 1967. Scour at culvert outlets. M.S. thesis. 82 pp. [On file at the Colorado State University, Fort Collins.]
- Rajaratnam, N. 1981a. Erosion of sand beds by submerged impinging circular turbulent water jets. The University of Alberta Water Resources Engineering Technical Report 81-1, 15 pp.
- Rajaratnam, N. 1981b. Erosion of a loose polystyrene bed by obliquely impinging circular turbulent air jets. University of Alberta Department of Civil Engineering Water Resources Engineering Technical Report 81-2, 25 pp.
- Rajaratnam, N. 1981c. Erosion of sand beds by circular impinging water jets with minimum tailwater. University of Alberta Department of Civil Engineering Technical Report--Water Resources Engineering Group, 19 pp.
- Rajaratnam, N. 1981d. Erosion by plane turbulent jets. *Journal of Hydraulic Research* 19(4):339-358.
- Rajaratnam, N. 1982. Erosion by submerged circular jets. *Journal of the Hydraulics Division* 108(HY2):262-267.
- Rajaratnam, N., and Beltaos, S. 1977. Erosion by impinging circular turbulent jets. *Journal of the Hydraulics Division* 103(HY10):1191-1205.

- Rajaratnam, N., and Berry, B. 1977. Erosion by circular turbulent wall jets. *Journal of Hydraulic Research* 15(3):277-289.
- Rajaratnam, N., and Macdougall, R.K. 1983. Erosion by plane wall jets with minimum tailwater. *Journal of Hydraulic Engineering* 109(7):1061-1064.
- Rajaratnam, N.; Pochylko, D.S.; and Macdougall, R.K. 1981. Further studies of erosion of sand beds by plane water jets. University of Alberta Department of Civil Engineering Water Resources Engineering Rept. WRE 81, 43 pp.
- Raudkivi, Arved J. 1986. Functional trends of scour at bridge piers. *Journal of Hydraulic Engineering* 112(1):1-13.
- Robinson, A.R. 1971. Model study of scour from cantilevered outlets. *Transactions, American Society of Agricultural Engineers* 14(3):571-576 and 581.
- Rouse, H. 1940. Criteria for similarity in the transportation of sediment. *In Proceedings of 1st Hydraulics Conference, Bulletin 20, State University of Iowa, Iowa City, March 1940.* pp. 33-49.
- Ruff, J.R., and Abt, S.R. 1980. Scour at culvert outlets in cohesive bed material. Colorado State University Report CER79-80JFR-SRA61, 157 pp.
- Ruff, J.R.; Abt, S.R.; Mendoza, C.; and others. 1982. Scour at culvert outlets in mixed bed materials. U.S. Department of Transportation, Federal Highway Administration, Offices of Research and Development Report No. FHWA/RD-82/011, 103 pp.
- Sarma, K.V.N. 1967. Existence of limiting scour depth. *Journal of the Institution of Engineers (India)* 48(1, C11):84-92.
- Sarma, K.V.N., and Sivasankar, R. 1967. Scour under vertical circular jets. *Journal of the Institution of Engineers (India)* 48(3, C12):569-579.
- Seaburn, G.E. 1965. Incipient motion caused by a jet. M.S. thesis. [On file at the University of Cincinnati, Cincinnati, OH.]
- Seaburn, G.E., and Laushey, L.M. 1967. Velocities of culvert jets for incipient erosion. *In Proceedings of the 12th Congress of the International Association for Hydraulic Research, Colorado State University, Fort Collins, September 11-14, 1967,* vol. 3, pp. 1-8.

Shaikh, A. 1980. Scour in uniform and graded gravel at culvert outlets. M.S. thesis. 105 pp. [On file at the Colorado State University, Fort Collins.]

Shen, H.W.; Schneider, V.R.; and Karaki, S.S. 1966. Mechanics of local scour. Colorado State University Engineering Research Center Report No. CER66HWS22, 56 pp.

Simons, D.B.; Stevens, M.A.; and Watts, F.J. 1970. Report: flood protection at culvert outlets. Colorado State University Report No. CER69-70DBS-MAS-FJW4, 218 pp.

Smith, C.D., and Johnson, S.R. 1983. Scour control at overhanging pipe outlets. In Proceedings of the 6th Canadian Hydrotechnical Conference, Ottawa, Ontario, June 2 and 3, 1983, pp. 581-598. Canadian Society for Civil Engineering.

Smith, G.L. 1957a. An analysis of scour below culvert outlets. M.S. thesis. 152 pp. [On file at the Colorado State University, Fort Collins.]

Smith, G.L. 1957b. Scour and energy dissipation below culvert outlets. Colorado Agricultural and Mechanical College Department of Civil Engineering Report No. CER57GLS16, 122 pp.

Smith, G.L. 1961. Scour and scour control below cantilevered culvert outlets. Colorado State University Research Foundation Report No. CER61GLS14, 109 pp.

Smith, G.L., and Hallmark, D.E. 1961. New developments for erosion control at culvert outlets. National Academy of Sciences--National Academy of Engineering, National Research Council, Highway Research Board Bulletin 286, pp. 22-31.

Stevens, M.A. 1969. Scour in riprap at culvert outlets. Ph.D. thesis. 203 pp. [On file at the Colorado State University, Fort Collins.]

Stevens, M.A.; Simons, D.B.; and Watts, F.J. 1971. Riprapped basins for culvert outfalls. National Academy of Sciences--National Academy of Engineering, National Research Council, Highway Research Record No. 373, pp. 24-38.

Taylor, B.D. 1971. Temperature effects in alluvial streams. California Institute of Technology, W.M. Keck Laboratory of Hydraulics and Water Resources Report No. KH-R-27, 204 pp.

Taylor, B.D. 1974. Temperature effects in flows over nonplanar beds. Journal of the Hydraulics Division 100(HY12):1785-1807.

Taylor, D.B., and Vanoni, V.A. 1972. Temperature effects in low-transport, flat-bed flows. *Journal of the Hydraulics Division* 98(HY8):1427-1445.

Thomas, R.K. 1953. Scour in a gravel bed at the base of a free overfall. M.S. thesis. [On file at the Colorado Agricultural and Mechanical College, Fort Collins.]

Thomas, Z. 1971. Time development of the deformation of an alluvial bottom. In *Proceedings of the 14th Congress of the International Association for Hydraulic Research*, Paris, France, August 29-September 3, 1971, vol. 3, pp. 347-354.

Thomas, Z. 1972. Časový vývoj rozměrů Lokálního Výmolu a Násou [Time development of the dimensions of a local scour and deposit]. *Vodohospodářský Časopis* [Bratislava, Czechoslovakia] 20(1):33-65. [Translated for the U.S. Department of Agriculture, Agricultural Research Service, and for the National Science Foundation by Franklin Book Programs, Inc., 1975.]

Vanoni, V.A., ed. 1975. *Sedimentation engineering*. 745 pp. American Society of Civil Engineers, New York.

Varga, L. 1966. Effect of tailwater on incipient erosion at culvert outlets. M.S. thesis. [On file at the University of Cincinnati, Cincinnati, OH.]

Varga, L., and Laushey, L.M. 1967. Application of the wall jet theory to erosion at the outlet of hydraulic structures. In *Proceedings of the 12th Congress of the International Association for Hydraulic Research*, Colorado State University, Fort Collins, September 11-14, 1967, vol. 3, pp. 202-206.

Whittaker, J.G., and Schleiss, A. 1984. Scour related to energy dissipators for high head structures. *Mitteilungen der Versuchsanstalt für Wasserbau, Hydrologie und Glasiologie*, Nr. 73, Zurich, 73 pp.